Reliability of timber structures

Report

Author(s):
Köhler, Jochen

RELIABILITY OF TIMBER STRUCTURES

Jochen Köhler

Institute of Structural Engineering
Swiss Federal Institute of Technology

Zurich
May 2007

FOREWORD

In the last few years the interest in designing timber structures has steadily increased. The reason for this being an increased focus in society on sustainability and environmental aspects but also due to the positive effects on the inner climate in accommodation buildings and the increased architectural possibilities. Furthermore, timber is technically and economically competitive compared with steel and concrete as a building material for a broad range of normal building structures such as e.g. accommodation buildings.

So far the basis for design of timber structures has by far and large not achieved the same level of refinement and detail as the basis for the design of steel and concrete structures for several reasons. First of all the variability of the material properties is much higher than for other building materials; the raw timber material is not engineered but the result of natural processes. The material properties cannot be designed as for other materials but must be ensured by quality control schemes. Secondly the material properties, and therefore the reliability, depend on the whole load and moisture history of the structure. These two effects interact in a complicated manner for the timber materials used in timber structures, structural timber, glued laminated timber, panel-products together with the joints between them.

The result of this being that the design of timber structures to a large degree is based on experience, subjective engineering judgement and in many cases excessive conservative assumptions. However, despite an in general conservative attitude the present basis for design of timber structures does not consistently account for the uncertainties influencing the structural performance. As a consequence hereof the presently applied basis for the design of timber structures may lead to designs which in terms of reliability are not comparable to equivalent structures made of steel and concrete.

The main contribution of the present thesis by PhD J. Köhler addresses the problem complex outlined in the above and can be summarized as to establish a probabilistic model framework (or probabilistic model code) for the design of timber structures. In this process special emphasis is directed on the aspects of consistent modelling of the performance of timber components subjected to different types of loading and environmental exposures.

In the thesis a rather rigorous phenomenological and hierarchical modelling of uncertainties associated with the characteristic of timber materials in dependency of scale, applied models and available information is developed. On this basis specific models are developed and/or further extended with the aim to represent the performance of timber components and joints in consistency with experimental data and engineering understanding. The introduced models are rigorously analysed and simplified to the extent reasonable and relevant with due consideration to their practical applicability.

The probabilistic model code developed within the present thesis has by now already been

adopted by the Joint Committee on Structural Safety. In this way the thesis has been ensured a significant impact in a pre-normative context and thereby contributes to the future increased rational, efficient and sustainable use of timber as a building material

Zürich, May 2007   Prof. Dr. M. H. Faber

SUMMARY

During the last decades structural reliability methods have been further developed, refined and adapted and are now at a stage where they are being applied in practical engineering problems as a decision support tool in connection with design and assessment of structures. For materials such as concrete and steel, the application of modern structural reliability methods has led to an increasingly more consistent evaluation of the safety or reliability. Whereas some efforts in this direction have been undertaken also for timber, the developments, however, have been less impressive. One of the main reasons for this is that the variability of the timber material properties is much higher than for other building materials. Furthermore, the timber material properties depend on the entire load and moisture history of the structure.

It is important that a consistent basis for design of timber structures is established and documented in such a way that it may be accepted for implementation by the timber engineering and research community. The development of a consistent basis of design of timber structures is the focal point of this thesis.

The proposed basis of design is structured into several levels of sophistication. The basic level reflects the recent practice for reliability based code calibration. The bending strength and stiffness and the density of timber are referred to as reference material properties and are introduced as simple random variables. The basic limit state functions for components and connections are given. Furthermore, proposals are made regarding the different characteristics of timber on this simple level. Functional relationships for other material properties (based on the reference material properties) are given and probability distribution functions for the other material properties are proposed. Starting from this level, several possible refinements are proposed. New information might be introduced, and it is shown how different types of new information can be integrated by using a Bayesian updating scheme. Refinements in regard to the modelling of damage as a consequence of time load duration are proposed. For the bending strength, a hierarchical spatial variability model is proposed and a method is presented for linking the properties of a cross section (which is considered as the reference starting point for the modelling of spatial variability) with the properties of a test specimen.

The main outcomes of this thesis are related to necessary pre-codification modelling aspects concerning the reliability of timber components in regard to strength and stiffness properties. An achievement of this thesis is that the work performed is fully compatible with the general probabilistic framework for establishing design basis developed by the Joint Committee on Structural Safety (JCSS).

ZUSAMMENFASSUNG

Die Methoden zur Beurteilung der Bauwerkszuverlässigkeit wurden in den letzten Jahrzehnten weiterentwickelt, verbessert und angepasst, so dass sie heute im praktischen Ingenieurwesen ihre Anwendung finden; zum Beispiel als Entscheidungshilfe bei dem Entwurf und dem Unterhalt von Bauwerken. Für Bauwerke aus Stahl und Beton führte die Anwendung dieser Methoden zu einer konsistenteren Beurteilung der Sicherheit und der Zuverlässigkeit. Obschon für Bauwerke aus Holz einige Anstrengungen unternommen wurden, diese Methoden zur Anwendung zu bringen, sind die erreichten Entwicklungen im Vergleich zu anderen Baumaterialien weniger fortgeschritten. Einer der Hauptgründe für diesen Unterschied ist die hohe Komplexität des Baumaterials Holz; um das volle Potential des Baumaterials Holz auszuschöpfen ist ein hohes Mass an Fachkenntnis erforderlich.

Es ist wichtig, dass eine konsistente Basis für die Bemessung von Holzkonstruktionen entwickelt wird, die breite Anwendung auf dem Gebiet des Ingenieurholzbaus findet. Die Entwicklung einer solchen Bemessungsbasis steht im Focus dieser Dissertation.

Die hier vorgeschlagene Bemessungsbasis ist in mehrere Modellierungsstufen aufgeteilt. Die Grundstufe repräsentiert die allgemein gängige Praxis bei der Kalibrierung von Bemessungsrichtlinien. Die Biegefestigkeit, das Elastizitätsmodul in Biegung und die Holzdichte sind als Referenzmaterialeigenschaften definiert und werden als Zufallsvariablen eingeführt. Einige grundlegende Grenzzustandsfunktionen für Komponenten und Verbindungen sind angegeben. Des Weiteren werden Vorschläge zur Modellierung der speziellen Holzmaterialeigenschaften gemacht. Andere Holzmaterialeigenschaften werden basierend auf den Referenzmaterialeigenschaften ermittelt und ebenfalls als Zufallsvariablen eingeführt. Ausgehend von dieser Grundstufe werden mehrere Modellerweiterungen vorgeschlagen. Es wird aufgezeigt, wie verschiedenartige neue Information dazu benutzt werden kann, die Parameter der vorgeschlagenen Modelle anzupassen. Modellverbesserungen in Bezug auf die Berücksichtigung der Schadensakkumulierung infolge von Langzeitbeanspruchung werden vorgeschlagen. Ein hierarchisches Model, welches die räumliche Variabilität der Biegefestigkeit berücksichtigt, wird entwickelt. Dieses Modell dient als Grundlage für eine Methode, die die Biegefestigkeit eines Querschnitts mit der Biegefestigkeit eines Probekörpers in Beziehung setzt.

Die vorgestellte Bemessungsbasis soll den Ausgangspunkt für die Weiterentwicklung von Bemessungsrichtlinien wie den Eurocode 5 und die SIA 265 bilden und den effizienten Gebrauch von Holz als Baumaterial ermöglichen. Die Ergebnisse dieser Arbeit sind kompatibel mit dem allgemeinen wahrscheinlichkeitsbasierten Rahmenwerk für die Entwicklung von Bemessungsrichtlinien, dem Probabilistischen Model Code, der vom Joint Committee on Structural Safety (JCSS) entwickelt und herausgegeben wurde.

TABLE OF CONTENTS

Annex

1 INTRODUCTION

Timber is an efficient building material, not only in regard to its mechanical properties but also because it is a highly sustainable material considering all phases of the life cycle of timber structures; production, use and decommissioning. Timber is a widely available natural resource throughout Europe; with proper management, there is a potential for a continuous and sustainable supply of raw timber material in the future. Due to the low energy use and the low level of pollution associated with the manufacturing of timber structures, the environmental impact of timber structures is much smaller than for structures built using other building materials. In addition timber, is a rather advantageous building material due to its material properties. Timber is a light material and, compared to its weight, the strength is high; the strength/weight ratio is even higher than for steel.

However, timber is still not utilized to its full potential in the building and construction sector considering its beneficial properties. Many building owners, but also architects and structural engineers, do not consider timber as a competitive building material compared to concrete, steel or masonry. Attributes such as high performance in regard to reliability, serviceability and durability are generally not associated with timber as a building material. One of the main reasons for this is that timber is a highly complex material; it actually requires a significant amount of expertise to fully appreciate the potential of timber as a structural building material. In addition to this there are still a number of issues which need to be further researched before timber materials can achieve the same recognition as a high quality building material such as e.g. steel and concrete.

In daily practice the engineering codes and regulations form the premises for the use of timber as a structural material. It is therefore of utmost importance that the codes and regulations are based on the most relevant and exact information available in regard to the reliability of timber structures. Traditionally, codes and regulations have been based to a very large degree on experience. This statement is true not just for timber structures, but also for concrete and steel structures. However, whereas the codes and regulations for the design of concrete and steel have undergone a remarkable modernisation through the last 2-3 decades, the codes and regulations for the design of timber structures are still falling significantly behind. The principle for the development of the scientific basis for codes and regulations for the design and assessment of structures is illustrated in Figure 1-1.

Whereas the various steps in the process of developing a scheme for design and assessment are illustrated to the left in the figure, the scientific constituents required in the process are illustrated in the right part of the figure. For identified design and assessment situations, models for describing the performance of structures are derived. The models take basis in physical hypotheses and experimental evidence. In general these models are associated with uncertainties and an important task within the modelling process is to take into account these uncertainties in a consistent manner. A set of probabilistic models, which reflects the current

best engineering practice, may be specified in so-called (probabilistic) model codes, which build the basis for all further simplified design codes.
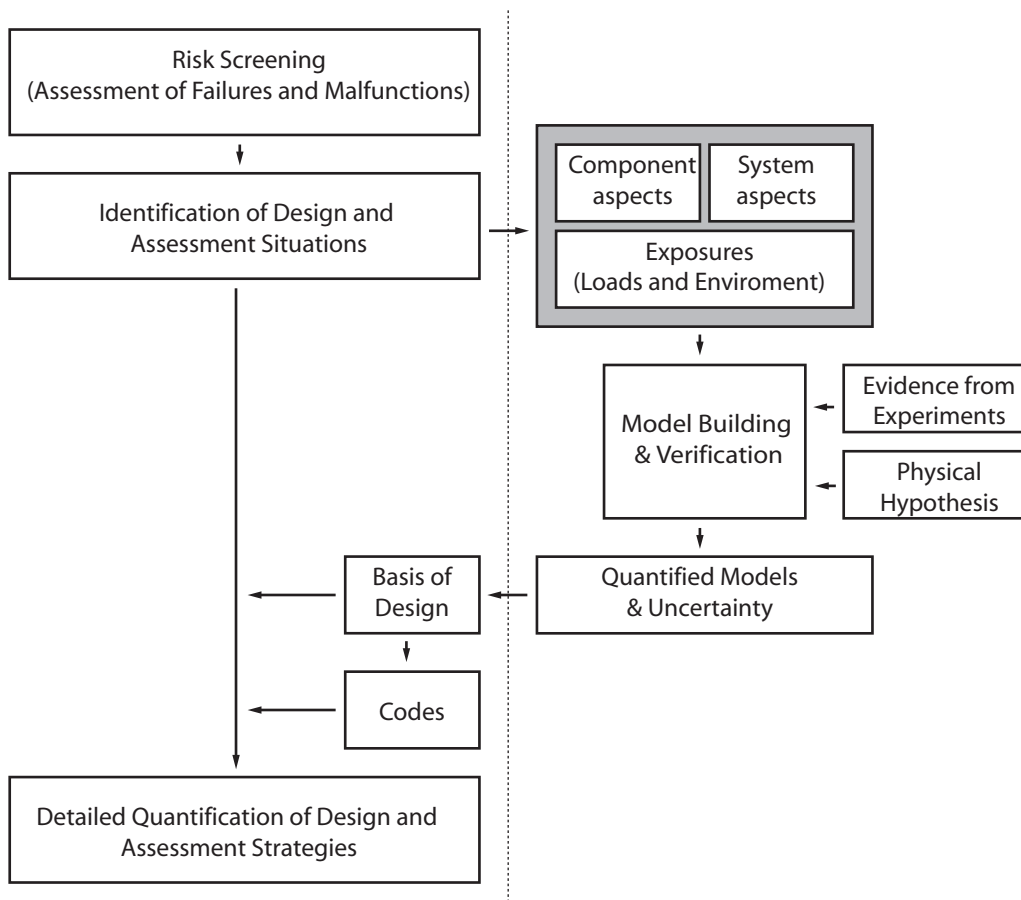
Figure 1-1 *Schematic representation of the framework required for establishing the basis for codes and regulations for design and assessment of structures.*

Presently the existing codes and regulations for the design of timber structures are not fully based on a framework as illustrated in Figure 1-1, but rather on a framework taking basis in general physical understanding combined with experience achieved through hundreds of years of use of timber as a structural material. In order to achieve the goal of optimizing the potential benefit of timber as a building material, it is thus necessary to establish a firm scientific basis for codes and regulations according to the process indicated in Figure 1-1.

1.1   SCOPE OF WORK AND LIMITATIONS

The main objective of the thesis is the development of a basis of design for timber structures. It is considered that timber is a material with special properties in regard to its high variability and its sensitivity to loading mode, load duration and changes in the surrounding climate. The schematic layout given in the right part of Figure 1-1 is used as a working thesis, focus is

placed on modelling aspects of timber components exposed to different load types and environmental conditions. This includes:

- a discussion of existing modelling approaches for the various aspects of timber components,

- a discussion of modelling alternatives,

- the selection of the most promising models,

- the calibration of parameters,

- the presentation of selected models and parameters in a consistent format,

- example calculations.

An important issue for the design of timber structures is the behaviour of structural systems made of a number of different components. These aspects are not considered explicitly within this thesis. However, the discussion on spatial variability of timber material properties and the respective modelling proposal delivers the basis for further research of the system behaviour of timber structures.

1.2   OUTLINE AND THESIS OVERVIEW

A thesis overview is given in Figure 1-2. In chapters 2 and 3 a brief introduction into the fields of structural reliability and timber engineering is given. Existing knowledge is reviewed and summarized. Focus is placed on the issues which are considered as a relevant basis for the subsequent chapters. Chapters 4 and 5 are the development parts of this thesis. In chapter 4 the focus is placed on the probabilistic modelling of timber material properties; in chapter 5 the modelling of timber connections with dowel type fasteners is discussed. These two chapters build the basis for the development of a proposal of a probabilistic model code for timber structures that is presented in chapter 6. In chapter 7 some further examples are given regarding e.g. the assessment of experimental data, Bayesian updating, etc. The thesis is concluded with chapter 8, where the main content is summarized and a discussion of proposed further research is given.

	Chapter 1
	Introduction

	Chapter 2	Chapter 3
Tools	**Basic Principles of Structural Reliability** Limit State Principle → Uncertainty → Basic Variables → Methods → Code Calibration	**Timber as a Structural Material** Tree → Wood → Timber → Timber Design

	Chapter 4	Chapter 5
Component	**Modelling Timber Material Properties** Grading → Spatial Variability → DOL → Framework	**Modelling Timber Connections** Dowel Type → Mechanical Models → Material Properties → Code Formats → Model Proposal → Verification → Model Uncertainty

	Chapter 6	Chapter 7	
Inference	**Probabilistic Model Code**	**Applications**	Parameter Estimation Influence of Test Standards Updating

Chapter 8
Conclusions and Outlook

Figure 1-2   Schematic overview of the thesis.

2 ASPECTS OF STRUCTURAL RELIABILITY

Typical problems in structural engineering such as design, assessment, inspection and maintenance planning are decision problems subject to a combination of inherent, modelling and statistical uncertainties. The structural reliability theory is concerned with the rational treatment of these uncertainties. In the subsequent chapter some basic aspects of structural reliability are introduced, whereas the content of the chapter is based on standard structural reliability literature, as Madsen et al. (1986), Melchers (1999) and Faber (2003). The interested reader is also referred to these publications for more detailed and complete information.

2.1 THE LIMIT STATE PRINCIPLE

The performance of an engineering structure depends on the type and magnitude of the applied load and the structural strength and stiffness. Whether the performance is considered satisfactory depends on the requirements which must be satisfied. Among others these include reliability of the structure against collapse, limitation of damages or of deflections, or other criteria. In general any state, that may be associated with consequences in terms of costs, loss of lives and impact to the environment are of interest. In the following it is not differentiated between these different types of states but for simplicity refer to all these as being failure events.

It is convenient to describe failure events in terms of functional relations, which if they are fulfilled, define that the failure event $\mathbf{F}$ will occur:

$$\mathbf{F} = \left\{ g(\mathbf{x}) \le 0 \right\} \tag{2.1}$$

where $g(\mathbf{x})$ is termed a limit state function. The components of the vector $\mathbf{x}$ are the realisations of the so-called basic random variables $\mathbf{X}$ representing all relevant uncertainties influencing the problem at hand. The failure event $\mathbf{F}$ is defined as the set of realisations of the limit state function $g(\mathbf{x})$, which are zero or negative.

Some typical limit states are given in Table 2-1.

Table 2-1   Typical limit states for structures.

Limit State Type	Description	Examples
Ultimate	Collapse of the structure or part of it	Rupture, plastic mechanism, instability, progressive collapse, fatigue, deterioration, fire.
Damage	(often included in above)	Excessive permanent cracking, permanent irreversible deformation.
Serviceability	Disruption of normal use	Excessive deflection, vibration, local damage.

Due to the associated consequences, failure events linked with the most serious limit states such as collapse and major damage should be relatively rare events. The study of structural reliability is concerned with the assessment of the probability of failure events for engineered structures at any stage during its service life.

The probability of occurrence of a failure event is a measure of the chance of its occurrence. This chance may be quantified by observing the long term frequency of the event for generally similar structures or components, or may be simply a subjective estimate of its numerical value. Engineering structures are mostly exclusive in regard to the structural assembly and their exposure to loads and environment which in general precludes the assignment of relative frequencies of events within many similar structures. However, a more generic description can be given for structural components and material. Thus in practice a combination of subjective estimates and frequency observations about structural components and structural assemblies is utilized to assess the probability of limit state violation of a structure.

The probability of failure p_f may be determined by the following integral:

$$p_f = P\big(g(\mathbf{X}) \le 0\big) = \int_{g(\mathbf{x}) \le 0} f_{\mathbf{X}}(\mathbf{x}) d\mathbf{x} \tag{2.2}$$

where $g(\mathbf{X})$ is the limit state function, $\mathbf{X}$ is a vector of basic random variables and $f_{\mathbf{X}}(.)$ is the joint probability function of the variables $\mathbf{X}$.

In general the basic variables $\mathbf{X}$ are functions of time. E.g. the loads which are applied to a structure are varying in time and are of uncertain magnitude at any point in time; consequently the situation is similar for the corresponding load effects s. The resistance of a structure or component r is also a function of time; commonly a structure is subject to some (random) deterioration process and the resistance is decreasing with time. The situation is illustrated in Figure 2-1. Both, the load effect and the resistance can be represented as random processes and probability density functions for given times $t = t_a, t_b$ can be formulated.
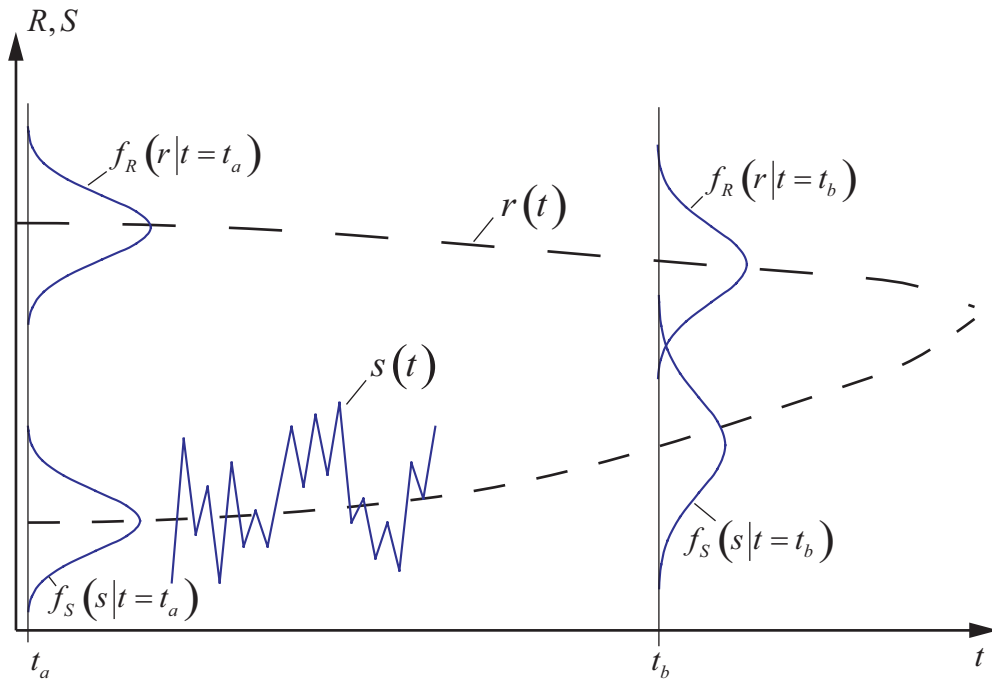
Figure 2-1   Schematic time-dependent reliability problem.

A situation as illustrated in Figure 2-1 is referred to as the time-dependent reliability problem. Failure occurs when the process $g\big(\mathbf{x}(t)\big)\leq 0$ for some time, t, during the considered time interval, $[0;T]$. $\mathbf{x}(t)$ is a realisation of the random process $\{\mathbf{X}(t)\}$. The probability of failure p_f in the interval $[0;T]$ may be determined as:

$$p_f(T)=1-P\big(g\big(\mathbf{X}(t)\big)>0,\ \forall t\in[0;T]\big) \tag{2.3}$$

The evaluation of Equation (2.3) is in general difficult, and approximations are used in practical applications. Often an upper bound of the probability of failure in the time interval $[0;T]$ is used:

$$p_f(T)=\int_0^T v^+(t,\xi)dt \tag{2.4}$$

where the out-crossing rate $v^+(t,\xi)$ is determined by a suitable application of Rice's formula, see e.g. Madsen et al. (1986).

In many situations it is convenient (and sufficient) to assume that the basic variables $\mathbf{X}$ are not depending on the time t. Then Equation (2.2) can be used for the determination of the probability of failure.

2.2 BASIC PRINCIPLES OF RELIABILITY ASSESSMENT

The aim of structural reliability assessment is to quantify the reliability of structures under the consideration of all uncertainties associated with the formulation of the failure criteria. The formal framework for the calculation of the failure probability is given in Equation (2.2), whereas the term reliability is defined as the complement of the failure probability $\left(= 1 - p_f \right)$. A failure criterion is expressed through the limit state function $g(\mathbf{X})$.

2.2.1 UNCERTAINTIES IN RELIABILITY ASSESSMENT

The limit state function $g(\mathbf{X})$ is formulated by means of models based on physical understanding and empirical data. Due to idealizations, inherent physical uncertainties and inadequate or insufficient data, the models themselves and the parameters entering the models such as material properties and load characteristics are uncertain. Consequently, uncertainties are grouped into:

- Inherent Uncertainties,

- Model Uncertainties,

- Statistical Uncertainties.

Inherent uncertainty refers to the randomness of a phenomenon. This randomness is a result from a combination of uncontrollable fluctuations of many different factors. An example is a strength property of a structural timber element, which is a product of several quality control procedures during its production, but also growing conditions, sawing pattern and many other factors in the production line of the timber structural element. Another example for the randomness is the realization of loads on structures due to e.g. snow or wind events. The described type of uncertainty is also referred to as physical uncertainty.

Model uncertainty is associated with the crudeness and incompleteness of mathematical models which describe a phenomenon.

The statistical uncertainties are associated with the statistical evaluation of test results or observations. They may result from limited numbers of tests or observations which cause uncertainty in the estimation of statistical parameters.

2.2.2 BASIC VARIABLES AND THEIR QUANTIFICATION

In structural reliability assessment the set of basic variables of a problem in general is constituted of both random and deterministic variables for the geometry, material properties and load characteristics. In this section only very general remarks are made in regard to the different physical characteristics of the different types of random basic variables. In general, the quantification of the basic random variables can be divided into three parts:

- Definition of the considered populations.

- Selection of a suitable types or families of probability distribution for the basic variable.

- Estimation of suitable distribution parameters from available data and any prior knowledge.

2.2.2.1 Population

The basic random variables should always be related to a meaningful and consistent set of populations. The description and modelling of these random variables should correspond to this set. A reliability analysis based on these random variables is only valid for the considered set of populations. The basis for the definition of a population is in most cases the physical background of the quantity. Factors which define a population are the nature and the origin of the random quantity (e.g. strength, load or geometry), the spatial characteristics (e.g. size of structural component, geographical origin of the considered material, regional wind speed characteristics) and temporal conditions (e.g. duration of exposure). The choice of specifications which define a population may depend on the objective of the analysis, the amount and nature of the available data and the amount of resources which can be afforded. A population with a unique set of specifications is referred to as elementary population; a population in which specification parameters vary is referred to as a composite population. The set of measurements associated with a certain population is referred to as an elementary or composite sample respectively. A sampling procedure may be representative or artificial. Representative samples or representative realisations of random variables are obtained through random sampling. Artificial means that no direct relation exist between the statistical properties of the sample and the statistical properties of the population. An artificial sample is e.g. when only weak specimen are selected for testing by engineering judgment or proof loading. Artificial samples are also termed censored samples.

Observations on a representative sample may be undertaken according to a standardised test procedure. Hereby the test standard specifies partly the population; e.g. if a sample of timber specimen is tested in bending and all spatial and temporary conditions are specified. Then, the statistical properties of the sample are assumed to be the same as the statistical properties of the population.

The statistical properties of the sample are described by a suitable probability distribution function. The physical characteristic of the random variable determines the possible type of distribution function.

2.2.2.2 Selecting a Suitable Probabilistic Model

Resistance Variables

The resistance of a structure is governed by so-called resistance variables. Dimensions,

geometrical imperfections and material properties are resistance variables. Resistance variables can be modelled as random properties by random variables. Assuming that the random properties belong to an elementary population, standard probability distribution models can be utilised to represent the random variables. The following distribution models are generally used to model resistance variables:

Normal Distribution: This is one of the most important probability distribution. It can be shown that a sum of many independent random properties gets normal distributed. This property is also known as the central limit theorem; see e.g. Benjamin and Cornell (1970). The normal distribution gives finite probability for negative values. For that reason the logarithm of the normal distribution is often preferred for modelling resistance variables.

Lognormal Distribution: The lognormal distribution arises naturally as a limiting distribution when the random resistance is a product of a number of independent random quantities. The lognormal distribution is frequently used to model resistance variables because it is precluding negative values.

Weibull Distribution: For strength related material properties the Weibull distribution is used quite frequently. It is based on the assumption that a structural body is composed of nearly an infinite number of elements. The strength of the elements is independent and identically distributed and the strength of the material body is assumed to be equivalent to the strength of the weakest element. The theory behind the Weibull distribution is described in more detail in section 4.2.4.2.

The distribution function for the Normal, Lognormal and the Weibull distribution is given in Annex A, Table A1.

Other distributions: A number of other distributions are sometimes used to model resistance variables; e.g. the beta-, rectangular-, t- or gamma distribution. For information about these models it is referred to standard literature, e.g. Benjamin and Cornell (1970).

Caution is necessary if the considered sample is not homogeneous, i.e. if the source of the considered specimens is not the same. When data from one or more sources is analysed as a single sample, the shape of the distribution function is likely depending equally on relative number taken from each source than on the actual, but unknown, distribution function of every single source.

Load Variables

Loads are generally understood as forces acting on a structure which arise from external influences, e.g. self weight, snow load, wind force, etc. Imposed deformations as dimensional changes arising from temperature or humidity changes are also considered as loads. In a structural analysis, so-called load effects are considered directly. They are commonly a combination of different variables, as e.g. roof shape, snow load, wind exposition, dimensions, etc., which make the effect of the snow load on the structure. This effect is

10

measured in the same dimension as the resistance (e.g. stress) and can be directly compared.

Load effects can be classified as follows in:

- permanent or variable (variability in magnitude with time),

- fixed or free (variability in position with time),

- static or dynamic (the nature of the induced structural response).

It should be noted that similar loads can be considered as different load effects according to the classification made above. (E.g. a traffic load on a bridge can be seen as the effect of the static weight of the heaviest truck or as the magnitude and number of load cycles caused by passing vehicles, etc.).

Permanent Loads: Permanent loads on structures can be seen as a sum of dead load of many different components of the structure and other parts. Therefore, the random character of permanent loads is well represented by a normal distribution. Furthermore, it can be shown that the coefficient of variation of the weight of the sum of many (independent) components is decreasing with the number of components considered.

Variable Loads: Most loads on structures are varying in time. Examples are wind loads, snow loads or traffic loads. Time varying loads can be modelled with random processes. Different types of random processes are illustrated in Figure 2-2. Very often structural analysis is simplified to be time invariant. Then only the distribution of the maximum realisations of a process in a specified time interval is of interest. Extreme value distributions can be utilised to model these extreme realisations. Several extreme value distributions are well described in the literature, e.g. Benjamin and Cornell (1970).
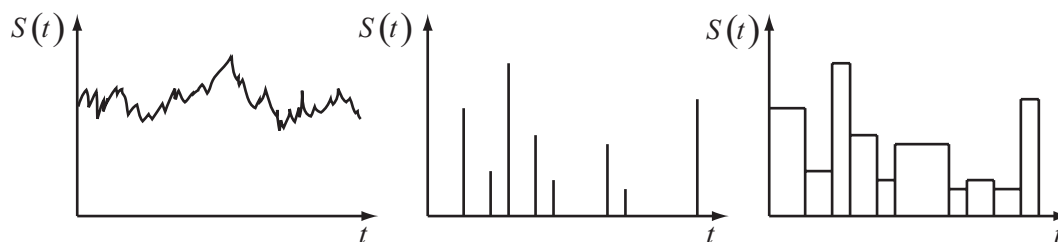
Figure 2-2   Different types of random load processes.

Load combinations

An important issue when considering load modelling is the representation of the extremes of combinations of different load effects – the load combination problem. Different individually acting loads may be modelled as the sum of the load effect processes $X_i(t)$ and the maximum $X_{max}(T)$ is calculated by:

$$X_{max}(T) = \max_T \left\{ X_1(t) + X_2(t) + ... + X_n(t) \right\}$$

(2.5)

A general solution to Equation (2.5) is hardly attainable but solutions exist for special cases of continuous load processes and different types of non-continuous processes, see e.g. Thoft-Christensen and Baker (1982) or Melchers (1999). Some approximate solutions to Equation (2.5) exist and the most widely used approaches, the Turkstra Load Combination Rule and the Ferry Borges – Castanheta Load Combination Rule are briefly introduced next.

The Turkstra Load Combination Rule

When n loads are combined it seems to be clear that the event of all individual loads attain the maximum at the same point in time is highly unlikely; even if the number of different loads n considered is high. However, it can be formulated as an upper bound for the maximum of n combined loads:

$$X_{\max}(T) \le \max_T \{X_1(t)\} + \max_T \{X_2(t)\} + ... + \max_T \{X_n(t)\} \tag{2.6}$$

This formulation is considered as too conservative and alternatively it is proposed in Turkstra (1970) to evaluate the maximum load for the individual loads for the given reference period and combining them in accordance with the scheme shown in Equation (2.7).

$$Z_1 = \max_T \{X_1(t)\} + X_2(t^*) + X_3(t^*) + ... + X_n(t^*)$$

$$Z_2 = X_1(t^*) + \max_T \{X_2(t)\} + X_3(t^*) + ... + X_n(t^*)$$

$$\vdots \tag{2.7}$$

$$Z_n = X_1(t^*) + X_2(t^*) + X_3(t^*) + ... + \max_T \{X_n(t)\}$$

and approximating the maximum combined load $X_{\max}(T)$ by

$$X_{max}(T) \approx \max_i \{Z_i\} \tag{2.8}$$

$X_i(t^*)$ is an arbitrary point in time value of $X_i(t)$ and in general taken into account as the mean value, provided that the process is stationary.

This approximation is called Turkstra's rule and is commonly used as a basis for codified load combination rules.

The Ferry Borges – Castanheta Load Combination Rule

A more sophisticated approximation to the load combination problem is based on the load model is suggested in Ferry Borges and Castanheta (1971). A highly simplified representation of the real load processes is utilized which facilitates a solution of the load combination problem as defined by Equation (2.5) by use of modern reliability methods such as FORM outlined in section 2.3.1.
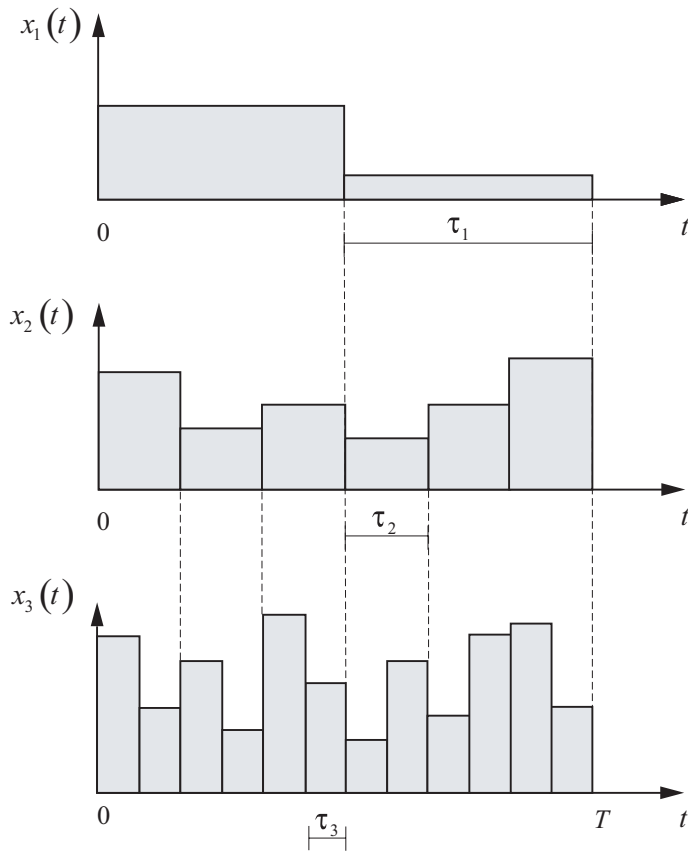
Figure 2-3   *Illustration of the Ferry Borges – Castanheta Load Process.*

For each process $X_i(t)$ it is assumed that the load changes after equal so-called elementary intervals of time τ_i. Further it is assumed that the load is constant within each elementary time interval. This is illustrated in Figure 2-3 where the reference period T has been divided into n_i intervals of equal length $\tau_i = T/n_i$. The integer n_i is called the repetition number for the ith load. The loads in the elementary time intervals are assumed to be identically distributed and mutually independent random variables with a point in time probability distribution function $F_{X_i}(x_i)$. The n_i pulses of the process may be understood as a vector of mutually independent random variables.

When combinations of load processes $X_1(t)$, $X_2(t)$, ..., $X_n(t)$ are considered it is assumed that the loads are stochastically independent with repetition numbers n_i, where:

$$n_1 \leq n_2 \leq ... \leq n_i \leq ... \leq n_r \qquad (2.9)$$

and

$$n_i / n_{i-1} \in Z_+ \qquad \text{for } i = 2,3,...,j \qquad (2.10)$$

where Z_+ is the set of positive natural numbers. E.g., in Figure 2-3 $j = 3$ and $n_1 = 2$, $n_2 = 6$ and $n_3 = 12$.

The distribution function of the maximum value of a period with m repetitions is calculated

as:

$$F_{\max_T X_i}(x_i) = \left(F_{X_i}(x_i)\right)^m \tag{2.11}$$

According to Ferry Borges – Castanheta different combinations of individual load processes i have to be taken into account, whereas the number of repetitions is varying and depending on the number of elementary time intervals n_i. The following combination rules are for the case of 3 different load sequences ($j = 3$):

Table 2-2   Load combination rules for 3 different load sequences ($j = 3$).

Combination No.	No. of repetitions m		
	Load 1	Load 2	Load 3
1	n_1	n_2/n_1	n_3/n_2
2	1	n_2	n_3/n_2
3	n_1	1	n_3/n_1
4	1	1	n_3

I.e. for the load distributions $F_{X_1}(x), F_{X_2}(x), F_{X_3}(x)$ of the loads 1, 2, 3 in Figure 2-3, the following combinations have to be considered:

1: $\qquad Z_1 = \left(F_{X_1}(x)\right)^2 + \left(F_{X_2}(x)\right)^3 + \left(F_{X_3}(x)\right)^2$

2: $\qquad Z_2 = \left(F_{X_1}(x)\right)^1 + \left(F_{X_2}(x)\right)^6 + \left(F_{X_3}(x)\right)^2$

3: $\qquad Z_3 = \left(F_{X_1}(x)\right)^2 + \left(F_{X_2}(x)\right)^1 + \left(F_{X_3}(x)\right)^6$

4: $\qquad Z_4 = \left(F_{X_1}(x)\right)^1 + \left(F_{X_2}(x)\right)^1 + \left(F_{X_3}(x)\right)^{12}$

The governing maximum load is $X_{\max}(T) \approx \max\limits_{i}\{Z_i\}$.

2.2.2.3   Estimation of Distribution Parameters

An important task within the framework of reliability analysis and assessment is the quantification of model parameters based on observations of the quantity to be modelled. In general the observations are performed through measurements of the quantity in the context of a specified test configuration or through continuous observations of the state of nature. The

output of these measurements is a set of numerical data, the so-called sample values. It is assumed that the sample values are realisations of the random variable X. The statistical properties of X can be assessed considering the sample values. Several methods can be found in the literature, e.g. a good overview of the methods is given in Benjamin and Cornell (1970). The most important methods are outlined in Annex A.

2.3   METHODS OF STRUCTURAL RELIABILITY

Several methods can be found in the literature to calculate the probability failure by solving the integral in Equation (2.2). An overview and a discussion of different approaches is presented in e.g. Ditlevsen and Madsen (1996), Melchers (1999) and Faber (2003). The most straightforward method is that of Monte Carlo simulation, while probably the more efficient are the so called approximate methods based on the calculation of the reliability index β (FORM and SORM). There are also methods to increase the efficiency of the Monte Carlo simulation like Importance Sampling or Adaptive Sampling. In this section only the main ideas of FORM (First Order Reliability Method) and the Monte Carlo Simulation are briefly outlined. For further information also about the other methods it is referred to standard literature, e.g. Melchers (1999).

2.3.1   FIRST ORDER RELIABILITY METHOD (FORM)

2.3.1.1   Linear Limit State Functions and Normal Distributed Variables

At first a simple case where the limit state function $g(\mathbf{x})$ is a linear function of the basic variables $\mathbf{X}$ is considered. Then the limit state function can be written as:

$$g(\mathbf{x}) = a_0 + \sum_{i=1}^{n} a_i x_i \tag{2.12}$$

If the basic random variables are normally distributed the so-called safety margin M is defined as:

$$M = a_0 + \sum_{i=1}^{n} a_i X_i \tag{2.13}$$

and is normal distributed with mean value μ_M and standard deviation σ_M as:

$$\mu_M = a_0 + \sum_{i=1}^{n} a_i \mu_{X_i} \tag{2.14}$$

and

$$\sigma_M^2 = a_0 + \sum_{i=1}^{n} a_i \sigma_{X_i}^2 + \sum_{i=1}^{n} \sum_{j=1, j \neq i}^{n} \rho_{ij} a_i a_j \sigma_{X_i} \sigma_{X_j} \qquad (2.15)$$

where ρ_{ij} are the correlation coefficients between the variables X_i and X_j. Defining the failure event as in Equation (2.1), the probability of failure can be defined as:

$$p_f = P(g(\mathbf{X}) \leq 0) = P(M \leq 0) \qquad (2.16)$$

which in this case reduces to the evaluation of the standard normal distribution function, as:

$$p_f = \Phi(-\beta) \qquad (2.17)$$

Where β is the so-called reliability index (due to Cornell (1969) and Basler (1961)) given as:

$$\beta = \frac{\mu_M}{\sigma_M} \qquad (2.18)$$

If the two dimensional case of two independent normal distributed random variables is considered the reliability index β has a geometrical interpretation as illustrated in Figure 2-4.
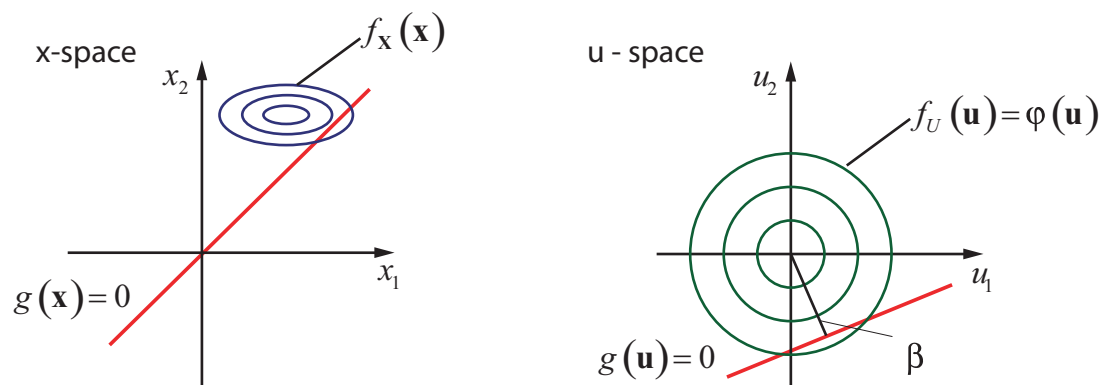
Figure 2-4   *Illustration of the two-dimensional case of a linear limit state function and standardized normally distributed variables U_1, U_2. (adapted from Faber (2003)).*

In Figure 2-4 the limit state function $g(\mathbf{x})$ is transformed into the limit state function $g(\mathbf{u})$ by normalisation of the independent normal distributed random variables $\mathbf{X}$ into standardized normally distributed random variables $\mathbf{U}$ as:

$$U_i = \frac{X_i - \mu_{X_i}}{\sigma_{X_i}} \qquad (2.19)$$

such that the random variables U_i have zero means and unit standard deviations.

The reliability index β has the geometrical interpretation as the smallest distance from the

line (or in general the hyper-plane) forming the boundary between the safe domain and the failure domain, i.e. the line (or hyper-plane) described by $g(\mathbf{u}) = 0$ (Hasofer and Lind (1974)). The point of the smallest distance is referred to as the design point $\mathbf{u}^*$.

2.3.1.2 Non-linear Limit State Functions

When the limit state function $g(\mathbf{x})$ is non-linear in the basic random variables $\mathbf{X}$, the failure probability can only be approximated. In Hasofer and Lind (1974) it is suggested to perform a linearization in the design point of the failure surface represented in the normalized space.

The approach is illustrated in the two dimensional space in Figure 2-5.
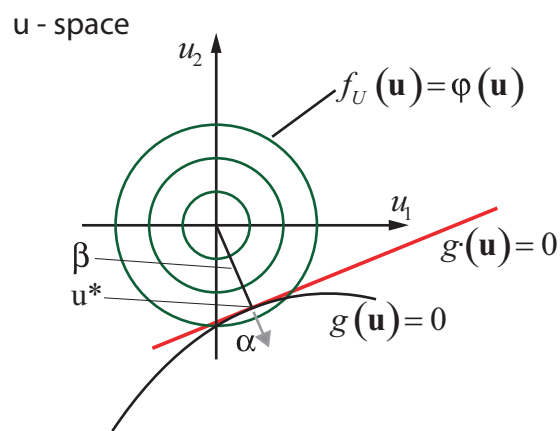
Figure 2-5   Illustration of the linearization proposed in Hasofer and Lind (1974) in the standard normal space.

In Figure 2-5 the failure surface $g(\mathbf{u}) = 0$ is linearised in the design point $\mathbf{u}^*$ by the line $g'(\mathbf{u}) = 0$. The vector $\boldsymbol{\alpha}$ is the out ward directed normal vector to the failure surface in the design point.

As the limit state function is in general non-linear, the design point is not known in advance and has to be found iteratively, e.g. by solving the following optimisation problem:

$$\beta = \min_{\mathbf{u} \in \{g(\mathbf{u})=0\}} \sqrt{\sum_{i=1}^{n} u_i^2} \tag{2.20}$$

This problem can be solved in several different ways. Provided that the limit state function is differentiable the following simple iteration scheme can be followed:

$$\alpha_i = \frac{-\dfrac{\partial}{\partial u_i} g(\beta \boldsymbol{\alpha})}{\left[\displaystyle\sum_{j=1}^{n} \dfrac{\partial}{\partial u_i} g(\beta \boldsymbol{\alpha})^2 \right]^{1/2}} \quad , \; i = 1, 2, ..., n \tag{2.21}$$

$$g\left(\beta\alpha_1, \beta\alpha_2, ..., \beta\alpha_n\right) = 0 \tag{2.22}$$

First the design point is guessed with $\mathbf{u}^* = \beta\boldsymbol{\alpha}$ and inserted into Equation (2.21) whereby a new vector $\boldsymbol{\alpha}$ to the failure surface is achieved. Then this $\boldsymbol{\alpha}$-vector is inserted into Equation (2.22) from which a new β-value is evaluated. The iteration scheme converges normally after a view, say 6-10, iterations and provides the design point $\mathbf{u}^*$ as well as the reliability index β and the outward normal vector to the failure surface in the design point $\boldsymbol{\alpha}$. The components of the vector $\boldsymbol{\alpha}$ may be interpreted as sensitivity factors giving the relative importance of the individual random variables for the reliability index.

For the general case, i.e. where the basic random variables $\mathbf{X}$ may be not normal distributed and correlated, the above requirements in regard to non-correlation and normality can be met by proper transformations of the correlated non-normal variables into uncorrelated normal ones. It is referred to Hohenbichler and Rackwitz (1981) and Der Kiureghian and Liu (1986), or Ditlevsen and Madsen (1996) where a detailed overview upon these transformation methods is given.

2.3.2 MONTE CARLO SIMULATION METHODS

A very simple approach to estimate probability of failure e.g. according to the general expression in Equation (2.2) is the Monte Carlo Simulation Method. Assuming that the basic random variables are represented through a set of independent random variables $\mathbf{X}$, then outcomes of the limit state function $g(\mathbf{X})$ can be processed by sampling the basic random variables at random virtually according to their distribution functions. The outcomes might be in the failure domain ($g(\mathbf{x}) \leq 0$) or in the safe domain ($g(\mathbf{x}) > 0$) and after an infinite number of 'tests' the failure probability is:

$$p_f = P\left(g(\mathbf{x}) \leq 0\right) = \lim_{n \to \infty} \frac{n_f}{n} \tag{2.23}$$

where n is the total number of trials and n_f is the number of outcomes where $g(\mathbf{x}) \leq 0$. Virtual random sampling or simulation is often consuming considerable computation time; therefore the number of simulations is limited to a certain extent. With a limited number of simulations the failure probability can only be estimated and the uncertainty of these estimations is of interest. It can be shown that the uncertainty associated with the estimate is proportional to $1/\sqrt{n_f}$.

Since in structural reliability analysis the failure probability of interest is small, i.e. in the order of 10^{-6} the number of simulated failures n_f is scarce. To estimate the failure probability of 10^{-6} with proper accuracy, e.g. a coefficient of variation of the estimate of 10%, the number of simulations should be 10^8.

2.4 DESIGN FORMATS IN STRUCTURAL ENGINEERING

In probabilistic assessments any uncertainties about a variable are taken into account explicitly. This is not the case for more traditional ways of measuring safety, such as the "factor of safety" and "partial safety factor" formats, which build the framework for presently used design formats in structural engineering. Within these formats safety is expressed as a deterministic measure since load and resistance are introduced as fixed values, whereas the estimate of the load is considered as sufficiently high and the estimate of the resistance as sufficiently low to guarantee an appropriate safety level.

2.4.1 ALLOWABLE STRESS FORMAT – THE SAFETY FACTOR

A customary method to define structural safety is through the factor of safety, usually associated with elastic stress analysis and which requires that:

$$s_i\left(\psi_g\right) \le s_{pi} \tag{2.24}$$

where $s_i\left(\psi_g\right)$ is the ith applied stress component calculated at the generic point ψ_g in the structure, and s_{pi}^* is the allowable stress for the ith stress component. The allowable stresses s_{pi} are in general defined in structural design codes and they are derived from material strengths as the ultimate moment, tension or compression stress, expressed in stress terms s_{ui} but reduced by a factor ϕ_r:

$$s_{pi} = s_{ui}/\phi_r \tag{2.25}$$

where ϕ_r is referred to as the factor of safety. The factor ϕ_r may be selected on the basis of experimental observations, prior experience, economic and possibly political considerations. Usually, its selection is the responsibility of a code committee.

According to Equation (2.24) failure of a structure is assumed when the calculated i^{th} elastic stress $s_i\left(\psi_g\right)$ component reaches the local permissible stress component s_{pi}. Whether failure actually does occur depends completely on how accurate $s_i\left(\psi_g\right)$ represents the actual stress in the real structure and how well s_{pi} represents the actual material strength.

By combining Equations (2.24) and (2.25) the condition of limit state violation can be written as:

$$\frac{s_{ui}\left(\psi_g\right)}{\phi_r} \le s_i\left(\psi_g\right) \qquad \text{or} \qquad \frac{s_{ui}\left(\psi_g\right)}{\phi_r}\Bigg/ s_i\left(\psi_g\right) \le 1 \tag{2.26}$$

When the inequality sign is replaced by an equality sign, Equations (2.26) are limit state functions. By appropriate integration these Equations can also be expressed by stress resultants:

$$\frac{r_i\left(\psi_g\right)}{\phi_r} \leq s_{q,i}\left(\psi_g\right) \quad \text{or} \quad \frac{r_i\left(\psi_g\right)}{\phi_r} \bigg/ s_{q,i}\left(\psi_g\right) \leq 1 \tag{2.27}$$

where r_i is the ith resistance at location ψ_g and $s_{q,i}$ is the ith stress resultant in general made up of the effects of one or more applied loads q_i.

The design formats where Equation (2.26) is utilized as a basis are referred to as 'Allowable Stress Design' (ASD) formats.

2.4.2   LOAD AND RESISTANCE FACTOR DESIGN FORMAT – PARTIAL SAFETY FACTORS

A format which is derived from the allowable stress format but allows for a more differentiated treatment of loads and resistances is the so called load and resistance factor design (LRFD) format. The limit state can be expressed at the level of stress resultants (i.e. member design level) as:

$$\frac{z_d \, r_k}{\gamma_M} = \gamma_G \, s_{G,k} + \gamma_Q \, s_{Q,k} + \ldots \tag{2.28}$$

where r_k is a characteristic member resistance, γ_M is the partial factor on r_k and $s_{G,k}$, $s_{Q,k}$ are the characteristic dead and live load effects respectively with associated partial factors γ_G, γ_Q and z_d is the design variable. Characteristic values are generally given in the design codes and correspond to fractile values of the underlying distributions of the variables.

2.5   RELIABILITY BASED CODE CALIBRATION

In the daily practice the engineering codes and regulations form the premises for the design of safe and cost efficient structures. Code regulations in North America, Australia and Europe are based on the limit states design (LSD) approach which is implemented via load and resistance factor design (LRFD) formats, e.g. CIRIA (1977), CEB (1976), Eurocodes (2001), AHSTO (1994) and OHBDC (1983). The LRFD format is outlined in Section 2.4.2. Originally, LRFD methods where adapted as so called "soft conversions" of allowable stress design (ASD), the design method which was prevalently used in code regulations before LRFD was introduced and which is commonly based to a major part on experience, tradition and judgment. Engineering traditions might be considered as the accumulation of knowledge and experience collected over a long period of time; i.e. the in that way developed rules and regulations imply an inherent level of safety. However, for the design of new types of structures with new materials or subject to new environment and loading conditions, existing design rules have to be adapted by means of careful extrapolation. Thereby it is assumed that

the safety and cost efficiency is still satisfactory.

In the last 3 to 4 decades the development of structural reliability methods has provided a more rational basis for the design of structures. These methods provide a consistent basis for the comparison between the reliability of well tested structural design and the reliability of new types of structures. The determination of consistent design formats, i.e. the allocation of characteristic values and partial safety factors, which provide consistent safety levels for different types of structures based on structural reliability methods together with the choice of desired target reliability, is commonly understood as reliability based code calibration. Reliability based code calibration has been formulated by several researchers, see e.g. Ravindra and Galambos (1978), Ellingwood et al. (1982) and Rosenblueth and Esteva (1972) and has been already implemented in several codes, see e.g. OHBDC (1983), NBCC (1980), and more recent the Eurocodes (2001). An overview about reliability based code calibration can be found in Faber and Sørensen (2003).

2.5.1 SIMPLE CODE CALIBRATION WITH GIVEN TARGET RELIABILITY

The central task within the framework of reliability based code calibration is to evaluate partial safety factors for already existing design concepts, which are formulated e.g. by means of a Load and Resistance Factor Design format (LRFD). Within structural codes, characteristic values, partial safety factor and load combination factors are utilized to achieve target reliability for a variety of load combinations. The characteristic values are in general determined by the code; e.g. 98%- or 50%-fractile values of the underlying probability distribution function for loads and 5%-fractile values for resistance variables. The partial safety and load combination factors can be calibrated so that a uniform level of reliability is obtained for all load combinations.

As an example the calibration of partial safety factors for a set of limit states is considered. The load is assumed to be a linear combination of a permanent load with the load effect S_G and a variable load with the load effect S_Q . The material property e.g. the yield strength is given by R and the design variable e.g. the cross-sectional area is $z_{d,i}$. $\alpha_{S,i}$ is a factor taking into account the ratio of the effect due to the characteristic permanent load to the effect due to the characteristic variable and permanent loads. Therefore, all possible load situations comprising the two loads can be described by different $\alpha_{S,i}$ factors as e.g. $\alpha_{S,i}$ = 0, 0.1, 0.2, …, 1.0.

For a given set of partial safety factors the reliability index is evaluated as follows. Firstly, the design variable $z_{d,i}$ is determined in accordance with Equation (2.28) as:

$$z_{d,i} = \frac{\gamma_M}{r_k}\left(\alpha_{S,i}\ \gamma_G\ s_{G,k} + \left(1-\alpha_{S,i}\right)\gamma_Q\ s_{Q,k}\right)$$
(2.29)

Secondly, the design variable z_i is inserted into the corresponding limit state function $g(\mathbf{X})$:

$$g_i(\mathbf{X}) = z_{d,i} R - \left(\alpha_{S,i} S_G + \left(1 - \alpha_{S,i} \right) S_Q \right) \tag{2.30}$$

with $\mathbf{X} = \left(R, S_G, S_Q \right)^T$ is the vector of the basic random variables. The failure probability is calculated using Equations (2.30) and (2.2) together with e.g. FORM or SORM as a solution scheme (see Section 2.3).

The optimal set of partial safety factors is determined by the optimization formulation:

$$\min_{\gamma_M, \gamma_G, \gamma_Q} \left\{ \sum_i \left(\beta_{target} - \beta_i \left(\alpha_{S,i}, z_i, \gamma_M, \gamma_G, \gamma_Q \right) \right)^2 \right\} \quad \text{with e.g. } i = 1, 2, 3, ..., 10; \ \alpha_{S,i} = \frac{i}{10} \tag{2.31}$$

β_{target} is the target reliability.

2.5.2   TARGET RELIABILITIES

In general, the requirements to the safety of a structure are expressed in terms of the accepted minimum reliability index or the accepted maximum failure probability. In a rational analysis the target reliability is considered as a control parameter subject to optimisation, Faber and Sørensen (2003).

The objective function may include in a general form cost benefit considerations in the sense of how much has to be invested (by e.g. increasing partial safety factors) to attain the intended benefit (e.g. the reliability of a structural system). As a consequence of this cost benefit formulation the target reliability is not common for different types of structures; it depends on the relative cost of a safety measure (e.g. increasing the cross section of a component) and the expected consequences in the case of failure of the structure.

In Table 2-3 target failure probabilities and corresponding target reliability indexes are given for ultimate limit states based on the recommendations of JCSS (2001). Note that the values given correspond to a year reference period and the stochastic models recommended in JCSS (2001).

Table 2-3   *Tentative target reliability indices β (and associated target failure probabilities) related to a one-year reference period and ultimate limit states (JCSS (2001)).*

Relative cost of safety measure	Minor consequences of failure	Moderate consequences of failure	Large consequences of failure
High	$\beta=3.1$ ($p_f \approx 10^{-3}$)	$\beta=3.3$ ($p_f \approx 5 \ 10^{-4}$)	$\beta=3.7$ ($p_f \approx 10^{-4}$)
Normal	$\beta=3.7$ ($p_f \approx 10^{-4}$)	$\beta=4.2$ ($p_f \approx 10^{-5}$)	$\beta=4.4$ ($p_f \approx 5 \ 10^{-5}$)
Low	$\beta=4.2$ ($p_f \approx 10^{-5}$)	$\beta=4.4$ ($p_f \approx 10^{-5}$)	$\beta=4.7$ ($p_f \approx 10^{-6}$)

The value for the most common design situation is indicated with grey shading in Table 2-3. Guidelines for the classifications in this table can be found in the probabilistic model code, JCSS (2001).

3 TIMBER AS A STRUCTURAL MATERIAL

It is the intention of this chapter to give an overview of timber as a structural material. This includes the description of wood as a fibre composite material on a micro scale[1] and the specification of irregularities like knots and fissures on a meso scale[2]. Furthermore it is described how timber material is usually used in construction and the relevant material properties are identified and defined.

In order to gain a better understanding of the reason for the special behaviour of wood and timber material it is helpful to start thinking about where the wood and the timber are 'produced'; in the stem of a tree.
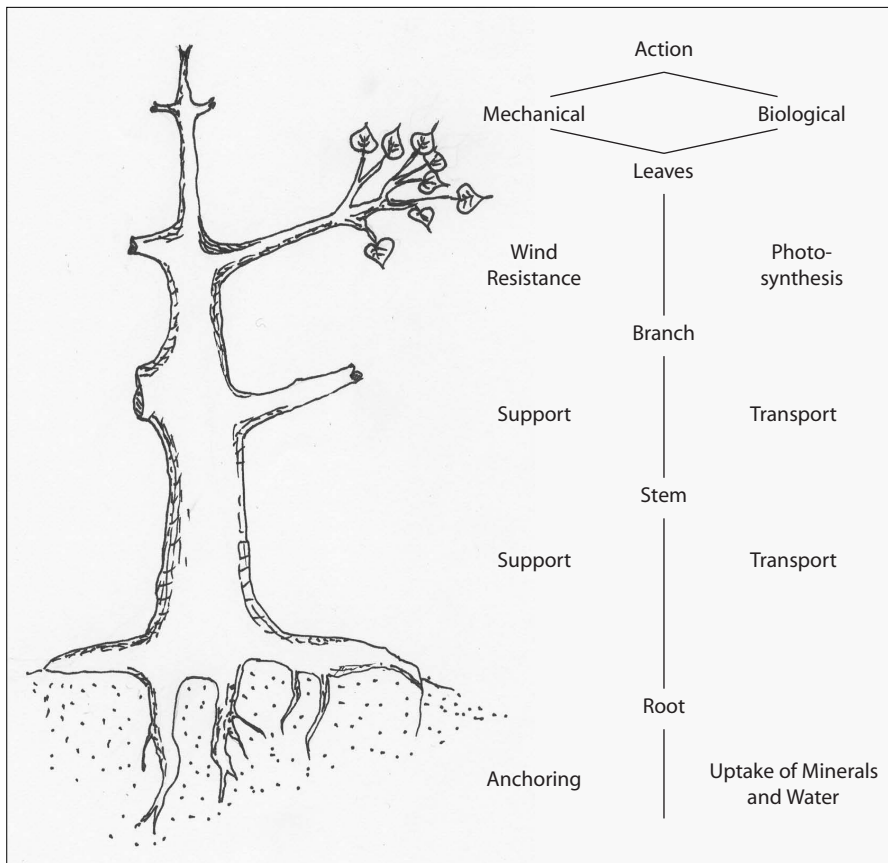
3.1 THE TREE

Figure 3-1   The tree.

A tree can be seen as a structure that faces an ongoing optimisation process over millenniums.

---

[1] In this context micro scale specifies a spatial reference most conveniently measured in μm.

[2] In this context meso scale specifies a spatial reference most conveniently measured in cm.

Its function is to expose leafs to sunlight and due to the competitive situation with other plants leafs have to be lifted up far above the ground. As illustrated in Figure 3-1 every part of the tree has different mechanical and biological functions. The uptake of water and minerals in the roots, the transport of these nutritional agents, the sap, through the stem and the branches and the photosynthesis in the leafs exposed to the sunlight describes briefly the biological function of the different parts. Mechanically the leafs have to resist the direct exposure to wind, rain and snow whereas the branches and the stem have to support the crown and transfer the corresponding load effects to the roots where the tree is anchored into the ground. As evident from Figure 3-1, the design of the tree must necessarily be a compromise. Even though it is a good photoreceptor, a large crown is heavy and more susceptible to wind loads; consequently many supporting members (stem and branches) are required and the stem must be more resistant to bending. Furthermore, the load has to be transferred through a large and efficient root system. A large crown also looses much water by transpiration. The water evaporated must be replaced by sufficient quantities of fresh supplies transported to the shoots by an equivalent root system. The available space for the root system is limited, since the ground has to be shared with other plants.

All these counteracting requirements result in an ideal compromise tree characterised by the largest possible crown but the smallest number of supporting members, all of which are of sufficient strength, but not so large as to add weight and increase energy consumption. Over millenniums this optimal design set up has been achieved, moreover trees have developed the ability to react continuously on every specific boundary condition; i.e. during growth, trees are able to optimise their shape and their mechanical properties. Regarding this aspect, the so-called secondary growth in the thickness direction of the tree components is of high importance. The thickness of branches and stems is determining the strength and the stiffness; the supporting qualities of the tree. Secondary growth takes place just below the outer surface of the stem or branch in the cambium, where phloem and finally bark are produced outwards, and wood is grown inwards, Niemz (2004). The inwardly grown wood is an annual tree ring consisting mostly of more porous early wood, and denser and stronger late wood[1]. Aiming at an even stress distribution in the supporting part of the tree the mechanical performance is continuously reassessed and more and stronger material is accumulated by secondary growth on the locations where the stresses are the highest. Simultaneously, the primary growth is aspiring to a tree design which is balanced between light exposure and affordable moment forces in the supporting parts. A more complete description of a tree as a highly optimised structure can be found e.g. in Mattheck (1998).

Coming back to the issue of interest – to describe and understand the composition of wood and structural timber, the briefly described self-optimisation property of trees should be kept in mind. On every scale it can be recognised that wood is a material with highly optimised properties as long as the original purpose is aimed at – the mechanical support and the

---

[1] The terms 'early wood' and 'late wood' are further explained in section 3.2.2.1.

transportation of sap in a tree. However, the material properties become sub-optimal when wood material is reused for human purpose, e.g. as timber for building structures.

3.2   WOOD

3.2.1   CELLS AND FIBRES – THE ULTRASTRUCTURE OF WOOD

Wood is a natural, organic cellular solid. Wood cells are also called tacheids which are long (2 – 5 *mm*) and slender (0.01 – 0.05 *mm*) and which have tapered or flattened ends. The mechanical design of wood cells is found to be common among many wood species.
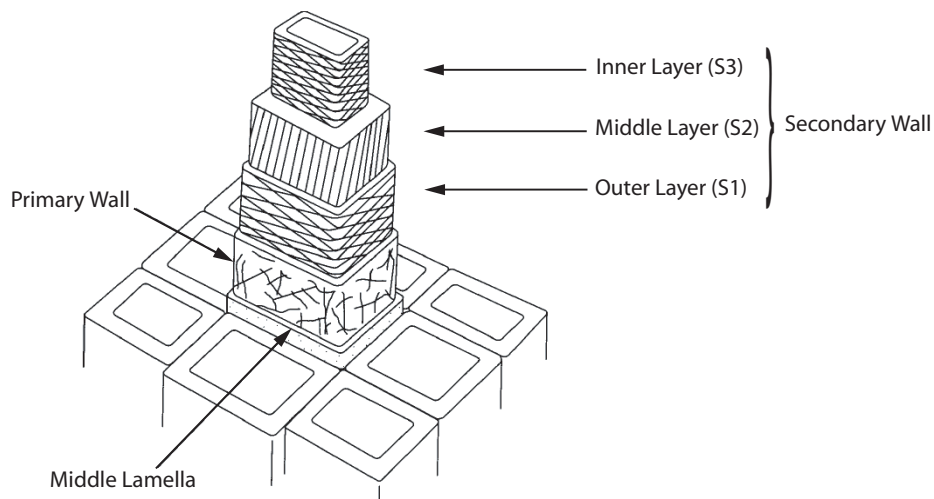
Figure 3-2   *The composition of a wood cell and its bonding in a lignin matrix (middle lamella).*

The basic skeletal substance of the wood cell wall is cellulose. Cellulose is made up of sugar molecules that fit together in a regular manner with their long-chain direction parallel to each other. The cellulose molecules form bundles called micro fibrils. As illustrated in Figure 3-2 the cell wall consists of 2 main layers; the primary wall in which the micro fibrils are arranged in a random, irregular network and a secondary wall which normally determines the static behaviour of the wood cell. The secondary wall itself consists of three fairly distinct layers. The outermost so-called *S1* layer is very thin (around 0.1 μm) and exhibits an average micro fibril angle of about 60° relative to the longitudinal axis of the cell. The main part of the secondary wall is the *S2* layer, which is typically several micro meters thick. The micro fibrils are oriented in a very small angle to the fibre axis. Within the *S3* layer the micro fibrils are arranged with a gentle slope but not in a strict order, Hoffmeyer (1995).

From an engineering point of view, the cell wall structure is a very effective construction. The predominant *S2* layer with the mainly axially oriented micro fibrils takes up tension forces. In compression the long and slender micro fibrils of the *S2* layer are prevented from buckling by

the outer and inner *S1* and *S3* layer.

The wood cells are orientated and glued together by a matrix of lignin, the middle lamella (Figure 3-2), forming the characteristic wood tissue (see also Figure 3-3) whose mechanical properties are tuned to fulfil the special supporting functions of the stem and branches. Along the fibre orientation the strength and stiffness properties for compression and tension are high compared to the strength and stiffness perpendicular to the fibre orientation.

3.2.2   GROWTH RINGS AND VESSELS – THE MICROSTRUCTURE OF WOOD

Wood is obtained from two main categories of trees known in colloquial terms as hardwoods (deciduous trees) and softwoods (coniferous trees or conifers). The observable difference between these two categories is that in general deciduous trees have leafs and covered seeds and coniferous trees evergreen needles and uncovered seeds. But there are also differences in the microstructure of the wood, namely the specific assembly, function and production strategy of wood cells.

Coniferous wood consists of 90% - 95% tracheids, which are prearranged in radial arrays, and their longitudinal direction is oriented along the axis of the stem of the tree. In evolving from early wood to latewood the cell walls become thicker, while the cell diameters become smaller. This difference in growth may result in a ratio between latewood density and early wood density as high as 3:1. The storage and transportation of sap takes place within parenchyma cells which in conifers are mostly arranged in radial rays. In Figure 3-3a and Figure 3-3b, two microscopic exposures of a southern pine specimen are shown. The different proportions of the early- and late wood tracheids can be observed. The parenchyma cells can be seen in Figure 3-3b. The interchange of sap between the cells is facilitated by small openings in the fibre wall, the so-called pits.

| a | 0.3 mm ⊢———— | b | 0.3 mm ⊢———— | c | 0.3 mm ⊢———— | d | 0.3 mm ⊢———— |
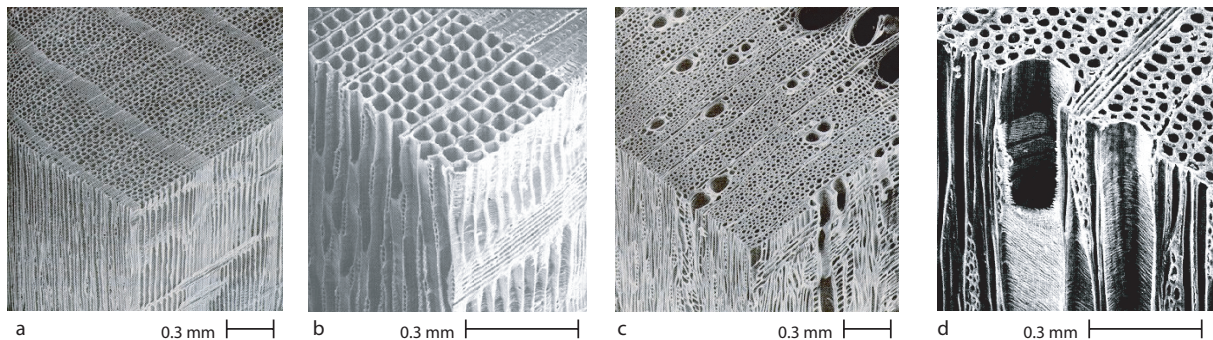
Figure 3-3   *The microstructure of coniferous wood – southern pine (a and b) and deciduous wood*
– white ash (c and d). (Pictures adapted from Niemz (2004))

The anatomy of deciduous wood is more varied and complicated than that of coniferous wood, but most of the structural characteristics are similar. The difference between early

wood and late wood is minor and the tracheids have mainly strengthening function. The transport of sap is assured through special vessels in between the tracheids; see Figure 3-3c and Figure 3-3d. Deciduous wood fibres have thicker cell walls and smaller Lumina than those of fibres from coniferous wood (compare Figure 3-3b, coniferous with Figure 3-3d, deciduous), Kollmann et al. (1968).

3.2.2.1 Variations of the Properties of Wood on a Micro Scale

Growth Rings

Within a very small volume in the stem of a tree the properties of the wood are varying systematically. The different properties of wood cells build in spring and early summer (early wood) and the cells produced from summer to fall (late wood) are well pronounced for many wood species grown in a temperate climate. Conifers tend to produce high density late wood rows of a relatively constant thickness and the variation of the thickness of the entire annual rings is governed by low density bands of early wood. In Figure 3-4 late and early wood can be distinguished as dark and bright coloured ring pattern. For some deciduous wood species, the so-called ring-porous species such as oak and ash, there is a high concentration of open vessels in the early wood which forms also the typical annual ring pattern (compare Figure 3-3). The width of these rings is relatively constant and the variation of growth ring width is mainly caused by the variation in the thickness of the high density rings of latewood tracheids. This can not be observed for so-called diffuse porous deciduous wood as poplar and beech, Hoffmeyer (1995).

Sapwood and Heartwood

The young outer part of a tree stem conducts the upward flow of sap from the root to the crown. This part of the stem is known appropriately as sapwood. As the cells grow old, they stop functioning physiologically; this inner part of the stem is known as heartwood. In most species heartwood is darker in colour due to the incrustation with organic extractives (compare with Figure 3-4). These chemicals provide heartwood with a better resistance to decay and wood boring insects. Heartwood formation normally results in a significant reduction in moisture content; in conifers the pits in the wood cell wall constrict, in deciduous wood the vessels become plugged. This results in a marked reduction of permeability, Kollmann et al. (1968).

Juvenile Wood

The wood of the first 5 to 20 growth rings (depending on species) of any stem cross section is called juvenile wood and exhibits properties different from those of the outer part of the stem (mature wood). This is particularly significant for coniferous wood. In juvenile wood, the wood cells are relatively short and thin walled with a remarkable slope of the micro fibrils or

the *S2* layer of the secondary wall. Therefore, juvenile wood typically exhibits lower strength and stiffness particularly in tension. The longitudinal shrinkage is much greater than in non-juvenile wood. Often heartwood holds all the juvenile wood, which possesses inferior quality with respect to the mechanical properties. The boundary between juvenile and mature wood is gradual and not visible, Thörnquist (1990).

anual growth ring pattern

sap wood

pith

juvenile wood

heart wood
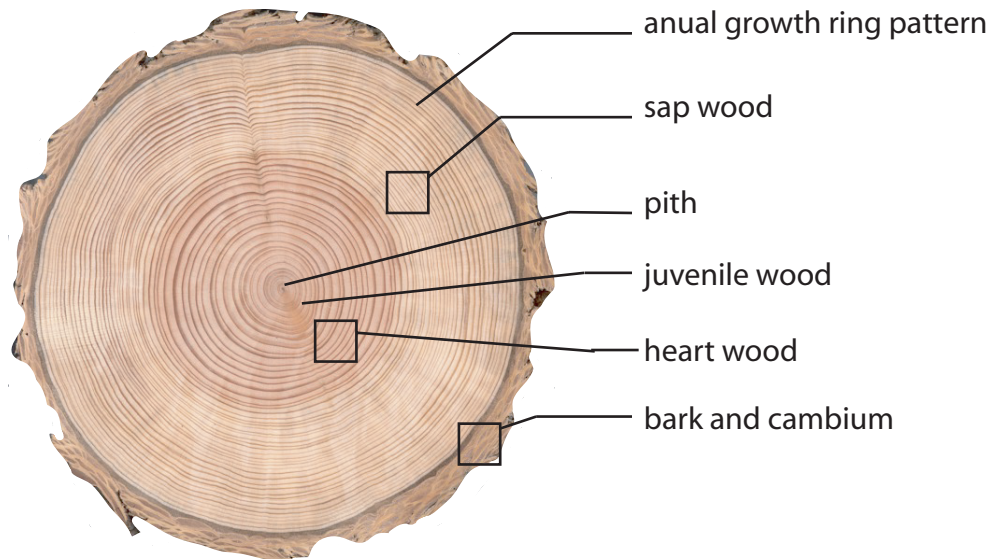
bark and cambium

Figure 3-4   *Cross section of a stem of a tree, Douglas-fir, annual growth ring pattern, juvenile wood, heart wood, bark and cambium.*

3.2.3   KNOTS AND GRAIN DEVIATIONS – THE MESO STRUCTURE OF WOOD

As seen in the preceding section wood is a material optimised to fulfil its biological and mechanical function in the supporting parts of a tree. Wood as a mechanical body is highly anisotropic mainly due to the elongated shapes of the wood cells and the oriented structure of the cell walls; i.e. the strength and stiffness along the grain direction is much larger than perpendicular to the grain direction. In a living tree this property is used in such a way that the fibre direction is following the direction of the main stresses in the supporting components; mainly along the axis of the stem and the branches. However, where branches are connected to the stem or where specific load circumstances cause torsion forces in the supporting components the fibre direction deviates from the direction of the axis of the components.

Knots

Knots are parts of branches that are embedded and anchored in the main stem of a tree. The lateral branch is connected to the pith of the main stem. As the perimeter of the stem increases, successive growth rings form continuously over the stem and branches and a cone

of branch wood (the inter-grown knots) develops within the stem. The result is a notch-free transition from stem to branch with minor stress concentrations where the fibre direction is following the predominant main stress direction in the 'joint'. Sometimes the branch may die or brake off. The succeeding growth rings added to the main stem simply encircle the dead limb stub and the dead part of the stub becomes a so-called encased or entrapped knot. Softwoods are characterised by having a dominant stem from which clusters of lateral branches occur at regular intervals, Isaksson (1999).

Grain Deviations

Some specific but permanent loading conditions on a tree are inducing cell orientation forming a helix around the stem axis (spiral grain). This is the case when torsion forces mainly in one direction due to e.g. asymmetric wind loading, are present in the stem.

Reaction Wood

A tree reacts on systematic external forces on the supporting components by forming so-called reaction wood. Conifers develop compression wood in areas with subdominant high compression, whereas deciduous species develop tension wood in regions where tension forces are prevailing. Compression wood has the appearance of wider growth rings and a higher late wood proportion than normal coniferous wood. Furthermore, the structural arrangement of the wood cell walls is different for compression wood, i.e. the micro fibrils of the S2 layer are arranged with a 45° slope which results in excessive longitudinal shrinkage property, similar to juvenile wood. The compression strength and stiffness of compression wood is higher than of normal wood whereas the tension strength and stiffness is approximately the same, i.e. the 45° angle of the S2 layer and their increased thickness are effects compensating each other. For deciduous species tension wood differ from normal wood for a number of biochemical, anatomical and mechanical characteristics. Mechanically, the frequency of vessels and their porosity is significantly lower in tension wood, whereas fibre and vessel lengths are significantly longer, Jourez et al (2001). However, in a number of tree species such as poplar the most striking differences are found in the fibres of tension wood. In these fibres, named G-fibres, one layer of the secondary wall (generally the S3 layer) is replaced by a very thick layer in which the micro fibrils are almost parallel to the axis of the cell which contributes, to the specific mechanical properties of tension wood, Timell (1969).

3.2.4   CLEAR WOOD SPECIMENS AND THEIR PROPERTIES

The characteristics of wood are usually obtained from tests of small pieces of wood termed "clear" or "straight grained" because they do not contain characteristics such as knots, cross

grain and splits[1]. These test pieces have anatomical characteristics such as growth rings that occur in consistent patterns within each piece. Clear wood specimens are usually considered "homogeneous" in wood mechanics, Niemz (2004).

Moisture Content

The moisture content is defined as the ratio of the mass of removable water to the dry mass of the wood. The dry mass is obtained by oven drying. The moisture content may be expressed as a fraction or in percentage terms. In so-called green wood, i.e. wood of a freshly cut tree, the moisture content could be higher than 100%; the so-called free water in the cell lumen together with the water in the saturated wood cell walls have a larger mass fraction than the oven dry wood. At a moisture content of around 28%, the so-called fibre saturation point, the wood cell walls are still saturated, whereas there is no free water in the cell lumen. Below the fibre saturation point the cell wall is loosing water which has a mayor influence on the mechanical properties of the wood. Above the fibre saturation point the mechanical properties are nearly independent of moisture content, Hoffmeyer (1995).

Shrinkage and Swelling
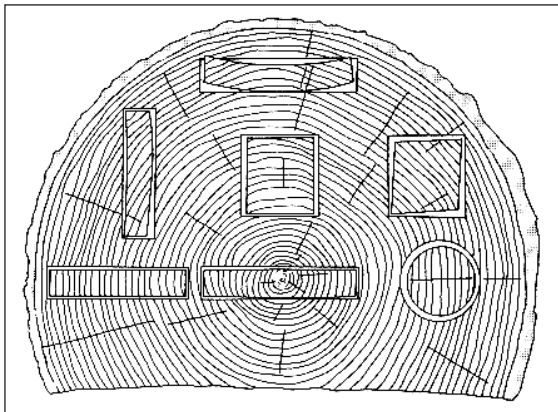
Figure 3-5   Distortions of wood prisms cut out at different spots in the stem due to shrinkage. (Niemz (2004))

Wood is dimensionally stable when the moisture content is greater than the fibre saturation point. Wood changes dimension as it gains or looses moisture below that point. It shrinks when loosing moisture from the cell walls and swells when gaining moisture in the cell walls. Shrinkage and swelling are also termed movements. The magnitude of these movements is depending on the direction to the wood cells and is mainly governed by the substantial S2 layer of the wood cell wall, compare Figure 3-2. The micro fibrils in the S2 layer are nearly parallel oriented to the longitudinal axis of the cell and the water is absorbed between the

---

[1] Splits are cracks along the fibre direction due to shrinkage of the wood

micro fibrils. This means that movements in the transverse direction are much more pronounced than in the longitudinal direction; the ratio is in the order of 20:1. Juvenile wood and compression wood exhibit micro fibril angles much larger than non juvenile wood, which result in much larger longitudinal movements.

In the transverse direction a differentiation between the radial and the tangential direction to the growth rings can be made. The movements in the tangential direction may, for practical purposes, be taken as twice as radial movements. The consequence of this property can be observed in Figure 3-5. Wood prisms are deformed due to shrinkage in different manner, depending on the orientation of the annual rings in the prism; these deformations are in general referred to as distortions, Hoffmeyer (1995).

Density

The wood density is the most important physical characteristic of wood. The density ρ_{den} is defined as:

$$\rho_{den} = \frac{m_g}{v_{Vol}} \tag{3.1}$$

where m_g is the mass in kg and v_{Vol} is the volume in m^3. In wood science and engineering the dry density $\rho_{den,0}$ and the density $\rho_{den,12}$ at 12% moisture content are most frequently used. While the density of the cell wall material is relatively constant among wood species, which is about $1500\ kg/m^3$ (Kollmann et al., 1968), the density of wood depends mainly on the ratio between cell lumen and cell wall. The density ranges from $200\ kg/m^3$ to $650\ kg/m^3$ for coniferous wood and from $300\ kg/m^3$ to $1100\ kg/m^3$ for deciduous wood.

Strength and Stiffness Properties

The strength and stiffness properties of wood depend on which direction the fibres are stressed. For small clear wood specimens it is in general distinguished between properties parallel and perpendicular to the grain.

Table 3-1   Strength properties and density of some structural materials (Thelandersson and Larsen (2004)).

Material	Density kg/m^3	Strength MPa	Strength / Density $10^{-3}\,MPa \cdot m^3/kg$
Structural Steel	7800	400-1000	50-30
Aluminium	2700	100-300	40-110
Concrete, compression	2300	30-120	13-50
Clear coniferous wood, tension parallel to the grain	400-600	40-200	100-300
Clear coniferous wood, compression parallel to the grain	400-600	30-90	70-150
Clear coniferous wood, tension perpendicular to the grain	400-600	2-8	5-10

Due to the fact that wood in a tree is a highly optimised structural material it is no surprise that its performance is impressive if it is stressed as in nature. E.g. clear wood exhibits high strength and stiffness in tension parallel to the grain; the ratio between strength and density is even higher than for steel (compare Table 3-1). On the other hand, if clear wood is loaded perpendicular to the grain the load carrying capacity is very low, Thelandersson and Larsen (2004).

Moisture Content and Mechanical Properties

The mechanical properties of wood depend on the moisture content. An increase in moisture leads to lower values for strength and stiffness properties. Water, when penetrating the cell wall, weakens the coherence of the cell wall. Moisture variations above the fibre saturation point of around 28% have no effect on the mechanical properties, since such variations are related to free water in the cell lumen. Not only the moisture content is important for the strength properties of wood specimen; fast changes cause moisture gradients in wood which induce stresses perpendicular to the grain direction. Wood is a hygroscopic material that takes water from the surrounding air, and the moisture content of wood tends to attain equilibrium with the air humidity.

The effect of moisture on the mechanical properties of wood is given in Table 3-2. For moisture contents between 8% and 20% a linear relationship between moisture content and strength can be assumed, Hoffmeyer (1995).

Table 3-2   Approximate change (%) of clear wood properties for a one percentage change of moisture content. (Hoffmeyer(1995)).

Material Property	Change [%]
Compression strength parallel to the grain	5
Compression strength perpendicular to the grain	5
Bending strength parallel to the grain	4
Tension strength perpendicular to the grain	2.5
Tension strength parallel to the grain	2
Modulus of elasticity parallel to the grain	1.5

Duration of Load

Wood experiences a significant loss of strength over a period of time. The failure mechanism of wood under long term load is referred to as creep rupture. The first major investigation on the duration of load effect on small clear wood specimen is published in Wood (1947). On the basis of bending tests of duration of up to 7 years, a stress – lifetime relationship is established, which predicts the 10-years strength to be slightly less than 60% of the approximated short term strength. Similar effects are observed in the literature for loading modes different from bending.

3.3   STRUCTURAL TIMBER

"Timber is as different from wood as concrete is different from cement." - Borg Madsen

Structural timber components are sawn from logs[1]. Apart from some exceptions they have a prismatic shape with a rectangular cross section. In contrast to small clear wood specimens timber components have structural dimensions. The maximum possible dimension of the timber components is determined by the size of the trees in the forest. E.g. one hundred years ago timber components with a length of 20 m and a rectangular cross section of about 150 x 450 mm were commonly available. Nowadays, the forestry strategy has changed and in most countries timber with a cross section over 75 x 225 mm and a length more than 5 m attracts a cost premium due to scarcity, Steer (1995). Timber components are applied for load carrying functions in structures; therefore there are several provisions in the production line to obtain appropriate structural elements. For example it is aimed for that the longitudinal axis of the timber structural component coincides with the grain direction of the wood cells. Due to the dimension of the timber components this is mostly not strictly possible. So called growth irregularities as knots and grain deviations are affecting the uniform and parallel grain direction. It should be remembered that these 'growth irregularities' are just part of the excellent property of a tree to react on stress peaks and special load conditions constantly during its growth. However, for a sawn piece of timber these growth irregularities are sub-optimal.

3.3.1   GROWTH IRREGULARITIES IN TIMBER STRUCTURAL COMPONENTS

3.3.1.1 Knots
Being an optimal stress reducing connection of the stem with the branches in a tree, knots in sawn structural timber are by far the most important defects affecting the mechanical properties. It can be differentiated between inter grown knots and loose knots (see Section 3.2.3).

3.3.1.2 Cross Grain
The phenomenon, when the mean grain direction within a large section is not coinciding with the longitudinal axis of the timber component is referred to as cross grain. This is quite common, but only recognised at a certain magnitude. The reason for cross grain might be technical, i.e. due to sawing configurations, or due to growth particularities, e.g. helix-growth, or a cone shaped stem of the tree.

---

[1] A log is a cut proportion of the stem of a tree, in general already prepared for transportation and further processing; i.e. the log is cylindrical shaped and free of branches.

3.3.1.3 Distortion

As for clear wood prisms, distortion due to inhomogeneous shrinkage and swelling properties is also present for timber structural elements. (compare shrinkage and swelling in section 3.2.4)

3.3.1.4 Wane

Timber structural elements, in general, have a rectangular shaped cross section. Due to sawing practice it is possible that the edge of the timber log becomes visible after cutting the rectangular shaped elements from the conical shaped log. This is in general referred to as wane.

3.3.1.5 Permanent Compressive Yield

Permanent compressive yield is a local phenomenon due to an instant compression in the stem of the living tree. E.g. during a storm the compression strength can be reached on a spot where local buckling of the fibres occurs. This happens without further consequences for the tree. In a sawn timber component these spots can be very disadvantageous due to very low strength characteristics. Permanent compressive yield is very hard to detect by visual quality control, Arnold and Steiger (2005).

3.3.2 MATERIAL PROPERTIES OF INTEREST OF TIMBER STRUCTURAL COMPONENTS

Structural timber is a non-homogeneous material. It's also known as orthotropic, whereas in structural timber the major irregularities in a component (knots or cross grain) weaken this statement. However, material properties of timber components are considered as the property of an entire structural component, i.e. tension parallel to the grain means tension parallel to the axis where a coincidence with the main fibre direction is assumed. Consequently, both, stresses perpendicular to the grain and parallel to the grain exist in such a component, whereas the latter case is the dominant.

Timber components are mainly used in structures in form of beams, columns and bars which are loaded in transversal bending and parallel compression and tension correspondingly. In these elements the stress bearing capacity of the wood material is used to its full potential. The wood fibres and the stress directions are mainly orientated along the longitudinal axis of these elements. In structural design, timber components are also subjected to other loading modes, namely tension and compression perpendicular to the component axis or shear. These properties are comparatively weak and should be treated with care during design.

In timber engineering, material properties are defined on an element level, i.e. material properties are defined as the load bearing capacity of timber material specimens of defined

size and conditioning[1] and assessed in accordance with an agreed testing procedure. E.g. the bending strength of timber is not an ultimate stress property of the timber material; it is rather the moment capacity of the test specimen, divided by the elastic section modulus. In this section timber material properties according to test standards are introduced. The principle test configurations are illustrated to show how material properties are defined at an element level (based on ISO 8375). Regional specifications for the test configuration of bending tests are given in section 7.3 according to the Australian/New Zealand Code, the US-American Code, the Canadian Code and the European Code.

3.3.2.1 Bending Strength, Bending Modulus of Elasticity

The bending strength according to test standards is determined with a test configuration illustrated in Figure 3-6. The load q is applied with constant rate until the collapse of the beam. The maximum load q_{max} is observed. The projected test time to failure t_f is also specified in the standards. The bending strength r_m is expressed in stress, assuming homogeneous ideal elastic material and pure bending as:

$$r_m = \frac{3qa}{h^2 b} \tag{3.2}$$
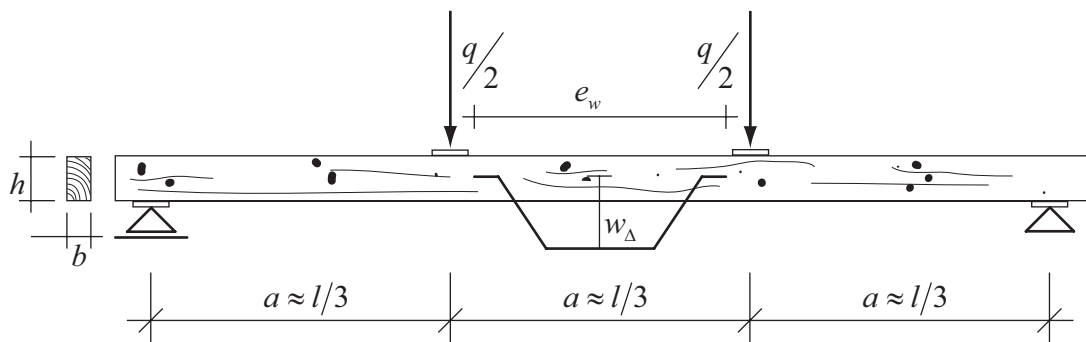
Figure 3-6   Typical bending test configuration; a, b, e_w, h are the specified dimensions, q and w_Δ are the measurements.

The bending stiffness is assessed with the same test configuration by observing the deflection w_Δ and the load at two different times during the test, i.e. $\left(w_{\Delta,1}, q_1\right)$ and $\left(w_{\Delta,2}, q_2\right)$. It has to be assured that the two measurements are made within the proportionality limit[2] of the beam. The bending stiffness, i.e. the bending modulus of elasticity moe_m is calculated as:

---

[1] Conditioning in terms of a predefined constant temperature and relative humidity surrounding.

[2] The proportionality limit confines the elastic domain of the stress strain relation ship of a material. In the elastic domain stress is proportional to strain.

$$moe_m = \frac{3}{4} \frac{a(q_2 - q_1)e_w^2}{h^3 b(w_{\Delta,2} - w_{\Delta,1})}$$ (3.3)

3.3.2.2 Tension Strength Parallel to the Grain, Tension Modulus of Elasticity

The tension strength according to test standards is determined with a test configuration as illustrated in Figure 3-7. The load q is applied with constant rate until failure of the specimen and the maximum load q_{max} is recorded. The projected test time to failure t_f is also specified in the test standards. Assuming ideal elastic and homogenous material behaviour the tension strength parallel to the grain $r_{t,0}$ is calculated as:

$$r_{t,0} = \frac{q_{max}}{bd}$$ (3.4)

where the index 0 specifies the angle to the grain.
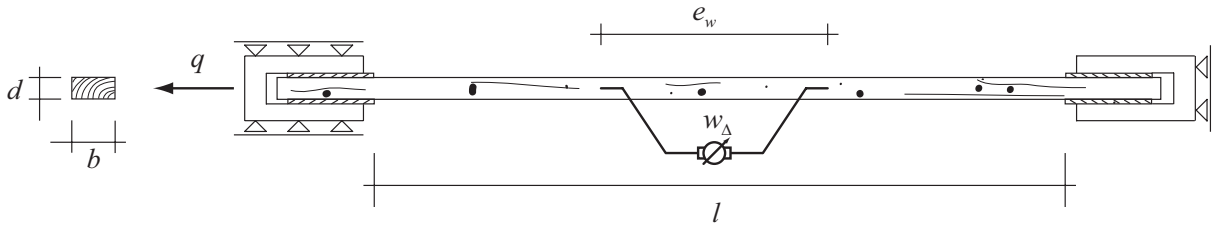
Figure 3-7   *Typical tension test configuration; l, b, d, e_w are the specified dimensions, q and w_Δ are the measurements.*

The tension stiffness is measured with the same test configuration by recording two simultaneous observations of the deflection w_Δ and the load at different times during the test. It has to be assured that the two measurements are made within the proportional limit of the specimen. The tension stiffness, i.e. the tension modulus of elasticity $moe_{t,0}$ is calculated with:

$$moe_{t,0} = \frac{e_w(q_2 - q_1)}{bd(w_{\Delta,2} - w_{\Delta,1})}$$ (3.5)

3.3.2.3 Compression Strength Parallel to the Grain, Compression Modulus of Elasticity

The compression strength according to test standards is determined with a test configuration as illustrated in Figure 3-8. The load q is applied with constant rate until the collapse of the specimen and the maximum load q_{max} is recorded. The projected time to failure t_f in the test is also specified in the standards. Assuming ideal elastic and homogenous material behaviour

38

the compression strength $r_{c,0}$ is calculated according to:

$$r_{c,0} = \frac{q_{max}}{bd}$$

(3.6)

The compression stiffness is measured with the same test setup by recording two simultaneous observations of the deflection w_Δ and the load at different times during the test. It has to be assured that the two measurements are made within the proportional limit of the specimen. The compression stiffness, i.e. the compression modulus of elasticity $moe_{c,0}$ is calculated with:

$$moe_{c,0} = \frac{e_w (q_2 - q_1)}{bd (w_{\Delta,2} - w_{\Delta,1})}$$

(3.7)
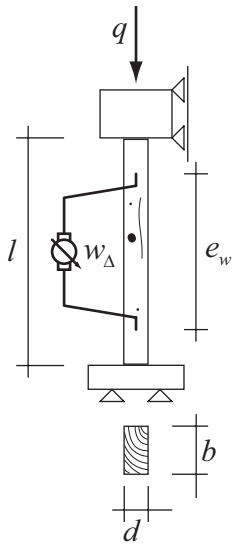
Figure 3-8   Typical compression test configuration; l, b, d, e_w are the specified dimensions, q and w_Δ are the measurements.

3.3.2.4 Tension and Compression Strength and Stiffness Perpendicular to the Grain

The compression and tension strength perpendicular to the grain according to test standards is determined with a test configuration as illustrated in Figure 3-9. The load q is applied with constant rate until the collapse of the specimen and the maximum load q_{max} is recorded. (For compression perpendicular to the grain q_{max} has to be estimated with proper iteration techniques). The projected time to failure t_f is also specified in the standards. Assuming ideal elastic and homogenous material behaviour the compression or tension strength perpendicular to the grain $r_{t,90}$, $r_{c,90}$ is calculated according to:

$$r_{t,90} = r_{c,90} = \frac{q_{max}}{bl} \tag{3.8}$$
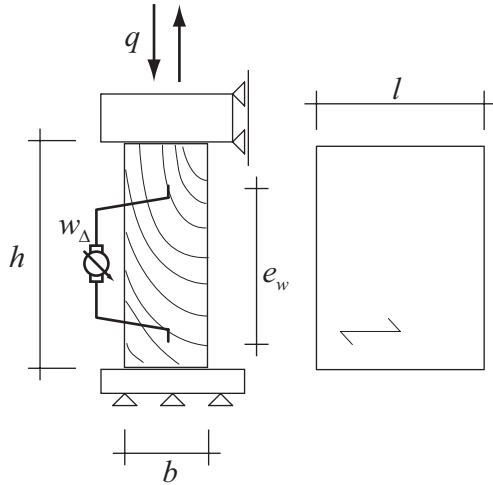
Figure 3-9   Typical compression and tension test configuration for perpendicular to the grain; l, b, h, e_w are the specified dimensions, q and w_Δ are the measurements.

The tension or compression stiffness perpendicular to the grain is measured with the same test configuration by recording two simultaneous observations of the deflection w_Δ and the load at different times during the test. It has to be assured that the two measurements are made within the proportional limit of the specimen. The tension or compression stiffness perpendicular to the grain, i.e. the tension or compression modulus of elasticity perpendicular to the grain $moe_{t,90}$, $moe_{c,90}$ is calculated with:

$$moe_{t,90} = moe_{c,90} = \frac{e_w (q_2 - q_1)}{bl (w_{\Delta,2} - w_{\Delta,1})} \tag{3.9}$$

3.3.2.5   Shear Strength, Shear Modulus

For evaluating the shear strength and stiffness different test configurations exist between different test standards, i.e. in contrast to the other material properties the differences are not only in dimension. For further particularities it is referred to the standards. Shear strength is in general understood as the resistance of a timber specimen against a shear load on the surface of the specimen in direction parallel to the grain combined with a compression load perpendicular to the shear load. The shear modulus is in general evaluated with a 3-point bending arrangement.

3.3.2.6 Density

A small volume is cut from the test specimen, whereas the removal shall be made over the entire cross section of the specimen. The volume has to be free of defects. After destructive tests the volume should be removed near the spot of the failure. The density is defined as the ratio between the mass and the volume (see also section 3.2.4). The density is highly dependent on the moisture content of the timber. Specifications are given in the test standards.

3.3.2.7 Test Standards

The test standards referred to are:

European Standards: EN 408 and EN 384

American Society for Testing and Materials: D 4761-88 and D 1990-91

Australian/New Zealand Standard: AS/NZ 4063:1992

3.4 TIMBER DESIGN

3.4.1 DESIGN FORMAT

The general layout of the most recent timber design codes is based on the load and resistance factor design (LRFD) format (see section 2.4.2), which can be written as in Equation (2.28). Several limit state equations are given in the codes, ultimate and serviceability, to cover the most typical situations in practical design. Characteristic values for the material properties are also given in these design codes which correspond to fractile values of the underlying distribution functions. As described above the material properties are defined as the properties of test specimen tested under specified conditions. In real structures these conditions may deviate in terms of the size of the elements, loading modes and duration, climate variations, etc. As seen before, timber material properties are rather sensitive to these deviations. In modern timber design codes modification factors on the strength and stiffness related material parameters are introduced to satisfy this circumstance. The calibration of these modification factors is the matter of ongoing discussions in the timber research community; some phenomena seem to be too complex to cope just with a multiplication of a factor, for other problems the experimental evidence is rather poor. These issues will be discussed in more detail in chapter 4.

Another particularity of timber is how its material properties are ensured to stay within some predictable limits.

3.4.2 TIMBER GRADING

In comparison to building materials such as steel and concrete, the properties of structural timber are not designed or produced by means of some recipe but may be ensured to fulfil given requirements only by quality control procedures – also referred to as grading. For this reason quality control and selection schemes are implemented in the production line, typically already at the sawmill where the construction timber is produced from the timber logs.

Various schemes for grading have been developed using different principles, however, the basic idea behind them all is that the material properties of interest are assessed indirectly by means of other properties, measured non-destructively such as e.g. the density, the modulus of elasticity or the visual appearance of the timber see Madsen (1992), Walker et al. (1993) or Green and Kretschmann (1997).

As a result of timber grading, timber is represented at the market as a graded material. The grades imply that the material properties lie within desirable and predictable limits. However, the material properties of timber grades have to be considered as random variables and the properties of timber grades are characterised (and communicated) through specific fractile values of the assumed probability distribution functions of the material properties of interest.

3.4.3 STRENGTH CLASS SYSTEMS

In general, structural timber is assigned to a specific strength class. Several strength class systems exist on an international scale, e.g. in Europe it is the EN 338 which constitutes the classification of timber based on the prescription of characteristic values or the mean values for the material properties; i.e. for every timber strength class a characteristic value or a mean value for every relevant material property is given. Timber that is assigned to a certain strength class is also referred to as a timber grade. In Table 3-3 an example for some strength classes according to EN 338 is given. The characteristic values for the strength properties and the density are defined as the 5% fractile values of the underlying distribution functions. The modulus of elasticity (MOE) and shear modulus are specified by mean values. For the qualification of a timber population to a certain grade, values for three material properties are mandatory; the 5% fractile value of the bending moment capacity, the 5% fractile value of the density and the mean value of the bending MOE. These material properties are subsequently also referred to as the reference material properties. It is in general assumed that the indicated values for other properties are representative for the specified grades. These values are based on empirical relationships with the reference material properties evaluated based on several tests on European softwoods and given in Glos (1995) as:

$$r_{t,0,k} = 0.6 r_{m,k} \tag{3.10}$$

$$r_{c,0,k} = 5r_{m,k}^{0.45} \tag{3.11}$$

$$r_{v,k} = 0.2r_{m,k}^{0.8} \tag{3.12}$$

$$r_{c,90,k} = 0.015\rho_{den,k} \tag{3.13}$$

$$r_{t,90,k} = 0.001\rho_{den,k} \tag{3.14}$$

$$moe_{0,mean} = moe_{m,mean} \tag{3.15}$$

$$moe_{90,mean} = moe_{90,mean} = moe_{m,mean}/30 \tag{3.16}$$

$$mog_{v,mean} = moe_{m,mean}/16 \tag{3.17}$$

For the nomenclature compare Table 3-3, the subscript k indicates the characteristic value of the material property; the subscript *mean* indicates the mean value of the material property. 0 and 90 indicate the angle of the main stress direction to the fibre direction.

Table 3-3   *The EN 338 strength classes C24, C30, C35 and C40; characteristic values for strength and stiffness properties and density. Mandatory properties are indicated with grey shading.*

		C24	C30	C35	C40
		$[MPa]$			
Bending moment capacity	$r_{m,k}$	24	30	35	40
Tension strength parallel to the grain	$r_{t,0,k}$	14	18	21	24
Tension strength perp. to the grain	$r_{t,90,k}$	0.4	0.4	0.4	0.4
Compression strength parallel to the grain	$r_{c,0,k}$	21	23	25	26
Compression strength per. to the grain	$r_{c,90,k}$	5.3	5.7	6	6.3
Shear strength	$r_{v,k}$	2.5	3.0	3.4	3.8
		$[GPa]$			
Bending MOE in bending	$moe_{m,mean}$	11	12	13	14
MOE - tension parallel to the grain	$moe_{0,mean}$	11	12	13	14
MOE - tension perp. to the grain	$moe_{90,mean}$	0.37	0.4	0.43	0.47
Shear modulus	$mog_{v,mean}$	0.69	0.75	0.81	0.88
		$\left[kg/m^3\right]$			
Density	$\rho_{den,k}$	350	380	400	420

4 PROBABILISTIC MODELLING OF TIMBER MATERIAL PROPERTIES

4.1 INTRODUCTION

Timber is a rather complex building material. Its properties are highly variable, spatially and in time. In structural engineering, material properties of timber are in general understood as the stress and stiffness related properties of standard test specimen under given (standard) loading and climate conditions and the timber density. Test configurations according to ISO 8375 are defined in section 3.3.2.

As introduced in section 3.4.2 timber is a graded material. Due to the grading process, the material properties are associated with some control scheme, whereas only the so-called reference material properties are considered explicitly. The so-called other material properties are only assessed implicitly. Following the European standard EN 338 the distinction between reference properties and other properties is made as illustrated in Figure 4-1. The bending moment capacity, the bending modulus of elasticity and the timber density are referred to as the reference material properties.

When modelling timber material properties in a structure, i.e. at any generic point, in time and in space, several issues have to be taken into account, see also chapter 3. As illustrated in Figure 4-2 the cornerstone of the modelling of timber material properties are the reference material properties under reference conditions. The material property of interest at any generic point may deviate in terms of type ('other material properties'), of dimensions ('scale') and of specific loading and climate conditions ('time (load/moisture)'). In general, these aspects are treated separately, i.e. research and modelling scheme proposals are focused on one dimension in Figure 4-2. This scheme is also followed in this chapter. In Section 4.2 focus is directed to the spatial variability of timber material properties, i.e. material properties are considered at different scales. The time dependency of timber material properties is discussed in section 4.3 (load dependency) and section 4.4 (moisture dependency). A framework for the interrelation of reference material properties and other material properties is given in section 4.5.

Reference Material Properties	Other Material Properties
r_m = bending moment capacity	$r_{t,0/90}$ = tension strength
moe_m = bending MOE	$moe_{t,0/90}$ = tension MOE
ρ_{den} = density	$r_{c,0/90}$ = compression strength
	$moe_{c,0/90}$ = compression MOE
	r_v = shear strength
	mog_v = shear modulus
	$r_{h,0/90}$ = embedding strength

Figure 4-1   Reference material properties and other material properties.
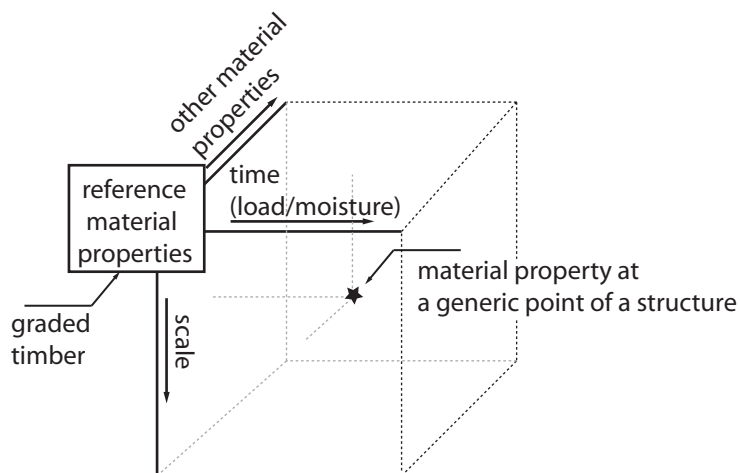
Figure 4-2   Outline of the modeling of timber material properties.

4.2   SPATIAL VARIATIONS OF TIMBER MATERIAL PROPERTIES

4.2.1   SCALES OF MODELLING

Timber material properties vary locally in space. A material property in one point of a structure might not be the same as in another point in the structure or in a point in a different structure. In general, three hierarchical levels of variation may be considered: micro, local (meso) and global (macro).

Timber from different origins is graded by applying different grading schemes by different

producers to one common grade. Every single sub-population of the timber grade might have differently distributed material properties. The variability of the distribution parameters represents a typical global parameter variation. Parameter variations may also be due to statistical uncertainties.

The variations between timber test specimens or components of one specific sub-population are modelled at the meso level. Information about the specific sub-population may be obtainable from tests with the purpose of reducing the parameter variation. The geometrical scale of the test specimens is in the same order as the size of a structural element and probably most conveniently measured in meters.

At the micro-level the irregularities in the timber material itself are represented. These are basically uncontrollable as they originate from natural variability such as the random distribution of knots fissures and grain deviations. The geometrical scale of these irregularities could be measured in *μm* at wood cell level or in *cm* if knots and weak sections are considered.
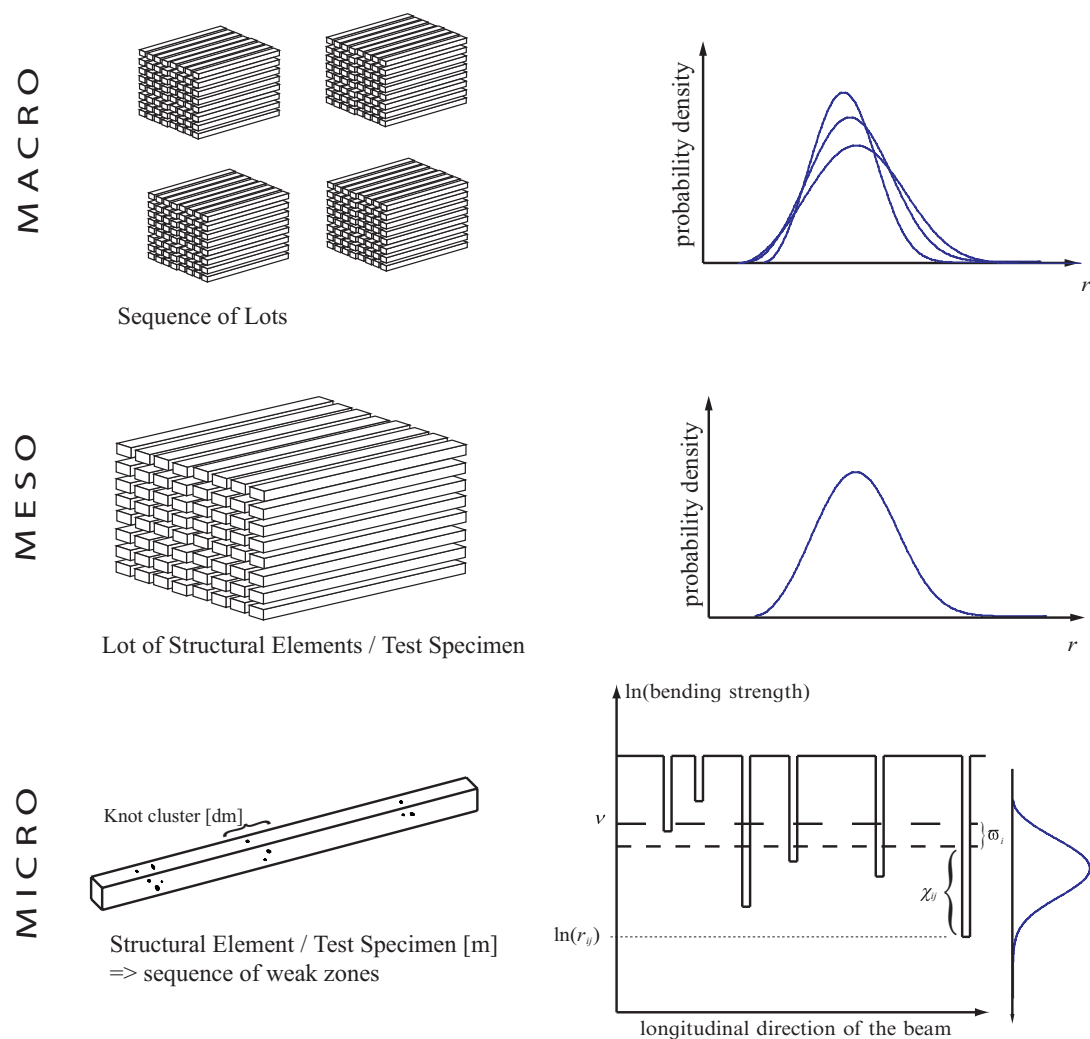
Figure 4-3   Different scales of modelling of timber material properties.

4.2.2 MODELLING REFERENCE MATERIAL PROPERTIES UNDER REFERENCE CONDITIONS – MESO LEVEL VARIATIONS

Material properties are in general defined on the scale of test specimen capacity and the loading history and climate conditions until failure are also specified in test standards, see section 3.3.2. Deriving a probabilistic model for the material properties on this level, in general, is a straightforward task. Material properties can be represented by random variables $X_i,\ldots$, the statistical characteristics of these variables can be described by distribution models which parameters are calibrated according to data taken from standard tests. In section 2.2.2 a general outline is given, some basic approaches and an example how this should be performed is given in Annex A and in Chapter 7.

4.2.3 MACRO LEVEL VARIATIONS – TIMBER GRADING

In practical design the situation is different in regard to the amount and quality of available information. Typically it is known what timber grade will be utilized in the structure. Various grading schemes are calibrated to identify timber grades, i.e. sub-populations of timber elements for which the strength class requirements (see section 3.4.3) are fulfilled. The statistical characteristics of the material properties of these sub-populations are strongly dependent on the properties of the timber supply which is used for grading and the particular grading procedure which is applied (Faber et al. (2004) and section 4.2.3.2). This means that for different sub-populations all assigned to the same timber grade, but by applying different grading schemes and/or using different ungraded material, the statistical properties of the material properties might be different, although the target fractile values are similar. These macro variations have to be taken into account.

A possible method to quantify macro material variations is demonstrated in Rackwitz and Müller (1977), where the macro variability of concrete is analysed. Concrete from a particular grade but from several different producers is analysed. The sample moments of each sub-population are quantified and functional relationships between the sample moments are derived. A similar scheme can be realized for graded timber by taking timber from different regions and graded to the same grade but identified by different grading schemes. Alternatively the macro variability can be explicitly assessed if the applied grading scheme can be formalized to a probabilistic framework which takes into account all uncertainties involved into the grading procedure.

Coming back to this issue with a proposal in this direction in the second half of this sub-section, first existing grading practice is introduced and discussed.

4.2.3.1 Existing Grading Practice

It is in general differentiated between two different strategies of timber grading: visual

grading and machine grading.

Visual Grading

Visual grading is based on visual inspection of timber structural elements. Visible defects as knots, fissures and cross grain[1] are assessed and according to the appearance of timber structural elements in regard to these defects they are sorted to a certain grade. Some more or less rudimentary forms of visual strength grading have been used since timber was utilised as a construction material. The first formal visual grading rules, the USA ASTM Standard D245 were published in 1927 (Madsen (1992)). Since the 1930s formalized rules for visual grading were introduced in the European countries (Glos (1995)). These rules are further developed until today, however they differ widely with respect to grading criteria, number of grades and grade limits. Recent efforts to harmonize these visual grading rules at least throughout Europe have not been successful because no single set of grading rules would cover the different species, timber dimensions and uses in a satisfactory manner (Glos (1995)). However, for Europe some general requirements for regional visual grading codes are prescribed (prEN 14081-1); the following has to be taken into account:

- limitations for visible strength and stiffness reducing characteristics: knots, slope to the grain, rate of growth (annual ring width), fissures,

- limitations for geometrical characteristics: wane, distortion,

- limitations for biological characteristics: insect and fungal damage.

It has to be considered that the visual grading of a timber structural element in the usual production line takes place within 2-4 seconds (Glos (1995)); the before mentioned characteristics are not measured by some device, they are subjectively estimated and it is decided within seconds whether the structural element belongs to a certain grade or not. Visual grading has proven as an efficient tool to reduce the variability of timber material properties, however, the grading effect strongly depends on the person who is performing the visual grading. The statistical characteristics of the material properties of visual graded timber are therefore difficult to assess based on information about the applied visual grading rules.

Machine Grading

The above mentioned disadvantages of visual strength grading may be overcome by machine grading, where a more formal assessment of the grading process can be performed. In contrast to visual grading, machine grading is in general based on indicative characteristics of a timber structural element which can be measured non-destructively by some device. The indicative characteristics have to be related to the basic material properties of interest. Typical indicative properties are:

---

[1] See Section 3.3.1, Page 35.

- Directly related to the MOE:

     - flat wise bending stiffness,

     - ultrasonic pulse measurement,

     - frequency response measurement.

- Directly related to the density:

     - measurements on weight and dimensions,

     - γ-ray detection.

- Directly related to visible defects:

     - microwave response,

     - optical detection and subsequent image processing.

A good overview about the different measuring schemes can be found in Thelandersson and Larsen (2003). It is the result from several research projects, e.g. Johansson et al. (1992), Boström (1994) that measurements related to the MOE are also highly related to the bending strength. Several grading machines operate with a single MOE related indicator as the flat wise bending stiffness and deliver comparable results compared to more complex machines measuring several indicators (Thelandersson and Larsen (2003)).

Several grading machine systems can be found at the market, however they operate according to similar principles; one or more indicative properties of the timber to be graded are measured by the machine and based on these measurements a population of the un-graded timber is subdivided into sub-populations of graded timber material. The grading acceptance criteria are formulated in form of boundary values for indicative properties which have to be matched to qualify a piece of timber to a certain grade. These boundaries are also termed grading machine settings. The performance, i.e. the statistical characteristics of the output of grading machines strongly depends on these settings, and in general very much attention is kept on how to control these machine settings.

Control of Grading Machine Settings

Grading machines can operate either machine controlled or output controlled. The output controlled grading system was developed in North America. Control is based on frequent destructive strength testing or proof loading of control samples of the machine graded timber. This system is relatively costly but it permits a modification of the machine settings in order to optimize the yield, i.e. the predictability of the properties of the graded timber material. This method requires large quantities of timber of similar dimension and origin, so that it can be assumed that the characteristics of the timber are stationary. These conditions rarely exist in Europe, where a variety of sizes, species and grades in small quantities are typical. For these conditions the machine controlled systems are developed. Machine control means that

the settings are derived within a substantial assessment procedure prior to the operation phase of the machine. The settings are optimized to a representative un-graded timber population which might be typical for the daily use of the grading machine. In general these assessments are done for entire geographical regions, e.g. assessments for the gross supply in France or Scandinavia suggest common settings for certain grading machines used in these countries or regions.

Rules for machine grading are described in building standards such as prEN 14081 in Europe, AS 4490, AS 3519 in Australia, ASTM D6570 in the US and NLGA SPS2 in Canada. Except of the US where in general exclusively the output control system is used, both, the output control and machine control system is used. For the output control in general the so called *CUSUM* methods are used for the continuous control of the grading machine output. In the prEN 14081 an explicit description of a machine control system is given. Both methods are briefly described in the following.

CUSUM – An Output Control Scheme

The most common used schemes for continuous output control machine grading systems are the cumulative sum (*CUSUM*) methods. *CUSUM* methods for quality control problems are described e.g. in Ewan and Kemp (1960) and linked to the timber grading problem in Warren (1978). To date *CUSUM* methods are proposed by building standards as the NLGA SPS2 (Canada) and prEN 14081 (Europe).

The principle feature of *CUSUM* techniques is that successive values of a variable, e.g. mean values of control samples, are compared with a predetermined target or reference value, and the cumulative sum of deviations from this value is plotted on a chart or recorded in tabulation. If the accumulation reaches or exceeds a pre-determined decision interval, this is taken to indicate that a change has occurred in the mean level of the variable. The decision interval may represent either an ordinal distance on a chart having time or sample number as its abscissa, or a constant for tabulation. To illustrate the main aspects of *CUSUM* methods a possible layout for output controlled machine timber grading is described, mainly following an example given in Leicester and Breitinger (1994).

It is differentiated between the attribute chart and the variable chart procedure. The attribute chart procedure is based on measuring the number of times that a required attribute, $c_{att,i}$ is missing. Specifically the attribute is taken as the event e.g. a strength value is in excess of the value of the proof load. The variable chart procedure is based on measuring a mean value, $m_{sc,i}$ of a control sample taken frequently from the output. The usual sample size for these samples is $n = 5$. The charting procedure is based on three control parameters k_c, y_c and z_c, where $y_c < z_c$. The values for the control parameters depend on the size n of the control sample, the coefficient of variation of the variable of interest and are different for the attribute and variable chart procedure. For example, if the size of the control sample is $n = 5$ and the coefficient of variation (cov) of the property to be controlled is 25% the control parameters

k_c, y_c and z_c can be specified as:

- Attribute Chart (Independent from cov): $(k_c, y_c, z_c) = (1, 1, 6)$
- Variable Chart : $(k_c, y_c, z_c) = (0.9625\mu, 0.475\mu, 0.672\mu)$

with μ, the mean value of the property to be controlled.

For the $i - th$ sample, a sum can be computed as:

$$SUM_i = CUSUM_{i-1} + \left(c_{att,i} - k_c\right) \tag{4.1}$$

for an attributes chart and

$$SUM_i = CUSUM_{i-1} + \left(k_c - m_{sc,i}\right) \tag{4.2}$$

for a variable chart. $CUSUM_{i-1}$ denotes the value of $CUSUM$ after the previous sample is tested. E.g. the actual $CUSUM_i$ for the variable chart is derived according to Table 4-1.

When the process switches to 'out-of-control', in general, some check on the stress grading process must be performed. If no processing errors are detected, an intensive sampling is performed, e.g. more samples are collected. If the process does not return to 'in-control' the production is halted. This procedure is illustrated in Figure 4-4.

Table 4-1   Rules for computing CUSUM (Leicester and Breitinger (1994)).

Previous $CUSUM_{i-1}$	Actual $CUSUM_i$				
	$SUM_i \leq 0$	$0 < SUM_i < y_c$	$SUM_i \leq y_c$	$y_c < SUM_i < z_c$	$SUM_i \geq z_c$
$CUSUM_{i-1} = 0$	0	SUM_i	z_c	z_c	z_c
$0 \leq CUSUM_{i-1} < y_c$	0	SUM_i	z_c	z_c	z_c
$y_c \leq CUSUM_{i-1} < z_c$	0	0	0	SUM_i	z_c
$CUSUM_{i-1} = z_c$	0	0	0	SUM_i	z_c

$CUSUM_{i-1} \leq y_c$: Process is in-control

$CUSUM_{i-1} > y_c$: Process is out-of-control
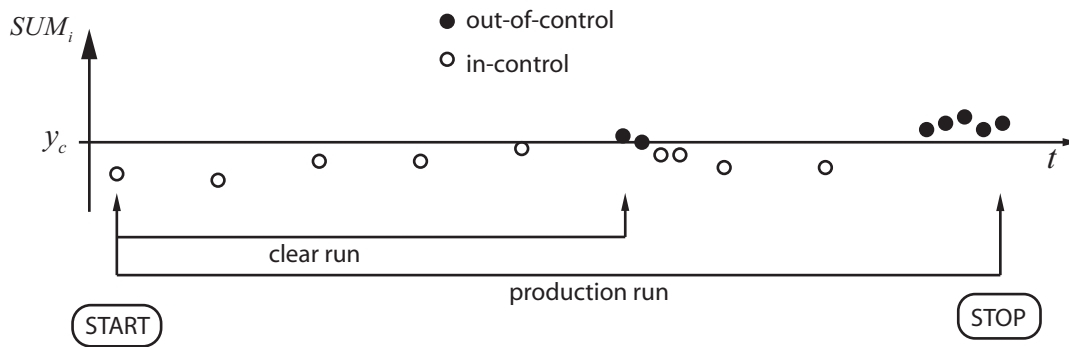
Figure 4-4 *Principle of CUSUM control procedure.*

Discussion of the CUSUM method

Being a common control procedure in the general field of quality control the *CUSUM* method has proven to be an operational scheme for the output control of machine grading systems. However, the control mechanism concentrates on mean values of variables of interest and is not sensitive to possible changes of the variance of the variables which are assumed to be known and constant. This could be seen as a reasonable assumption, but on the other hand it could be interpreted as a shortcoming of the method, since changes in variance may be present and lower fractile values are sensitive to these changes.

Alternatively to the *CUSUM* method, a Bayesian updating scheme (see Annex A) could be employed to integrate the gathered information more efficiently, i.e. continuously gain more information about the variable and its statistical properties.

The prEN 14081 approach for machine control systems

The new European grading code prEN 14081 prescribes an approach for the derivation of grading machine settings according to the machine control system. The basis of this approach is first introduced in Rouger (1996). The machine's grading performance is compared with that of a perfect machine capable of grading each piece of timber to its optimum grade. The comparison is made by assigning utilities for wrongly graded timber. In the following the main aspects of this approach are introduced and discussed.

1) Optimum Grade:

Timber grades are defined by requirements which have to be fulfilled in terms of the statistical properties of some material properties of the graded sub-population. In Europe these requirements are defined through a strength class system given in EN 338 (see section 3.4.3) and are referred to the:

- 5%-fractile value of the bending moment capacity,
- 50%-fractile value of the bending stiffness,
- 5%-fractile value of the timber density,

all properties measured in tests according to EN 408.

The optimal set of different timber grades for a given population is defined as a set where every single component is assigned to its highest possible grade. To obtain this set the following steps are examined (following Rouger (1996)):

- For a specific geographic region a large ($n \geq 900$) and representative sample is assessed in regard to measurements on the bending moment capacity $r_{m,i}$, the bending stiffness $moe_{m,i}$, the density $\rho_{den,i}$ and the indicative properties.

- The values of the measurements are ranked in ascending order that:

$$\mathbf{r}_m = \left(r_{m,1}, r_{m,2}, ..., r_{m,n} \right) \text{ with } r_{m,1} \leq r_{m,2} \leq ... \leq r_{m,n};$$

$$\mathbf{moe}_m = \left(moe_{m,1}, moe_{m,2}, ..., moe_{m,n} \right) \text{ with } moe_{m,1} \leq moe_{m,2} \leq ... \leq moe_{m,n};$$

$$\mathbf{\rho}_{den} = \left(\rho_{den,1}, \rho_{den,2}, ..., \rho_{den,n} \right) \text{ with } \rho_{den,1} \leq \rho_{den,2} \leq ... \leq \rho_{den,n}.$$

Note that following this approach $r_{m,i}, moe_{m,i}, \rho_{den,i}$ do not essentially correspond to the same specimen. The ranked data is plotted in quantile plot (see Annex A1).

- For the highest grade the sample is cut at a quantile level such, that the sub-sample above the cut level fulfils the requirements of this grade. If the cutting levels are at different quantiles for the different properties the cutting level with the greatest rank has to be taken as being the relevant.

- The sub-sample below the cutting level is taken to be cut again to obtain a sub-sample corresponding to the next timber grade below and so on (see Figure 4-5).

- The optimal grading is defined as the proportions of different grades assigned according to the segmentation procedure as described above. Typically the proportion of the highest grade is large. A possible optimal grading could be as given in Table 4-2.
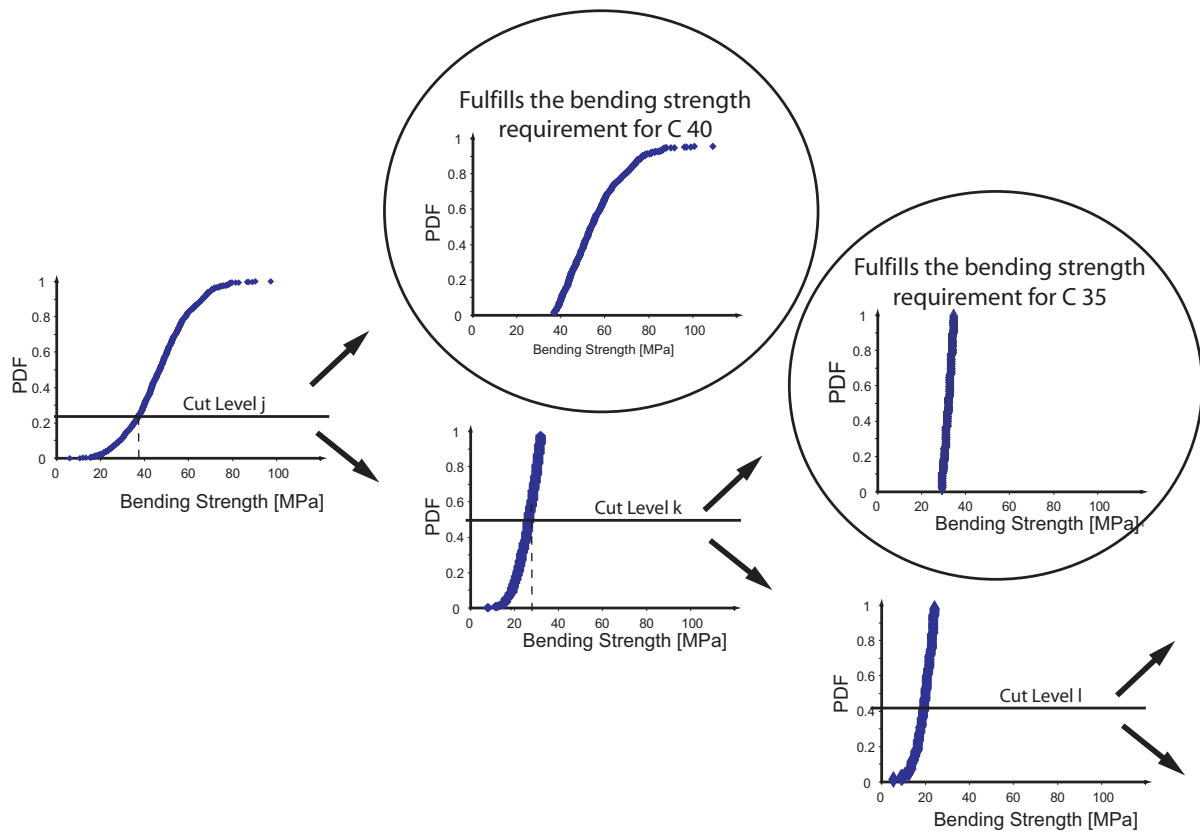
*Figure 4-5   The principle of the segmentation method exemplified on the bending strength
(arbitrary but typical example).*

Table 4-2   Optimal Grading (arbitrary but typical example).

Grade	Proportion
C40	720 (72%)
C30	130 (13%)
C24	89 (8.9%)
reject	61 (6.1%)

2) The establishment of a model which relates bending strength with the indicating properties of the machine. Beside linear regression models also more complex models can be used.

3) The determination of a set of machine settings which results in timber grades by using the model derived in 2.

4) The entire population is (virtually) graded according to these settings, into the so-called assigned grades.

5) The assigned grades are compared with the optimal grades in a so-called size matrix. A possible size matrix could be given as in Table 4-3.

Table 4-3   A possible size matrix for the grade combination C40-C30-C24-reject (arbitrary but typical example).

Optimum Grade	Assigned Grades			
	C40	C30	C24	reject
C40	254	412	51	3
C30	11	28	87	4
C24	1	20	45	23
eject	0	3	48	10

6) The determination of an elementary cost matrix.

According to Rouger (1997) it is considered as unprofitable if timber is assigned to a grade greater than its optimal grade (upgrading) or if timber is assigned to a grade less than its optimal grade (downgrading). Both up- and downgrading is assumed to be associated with costs derived according to the scheme described next.

a) Upgrading:

The mean value of the optimum grade $\mu_{X,opt}$ is calculated based on its characteristic value, i.e. the 5%-fractile value $x_{0.05,opt}$ and assuming that the property is lognormal distributed with a coefficient of variation (cov) of 30%:

$$\mu_{X,opt} = \exp\left(\ln\left(x_{0.05,opt}\right) + \left(0.5\,\text{cov}^2 + 1.65\,\text{cov}\right)\right) \tag{4.3}$$

Similar, the mean value of the assigned grade $\mu_{X,ass}$ is estimated.

By assuming a target reliability index of $\beta_{target} = 3.0$, an applicable stress to the timber of the assigned grade s_{ass} is calculated as:

$$s_{ass} = \mu_{X,ass} - \beta_{target}\mu_{X,ass}\,\text{cov} \tag{4.4}$$

s_{ass} is then applied to the timber sub-population corresponding to the optimum grade and a reliability index β is calculated as:

$$\beta = \frac{\mu_{X,opt} - s_{ass}}{\mu_{X,opt}\,\text{cov}} \tag{4.5}$$

A cost of upgrading is then defined as the difference between this reliability index and the target reliability index:

$$Cost\left(upgrading\right) = \beta_{target} - \beta \tag{4.6}$$

b) Downgrading:

The cost of downgrading is assigned to be related to the over dimensioning of bending elements in deflection (it is considered that deflection is the most common design criteria):

$$Cost\left(downgrading\right) = \sqrt[3]{\frac{moe_{m,opt}}{moe_{m,ass}}} - 1 \tag{4.7}$$

where $moe_{m,opt}$ and $moe_{m,ass}$ are the MOE's of the optimum and the assigned grade.

Based on the above calculations a so-called cost matrix can be derived. A possible cost matrix is illustrated in Table 4-4.

Table 4-4   A possible elementary Cost Matrix (upgrading, dark grey; downgrading, light grey), (arbitrary but typical example).

Optimum Grade	Assigned Grades			
	C40	C30	C24	eject
C40	0	0.053	0.084	0.326
C30	0.111	0	0.029	0.26
C24	0.222	0.083	0	0.224
eject	0.778	0.5	0.333	0

7) The determination of the global Cost Matrix.

Each value $global_{ij}$ in the global cost matrix is obtained by multiplying the corresponding number in each cell of the size matrix $size_{ij}$ by the corresponding value of the elementary cost matrix $elementary_{ij}$ and then by dividing with the total number of pieces in the assigned grade, as:

$$global_{ij} = \frac{elementary_{ij} size_{ij}}{\sum_i size_{ij}} \tag{4.8}$$

A possible global cost matrix is given in Table 4-5.

Table 4-5   A possible global Cost Matrix (arbitrary but typical example).

Optimum Grade	Assigned Grades			
	C40	C30	C24	eject
C40	0	0.047162	0.018545	0.02445
C30	0.00459	0	0.010922	0.026
C24	0.000835	0.003585	0	0.1288
eject	0	0.00324	0.069195	0

8) Assessment of the global cost matrix.

The grading machine settings are considered as appropriate when all global upgrading costs are lower than 0.02. In Table 4-5 this requirement is violated.

Discussion on the prEN 14081 approach

The principles of the procedure for the derivation of grading machine settings according to prEN 14081 part II are briefly summarized above. In the opinion of the author the procedure exhibits several shortcomings in both, the practical and the theoretical point of view:

Practically, it is considered as a disadvantage that the procedure does not allow for a probabilistic assessment of the material properties based on the derived grading settings. I.e. the gathered information cannot be directly used for the estimation of distribution parameters of the graded timber.

From the theoretical viewpoint several inadequacies can be identified, which, in the opinion of the author, are too serve to be considered as simplifications or assumptions. The general set up of the method, the assignment of so-called optimum grades by the segmentation technique (compare Figure 4-5) and taking these segments as a reference is debatable. Furthermore, it seems incorrect to assign Lognormal distributions with a coefficient of variation (cov) of 30% to these segments and perform a reliability calculation (see Equations (4.3) and (4.5)). By inspecting the right part of Figure 4-5 it is clear that the segments are not log-normally distributed and the coefficient of variation is not 30%. In addition, the assumption is not consistent, i.e. for some of the optimum grades the assumption is less inadequate than for others. Another feature which appears inappropriate is the assumption that the cost for upgrading is proportional to the reliability index. Possible cost, however, would better be related to the probability of failure.

Even more features of the method could be questioned; however, the discussion is not continued here.

Quite recently the prEN 14081 reached its approval phase. A future task for the research community is to reflect upon the proposed method for the derivation of grading machine settings. Real costs are involved in the structural timber production line and one major issue

of competitiveness of structural timber is the consistent representation of the uncertainties according to the timber material properties. It is expected that new more efficient methods will come up soon.

An example for an alternative procedure is presented in the following. Referring to Faber et al. (2004) and Köhler and Faber (2003) a procedure for the probabilistic modelling of graded timber material properties is derived. In section 4.2.3.2 the procedure is introduced with the example of one relevant (or grade determining) material property. In section 4.2.3.4 the method is followed further and a framework for the optimal assignment of grading machine settings is presented.

4.2.3.2 Probabilistic Modelling of Grading Schemes

In structural reliability applications it is necessary to be able to assess the probability distribution function of the relevant material properties. Assuming that a sufficiently large number of experiments have been performed regarding the relevant material property X of the ungraded timber, it is in principle a straightforward task to select a probability density function and to estimate the parameters of this correspondingly. The resulting density function might be considered as a prior density function $f_X'(x)$, i.e. the probability density function, which might be assumed if no grading schemes are invoked. However, when a grading scheme has been applied the prior density function is no longer representative for the graded timber specimens. In order to assess the representative probability density function use may be made of Bayes's rule, see e.g. Benjamin and Cornell (1970), yielding the posterior probability density function $f_X''(x)$, i.e. the probability density function, which can be assumed for the material properties, categorised into a particular grade by application of the grading acceptance criteria A_C:

$$f_X''(x) = P(X = x | A_C) = \frac{1}{c} f_X'(x) P(A_C | X = x) \tag{4.9}$$

where $c = P(A_C)$.

The grading acceptance criteria A_C is the rule applied for the categorisation of timber into different grades and also refered to as the grading machine settings. The grading acceptance criteria A_C may be formulated in terms of the values of the indicators. Typically the criteria have the following appearance:

$$A_C = \{b_L \leq I \leq b_U\} \tag{4.10}$$

where b_L and b_U are lower and upper bounds for the indicator for a particular grade.

It is seen from Equation (4.9) that it is necessary to estimate the likelihood of the implementation of the grading acceptance criteria, i.e. $P(A_C | X = x)$ as a function of the specific value of the material property X. This likelihood may be assessed if test results are

available from timber specimens tested both, in regard to the indirect characteristic, e.g. the flatwise bending stiffness, and the relevant material property, e.g. the edgewise bending strength. Assuming that such test results are available a regression analysis can be performed based on which the statistical characteristics of the indicator, e.g. the flatwise bending stiffness can be assessed for a given value of the relevant material property. The prior probability distribution function for the un-graded timber material properties together with the likelihood of implementing a given selection criteria for a given sample thus forms the basis for assessing the posterior probability distribution function using Bayes's rule.

The regression analysis takes basis in n simultaneous observations of the relevant material property $\mathbf{x} = (x_1, x_2, ..., x_n)^T$ and the indicator $\mathbf{\iota} = (\iota_1, \iota_2, ..., \iota_n)^T$. Assuming that at least locally a linear relationship between x and ι exist the regression may be performed on the basis of:

$$\iota = a_0 + a_1 \cdot x + \varepsilon \tag{4.11}$$

where a_0 and a_1 are the regression coefficients and where ε is an error term. Assuming that the error term ε is normal distributed with zero mean and unknown standard deviation σ_ε the maximum likelihood method, see e.g. Lindley (1965) may be used to estimate the mean values and covariance matrix for the parameters a_0, a_1, σ_ε.

The likelihood is then given as:

$$L(a_0, a_1, \sigma_\varepsilon) = \prod_{i=1}^{n} \frac{1}{\sqrt{2\pi}\sigma_\varepsilon} \exp\left(-\frac{1}{2}\left(\frac{-\iota_i + a_0 + a_1 \cdot x_i}{\sigma_\varepsilon}\right)^2\right) \tag{4.12}$$

The parameters are estimated by the solution $\mathbf{p}^*$ to the optimisation problem:

$$\max_{\mathbf{p}} L(\mathbf{p}) \tag{4.13}$$

where $\mathbf{p} = (a_0, a_1, \sigma_\varepsilon)^T$.

Having performed the regression analysis, it is possible to assess the acceptance probability i.e. $P(A_C | X = x)$ by:

$$P(A_C | X = x) = P(b_L \leq a_0 + a_1 X + \varepsilon \leq b_U | X = x) = P(b_L \leq a_0 + a_1 x + \varepsilon \leq b_U) \tag{4.14}$$

which is straightforward to assess recognising that the indicator I is normal distributed.

For structural reliability applications the probability distribution function for the relevant material characteristic is often more directly useful than the probability density function. Considering the probabilistic modelling of the relevant material characteristics corresponding to the different grades it may, e.g. in the context of First Order and Second Order Reliability (FORM/SORM) analysis be more appropriate to consider the probability distribution function given in Equation (4.15) instead of the probability density function from Equation (4.9):

$$P\left(X \le x \middle| A_C\right) = \frac{P\left(X \le x\right)P\left(A_C \middle| X \le x\right)}{P\left(X \le x\right)P\left(A_C \middle| X \le x\right) + P\left(X > x\right)P\left(A_C \middle| X > x\right)} \tag{4.15}$$

However, the probability distribution defined by Equation (4.15) is also not always straightforward to work with because it involves the calculation of the terms $P\left(A_C \middle| X \le x\right)$ and $P\left(A_C \middle| X > x\right)$ which in general are difficult to express analytically.

If the only aim is to assess the probability distribution function FORM/SORM (Madsen et al. (1986)) as well as Monte Carlo based simulation techniques (Melchers (1987)) may, however, also be directly applied by use of the following formulation:

$$P\left(X \le x \middle| A_C\right) = \frac{P\left(X \le x \cap A_C\right)}{P\left(A_C\right)} \tag{4.16}$$

Example

As an example the case where the grading of the timber material is performed using the Computermatic grading machine is presented. A data set from Johansson (1992) is considered concerning the bending strength of 239 timber specimens of European spruce.
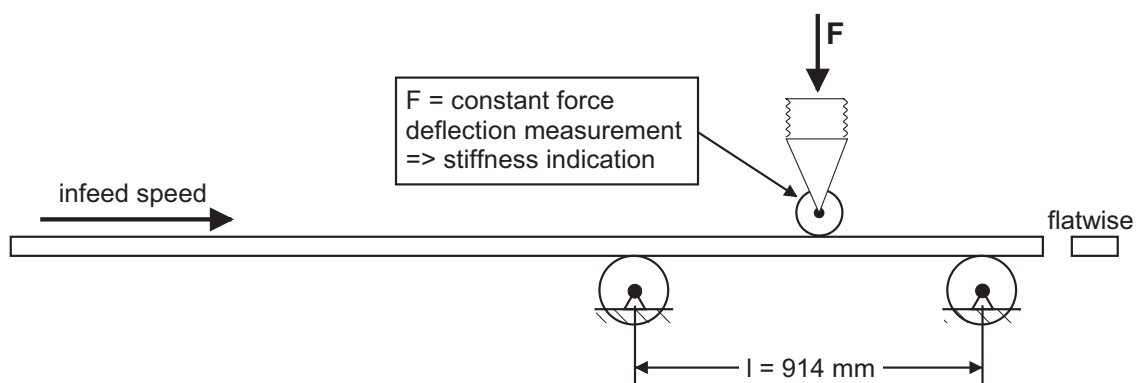
Figure 4-6   Principles of the Computermatic Grading Machine.

The Computermatic grading machine is a widely used grading machine which considers the flatwise bending stiffness as an indicator of the bending strength. As illustrated in Figure 4-6, the stiffness characteristic is obtained through a measurement of the deflection under a fixed load applied at the centre of a span of 914 mm. The bending strength is obtained in four-point bending tests according to the European standard EN 408, compare section 7.3.1. Further information regarding the Computermatic grading machine can be found in the literature, e.g. Computermatic user manual (2000). The entire population of the 239 timber specimen is assumed to be un-graded. The probability distribution function of the bending strength, i.e. the prior probability distribution function, is assumed to be 2-parameter Weibull min distributed. The 2-parameter Weibull min distribution function is given in Annex A. It is observed e.g. in

Glos (1978) that the 2-parameter Weibull distribution gives too conservative estimates for the lower tail region of the distribution. The parameters of the Weibull distribution are therefore also estimated with explicit consideration of the lower tail region of the data.

In Figure 4-7 the probability distribution function representing all data is compared to the probability distribution function estimated by using the censored maximum likelihood estimation according to section 7.1 with a threshold value corresponding to the lower 30 % quantile. For the purpose of comparison the sample probability distribution function using all observations is also illustrated.

In Figure 4-7 it is seen that a significant refinement of the representation of the strength data in the lower tail domain can be achieved, by using the distribution model fitted to the lower data set domain.

In Johansson (1992) not only the bending strength of the 239 specimens but also the Computermatic based indicator of the bending strength for each specimen has been observed and recorded prior to the bending strength tests. By regression analysis of simultaneously measured bending strengths and the observed Computermatic based indicators the regression coefficients are estimated according to Equations (4.11)-(4.13). Using the Method of the Maximum Likelihood both the parameters of the prior probability distribution functions and the regression parameters are estimated as normal distributed random variables with mean values, standard deviations and correlations as given in Table 4-6. Ignoring the statistical uncertainty associated with the estimated parameters, which for the present case is insignificant, the acceptance probability may thus be assessed directly from Equation (4.14).
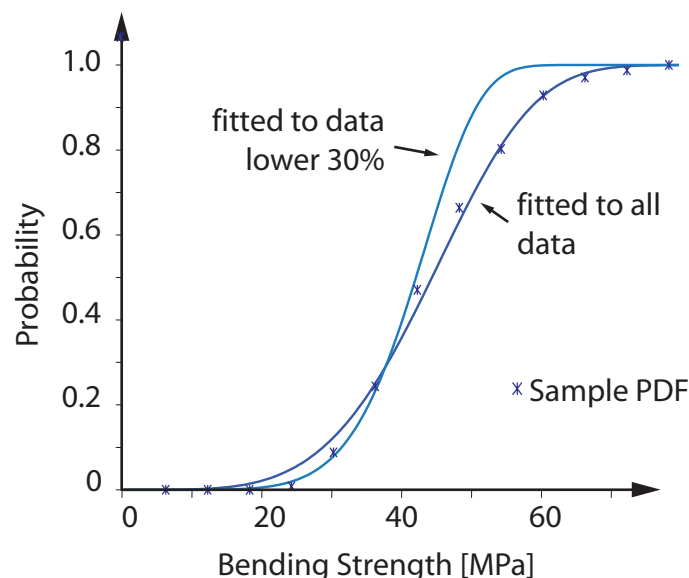

Figure 4-7   *2-parameter Weibull min probability distribution functions with parameters estimated using all data and data below 30%, compared with the sample probability distribution function (Sample PDF).*

Table 4-6 *Mean values, standard deviations and correlations of the parameters of the prior probability distribution function (w, k see also the definition in Annex A) together with the estimated regression parameters.*

	Prior Distribution Parameters (bending mod. of rupture)			Regression Parameters (Computermatic)			
	Weibull parameters as normal distributed random variables		correlation	as normal distributed random variables			correlation
	w [MPa]	k [MPa]	ρ	a_0 [Comp]	a_1 [Comp/MPa]	σ_ε [Comp]	ρ
All data	$\mu = 48.0$ $\sigma = 0.76$	$\mu = 4.32$ $\sigma = 0.21$	$(w,k) = 0.33$	$\mu = 4673$ $\sigma = 291$	$\mu = 98.6$ $\sigma = 6.45$	$\mu = 1073$ $\sigma = 40.08$	$(a_0, a_1) = -0.02$ $(\sigma_\varepsilon, a_1) = 0$ $(\sigma_\varepsilon, a_0) = 0$
Data lower 30%	$\mu = 43.9$ $\sigma = 0.02$	$\mu = 6.44$ $\sigma = 0.49$	$(w,k) = -0.06$				
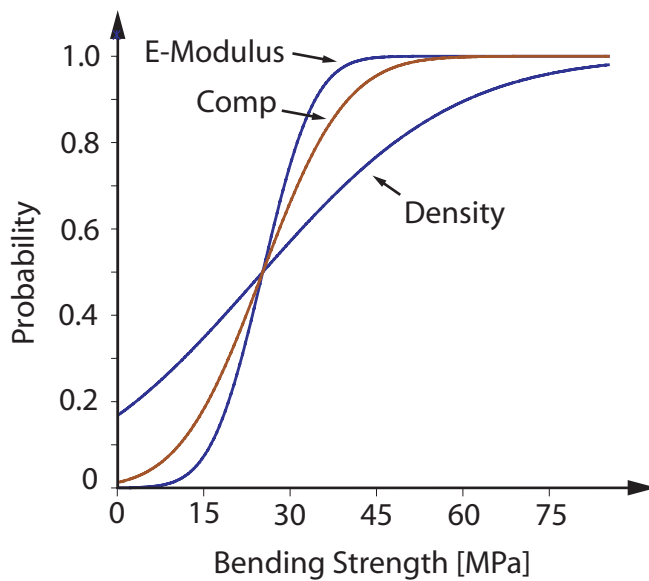
Figure 4-8 *Acceptance probability of different indicators.*

In Figure 4-8 the acceptance probability (Equation (4.14)) for three different types of indicators is illustrated. The Computermatic based indicator is compared with the case when the timber density and edgewise modulus of elasticity are used as an indicator. The grading acceptance criterion for each probability curve is chosen such that the mean value of the expected bending strength is the same in all three cases. It is not surprising that the 'better' the linear regression is between the indicator and the relevant material property, the steeper is also the corresponding acceptance probability curve. The steepness of the acceptance probability curves thus forms a basis for comparison of the efficiency of different grading methods.

Assuming that the timber specimens are categorised in three grades of same volume according

to the observed Computermatic indicators, i.e. 1) 4000 – 8100 MPa, 2) 8100 – 9650 MPa and 3) 9650 – 15000 MPa, the probability density function for the graded timber can be obtained directly from Equation (4.9).

In Figure 4-9 the prior probability density function of the bending strength for the un-graded timber (2-parameter Weibull min distributed with mean value 43.7 MPa and standard deviation 11.4 MPa) is shown together with the probability density functions for the three timber grades in accordance with the abovementioned grading acceptance criteria. Note that the grading is performed using the prior probability density function with parameters estimated based on all data.
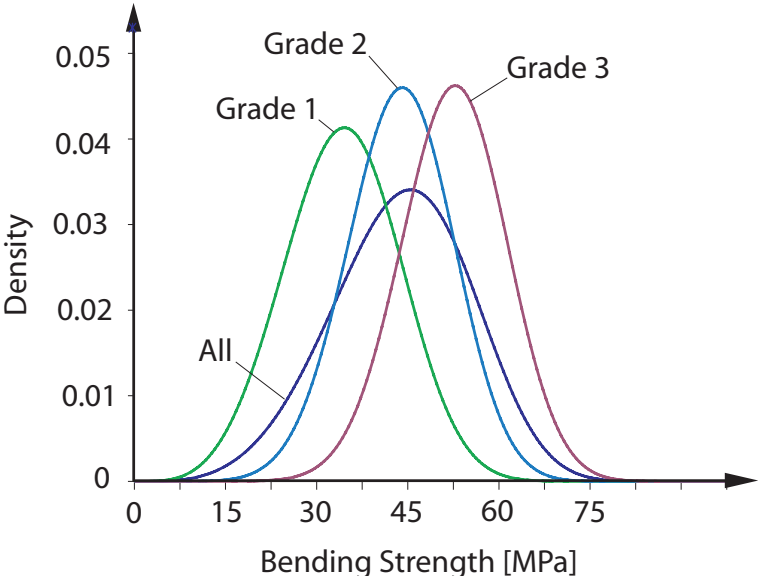
Figure 4-9   Illustration of the probability density functions for the bending strength for un-graded and graded timber specimens.

In Figure 4-10 the probability distribution functions for the different grades are shown in comparison with the sample probability distribution functions (sample PDF's) established from the experimental data fulfilling the respective grading acceptance criteria.

64
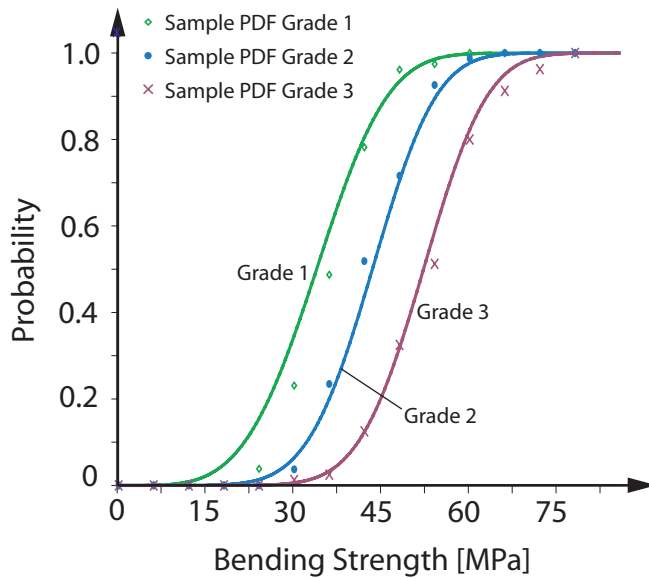
Figure 4-10   Probability distribution functions for the bending strength for the three different grades together with the corresponding sample probability distribution functions.

In Figure 4-10 the lower tail domain of the probability distribution functions are shown in larger scale together with the lower 5% fractile values.
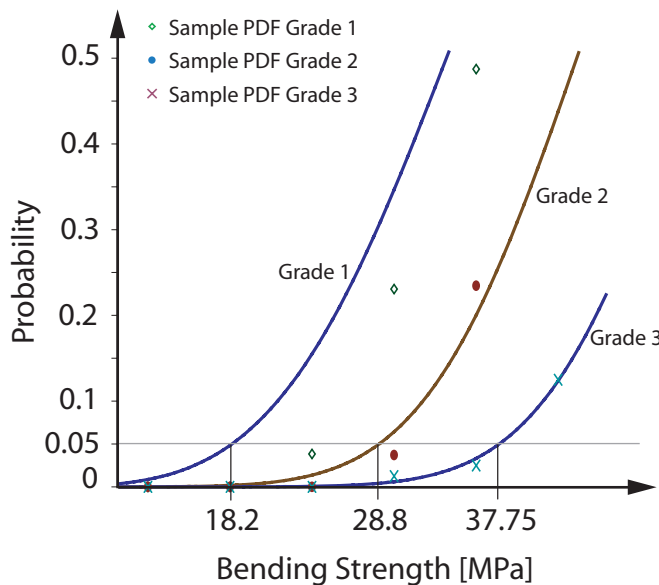
Figure 4-11   Lower tail domain of the graded probability distribution functions. Estimates of the lower 5% fractiles (characteristic values) are shown.

Note, that especially the representation of the data by the probability distribution function for grade 1 is not satisfactory. For the weaker timber, e.g., grade 1 and grade 2, special emphasis on the lower tail domain in the representation of the prior probability distribution function is thus required. Figure 4-12 and Figure 4-13 shows the three probability distribution functions compared with the sample probability distribution functions. For identifying the probability

density function of grade 1 and 2, now, the prior probability density function is fitted with special emphasis on the lower tail domain using the censored maximum likelihood method according to section 7.1. The data which fulfils the grade 3 acceptance criteria are mostly taken from the middle and upper part of the prior distribution. For that part the prior probability distribution function modelled under consideration of all data can be used. The sample cumulative probability distribution functions corresponding to the graded observations are also shown in Figure 4-12.

Figure 4-12   Probability distribution functions for the bending strength for the three grades. The prior probability distribution function for grade 1 and 2 is fitted to the lower tail.

Figure 4-13   Lower tail domain of the probability distribution functions for the bending strength for the three grades. Estimates of the lower 5% characteristic values are shown.
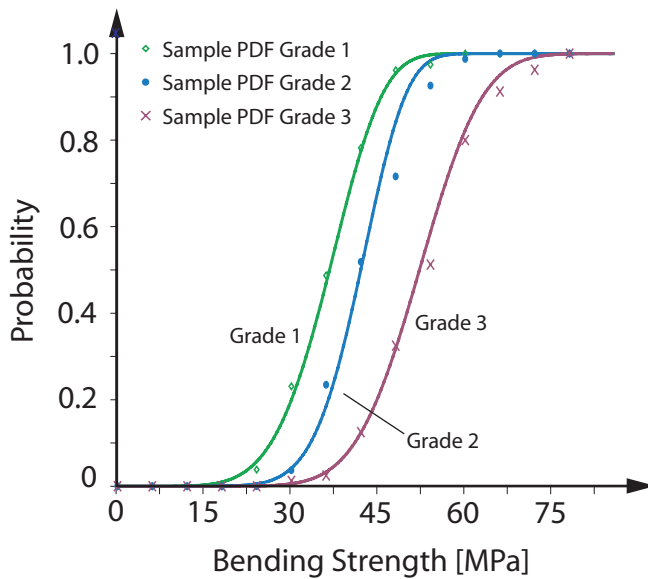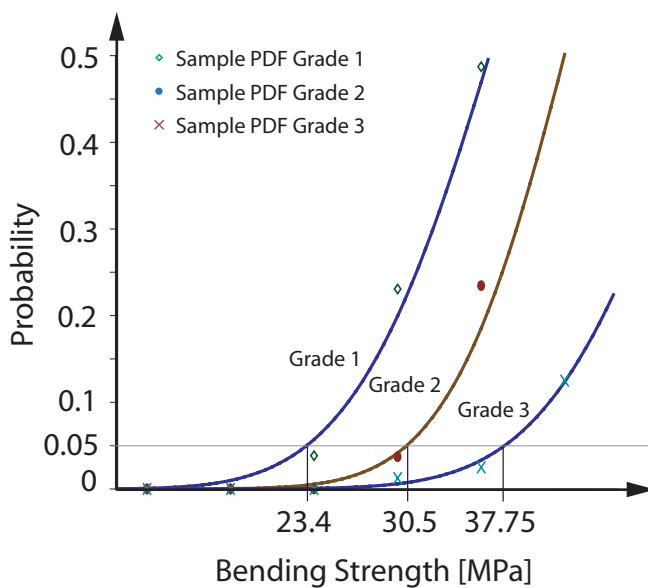
In Figure 4-13 the lower tail domain is shown in larger scale. It is seen by comparison between the theoretically derived probability distribution functions and the sample probability distribution functions (corresponding to the experimental observations in the considered intervals) that a rather satisfactorily agreement in the lower tail domain is achieved.

In Table 4-7 the lower 5 % fractile values are given for the different grades with and without estimating the parameters of the prior probability distribution function in the lower tail domain using the censored maximum likelihood method compared with the 5% fractile values resulting directly from the data.

From Figure 4-13 it is seen that a great benefit may be obtained by estimating the prior probability distribution with special consideration of the tail domain before the probability distributions of the graded specimens are evaluated.

Whether a prior fitted with special emphasis to the goodness of fit in the lower tail domain has to be preferred or not, depends on the domain for which the posterior is of special interest. It is thus difficult to provide any generally applicable rules for this selection. However, in most normal cases the selection would follow naturally from the available data on the simultaneous observations of an indicator and the bending strength together with previous experience to judge which approach is appropriate.

Table 4-7   Lower 5% fractile values for the graded timber specimens.

acceptance interval	char. value [MPa] f'_{R_m} fitted to lower tail	char. value [MPa] f'_{R_m} fitted to all	char. value [MPa] sample values
4000 - 8100	23.4	18.2	25.0
8100 - 9650	30.5	28.8	30.5
9650 - 15000	-	37.71	36.3
All data (ungraded)	24.1		28.4

4.2.3.3   Probabilistic Model Format for Timber Materials in consideration of grading

As a prerequisite to the consistent probabilistic design of timber structures and correspondingly, the calibration of e.g. load and resistance factor design formats, it is necessary to establish a standardised format for the representation of the relevant timber material properties. Such a format must contain both a description of the prior probability distribution of the relevant timber material properties as well as a description of the quality of the different quality control and selection for grading procedures.

In Table 4-8 a possible format for probabilistic models of relevant timber material properties of interest is suggested. First the distinction of different prior timber populations is proposed e.g. in respect to the geographical origin of the timber, the species, the dimension of the considered timber elements and other possible characterising properties. Representative prior probability distribution models of the relevant material property may be specified in terms of

probability distribution functions, their parameters and the uncertainties associated with their parameters. Furthermore the different schemes for quality control and grading may be represented in terms of their linear regressions and associated uncertainties.

To establish a probabilistic description of timber material properties in a code format such as e.g. the Probabilistic Model Code by the Joint Committee on Structural Safety, the parameters and their uncertainties should be represented in the same way. The procedure described in this chapter is a proposal in this direction and should be taken as a basis for further discussions.

Table 4-8   Suggested Format for Probabilistic Models for relevant Material Properties of Timber Materials.

characteristics of the population				Prior distibution Parameters (relevant material property)			Regression Parameters (for a given grading method)			
origin	timber species	size	....	w	k	ρ	a_0	a_1	σ_ε	ρ
Region or Country 1	Specie or speciegroup 1			$\mu =$ $\sigma =$	$\mu =$ $\sigma =$	$(w,k) =$	$\mu =$ $\sigma =$	$\mu =$ $\sigma =$	$\mu =$ $\sigma =$	$(a_1,a_0) =$ $(a_1,\sigma_\varepsilon) =$ $(a_0,\sigma_\varepsilon) =$
	Specie or speciegroup 2			$\mu =$ $\sigma =$	$\mu =$ $\sigma =$	$(w,k) =$	$\mu =$ $\sigma =$	$\mu =$ $\sigma =$	$\mu =$ $\sigma =$	$(a_1,a_0) =$ $(a_1,\sigma_\varepsilon) =$ $(a_0,\sigma_\varepsilon) =$
	⋮	⋮	⋮	⋮	⋮	⋮	⋮	⋮	⋮	⋮
Region or Country 2	Specie or speciegroup 1			$\mu =$ $\sigma =$	$\mu =$ $\sigma =$	$(w,k) =$	$\mu =$ $\sigma =$	$\mu =$ $\sigma =$	$\mu =$ $\sigma =$	$(a_1,a_0) =$ $(a_1,\sigma_\varepsilon) =$ $(a_0,\sigma_\varepsilon) =$
	⋮	⋮	⋮	⋮	⋮	⋮	⋮	⋮	⋮	⋮
⋮	⋮	⋮	⋮	⋮	⋮	⋮	⋮	⋮	⋮	⋮
User specified populations										
Pop 1				$\mu =$ $\sigma =$	$\mu =$ $\sigma =$	$(w,k) =$	$\mu =$ $\sigma =$	$\mu =$ $\sigma =$	$\mu =$ $\sigma =$	$(a_1,a_0) =$ $(a_1,\sigma_\varepsilon) =$ $(a_0,\sigma_\varepsilon) =$
Pop 2										

The statistical properties of the graded timber materials depend as discussed previously also on the grading acceptance criteria (grading machine settings) implemented for the different grades. It is hardly possible to prescribe how these should be selected as this should be a matter of economical optimisation for the individual saw mills. The selection of a quality control and grading scheme must be made on the basis of cost benefit considerations. These aspects are considered in the next section.

4.2.3.4   Assessment of the Optimal Grading Procedure

Based on the proposed statistical modelling of timber properties as a function of the type and efficiency of the grading procedures, a cost optimisation scheme may be formulated for the identification of the optimal grading procedure. Therefore, the cost of the control and the benefit of fulfilling the requirements set for the material characteristics belonging to different grades have to be given.

The benefit B_T of a set of timber grades identified by the grading procedure GP may be written as:

$$B_T(f_X'(x), A_C, GP) = \mathbf{V}^T \cdot \mathbf{C}_{Grade} \qquad (4.17)$$

where $\mathbf{V}$ is a vector of volumes of particular grades, which can be identified depending on the prior probability distribution of the relevant material property, the set of grading acceptance criteria and the grading procedure. $\mathbf{C}_{Grade}$ is a vector of the (monetary) benefit of the timber grades per unit volume. If the prior probability distribution of the relevant material property, the grading procedure, the set of timber grades and their monetary benefits are known, the optimal set of grading acceptance criteria A_C may be found by solving the following optimisation problem:

$$\max_{A_c} \ B_T(f_X'(x), A_C, GP) \qquad (4.18)$$
$$\text{subject to: } \mathbf{N}_{req}, \mathbf{C}_{Grade}$$

subject to normative requirements which have to be fulfilled by the grades, $\mathbf{N}_{req}$, and the cost vector $\mathbf{C}_{Grade}$. Involving the investment, maintenance over lifetime costs, costs for personnel, etc. of a particular grading procedure by the function $C_G(GP)$ the optimal grading procedure may be identified by solving the following optimisation problem:

$$\max_{GP} \left[\left(\max_{A_c} \ B_T(f_X'(x), A_C, GP) \right) - C_G(GP) \right] \qquad (4.19)$$
$$\text{subject to: } \mathbf{N}_{req}, \mathbf{C}_{Grade}$$

Example - continuation

Considering the data and the inference from the example in section 4.2.3.2, it can now be demonstrated how an optimal set of grading acceptance criteria for the considered grading procedure of the Computermatic grading machine can be found by applying Equation (4.18). The intention is to set up three different grading acceptance criteria to select three different timber grades. The grades have to fulfil the requirements for the strength classes according to EN 338 in terms of the 5% fractile value of the bending strength and the mean of bending modulus of elasticity and the 5% fractile value of the density. The prior population is assumed to be checked according to visual defects of the timber as warp, insect damage etc. Five different grades according to EN 338 are selected to be possible grades and a reject domain is defined for timber, which not has to fulfil any requirements. They are shown together with example values for the monetary benefit and the material requirements in Table 4-9, therefore the vector $\mathbf{C}_{grade}$ (units: monetary unit per volume) becomes:

$$\mathbf{C}_{grade} = (0.5, \ 1.0, \ 1.4, \ 1.6, \ 1.8, \ 2.0)^T.$$

To identify three different grades, three different grading acceptance criteria have to be

defined:

$$A_{C_1} = \left\{ b_{L,1} \leq I < b_{L,2} \right\}; A_{C_2} = \left\{ b_{L,2} \leq I < b_{L,3} \right\}; A_{C_3} = \left\{ b_{L,3} \leq I \leq b_{U,3} \right\} \qquad (4.20)$$

Table 4-9   Monetary benefit (example values) and requirements for grades according to EN 338.

	'reject'	C16	C24	C30	C35	C40
Monetary Benefit	0.5	1.0	1.4	1.6	1.8	2.0
Bending strength, 5%-frac [MPa]	-	>16	>24	>30	>35	>40
Modulus of elasticity, mean value [MPa]	-	>8000	>11000	>12000	>13000	>14000
Density, mean value [kg/m³]	-	>310	>350	>380	>400	>420

In addition to the posterior distributions of the ultimate bending strength for these three grading acceptance criteria $P\left(R_m \leq r_m \big| A_{C_i} \right)$, the posterior distributions of the bending modulus of elasticity $P\left(MOE_m \leq moe_m \big| A_{C_i} \right)$ and of the density $P\left(P_{den} \leq \rho_{den} \big| A_{C_i} \right)$ have to be assessed, according to the prior distribution parameters and the regression parameters given in Table 4-6, Table 4-10 and Table 4-11. These posterior distributions are representing timber sub-populations with the property $I \in A_{C_i}$ and can be checked in regard to the requirements in Table 4-9.

The three grading acceptance criteria are defined through the values of $b_{L,1}, b_{L,2}, b_{L,3}$ and $b_{U,3}$ in Equation (4.20). The value $b_{U,3}$ is fixed to an upper threshold value, namely $b_{U,3} = 16000$ MPa. The optimal values of $b_{L,1}, b_{L,2}$ and $b_{L,3}$ are then found by solving Equation (4.18) using the simplex algorithm, see e.g. Nelder and Mead (1965), for which differentiability of the objective function and constraints is not required. The applied algorithm does not allow for the definition of the constraints explicitly. Therefore the constraints have been included directly into the formulation of the objective function $B_T(f'_X(x), A_C, GP)$ in line with the requirements given in EN 338. Due to the discrete character of the objective function the simplex algorithm is applied in conjunction with a random search to facilitate the identification of the optimal solution over the set of discrete optimisation variables. In this search it has been found that 100 simulations provided stable results.

Table 4-10 *Mean values, standard deviations and correlations of the parameters of the prior probability distribution function together with the estimated parameters for the regression between bending modulus of elasticity and the Computermatic indicator.*

Prior Distribution Parameters (bending modulus of elasticity)			Regression Parameters (Computermatic)			
Log-normal parameters as normal distributed random variables		correlation	as normal distributed random variables			correlation
ξ [MPa]	δ [MPa]	ρ	a_0 [Comp]	a_1 [Comp /MPa]	σ_ε[Comp]	ρ
$\mu = 12749.1$	$\mu = 0.1949$	$(\xi,\delta)=0$	$\mu = 2892$	$\mu = 0.469$	$\mu = 961.7$	$(a_0,a_1) = -0.03$
$\sigma = 160.7$	$\sigma = 0.0089$		$\sigma = 332.1$	$\sigma = 0.025$	$\sigma = 35.91$	$(\sigma_\varepsilon,a_1) = 0$
						$(\sigma_\varepsilon,a_0) = 0$

Table 4-11 *Mean values, standard deviations and correlations of the parameters of the prior probability distribution function together with the estimated parameters for the regression between density and the Computermatic indicator.*

Prior Distribution Parameters (density)			Regression Parameters (Computermatic)			
Normal parameters as normal distributed random variables		Correlation	as normal distributed random variables			correlation
μ[kg/m^3]	δ [kg/m^3]	ρ	a_0 [Comp]	a_0 [Comp/ kg/m^3]	σ_ε [Comp]	ρ
$\mu = 406.3$	$\mu = 35.47$	$(\xi,\delta)=0$	$\mu = 1063.6$	$\mu = 19.51$	$\mu = 1341.0$	$(a_0, a_1) = -0.02$
$\sigma = 2.295$	$\sigma = 1.622$		$\sigma = 997.24$	$\sigma = 2.44$	$\sigma = 50.1$	$(\sigma_\varepsilon, a_1) = 0$
						$(\sigma_\varepsilon, a_0) = 0$

Table 4-12 *Optimal set of timber grades, limiting properties are shaded and framed.*

	I [MPa]	V_i	bending mod. of rupture 5%-fractile value [MPa]	bend. mod. of elasticity mean value [MPa]	density 5%-fractile value [kg/m3]	Grade EN 338
A_{C_r}	[0,5255)	0.5%		reject		
A_{C_1}	[5255,8094)	29.5%	26.0	11000.4	339*	C24
A_{C_2}	[8094,10161)	49%	30.3	12952.34	351.6*	C30
A_{C_3}	[10161,16000]	21%	40.1	15738.9	366*	C40

*)density is not taken into account as a requirement.

Subject to the given conditions summarised in Table 4-9, the optimal set of grading

acceptance criteria is given in Table 4-12. From the assumed set of data the grades C24, C30 and C40 have been identified, where for the grade C24 the mean value of the bending modulus of elasticity is the limiting property. For the grades C30 and C40 the bending strength is limiting. The relationship between the Computermatic indicator and the timber density is too weak to make any quantitative prediction about the density based on a Computermatic indication. Therefore, in this example the density is not taken into account as a requirement for assigning grades.

As the Computermatic grading procedure apart from values of the flatwise bending stiffness (Indicator) also provides values of density, the parameters of Table 4-11 can be updated continuously. By doing spot test, e.g. for every 100th timber specimen, of the bending strength and the bending modulus of elasticity the parameters of Table 4-6 and Table 4-10 can also be updated continuously.

4.2.3.5   Summary and Concluding Remarks on Grading

A brief overview about timber grading is given, with focus on the control of grading machines. Grading machines can be either output controlled or machine controlled. A common output controlled procedure is the so-called *CUSUM* method and the main features of this method are briefly explained and discussed. A procedure for machine control is introduced following the method which is prescribed in the European standard prEN 14081. It is noted that both control methods do not allow for a probabilistic assessment of the graded timber material properties based on the corresponding formalism of the control methods. Furthermore, several shortcomings within the machine control method according to the European standard prEN 14081 are outlined and discussed.

Alternatively to the described methods, the statistical assessment of timber material properties has been considered with special emphasis on the modelling of the effect of different schemes for quality control and grading of timber. It is shown that typically applied indicators for the relevant material properties such as measurements of the flatwise bending stiffness, the measurement of densities and others may be utilised for the statistical differentiation of different populations of the strength characteristics. The suggested approach not only forms a very strong tool for the statistical quantification of the material characteristics of timber but furthermore provides a consistent basis for quantifying the efficiency of different quality control and grading procedures. The probabilistic models for the graded timber material properties have been formulated such that they readily may be applied in structural reliability analysis.

It has been found that the assessment of the statistical characteristics of the graded timber should be performed on the basis of a probabilistic modelling of the un-graded timber where special emphasis is made on the representation of the probability distribution function in the lower tail domain.

It is of utmost importance that the statistical characteristics of timber material properties are

assessed and treated in consistency with the implemented quality control and grading procedures. Only then a consistent basis may be established for the quantification of the reliability of timber structures - the basis for codification of design and assessment. The suggested probabilistic modelling seems to provide the required framework for establishing such a basis by means of quantifying the efficiency of the different quality control and grading procedures. It is envisaged that different quality control grading procedures may be described by means of their regression characteristics and acceptance probability curves corresponding to different grading criteria. A format for the standardisation of the probabilistic modelling of timber materials subject to different quality control and grading procedures is suggested. It is important that the appropriateness of such a format is discussed and that a consensus is achieved in this respect in the near future.

In section 4.2.3.4 it has been demonstrated how an optimal (in terms of monetary benefit) set of timber grades can be identified through the solution of an optimisation problem. The objective function of the optimisation problem is defined based on the findings of section 4.2.3.2. The identified timber grades can be described by means of the probabilistic characteristics of the relevant material properties as e.g. the bending strength, the bending modulus of elasticity and the density of the timber. The simplex algorithm for the optimisation of non-differentiable objective functions in conjunction with a simulation procedure has been applied for the identification of the optimal grading procedure. The constraints to the optimisation problem, in terms of the requirements for timber grades according to EN 338 have been incorporated directly into the objective function.

An example has been presented illustrating the suggested approach to cost optimal timber grading. The assignment of monetary benefit to the different grades of timber has, however, been based on judgement rather than true values. In practice the benefit associated with timber of a particular grade would depend on a number of factors such as the size of the individual timber specimen, the total amount of available timber for a given grading, the production capacity of a given sawmill, the available grading machines and not least the market price for the different timber grades. The implementation of the proposed approach in practice would have to incorporate these and other factors more accurately into the formulation of the benefit function. Further studies in close collaboration with the timber industry should be undertaken and discussed to clarify these aspects and to set up a rational basis for their assessment. However, according to the preferences of a sawmill owner the proposed approach facilitates the identification and the calibration of a grading procedure and thus an increase in the overall production benefit.

4.2.4   WITHIN MEMBER VARIATIONS – MICRO SCALE VARIATIONS

For modelling the variations of strength related timber material properties within a component, the variability on a micro scale has to be taken into account. In general, assumptions about the micro system behaviour of the material are providing guidelines for the

development of stochastic material models. Two classical probabilistic strength models can be found in the literature: the ideal brittle material model and the ideal plastic material model.

4.2.4.1 Classical Probabilistic Strength Models

Ideal Brittle Material

An ideal brittle material is defined as a material that fails if a single particle fails, see e.g. Bolotin (1969). The strength of the material is thus governed by the strength of the 'weakest' particle; therefore the model for ideal brittle materials is also called the weakest link theory proposed by Weibull (1939). If the strength X of the individual particles are assumed to be mutually independent and identically distributed with distribution function $F_X(x)$, the distribution function of the strength R of a body with nv_{Vol} identical loaded particles[1] is:

$$F_R(x) = 1 - \left(1 - F_X(x)\right)^{nv_{Vol}} = 1 - \exp\left(nv_{vol} \ln\left(1 - F_X(x)\right)\right) \tag{4.21}$$

The behaviour of $\ln\left(1 - F_X(x)\right)$ for small arguments can be represented as:

$$\ln\left(1 - F_X(x)\right) \cong -c\left(x - x_0\right)^k; \quad x \geq x_0 \tag{4.22}$$

where x_0 is the smallest possible value of x, c and k are positive constants. Equation (4.21) now can be written as:

$$F_R(x) = 1 - \exp\left(-cnv_{vol}\left(\left(x - x_0\right)^k\right)\right) \tag{4.23}$$

Considering an isotropic solid under a homogeneous stress distribution and by introducing a reference volume $v_{Vol,0}$, e.g. the volume of standard test specimen substituting by $cn = 1/v_{Vol,0} w^k$ in (4.23) gives:

$$F_R(x) = 1 - \exp\left(-\frac{v_{Vol}}{v_{Vol,0}}\left(\frac{x - x_0}{w}\right)^k\right) \tag{4.24}$$

which is the expression of a 3-parameter Weibull distribution. w is called the shape parameter and k the scale parameter. The expected value $E[R]$ and the variance $Var[R]$ of R can be given as:

$$E[R] = x_0 + w\Gamma\left(1 + \frac{1}{k}\right)\left(\frac{v_{Vol}}{v_{Vol,0}}\right)^{-1/k} \tag{4.25}$$

---

[1] n particles of finite volume v_{Vol}.

$$\text{Var}[R] = w^2\left(\Gamma\left(1+\frac{2}{k}\right) - \Gamma^2\left(1+\frac{1}{k}\right)\right)\left(\frac{v_{Vol}}{v_{Vol,0}}\right)^{-2/k} \tag{4.26}$$

where $\Gamma(.)$ is the gamma distribution.

The expected value function decreases with the considered volume v_{Vol} and for $x_0 = 0$ the coefficient of variation is independent of v_{Vol}. The size effect is observed for many brittle materials such as hardened steel, concrete and stiff clay. The coefficient of variation and the correlation of the strength of the reference volumes $v_{Vol,0}$ determine the importance of the volume effect.

Assuming unique failure probability for two material bodies with different volumes $v_{Vol,1}$ and $v_{Vol,2}$ gives the following expression:

$$F_R\left(x_1, v_{Vol,1}\right) = 1 - \exp\left(-\frac{v_{Vol,1}}{v_{Vol,0}}\left(\frac{x_1-x_0}{w}\right)^k\right) = 1 - \exp\left(-\frac{v_{Vol,2}}{v_{Vol,0}}\left(\frac{x_2-x_0}{w}\right)^k\right) = F_R\left(x_2, v_{Vol,2}\right) \tag{4.27}$$

which results in:

$$\frac{x_2-x_0}{x_1-x_0} = \left(\frac{V_1}{V_2}\right)^{1/k} \xrightarrow{\ x_0=0\ } \frac{x_2}{x_1} = \left(\frac{V_1}{V_2}\right)^{1/k} \tag{4.28}$$

Equation (4.28) can directly be used to compare the load bearing capacity of different volumes for loading modes resulting in constant stress fields and brittle failure modes.

If an inhomogeneous stress distribution can be considered by introducing the stress $s\left(\xi_1, \xi_2, \xi_3\right)$ as a product of a reference stress s, (e.g. the maximum stress in the body) and a dimension free function $h\left(\xi_1, \xi_2, \xi_3\right)$, the probability distribution function of the strength r of the body can be written as:

$$F_R\left(x\right) = 1 - \exp\left\{-\frac{1}{v_{Vol,0}}\int_{xh(\xi_1,\xi_2,\xi_3)>x_0}\left(\frac{xh\left(\xi_1,\xi_2,\xi_3\right)-x_0}{w}\right)^k dv_{Vol}\right\} \tag{4.29}$$

Equation (4.29) is utilised in Johnson (1953) to compare the mean strength of beams with various support and loading conditions and standard deviation of reference strength. A graphical representation of the result of these calculations is presented in Figure 4-14. The ordinate in the figure is the mean strength of the beam normalised to the strength of a beam loaded by a constant bending moment. It is seen that the mean strength of beams exposed to other load configurations is larger and also depending on the coefficient of variation of the material strength.
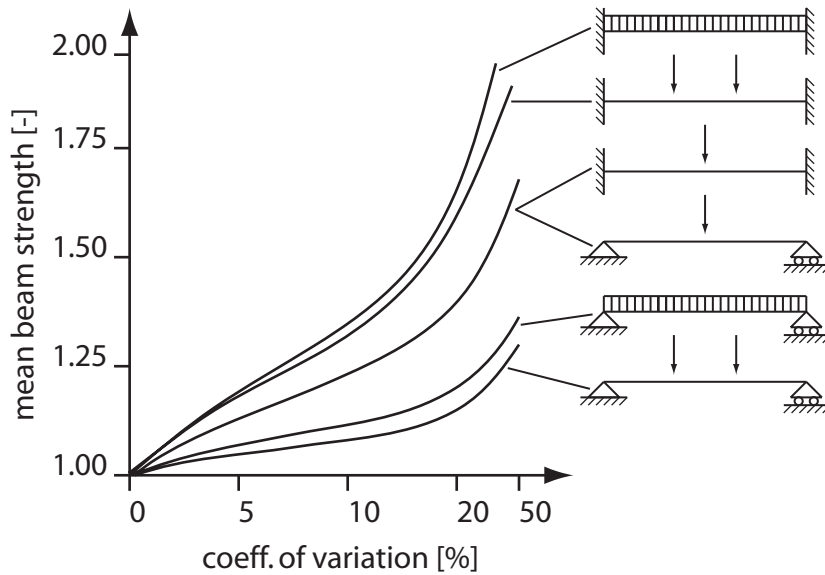
Figure 4-14   Comparison of mean strength of rectangular beams with various loading conditions and standard deviation of reference volume strength, from Johnson (1953).

Ideal Plastic Material

In an *ideal plastic material* a particle yields when reaching its maximum capacity (yield load), i.e. a particle is still capable of carrying the yield load but further load increments are transferred to other particles in the loaded material body. The maximum load is reached when yielding takes place in all particles in a cross section. The strength R of an ideal plastic material is thus equal to the sum of the strength R_i of the yielded particles. The cross section strength is:

$$R = \sum_i R_i \tag{4.30}$$

When the number of particles is large and the dependency between the particle strength is sufficiently low, the distribution of R converges to a normal distribution due to the central limit theorem.

The sum can be approximated by the integral:

$$R = \int_{a_{are}} s_u^*(\xi_1, \xi_2)\, da_{are} \tag{4.31}$$

where $s_u^*(\xi_1, \xi_2)$ is the yield stress at (ξ_1, ξ_2).

4.2.4.2   Timber Material as an ideal brittle material

Over the last 40 years, the ideal brittle material model has been widely applied to study the tension, bending, bending shear and compression strength variability of various wood products including sawn and glued laminated timber. However, whenever the theory is

utilised to explain some observed phenomena, inconsistencies to the theory have been noticed. In Bohannan (1966) one of the first studies is published, showing that size effects and load configuration effects on the bending strength could be explained by the weakest link theory for brittle materials. Clear wood specimens of different size and loading configurations are analysed. It is shown that increasing length or depth causes a decrease in bending strength but the bending strength is independent of the width of the specimen. Inductively, it is concluded that bending members do not exhibit a perfectly brittle material behaviour upon which the weakest link theory is based. In Madsen and Stinson (1982), the width effect on the bending strength of structural timber is studied. Their results suggest that bending strength increases as the member width increase, which is contrary to the concept of a weakest link fracture process. It is suggested in Madsen and Buchanan (1986) that this inconsistency could result from visual grading rules which limit knot sizes on the wide and narrow faces of the member. These rules tend to limit the maximum size of knots for a fixed member depth independent of member width. In the same study it is suggested to consider size effects on the strength of timber separately depending on every single dimension of the member. According to Equation (4.32) it is distinguished between length, width and depth effect:

$$\frac{r_{m,2}}{r_{m,1}} = \left(\frac{l_1}{l_2}\right)^{1/k_l} + \left(\frac{b_1}{b_2}\right)^{1/k_b} + \left(\frac{d_1}{d_2}\right)^{1/k_d} = \left(\frac{l_1}{l_2}\right)^{m_l} + \left(\frac{b_1}{b_2}\right)^{m_b} + \left(\frac{d_1}{d_2}\right)^{m_d} \tag{4.32}$$

where l is the length, b is the width and d is the depth of the specimen; r_m is the bending strength property of the specimen.

A similar distinction is made in a study of the size effect on the tension strength, Madsen (1992). In that comprehensive research project, specimen of different sizes, grades and species are analysed. Equation (4.32) is utilised to quantify m-values for two different fractile values of the underlying probability distribution functions of the tension strength. The following values are suggested, Madsen (1992):

Length effect: 50%-Fractile $m_l = 0,20$

                   10%-Fractile $m_l = 0,15$

Width[1] effect: 50%-Fractile $m_b = 0,15$

                   10%-Fractile $m_b = 0,10$

For tension perpendicular to the grain a nearly perfect agreement with the weakest link theory can be observed. In Barrett (1974) the work of several authors is reviewed and summarised. Data from clear wood specimens, structural timber and glued laminated timber is brought in

---

[1] For tension specimen the width refers to the wide face of the cross section.

one context.

Furthermore, in Barrett et al. (1975) and subsequently in Colling (1986) the perfectly brittle material model is successfully applied to model tension perpendicular to the grain failure modes in curved and pitched tapered beams and connections. These studies confirm that the Weibull model has wide application in modelling of wood fracture especially for tension perpendicular to the grain. In Foschi and Barrett (1975) and in Colling (1986) it is confirmed that shear strength of beams varies with member size and the effects are quantified by using the ideal brittle material model.

In Madsen (1992) it is shown that the bending strength of sawn timber of constant thickness varies with member length and loading condition in a manner consistent with the ideal brittle material model (Equation (4.28) and (4.29)). Further, tension and compression tests with different lengths are analysed. The length dependencies are quantified with the shape parameter k (compare Equation (4.28)); for tension and bending similar values are derived, $k_{tension} = k_{bending} = 5$, and for compression $k_{compression} = 10$ is established. In Barrett and Fewell (1990) Canadian, US and European species data is analysed and length effect factors for bending and tension are derived by also using the ideal brittle material model. Similar values for bending and tension are found; $k_{tension} = k_{bending} = 5.9$. An important result of these studies is the observation that length effects in tension and bending are very similar; i.e. inductively it could be concluded that the bending and tension strength of structural timber is both governed by the ultimate tension strength. On the other hand in Rouger and Fewell (1994) it is found that 60-90% of the bending specimens considered in this study showed ductile failure mode governed by the compression side.

In Larsen (1986) and Colling (1986) a formulation based on Equation (4.29) is utilised to investigate the stress distribution effect on the shear strength and the tension perpendicular strength of curved and tapered beams.

There is an ongoing list of further literature and many applications of the ideal brittle material model for timber can be found. However, the results of these investigations are delivering partly contrary results. Contrary in regard to the value of quantified parameters as e.g. the scale parameter k, but also in regard to the observed phenomena. This can be explained by the variability of the timber material at a macro scale, i.e. different species and grades exhibit different size effects (Rouger and Fewell (1994)); but also by the fact that the assumptions underlying the theory of brittle fracture are not strictly fulfilled when considering timber. Timber is referred to as an orthotropic material; strength and stiffness properties are depending on the stress direction in a timber solid. Therefore the theory can only be used for individual loading modes for which the stress direction can be assumed to be constant, i.e. timber components loaded to tension perpendicular or parallel to the grain, shear along the grain or pure bending of beam shaped timber specimen. The latter loading mode includes tension and compression and has to be considered with caution because the failure mode in compression is not brittle. The material irregularities are in the scale of μm if the fibre

configuration is considered or in the scale of *dm* when considering major defects as knots and grain deviations[1]. The latter ones are almost in the same scale as structural components, which is in conflict of the assumption of 'a big number of defects, identical distributed and independent' – the material is not statistically homogeneous.

In summary it can be concluded that the ideal brittle material model can be used in some cases as an empirical model basis which describes the major phenomenon, but where the parameters, i.e. scale and shape parameters do not have any physical meaning; but can be derived by fitting to experimental data. Especially for tension perpendicular to the grain the physical deviations to the initial theory seem to be small.

4.2.4.3 Weak section models for special load cases for timber structural elements

A typical timber structural element is of beam shape which means that its longitudinal extension is much larger than its transversal extensions and the main fibre direction is orientated along the longitudinal (main) axis of the element. These elements are mainly loaded in tension, compression and/or bending along the main axis. According to the inhomogeneous structure of these elements due to major defects such as knots and grain deviations, the direct application of the ideal brittle material model is questionable. Therefore, an alternative model for the variation of strength and stiffness related material properties is desirable. In regard to the variation of the modulus of elasticity (MOE) several references can be found in the literature, see e.g. in Corder (1965), Kass (1975), Suddarth and Woeste (1977) and Foschi and Barrett (1980). In Kline et al. (1986) a probabilistic approach to describe the lengthwise variation of bending stiffness is introduced. As illustrated in Figure 4-15 timber beams are divided in segments of identical length and the stiffness of segment 2 to segment $n-1$ is measured with a 4-point bending test. The correlation between the MOE_i's of the different segments is investigated and quantified by the so-called *Lag-k* serial correlation. The *Lag-k* serial correlation is the correlation of an observation from segment i and an observation from segment $i+k$; e.g. if $k=2$, *Lag-k* means the correlation of the MOE of segments 2 and 4 or of the segments 3 and 5 etc. For realisations of the $MOE = X$; $x_1, x_2, x_3, ..., x_n$ the *Lag-k* serial correlation ρ_k is defined as:

$$\rho_k = \frac{\sum_{i=1}^{n-k}(x_i - \bar{x})(x_{i+k} - \bar{x})}{\sum_{i=1}^{n}(x_i - \bar{x})^2} \tag{4.33}$$

with $\bar{x}$ being the sample mean value of X . It is found that the serial correlation decreases with increasing k . The lengthwise variation of X is modelled by a second order Markov model as:

---

[1] Grain deviation is defined as in section 3.3.1.2.

$$X_{i+1} = \beta_0 X_i + \beta_1 X_{i-1} + \varepsilon_{i+1} \tag{4.34}$$

where β_i, $i = 1, 2$ are regression parameters and ε is the vector of random errors, the components are assumed to be normal distributed with mean value 0 and unknown standard deviation.

Similar approaches are utilised to describe the lengthwise variation of tension and bending strength. Obviously only every second section can be tested destructively (compare Figure 4-15). In Showalter et al. (1987), Lam and Varoglu (1991) and Taylor and Bender (1991) the tension strength is considered, in Czmoch (1991) the bending strength is considered; all studies find decreasing serial correlation with increasing k.
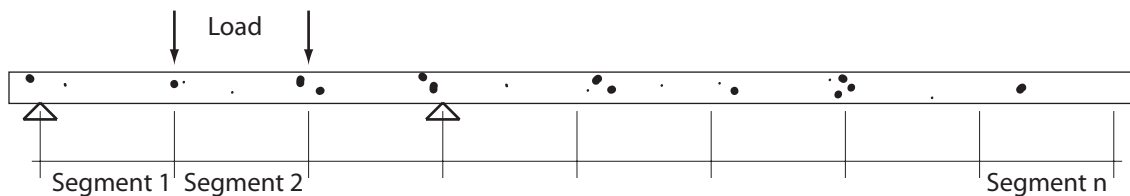
Figure 4-15   Separation in segments and test arrangement.

As seen in Figure 4-15 the regular segmentation does not facilitate the explicit consideration of observable irregularities in the beams. Examples for such observable irregularities are knots and knot clusters. In Riberholt and Madsen (1979) it is observed that low bending strength and bending stiffness coincides with the presence of knots and knot clusters. In this study it is assumed that failure can only occur at such weak sections and due to the discrete distribution of knots and knot clusters an idealised model is proposed in terms of discrete weak sections separated by strong sections – sections of clear wood, see Figure 4-16. Furthermore equicorrelation of the strength of weak sections is assumed, which means that the correlation between the strength of weak sections is independent on their distance over the length of the beam.
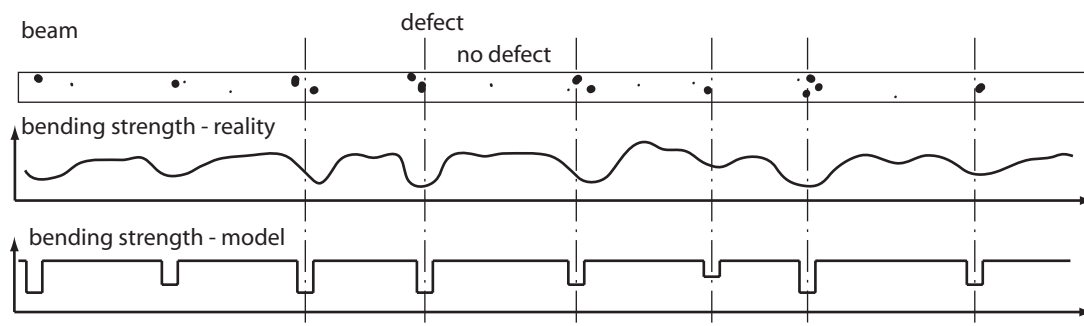
Figure 4-16   Bending strength of a timber beam; implied reality and as in the proposed model (Riberholt, Madsen (1979)).

Failure of one single weak section is determining the strength of the entire component and consequently the component can be modelled as a series system of weak sections. The strength of the weak section is described by a random variable whereas the location of the weak sections is modelled as an arrival 'time' of a Poisson process. The parameters of the Poisson process are estimated by direct measurements of the distances of knots and knot clusters. The parameters of the distribution function of the weak section strength is estimated indirectly; through measurements of the bending stiffness as an indicator for bending strength or by existing bending strength tests according to EN 408.

The proposed model for the variation of bending strength properties is investigated by Czmoch et al (1991). Here the length and load configuration effect of beams is studied and it is found that the available experimental information to verify the parameters of the proposed model is insufficient. This problem is considered in Isaksson (1999).

Following Isaksson (1999) the variability in bending strength within and between members can be modelled as:

$$\ln\left(r_{m,ij}\right) = v + \varpi_i + \chi_{ij} \tag{4.35}$$

where,

$r_{m,ij}$ is the strength of weak section j in component i.

v is the logarithm of the mean strength of all weak sections of all components.

ϖ_i is the realisation of the difference between the logarithm of the mean of the strength of the sections within a specific component i and v. ϖ is modelled by a normal distributed random variable with zero mean and standard deviation equal to σ_ϖ.

χ_{ij} is the realisation of the difference between the strength of weak section j in component i and $v + \varpi_i$, i.e. the variability within one particular component in one particular population. χ is modelled by a normal distributed random variable with zero mean and standard deviation equal to σ_χ.

Based on experiments with Norwegian spruce, the following random variables of the model are quantified:

Distance between weak sections

It is assumed that the weak sections (and correspondingly the number of weak sections) are distributed spatially according to events of a Poisson process X_i along the longitudinal axis of the component. Following this assumption the distances between the weak sections are exponentially distributed. However, due to the experimental evidence it is found that the Gamma distribution fits better to the data. The parameters of the Gamma distribution are given as: $\Gamma\left(2.55,194\right)$.

Length of weak sections

The length of the weak sections, i.e. the length of a knot cluster, is assumed to be constant with $150 mm$.

Bending strength of weak sections

Based on 673 observations the random variables from Equation (4.35) are quantified with the parameters as given in Table 4-13 (Isaksson (1999)).

Table 4-13   Parameters for the bending strength of weak sections according to Equation (4.35).

	ν	ϖ [Normal]	χ [Normal]
μ	4.03038	0	0
σ	0.24773	0.18747	0.16194

The model is illustrated in Figure 4-17.
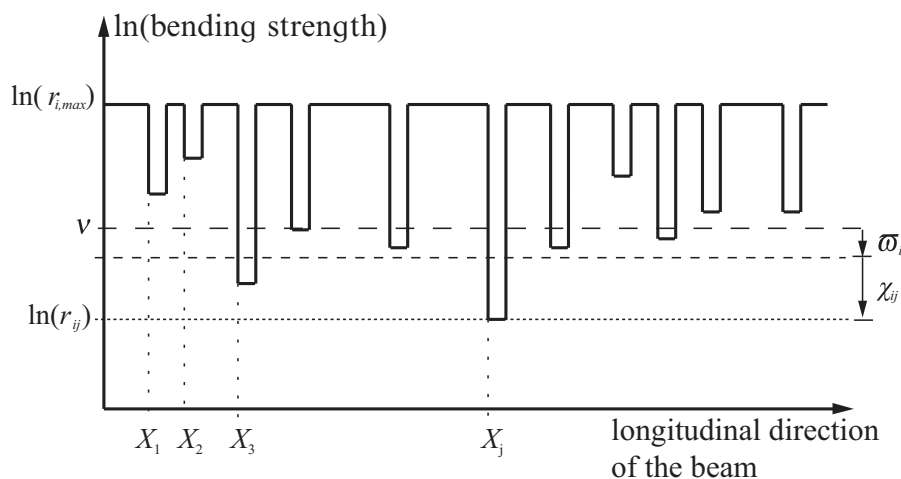
Figure 4-17   Modelling of the longitudinal variation of bending strength of a timber beam, Isaksson (1999).

Bending strength between weak sections

In Isaksson (1999) it is assumed that the strength of the strong sections is equal to the strength of the strongest weak section in the component.

A similar study on the lengthwise variation of bending strength is reported in Källsner and Ditlevsen (1994, 1997), Ditlevsen and Källsner (2004). Out of 26 beams 197 weak sections are identified and tested in regard to their bending strength by cutting them out, finger joining them between two pieces of stronger wood and testing them in a four point bending arrangement. A particular feature of this study is that unintentionally a large fraction of the test specimen did not fail in the section of interest, i.e. failure took place in the finger joints or

in the stronger wood. Due to the censored data special methods are introduced to consider the observations properly. However, the results are in general consistent with the results presented in Isaksson (1999). A hierarchical model is introduced with two levels to represent the variation of bending strength within and between members. The $Lag-k$ correlation is found to be constant, i.e. equicorrelation is assumed. The model proposed by Isaksson in Equation (4.35) can be interpreted as a two level hierarchical model if v is assumed to be constant. A closed form analytical expression for the distribution function of the bending strength with any given number of weak section is presented and the derivation is summarised in the following.

The ultimate strength of a timber component containing j weak sections and loaded with a constant load effect is defined by:

$$r_{m,i,\min} = \exp\left(\omega_i + \min\left\{\chi_{i,1}, \chi_{i,2}, ..., \chi_{i,j}\right\}\right) \tag{4.36}$$

with $\omega_i = v + \varpi_i$, compare Equation (4.35).

The probability distribution function $F_{\ln(R_m)}\left(z\mid j\right)$ of the logarithm of the ultimate bending strength $\ln(r_m) = z$ conditional on j, the number of weak sections, becomes:

$$F_{\ln(R_m)}\left(z\mid j\right) = P\left(\omega + \min\left\{\chi_1, \chi_2, ..., \chi_j\right\} \le z\right) = \frac{1}{\sigma_\omega} \int_{-\infty}^{\infty} \left[1 - \Phi\left(-\frac{z-x}{\sigma_\chi}\right)\right]^j \varphi\left(\frac{x-\mu_\omega}{\sigma_\omega}\right) dx \tag{4.37}$$

If j is considered as a discrete random variable with probability p_j, the probability distribution function becomes:

$$F_{\ln(R_m)}\left(z\right) = \sum_{j=0}^{\infty} F_{\ln(R_m)}\left(z\mid j\right) p_j = 1 - \frac{1}{\sigma_\omega} \int_{-\infty}^{\infty} E\left[\Phi\left(\frac{x-z}{\sigma_\chi}\right)^J\right] \varphi\left(\frac{x-\mu_\omega}{\sigma_\omega}\right) dx \tag{4.38}$$

with $E\left[\Phi\left(\frac{x-z}{\sigma_\chi}\right)^J\right] = \sum_{j=0}^{\infty} \Phi\left(\frac{x-z}{\sigma_\chi}\right)^j p_j$

which can be expressed by the so-called probability generating function $\psi(y) = E\left[y^J\right]$ of the integer random variable J. For J following a Poisson distribution with parameter λl the probability generating function is $\psi(y) = \exp\left(\lambda l(y-1)\right)$ in which case Equation (4.38) becomes:

$$F_{\ln(R_m)}\left(z\right) = 1 - \frac{1}{\sigma_\omega} \int_{-\infty}^{\infty} \exp\left[-\lambda l \Phi\left(\frac{z-x}{\sigma_\chi}\right)\right] \varphi\left(\frac{x-\mu_\omega}{\sigma_\omega}\right) dx \tag{4.39}$$

where l is the length of the considered component. Equation (4.39) is the probability distribution function of the logarithm of the bending strength of a component of length l.

4.3   DURATION OF LOAD EFFECTS

One of the distinctive characteristics of timber is that its strength is influenced by the intensity and the duration of the applied stresses. Although this phenomenon is similar to that of fatigue in metals, strength degradation in timber is observed even under static (permanent) loading. This effect is referred to as the duration of load (DOL) effect. Numerous experimental programs have focused on the investigation of the DOL effects in clear wood specimen and later on also in full size timber components. A variety of models have been proposed to describe the phenomenon. Hereby, it has been mainly focused on the duration of load effect of bending specimen. Some of the proposed models have a physical hypothesis of the phenomena as a basis; however, they all consist of variable model parameters which can be calibrated to observed experimental data.

4.3.1   ASSESSMENT OF DURATION OF LOAD EXPERIMENTAL DATA

The assessment of the DOL phenomenon by experimental data introduces a variety of challenging research problems. First of all by the nature of the problem, experiments involve long periods of time, are therefore costly and consequently rare. To reduce costs, the test configurations are rather simple, i.e. in general a constant (dead) load or a ramp-load is applied and time until failure is measured. A typical bending duration of load test configuration is the three- or four-point bending test as illustrated in Figure 4-18. Also illustrated in Figure 4-18 are the typical stress histories for short-term tests, long-term tests and impact load test.

In a short-term test, the stress is applied with a constant rate k_R, which in general is kept constant within the entire test program. k_R is calibrated so that the time to failure stays within some pre-defined limits; e.g. according to the test standard ISO 8375 failure should take place after t_s = 300 seconds +/- 120 seconds. If, for example, k_R is chosen such that in average the short-term bending test duration is 300 seconds and the coefficient of variation of the short-term bending strength is 25%, the test duration for a specimen with a low bending strength, say a value similar to the 5%-fractile value is only 176 seconds (300 - 124 seconds); i.e. the time limit from ISO 8375 would be violated.

In a long-term test the specimens are loaded with a constant stress $\hat{s}$ over a period of time and the time until failure t_f is measured. Therefore, the specimens have to be loaded at the beginning of the test. In general, this can be done by applying any specified load rate; often the same constant rate k_R as in the short-test (as illustrated in Figure 4-18) is applied. Or the stress is applied instantly, i.e. with a very large rate which in general is not specified.

The third type of duration of load test is the impact loading test. In this type of test the loading rate is greater than for shot- term tests, $k_I > k_R$ and the time to failure t_I is measured.
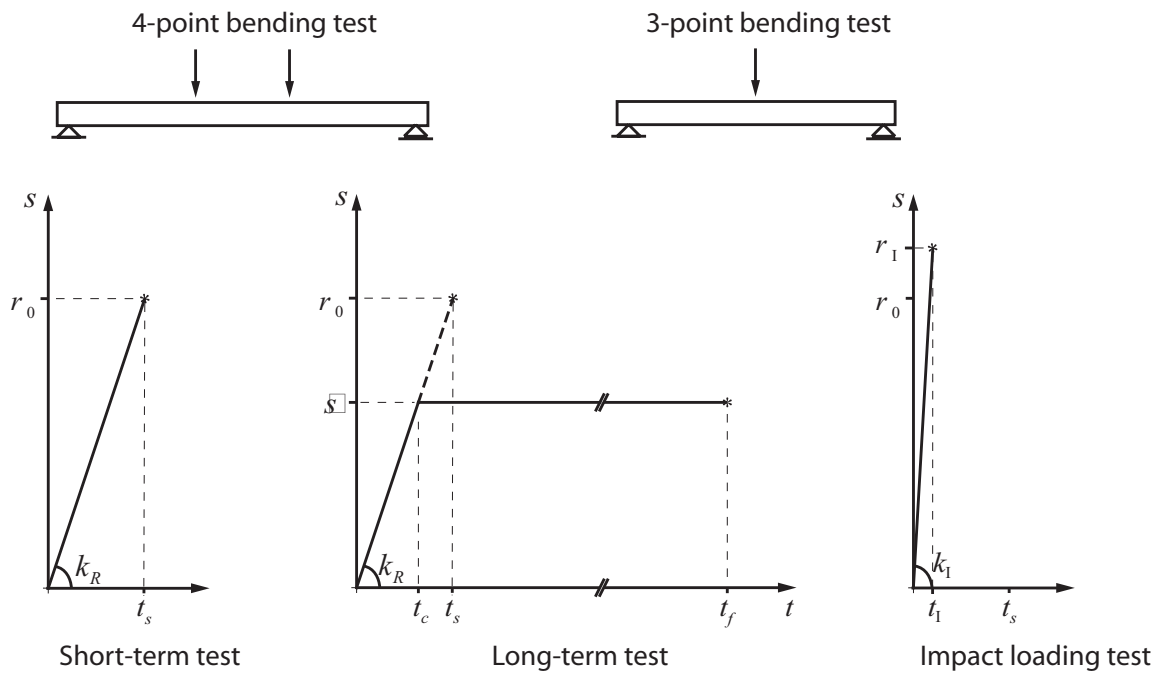
Figure 4-18   Stress history used in test set up; short-term and long-term tests and impact loading test.

The short-term strength r_0 is in general the reference property, i.e. the focus of duration of load experiments is for how long a specimen can sustain a constant fraction of its short-term strength. The ratio $\hat{s}/r_{0,i}$ is therefore of importance. Similarly, impact loading tests focus on measuring $r_{I,i}$ which is then expressed as the ratio $r_{I,i}/r_{0,i}$.

Obviously, $r_{I,i}$, $\hat{s}$ and $r_{0,i}$ cannot be measured for the same specimen and since the applied constant stress $\hat{s}$ respectively the impact load capacity $r_{I,i}$ are the targets, the short-term strength $r_{0,i}$ must be estimated indirectly. Several methods have been applied to overcome this problem.

One method does not rely on the comparison of $r_{I,i}$, $\hat{s}_i$ and $r_{0,i}$ of individual specimen, but in the comparison of average values of $r_{I,i}$, $\hat{s}_i$ and $r_{0,i}$ at average time to failures. This method is applied in Wood (1949) for the analysis of data from short-term, long-term and impact load tests and in Hanhijärvi et al. (1998) for the analysis of data from short-term and long-term tests.

Another method is pair matching, which is undertaken by sampling specimens in pairs cut out of the tree next to each other and therefore implying similar properties. One specimen is then tested in a short-term test while the other is long-term loaded. The method is mainly applied for clear wood specimen free of knots and other irregularities, but still has to allow for substantial short-term strength differences between the two specimens (Hoffmeyer (1990)). For structural timber, the pair matching method is assessed in Norén (1986). Pairs of specimens are obtained by very carefully placing the saw cut not only through the pith of a piece of timber, but even divide the critical knots into equally sized halves. However, short-term test on the paired specimen confirm that it is not possible to find a method for pair

85

matching timber with sufficient accuracy by applying this technique.

The predominant approach for estimating the short-term strength of duration of load test specimen is based on the so-called equal rank assumption. This method is e.g. applied in Madsen (1992). An adequate number n of specimen is assessed in regard to a strength related property which has to be measured non-destructively, e.g. machine grading indication or knot size measures. The measurements ι_i are ranked in ascending order, so that $\iota_1 \leq \iota_2 \leq \iota_3 \leq ...\iota_n$. The specimens are now sub-divided into two groups with similar distribution of the strength related properties, e.g. one group with $\left(\iota_1, \iota_3, \iota_5, ..., \iota_{n-1}\right)$ and the other group containing $\left(\iota_2, \iota_4, \iota_6, ..., \iota_n\right)$ given that $n/2 \in \mathbb{N}$. Now it is assumed that both groups have also similar bending strength distributions. One group – the short-term group – is tested in a short-term bending strength test, while the other group – the long-term group – is long-term loaded to a specific percentile of the short term strength distribution. Some of the specimens fail before the constant load level is reached. The specimens which survive the duration of the long-term test are taken to be tested in a short-term strength test. The strength measurements of the short-term group $r_{0,i}$ are ranked in ascending order, so that $r_{0,1} \leq r_{0,2} \leq r_{0,3} \leq ...r_{0,n/2}$. The time to failure measurements $t_{f,i}$ of the long-term group are also ranked in ascending order, so that $t_{f,1} \leq t_{f,2} \leq t_{f,3} \leq ...t_{f,n/2}$ (note that in general, the first time to failure measurements already take place in the ramp-load phase of the long duration test). In Figure 4-19 the strength measurements of the specimen of both groups are plotted against their rank. The basic idea of the equal rank assumption is that a specimen from the long-term group of rank i (failed at time $t_{f,i}$) has the same short term strength as the specimen of the short-term group with rank i, $r_{0,i}$. Following this assumption it is possible to express the so-called stress level sl_i as the ratio of the applied constant stress $\hat{s}$ and the expected short-term strength $r_{0,i}$:

$$sl_i = \frac{\hat{s}}{r_{0,i}} \tag{4.40}$$

In Figure 4-20 the stress levels for the specimen of the long-term group are estimated according to Equation (4.40) and plotted against the logarithm of the time to failure $\log_{10}\left(t_f\right)$.

In Figure 4-20 the common representation of duration of load data is illustrated. Many DOL models are represented in form of the stress level as the function of time to failure. Typically the data points are arranged on a string, which is the consequence of the equal rank assumption. The shape of the data string does not necessarily reflect the DOL behaviour of the single specimens; it may only reflect the DOL behaviour of the particular distribution of the considered sample, i.e. specimen within the sample which have a low quality and therefore have a low short-term strength always sustain a high stress level and fail after relatively short time, specimen with high quality have to sustain a low stress level and fail after relatively long time (Hoffmeyer (1990)).
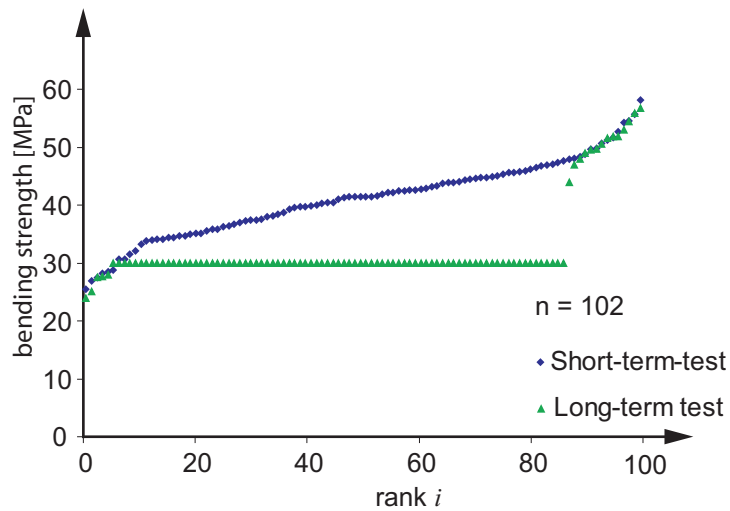
Figure 4-19   *Strength measurements from short-term and from long-term tests plotted against their rank (the data for this figure is taken from Hoffmeyer (1990)).*
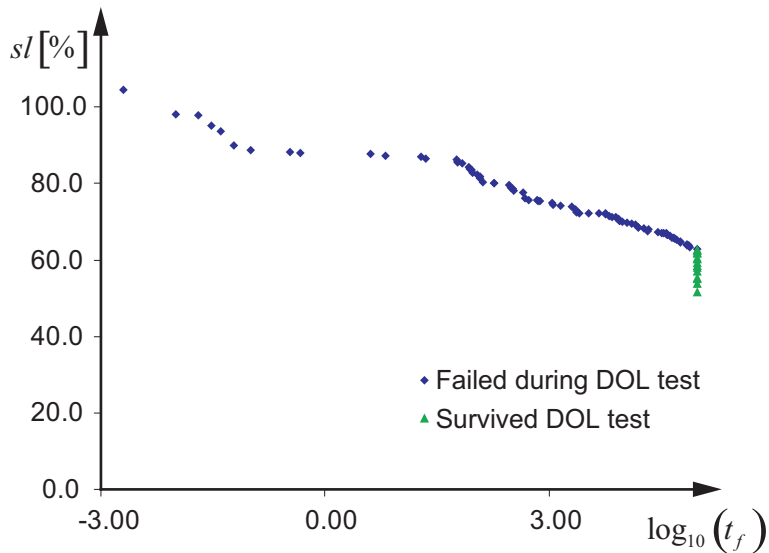
Figure 4-20   *Stress level in [%] against logarithmic time to failure in [log(hours)] (the data for this figure is taken from Hoffmeyer (1990)).*

4.3.2   MODELLING THE DURATION OF LOAD EFFECT

Several models for describing the duration of load effect for timber and timber materials can be found in the literature. Some of them have a conceptual framework from some physical mechanism leading to failure over time as a background; others are just empirically derived to represent DOL test data. The models can be divided into the following groups:

- Empirical formulations for time to failure. The parameters of simple mathematical formulations are fitted to DOL test results.

- Cumulative damage theories. A damage state variable without any precise physical

definition is introduced. Empirical parameters are fitted to test results. The models and their parameters are conditional on loading mode (e.g. bending, compression).

- Fracture mechanics. Relative damage is defined as the growth of cracks. Model parameters have direct physical meaning.

- Deformation kinetics. Rupture is completely determined by the magnitude and nature of deformation preceding rupture.

- Energy based models. Failure is defined as the excess of critical strain energy.

In the following sections all the different modelling approaches are briefly reviewed and the most relevant references are given.

4.3.2.1   Empirical Representation of time to failure – the Madison Curve

The so-called Madison curve (Wood (1951)) is formulated on the basis of results from laboratory tests on clear wood bending specimens, i.e. specimens, with no visible defects, exposed to loads of constant intensity. The aim of this model is to cover the effect of relatively long load durations and the effect of very short load durations. Therefore, data bases from several resources are pooled together to obtain a model capable to cover a duration of load ranging from 0.015 seconds to 156 days. The Madison curve is an empirical curve describing the stress level sl (see Equation (4.40)) as a function of the time to failure t_f. The curve is calibrated to three pre-selected points representing average values derived from several test programs:

- The short-term strength is defined as the failure load of a specimen loaded in a ramp load test with a corresponding average time to failure of 7.5 minutes. Correspondingly, the stress level is 100% at 7.5 minutes.

- From impact loading tests it is found that the average stress level sl of specimen loaded in a very fast ramp-load test of the duration of 0.015 seconds is 150%.

- From long-term loading tests it is found that the average stress level sl of specimen loaded in a constant load test of the duration of 156 days is 69%.

The resulting curve has the equation:

$$sl = 18.3 + 108.4 \, t_f^{-0.0464} \tag{4.41}$$

where sl is the stress level and t_f is the time to failure in seconds. The Madison curve is often taken as a reference for the duration of load effect for clear wood but also for structural timber.

In Pearson (1972) data from several investigations is reviewed, whereas it is focused solely on long-term data. Based on the analysis of the data an alternative formulation is found:

$$sl = 91.5 + 7 \, \log\left(t_f\right) \tag{4.42}$$

where t_f is the time to failure in hours.

In Figure 4-21 Equations (4.41) and (4.42) are compared. The models differ especially for very long durations of loading time. The up bend of the Madison curve can not be confirmed by explicitly considering long-duration data. Therefore the Pearson curve should be taken as a reference for the long-term DOL effect in clear wood.
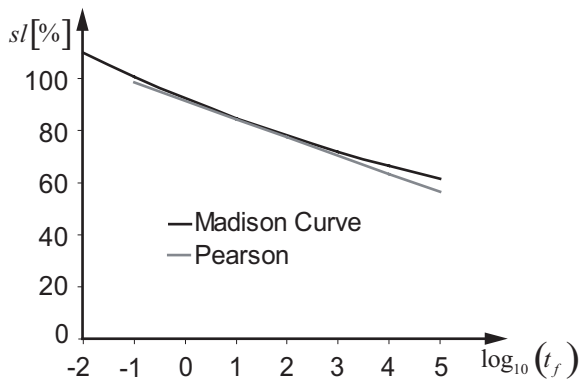
Figure 4-21   *Models for the DOL behavior of clear wood; the so-called Madison curve (Wood (1951), Equation (4.41)) and a model following Pearson (1972), Equation (4.42) represented in a stress level – log(time) diagram. (time in hours).*

4.3.2.2   Damage Accumulation Models

A major part of the models for describing the duration of load effect for timber involve a damage state variable to assess damage accumulation in timber structural members subject to their loading histories. These models are referred to as damage accumulation models. It should be noted that damage in the context of the damage accumulation models does not refer to a quantity with a direct physical interpretation; damage is simply deducted from the time to failure recordings of long-term loading experiments under a given loading history. However, possible interpretations could range from the creation and the propagation of micro cracks in the material, the increase of material porosity, local fibre buckling, the destruction of molecular bonds, some other irrecoverable process or a combination of these. (Hoffmeyer in Thelandersson and Larsen (2003)).

In general, damage is expressed by a damage state variable α_D, where $\alpha_D = 0$ is equivalent with no damage and $\alpha_D = 1$ is associated with full damage or failure. Damage accumulation models are usually given as rate equations of damage over time $d\alpha_D/dt$, as:

$$\frac{d\alpha_D}{dt} = h\left(s(t), r_0, \boldsymbol{\theta}\right) \quad \text{for} \quad 0 \leq \alpha_D \leq 1 \tag{4.43}$$

where $h(.)$ is a function of the applied stress $s(t)$, the short term strength r_0 and model

parameters $\boldsymbol{\theta}$; or:

$$\frac{d\alpha_D}{dt} = h\big(s(t), r_0, \alpha_D, \boldsymbol{\theta}\big) \quad \text{for} \quad 0 \le \alpha_D \le 1 \tag{4.44}$$

where $h(.)$ is a function of the applied stress $s(t)$, the short term strength r_0, the actual damage state α_D and model parameters $\boldsymbol{\theta}$.

The first damage accumulation model is proposed in Gerhards (1979), where the rate of damage accumulation is expressed as a function of the applied stress (equivalent to Equation (4.43)). Initially, the model is developed and calibrated to long-term test data on small clear wood specimen. In Gerhards and Link (1987) the same model is calibrated to long-term test on full- size timber specimen. In Barrett and Foschi (1978) a damage accumulation model is introduced, where the rate of damage is a function of the applied stress, the actual damage and a threshold value for the stress below which no damage accumulation occurs (equivalent to Equation (4.44)). In Foschi and Yao (1986) a model is presented, taking basis in the first two terms of the extension of a power series. The model is also presented as the damage rate as a function of the applied stress, the actual damage and a threshold value for the stress below which no damage accumulation occurs, i.e. is corresponding to Equation (4.44).

4.3.2.3   Models based on Fracture Mechanics

In contrast to the damage accumulation models, where damage is introduced as an abstract quantity without any direct physical background, the models based on fracture mechanics introduce damage as the increase of crack size in a viscoelastic solid.

An approach based on viscoelastic fracture mechanics is introduced in Nielsen (1979) with the so called Damaged Viscoelastic Material (DVM) theory. The main idea behind the DVM - model is that structural timber may be seen as an initially damaged material, where the damage is represented by cracks. The time dependent behaviour of timber under load is modelled by a single crack under stress perpendicular to the crack plane. The crack is modelled as a Dugdale crack with a time dependent modulus of elasticity; see e.g. Dugdale (1960).

Another approach using the Dugdale crack model applied to a viscoelastic material is presented in Mindess (1976), where it is focused on delayed crack propagation under constant or increasing load:

$$\frac{da_{crack}}{dt} = b_1 k_{stress}^{b_2} \tag{4.45}$$

where a_{crack} is the crack length, t is the time, k_{stress} is the stress intensity factor and b_1, b_2 are model parameters depending on the material. Equation (4.45) can be integrated for several load histories. In Sharpely (1975) Equation (4.45) is utilized and the model parameters b_1, b_2 are assigned based on theoretical considerations taking basis in the so called Barenblatt

theory, see Barenblatt (1962).

4.3.2.4 Models based on Chemical Kinetics

In Caultfield (1985) and van der Put (1986) two DOL models based on chemical kinetics are proposed that relate fracture times to bond breaking processes in the wood. These models are based on physical parameters, however, the governing equations are rather complex and the application to structural timber with its inherent defects and high material variability may be difficult (Morlier et al. (1996)).

4.3.2.5 Models based on Energy considerations

A strain energy model to predict load duration effects in timber is proposed in Fridley et al. (1991) and the model is developed further in Philpot et al. (1994). A critical strain energy density function is established from experimental observations. Failure is defined as the excess of a critical strain energy density, $g_{u,cr}$, which is assumed to correspond to the initiation of non-linear material behaviour. For instance, $g_{u,cr}$ in a standard short-term test would correspond to the proportional limit; in a long-term test $g_{u,cr}$ would correspond to the initiation of tertiary creep. The strain energy definition of failure is found to be invariant with respect to load history, environmental conditions and strength and stiffness related material property. Another proposal for an energy-based DOL model can be found in Bach (1973).

4.3.3 PROBABILISTIC MODELLING OF DURATION OF LOAD EFFECTS

The probabilistic modelling of duration of load effects is a prerequisite for reliability analysis and reliability based code calibration for timber structures. The analysis takes basis in the time dependent reliability problem as discussed in section 2.1, where Equation (2.3) specifies the time dependent failure criterion as:

$$R(t) - S(t) \leq 0 \tag{4.46}$$

at any time t; i.e. normally the considered time interval is limited to a projected service lifetime of a structure; $t \in [0, T_{sl}]$.

4.3.3.1 Modelling Scheme - Uncertainty

In principle, the probabilistic modelling of the life time of a timber structural element follows a scheme as illustrated in Figure 4-22. On the load side (the left hand side in Figure 4-22), relevant scenarios have to be identified which might be idealized and represented by proper random processes. The parameters of these processes are in general estimated based on observations. On the resistance side (the right hand side in Figure 4-22) the procedure starts with the identification of relevant failure mechanisms. In section 4.3.2 it is already discussed

how diverse the assumptions regarding the relevant mechanisms are. However, a mathematical model is formulated based on these assumptions and the parameters of the models are calibrated to experimental data. It is an important task within the probabilistic modelling that all uncertainties involved are consistently taken into account.
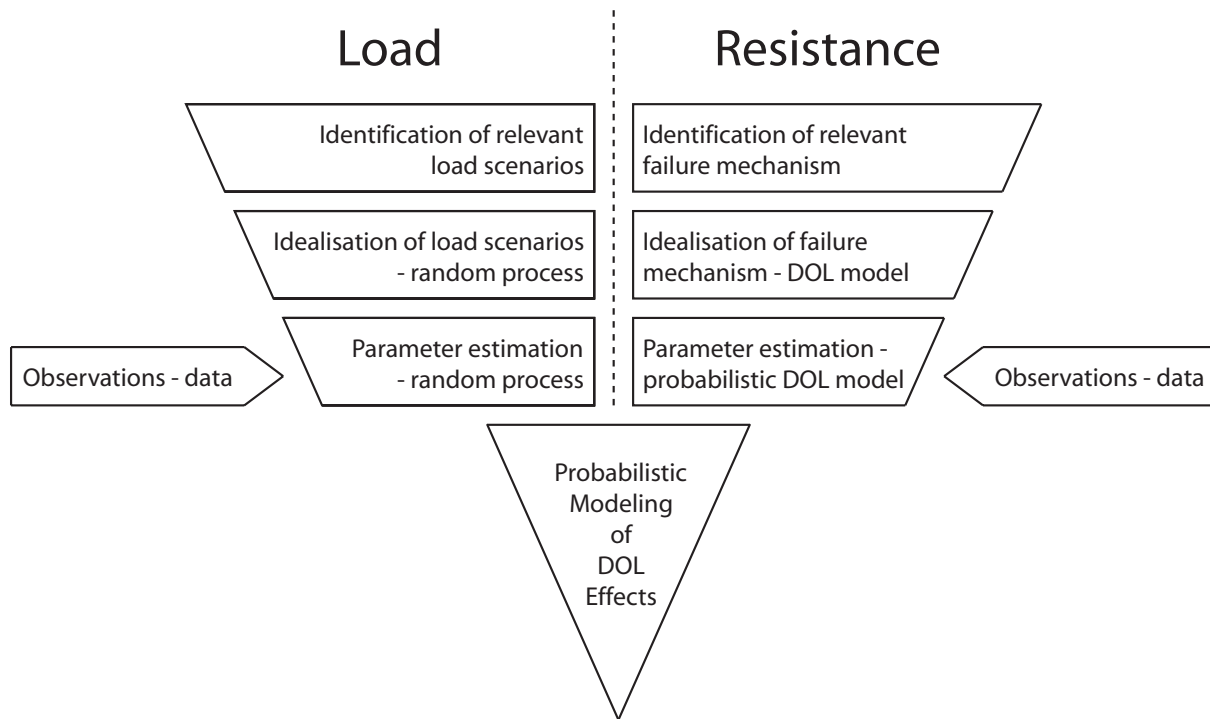
Figure 4-22   Scheme for the probabilistic modeling of duration of load effects.

The uncertainties involved in the long term resistance model are briefly discussed in the following:

- Failure mechanism assumptions/model formulations: The model can be formulated based on different assumptions about the failure mechanism. The basic assumptions and the possibly simplified mathematical representations are associated with uncertainties.

- Parameter estimation: the model parameters are calibrated with (limited) experimental data.

- Extrapolation to other load scenarios: due to the limited availability of experimental data, also the load scenarios applied within the experiments are limited. It has to be assumed that models can be applied to load scenarios different to the scenarios used in the experiments.

- Sampling techniques such as the equal rank assumption: as discussed in section 4.3.1 the stress ratio $sl_i = \hat{s}/r_{0,i}$ is a central measure for the analysis of long-term strength data. Assumptions such as the equal rank assumption induce additional uncertainty to the problem.

The uncertainties discussed above can be partly quantified by proper calibration methods as the maximum likelihood method. However, the remaining uncertainty e.g. due to the equal rank assumption or due to extrapolation has to be accounted for separately.

4.3.3.2 DOL model representations

In general, damage accumulation models are used for the probabilistic modelling of the DOL effect; see e.g. Ellingwood and Rosowsky (1991), Foschi et al. (1989), Sørensen et al. (2002). The basic characteristic of damage accumulation models is that the performance of the element is described by one single damage state variable α_D, which is in general a function of the short-term strength R_0 and the applied stress history $S(t)$. Taking this into account the limit state function in Equation (4.46) can be simplified to:

$$1 - \alpha_D \big(S(t), R_0, \mathbf{\theta} \big) \leq 0 \tag{4.47}$$

where $\mathbf{\theta}$ is a vector of model parameters.

The model parameters of the damage accumulation models are mostly calibrated to data from standard long-term experiments, i.e. where a ramp load phase is followed by a period of constant load until failure and the time to failure is measured (compare section 4.3.1). For reliability analysis and code calibration these models are used for any realistic and relevant load process. This includes the assumption that the failure mechanism is solely due to creep rupture, i.e. failure is assumed to be a consequence of accumulated time under load. This means that the effect of repeated load cycles is assumed to be irrelevant, a fact which provokes some scepticism, especially for load processes with a high number of load repetitions. Furthermore, the parameters of the damage accumulation models have no direct physical meaning and cannot be adapted to other situations in regard to climate or loading mode.

The model proposed by Nielsen (2000) (see section 4.3.2.3) seems to be promising in order to overcome these problems. For constant loads a relatively simple representation for this model can be given and parameters can be calibrated by using standard long-term experiment data as for the damage accumulation models. However, the parameters are linked to some physical meaning and an algorithm for taking into account repeated load cycles exist.

In the following, three damage theories are investigated further. The Gerhards model (Gerhards (1979) and Gerhards and Link (1987)) and the Foschi and Yao model (Foschi and Yao (1986)) are typical representatives for damage accumulation models. The Nielsen model (Nielsen (1979) and Madsen (1992)) with its promising properties is also discussed and compared with the two other models.

Gerhards Model

The Gerhards model has the form:

$$\frac{d\alpha_D}{dt} = \exp\left(-a_D + b_D \frac{s(t)}{r_0}\right) \quad \text{for} \quad 0 \le \alpha_D \le 1 \tag{4.48}$$

a_D and b_D are model parameters, r_0 is the short-term capacity and $s(t)$ is the applied stress. The Gerhards model corresponds to the general formulation given in Equation (4.43).

Equation (4.48) can be integrated for any stress history $s(t)$ to determine the accumulated damage α_D. The time to failure t_f is defined at $\alpha_D(t) = 1$.

$$\alpha_D(t) = \int_0^t \exp\left(-a_D + b_D \frac{s(t)}{r_0}\right) dt \tag{4.49}$$

For a constant load effect and assuming that the effect of the initial ramp loading can be neglected the time to failure according to the Gerhards model can be estimated as:

$$t_f = \exp\left(a_D - b_D \frac{\hat{s}}{r_0}\right) \tag{4.50}$$

where $\hat{s}$ is the constant stress level (Note that this format is equivalent to the one proposed by Pearson (1972), Equation (4.42)).

The Gerhards model allows for the consideration of the characteristics of the short-term test configuration. As illustrated in Figure 4-18 the short-term test involves a certain time of ramp loading with rate k_R. The integral given in Equation (4.49) can be solved for any ramp loading $s(t) = k_{R,a} t$, as:

$$\alpha_D(t) = \frac{r_0}{b_D k_{R,a}} \exp(-a_D) \left(\exp\left(b_D \frac{k_{R,a} t}{r_0}\right) - 1\right) \tag{4.51}$$

For the case of the short-term test, where $k_{R,a} = k_R$, $\alpha_D = 1$, $k_R t / r_0 = 1$ the parameter a_D can be represented by:

$$a_D = \ln\left(\frac{r_0 (\exp(b_D) - 1)}{b_D k_R}\right) \tag{4.52}$$

This means that whenever the short-term strength is linked to a certain short-term test loading rate k_R, a_D can be eliminated through Equation (4.52).

Considering this elimination, Equation (4.51) can be simplified to:

$$\alpha_D(t) = \frac{k_R}{k_{R,a}} \frac{\exp\left(b_D \dfrac{k_{R,a}t}{r_0}\right) - 1}{\exp(b_D) - 1} \tag{4.53}$$

The integral given in Equation (4.49) can be solved for the stress history of a long-term test as illustrated in Figure 4-18. A ramp loading with rate k_R is applied until the constant stress level $\hat{s}$ is reached after the time t_C. Damage accumulation can be assessed through $\alpha_D(t)$ as:

$$\alpha_D(t) = \frac{\left(\exp\left(b_D \dfrac{k_R t}{r_0}\right) - 1\right)}{\left(\exp(b_D) - 1\right)} \qquad \text{for } 0 \leq t < t_C$$

$$\alpha_D(t) = \frac{b_D(t - t_C)}{t_C} \frac{\exp\left(b_D \dfrac{\hat{s}}{r_0}\right)}{\left(\exp(b_D) - 1\right)} + \frac{\left(\exp\left(b_D \dfrac{\hat{s}}{r_0}\right) - 1\right)}{\left(\exp(b_D) - 1\right)} \qquad \text{for } t_C \leq t \tag{4.54}$$

When $\hat{s} < r_0$, the time to failure can be evaluated as

$$t_f = \frac{\hat{s}}{k_R} + \frac{r_0}{k_R b_D}\left(\exp\left(b_D\left(1 - \frac{\hat{s}}{r_0}\right)\right) - 1\right) \tag{4.55}$$

Equation (4.55) is used for calibrating model parameters with test results.

The residual strength r_r corresponding to the damage α_D can be derived such that $\alpha_D = 0 \Rightarrow r_r/r_0 = 1$ and $\alpha_D = 1 \Rightarrow r_r/r_0 = 0$. For Gerhards model the residual strength can be given as:

$$\frac{r_r}{r_0} = \frac{1}{b_D}\left(1 + (1 - \alpha_D)(\exp(b_D) - 1)\right) \tag{4.56}$$

Foschi and Yao Model

In Foschi and Yao (1986) a power series expansion is used to express damage accumulation according to the general form as given in Equation (4.44), as:

$$\frac{d\alpha_D}{dt} = h(s(t), r_0, \alpha_D, \boldsymbol{\theta}) = h_1(s(t), r_0, \boldsymbol{\theta}) + h_2(s(t), r_0, \boldsymbol{\theta})\alpha_D + \ldots + h_n(s(t), r_0, \boldsymbol{\theta})\alpha_D^{n-1} \tag{4.57}$$

As an approximation, Yao (1987) considered only the first two terms of the expansion. Accordingly the so called Foschi and Yao model is expressed as:

$$\frac{d\alpha_D}{dt} = a_D \left(s(t) - \eta_D r_0\right)^{b_D} + c_D \left(s(t) - \eta_D r_0\right)^{d_D} \alpha_D(t) \quad \text{for} \quad s(t) \geq \eta_D r_0$$

$$\frac{d\alpha_D}{dt} = 0 \qquad\qquad\qquad\qquad\qquad\qquad \text{for} \quad s(t) < \eta_D r_0$$

$$(4.58)$$

The accumulated damage is also depending on the actual value of the damage state variable $\alpha_D(t)$. a_D, b_D, c_D, d_D and η_D are model parameters. η_D defines the stress level threshold below which no damage is assumed to occur. The model can be rewritten as (Köhler and Svensson 2002):

$$\frac{d\alpha_D}{dt} = a_D \left(\frac{s(t)}{r_0} - \eta_D\right)^{b_D} + c_D \left(\frac{s(t)}{r_0} - \eta_D\right)^{d_D} \alpha_D(t) \qquad \text{for} \quad \frac{s(t)}{r_0} \geq \eta_D$$

$$\frac{d\alpha_D}{dt} = 0 \qquad\qquad\qquad\qquad\qquad\qquad\qquad \text{for} \quad \frac{s(t)}{r_0} < \eta_D$$

$$(4.59)$$

Equation (4.59) has the advantage to present stress as a dimensionless ratio of the applied stress and the assumed short-term strength.

By solving Equation (4.59) for the case of standard short-term tests, one will ascertain also for Foschi and Yaos' model one model parameter, a_D, with:

$$a_D = \frac{k_R(b_D + 1)}{r_0(1 - \eta_D)^{(b_D + 1)}} \tag{4.60}$$

where k_R is the rate of loading applied for evaluating r_0.

The time to failure, t_f, for a prior-to-testing undamaged component loaded with a ramp load, with the same rate of loading, k_R, as the standard test, until the constant load level, $\hat{s}$, is reached and held until failure occurs has the following expression (see Köhler and Svensson (2002)):

$$t_f = \frac{\hat{s}}{k_R} + \frac{1}{c_D \left(\frac{\hat{s}}{r_0} - \eta_D\right)^{d_D}} \ln\left(\frac{1 + \lambda_D}{\alpha_{D,0} + \lambda_D}\right) \qquad \hat{s} \geq \eta_D R_0, \ \hat{s} < r_0$$

$$t_f = \infty \qquad\qquad\qquad\qquad\qquad\qquad \hat{s} < \eta_D R_0$$

$$(4.61)$$

with

$$\lambda_D = \frac{k_R(b_D + 1)}{c_D r_0 (1 - \eta_D)^{(b_D + 1)}} \left(\frac{\hat{s}}{r_0} - \eta_D\right)^{b_D - d_D}, \alpha_{D,0} = \left(\frac{\hat{s}/r_0 - \eta_D}{1 - \eta_D}\right)^{b_D + 1} \tag{4.62}$$

where $\alpha_{D,0}$ is the degree of damage prior the studied period of constant load.

Equation (4.61) is used when calibrating the model against test results.

Residual strength r_r corresponding to the damage α_D for the Foschi and Yao model can be expressed as:

$$\frac{r_r}{r_0} = \eta_D + (1-\eta_D)(1-\alpha_D)^{1/(1+b_D)} \tag{4.63}$$

Nielsen Model

In case of constant load intensity, a damage accumulation law can be formulated from the DVM-theory as:

$$\frac{d\alpha_\kappa}{dt} = \frac{(\pi \cdot fl)^2}{8q_c\tau_c} \frac{\alpha_\kappa \cdot sl_\kappa^2}{\left((\alpha_\kappa \cdot sl_\kappa^2)^{-1} - 1\right)^{1/b_c}} \tag{4.64}$$

where sl_κ is the stress level (or load intensity) defined by the ratio $\hat{s}/r_{cr}$ between applied stress $\hat{s}$ (load intensity) and the strength r_{cr} measured in a very fast ramp-load test. fl is the strength level defined as the ratio r_{cr}/r_l between the strength r_{cr} (as defined above) and the intrinsic strength of the (hypothetical) non-cracked material r_l. $\alpha_\kappa = l/l_0$ is the damage, defined as the ratio between the actual crack length l and the initial crack length l_0. $\alpha_\kappa = 1$ corresponds to no damage and $\alpha_\kappa = sl_\kappa^{-2}$ to full damage. τ_c and b_c are (creep) material parameters depending e.g. on loading mode and moisture history. The parameter q_c is given as a function of the creep exponent b_c as:

$$q_c = (0.5(b_c+1)(b_c+2))^{1/b_c} \tag{4.65}$$

and considers a parabolic increasing crack opening progression.

Based on Equation (4.64) time to failure t_f under constant stress can be derived as:

$$t_f = \frac{8q_c\tau_c}{(\pi \cdot fl \cdot sl_\kappa)^2} \int_1^{sl_\kappa^{-2}} \frac{(\varphi-1)^{1/b_c}}{\varphi} d\varphi \tag{4.66}$$

where φ is a damage state variable. Nielsen's definition of the stress level sl_κ thus differs from the usual definition, which relates applied stress to short-term strength as it is defined in Figure 4-18, i.e. a ramp load test with a specified average time to failure of e.g. 5 minutes according to ISO 8375. The creep parameters τ_c and b_c are related to the viscoelastic behaviour around the crack tip. These are very local phenomena and cannot be consistently reflected in macro-scale creep tests. q_c is a function of the creep parameter b_c. The parameter fl indicates the state of initial damage of the material as it is defined by the ratio of the

material strength r_{cr} and the (hypothetical) material strength without any damage r_l which can only be assessed theoretically. This means that, although the model parameters have some physical meaning, they must be obtained by calibration, as it is the case for other damage accumulation models. Equation (4.66) can be used for calibrating the parameters of the Nielsen model to data from standard long-term tests. Therefore it is assumed that the Nielsen stress level sl_κ can be replaced by the conventionally defined stress level sl. Further, it is supposed that the initial ramp load phase of a standard long-term experiment (Figure 4-18) can be neglected.

The integral, included in Equation (4.66) can be solved for discrete realisations of the parameter b_c; in general values for $1/b_c = 3, 4, 5$ are used and the solutions can be given as (Bronstein and Semendjajew (1981)):

$$b_c = \frac{1}{3} \qquad t_f = \frac{3.1\tau_c}{sl_\kappa^2 fl^2}\left(\frac{x^3}{3} - \frac{x^2}{2} + x - \log(x+1)\right)$$

$$b_c = \frac{1}{4} \qquad t_f = \frac{3.2\tau_c}{sl_\kappa^2 fl^2}\left(\frac{x^4}{4} - \frac{x^3}{3} + \frac{x^2}{2} - x + \log(x+1)\right) \qquad (4.67)$$

$$b_c = \frac{1}{5} \qquad t_f = \frac{3.2\tau_c}{sl_\kappa^2 fl^2}\left(\frac{x^5}{5} - \frac{x^4}{4} + \frac{x^3}{3} - \frac{x^2}{2} + x - \log(x+1)\right)$$

with $x = sl_\kappa^{-2} - 1$.

The parameters fl and τ_c are not independent. The model therefore includes only one free parameter to calibrate.

For the Nielsen model the residual strength r_r is given by:

$$\frac{r_r}{r_0} = \alpha_\kappa^{-\frac{1}{2}} \qquad (4.68)$$

Fatigue modelling with the Nielsen model

Theoretical investigations as well as physical evidence from test results indicate that the duration of load failure mechanism in timber is not entirely due to creep rupture but also due to accumulated fatigue damage. Frequency dependent fatigue effects in timber have been considered theoretically in Nielsen (2000) and experimentally e.g. in Clorius (2001). Based on the solution for constant load intensity the DVM-model is developed further in Nielsen (2000) to consider rectangular pulse loading by introducing crack closure and contact effects due to unloading.

The load process which can be considered by the Nielsen model is a square wave loading with

constant amplitude and constant frequency. The load process is determined by frequency $f = 1/T$, maximum load intensity sl_{max}, load ratio $p_{sl} = sl_{min}/sl_{max}$ and fractional time under maximum load β_{sl}. The parameters are illustrated in Figure 4-23.
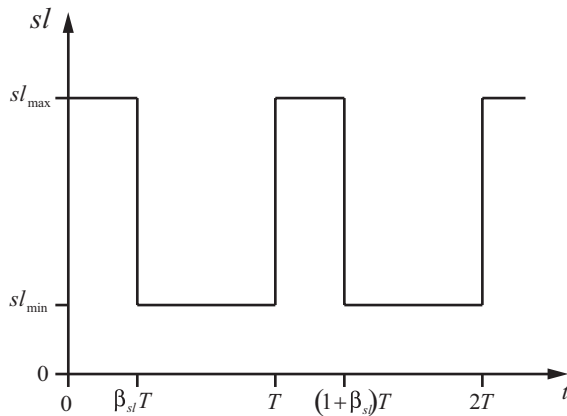
Figure 4-23   Basic load intensity variation considered: Square wave loading.

The algorithm proposed in Nielsen (2000) is illustrated in Figure 4-24 and starts with the input of material and load parameters; $\boldsymbol{\delta}$ is a vector of fatigue parameters. The other parameters are defined in the foregoing. After setting the start-values, a x which satisfies the Equation in step C3 is found by iteration. With the Equation in step C4 and the constant damage increment $\Delta\alpha_\kappa$ the number of load cycles Δn leading to that damage increment is calculated. The damage is accumulated until the failure criterion formulated in the Equation in step L1 is fulfilled. Load conditions may only be changed when the algorithm returns to step C3 again, i.e. after an unknown number of load cycles. Not that this circumstance restricts the model to consider only harmonic load pulse processes.

By setting Δn instead of $\Delta\alpha_\kappa$ to a constant value, e.g. $\Delta n = 1$, the load intensity can be changed after every load pulse and the corresponding damage increment is calculated. This facilitates the consideration of realizations of a random process with rectangular load pulses (see Köhler and Faber (2003)).

The model as it is presented in Figure 4-24 is referred to as the general Nielsen model. The model as it is presented in Equation (4.64) is also capable to model the duration of load effect; damage is then accumulated as a consequence of time under constant load. The model presented in Equation (4.64) is referred to as the simple Nielsen model.

Figure 4-24   Algorithm for predicting the time till failure.

4.3.3.3   Calibrating Models to experiment observations

Long-term experiments are illustrated in Figure 4-18. The experiments indicate a time to failure t_f after a certain stress history, where a period of constant stress $\hat{s}$ follows a period of loading with the rate k_R.
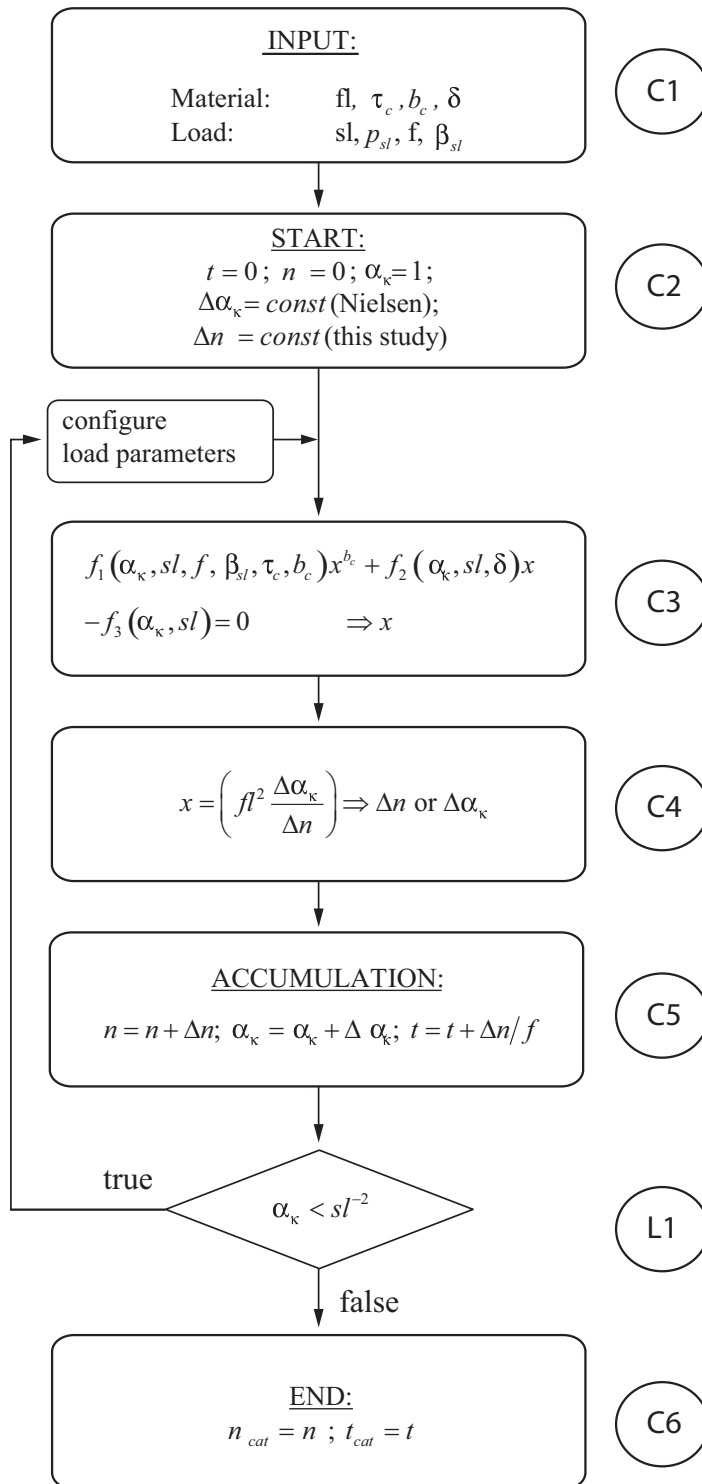
For the considered DOL models an expression for the time to failure considering the experiment stress history can be derived. These expressions can be written in the general form as:

$$t_f = t_f\left(sl, \boldsymbol{\theta}, k_R\right) \tag{4.69}$$

The estimation of the model parameters is performed considering n simultaneous observations of the time to failure $\mathbf{t}_f = \left(t_{f,1}, t_{f,2}, ..., t_{f,n}\right)^T$ and the stress level $\mathbf{sl} = \left(sl_1, sl_2, ..., sl_n\right)^T$. Assuming that (at least) locally the relationship between t_f and sl can be described with the models presented above, the parameter assessment may be performed by introducing an error term ε which takes account for the difference between observed time to failure t_f and modelled time to failure $t_{f,m}$:

$$t_f = t_{f,m}\left(sl, \boldsymbol{\theta}, k_R\right) + \varepsilon \tag{4.70}$$

Assuming that the error term is normally distributed with zero mean and unknown standard deviation, σ_ε, the maximum likelihood method, see e.g. Lindley (1965), may be used for estimating the mean values and covariance matrix for the parameters $\boldsymbol{\theta}$ and σ_ε.

The likelihood is then given as

$$L\left(\theta_1, \theta_2, ..., \theta_n, \sigma_\varepsilon\right) = \prod_{i=1}^{n} \frac{1}{\sqrt{2\pi}\sigma_\varepsilon} \exp\left(-\frac{1}{2}\left(\frac{-t_{f,i} + t_{f,m,i}\left(sl_i, \boldsymbol{\theta}, k_R\right)}{\sigma_\varepsilon}\right)^2\right) \tag{4.71}$$

The parameters are estimated by the solution of the optimization problem

$$\max_{\mathbf{p}} L(\mathbf{p}) \tag{4.72}$$

where $\mathbf{p} = \left(\theta_1, \theta_2, ..., \theta_n, \sigma_\varepsilon\right)^T$.

The parameters of the damage models are calibrated to results from long-term tests (Hoffmeyer (1990)):

The considered tests are performed on structural timber in four point bending. Two different test climate conditions are considered: constant climate corresponding to 20% and 11% moisture content of the timber. From the 20% moisture content timber, 306 specimens of graded Norway spruce are tested. One third is tested in standard short-term test with ramp load until failure (EN 408). The remaining specimens are tested with constant load corresponding to the 5 percentile of the short term strength for one half the remaining sample and the 15 percentile for the other half. From the 11% moisture content timber the approach is similar ($n = 204$) but for long term loading solely the 5th percentile of the short term strength is used as a load level. The matching of the short-term capacity for the long-term test is based on the assumption of equal rank (see section 4.3.1).

For the Gerhards damage model and the Foschi and Yao damage model the ramp load rate k_R, is considered and is set to 500 MPa/hour; for the Nielsen model the initial ramp load phase is neglected. The threshold ratio η_D in the Foschi and Yao model is set to a constant value of 0.5. For the Nielsen damage model the parameters b_c and fl are held constant with values 0.2 and 0.25, respectively.

Table 4-14   Model parameters for the Foschi and Yao damage model, the Gerhards model and the Nielsen model calibrated on results form DOL tests (Hoffmeyer, 1990) by the ML-method. The model parameters are represented as normal distributed random variables.

	Model parameter	Average Timber Moisture Content: 11%		Average Timber Moisture Content: 20%	
		Expected value	Standard deviation	Expected value	Standard deviation
Foschi and Yao	$b_D : B_D$	30.03	0.92	20.16	0.610
	$c_D : C_D$	17.05	12.30	12.06	7.29
	$d_D : D_D$	5.69	0.45	4.37	0.31
	$\sigma_{eps} : \Sigma_{eps}$	0.30	0.03	0.37	0.02
Gerharts	$b_D : B_D$	51.41	0.01	43.35	0.004
	$\sigma_{eps} : \Sigma_{eps}$	0.55	0.05	0.476	0.03
Nielsen	$\tau_c : T_c$	875	113	75.74	5.41
	$\sigma_{eps} : \Sigma_{eps}$	0.51	0.04	0.38	0.02

The correlations for the estimated parameters of the Foschi and Yao model can be given as:

Table 4-15   Correlations for the parameters of the Foschi and Yao model.

Average Timber Moisture Content: 11%					Average Timber Moisture Content: 20%				
	B_D	C_D	D_D	Σ_{eps}		B_D	C_D	D_D	Σ_{eps}
B_D	1	0.41	0.32	0	B_D	1	0.62	0.49	0
C_D		1	0.98	0	C_D		1	0.97	0
D_D			1	0	D_D			1	0
Σ_{eps}				1	Σ_{eps}				1

For the Nielsen and the Gerhards model as for the Foschi and Yao model (see Table 4-15) Σ_{eps} is not correlated with the model parameters.

The test results corresponding to a timber moisture content of 20% are plotted together with the expected realizations of the calibrated models in Figure 4-25. The stress level sl is plotted together with the logarithm of the time until failure in hours $\log_{10}\left(t_f\right)$. It can be observed that especially for the centre part, for time to failure between 1 hour and 1 year the differences between the models are quite minor.
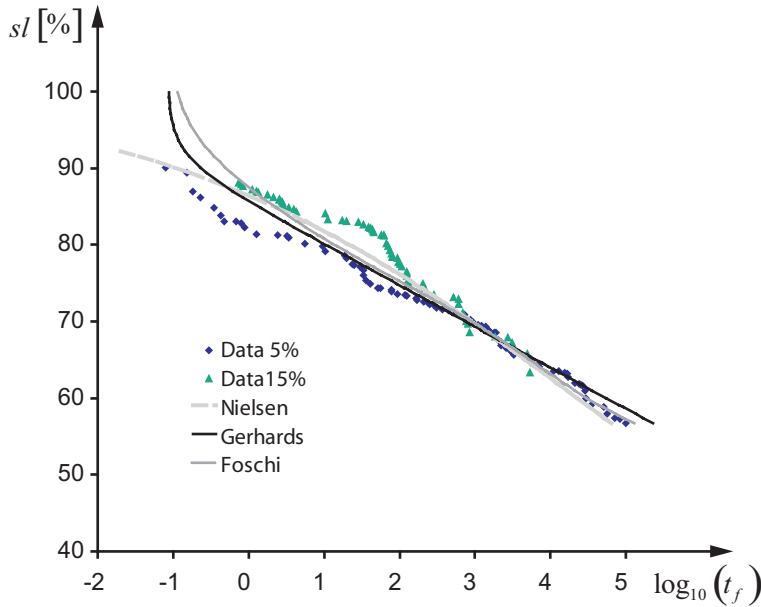
Figure 4-25   Duration of load data (Hoffmeyer, 1990) and damage models based on the mean value of the estimated parameters (time in hours).

4.3.3.4   Modelling Stress Histories

The DOL models presented above can be used for time variant stress histories. Therefore the stress histories have to be separated into incremental periods of constant load. Damage is accumulated according to the following scheme:

$$\alpha_{D,i} = \alpha_{D,i-1} + \Delta\alpha_{D,i} \tag{4.73}$$

where $\Delta\alpha_{D,i}$ can be calculated as:

$$\Delta\alpha_{D,i} = h_{model,i}\left(sl_i\right)\Delta t_i \tag{4.74}$$

where $h(.)$ is a function of the assumed constant stress level sl. For the Gerhards model and the Foschi and Yao model $h(.)$ can be written as (based on Equations (4.48) and (4.59)):

$$h_{Gerhards,i}(sl_i) = \exp(-a_D + b_D sl_i) \tag{4.75}$$

$$h_{F+Y,i}(sl_i) = a_D(sl_i - \eta_D)^{b_D} + c_D(sl_i - \eta_D)^{d_D} \alpha_{D,i-1} \quad \text{for} \quad sl_i - \eta_D > 0$$

$$h_{F+Y,i}(sl_i) = 0 \quad \text{for} \quad sl_i - \eta_D \leq 0 \tag{4.76}$$

The time increments Δt_i have to be chosen small enough to map the time-variant load process and the non-linear effect of the Foschi and Yao model. The starting condition of the calculation is $\alpha_D = 0$ for an undamaged material. The failure condition is $\alpha_{D,cr} = 1$.

For using the general Nielsen model, i.e. modelling damage as a consequence from both, time under load and number of load cycles (with a scheme as illustrated in Figure 4-24), the random load sequence has to be transformed into a square wave shaped load process. A harmonic square wave shaped load process is illustrated in Figure 4-23. As shown in Köhler and Faber (2003) the parameters from the harmonic square wave process can be modified after every load cycle as illustrated in Figure 4-24, i.e. random load variations can be reasonably idealized. Superior stress cycles can be modelled by standard rain flow counting algorithm, see e.g. in Downing and Socie (1982).

For moderately fluctuating load processes a similar damage accumulation scheme as presented above in Equation (4.74) can be applied by using the simple Nielsen formulation for the case of constant load, $h(.)$ can be written as (compare with Equation (4.64)):

$$h_{Nielsen,i}(sl_i) = \frac{(\pi fl)^2}{8q_c\tau_c} \frac{\alpha_D sl_i^2}{\left(\left(\alpha_D sl_i^2\right)^{-1} - 1\right)^{1/b_c}} \tag{4.77}$$

where the starting condition of the calculation is here $\alpha_D = 1$, failure condition is $\alpha_{D,cr} = sl^{-2}$.

As shown in Köhler and Faber (2003) for some load cases it is a reasonable simplification of the Nielsen model to consider only the time under load as the cause of damage accumulation instead of applying the model in it's fully developed general format as illustrated in Figure 4-24. According to the Nielsen model fatigue damage is due to fast unloading and it can be shown that this damage can be neglected if the unloading is slow enough (order of magnitude 6 hours) or seldom enough (the order of magnitude is around 60 unloadings per lifetime).

The limit state function as given for the damage accumulation models in Equation (4.47) is not valid for the Nielsen model. For the Nielsen model the limit state function becomes:

$$\alpha_{D,cr} - \alpha_D(S(t), R_0, \boldsymbol{\theta}) \leq 0 \tag{4.78}$$

where $\alpha_{D,cr} = SL^{-2}$.

4.3.4   APPLICATIONS FOR DOL MODELS

To gain a better understanding about the predictive behaviour of the three DOL models introduced above some example calculations are performed within this section. The models are used with the parameters as presented in Table 4-14.

4.3.4.1   Lifetime Prediction and Damage Accumulation for Constant Load

When comparing the DOL-model estimations of the time to failure for a constant load only minor differences can be found, as it can be seen in Figure 4-25 for e.g. a stress level $sl = 0.7$. When investigating the damage accumulation for a case with constant load, however, the models show very different behaviour. In Figure 4-26 the damage accumulation until failure for the case of constant load with load ratio $sl = 0.7$ is shown. The ordinate of the diagram in Figure 4-26 is the difference between damage, α_D, and damage at failure, $\alpha_{D,cr}$, on the abscissa is time. The damage accumulation according to the Gerhards model is for this load case linear with time. The Nielsen model shows for the same case high non-linearity as does the Foschi and Yao model. The latter is, however, smoother than the first. The model parameters for constructing Figure 4-26 are taken from Table 4-14, with a moisture content of the timber equal to 20% (Köhler and Svensson (2002)).
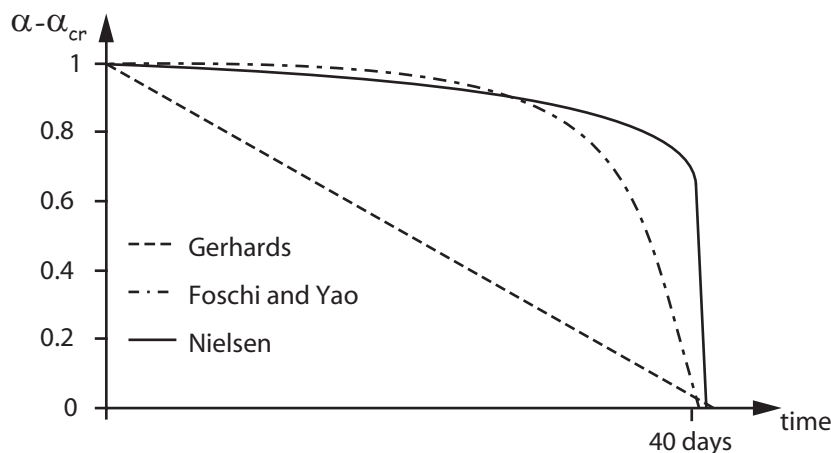
Figure 4-26   Damage accumulation for the case of constant load ratio of 0.7 according to the Gerhards model, the Foschi and Yao model and the Nielsen model.

4.3.4.2   Reliability based code calibration

In timber design codes, the effect of load duration is taken into account by a strength modification factor k_{mod}, which depends on the type of load acting on the structure. The loads are classified in terms of their expected duration time and intensity. The modification factor k_{mod} is calibrated by using a DOL model in a probabilistic analyses. k_{mod} calibration has been carried out and reported in e.g. Foschi et al. (1989), Ellingwood et al. (1991), Svensson et al.

(1999), Sørensen et al. (2002) and Köhler and Faber (2003). In the following an approach for determining k_{mod} is presented.

Procedure for calibrating the duration of load modification factor k_{mod}

1) Design Format:

The design codes specify by means of design equations that the design strength of structural components r_d is larger than or equal to the design load effect s_d. In modern LRFD code format, the design values are defined in terms of characteristic values and partial safety factors γ as (compare Equation (2.28)):

$$r_d = z_d \frac{r_{0,k}}{\gamma_M} \geq s_k \cdot \gamma_S = s_d \tag{4.79}$$

where the index k denotes characteristic value and z_d is the design parameter. Irrespective of the duration of load, the load description (right hand-side of Equation (4.79)) is based on the annual maximum load intensity, i.e. the description of the load effect will not change to account for the load duration. For materials being affected by the duration of the loading such as timber a modification factor, k_{mod}, is introduced on the short term capacity as:

$$r_d = z_d \frac{k_{mod} \cdot r_{0,k}}{\gamma_M} \tag{4.80}$$

The effect of the duration of the load is accounted for entirely by the k_{mod} factor. The partial safety factor for the timber material resistance γ_M, is thus independent of the load duration.

2) Limit State Functions:

Two failure modes are considered in the following: A) failure is defined as the load effect intensity exceeding the short-term strength and B) where failure is defined as the consequence of damage accumulation during long term load application. Hence, when conducting the reliability analyses each failure mode is associated with a specific limit state function.

For failure mode A) i.e. the failure mode where load effect intensity, S, is exceeding the short term strength R_0 the short-term limit state function is given as (compare Equation (4.46)):

$$g(\mathbf{X}) = z_d R_0 X_M - S \tag{4.81}$$

where X_M is the model uncertainty and z_d is a design variable.

For failure mode B) where failure occurs as a consequence of the accumulated damage exceeding the critical damage level $\alpha_{D,cr}$ the long-term limit state function is given as (compare Equation (4.78)):

$$g(\mathbf{X}) = \alpha_{D,cr} - \alpha_D \left(S(t), R_0, z_d, \mathbf{p} \right) \tag{4.82}$$

where α is the damage as a function of the model parameters $\mathbf{p} = \left(\theta_1, \theta_2, ..., \theta_n, \sigma_\varepsilon \right)^T$, $S(t)$ is the load process, and z_d is the design variable.

3) Procedure for determining k_{mod}:

By utilizing Monte Carlo simulation for generating random variables the modification factor k_{mod} is determined according to the following procedure. First the partial safety factor for the short-term strength $\gamma_{M,s}$ is calibrated to a target reliability index, β_{target}, using the limit state function given in Equation (4.81) and the design Equation (4.79) for constant γ_S. The probabilistic model for the load intensity is based on the maximum load for a reference period of 50 years. The partial safety factor for the long-term strength $\gamma_{M,l}$ is calibrated using the limit state function in Equation (4.82), and the design equation given in Equation (4.79) for constant γ_S. The realization of the load process $S(t)$ entering the limit state function given in Equation (4.82), is generated based on some specified load model. For the generated load process realization, the damage models calculate the accumulation of damage. After a sufficient number of simulations, the ratio of the number of failures n_f and the total number of realizations n estimates the probability of failure $p_f = n_f / n$. The corresponding reliability index β is determined from $\beta = -\Phi^{-1}(p_f)$. The long-term partial safety factor, $\gamma_{M,l}$, is re-calculated until the target reliability index, β_{target}, is reached. k_{mod} is then determined as:

$$k_{\mathrm{mod}} = \frac{\gamma_{M,s}\left(\beta_{target} \right)}{\gamma_{M,l}\left(\beta_{target} \right)} \tag{4.83}$$

The calculations may be based on several different load models. The short-term strength R_0 is modeled by a log-normally distributed random variable with expected value equal to one and coefficient of variation equal to 25%. Referring to the Joint Committee on Structural Safety (JCSS, 2001) and Faber and Sørensen (2003) a target reliability index $\beta_{target} = 3.2$ for a reference period of 50 years is used. When not specifically specified, the model uncertainty in the short-term limit state function (Equation (4.81)) is assumed log-normal distributed with mean value equal to 1 and standard deviation equal to 0.05.

4.3.4.3   Calibration Example – Live Load

Live Load Model

The live load model used in this example is equivalent to the model proposed in (CIB 1989) and recommended by the Joint Committee on Structural Safety (JCSS (2001)). The model contains two parts, sustained live load and intermittent live load. The sustained live load covers ordinary live load such as furniture, average utilization by persons, etc. The intermittent live load describes the exceptional load peaks, e.g. furniture assembly while re-

modelling, people gathering for special occasions, etc. The live load model is based on the following definitions:

The occurrences of changes in magnitude of the sustained load are modelled as a Poisson process. The duration of load is then exponential distributed with expected value λ_{sus}. The magnitude of the sustained load is modelled by a Gamma distribution with expected value μ_{sus} and standard deviation σ_{sus}:

$$\sigma_{sus} = \sqrt{\sigma_{sus,r}^2 + \sigma_{sus,sp}^2 \frac{a_{are,0}}{a_{are}} \kappa_P} \tag{4.84}$$

where $a_{are,0}$ is the reference area, a_{are} is the considered area ($a_{are,0} < a_{are}$), κ_P is the peak factor, $\sigma_{sus,\gamma}^2$ specifies the variation between structures, $\sigma_{sus,sp}^2$ is the small scale variation related to the area $a_{are,0}$.

The occurrences of intermittent loads are also modeled as a Poisson process. The duration between intermittent loads are thus exponentially distributed with expected value v_{int}. The magnitude of the intermittent load is modeled by a Gamma distribution with expected value μ_{int} and standard deviation σ_{int}:

$$\sigma_{int} = \sqrt{\sigma_{int,sp}^2 \frac{a_{are,0}}{a_{are}} \kappa_P} \tag{4.85}$$

where $\sigma_{int,sp}^2$ is the small scale variation related to the area $a_{are,0}$.

The duration of the intermittent load t_{int} is considered exponentially distributed with parameter λ_{int}. The parameters used for the live load model are given in Table 4-16.

Table 4-16:   Parameters used for model live load in office space.

Type of building	$a_{are,0}$ $\left[\mathrm{m}^2\right]$	μ_{sus} $\left[\frac{\mathrm{kN}}{\mathrm{m}^2}\right]$	$\sigma_{sus,\gamma}$ $\left[\frac{\mathrm{kN}}{\mathrm{m}^2}\right]$	$\sigma_{sus,sp}$ $\left[\frac{\mathrm{kN}}{\mathrm{m}^2}\right]$	$1/\lambda_{sus}$ $[\mathrm{year}]$	μ_{int} $\left[\frac{\mathrm{kN}}{\mathrm{m}^2}\right]$	$\sigma_{int,sp}$ $\left[\frac{\mathrm{kN}}{\mathrm{m}^2}\right]$	v_{int} $[\mathrm{year}]$	$1/\lambda_{int}$ $[\mathrm{days}]$
Office	2	0.5	0.3	0.6	5.0	0.2	0.4	0.3	2.0

In this example, a floor structure based on joists with a span of 4.5 m and a spacing of 0.6 m is considered. The area a_{are} is assumed to cover the span and twice the spacing of the joists $a_{are} = 5 \ \mathrm{m}^2$. The peak factor, κ_P is calculated for load influence on the joist for maximum mid-span bending moment, therefore $\kappa_P = 1.778$ (CIB 1989).

By using Monte Carlo simulation and the load model parameters from Table 4-16 the mean value and the coefficient of variation of the annual maximum load $S_{Q,1}$ and the 50 year maximum load $S_{Q,50}$ can be derived. In Table 4-17 the results of the simulation are given. A typical realization of a 50 years live load history is shown in Figure 4-27 (Köhler and

Svensson (2002)).

Table 4-17:   Results from simulations of live load in office space (non-parametric).

Annual max $S_{Q,1}$			50 year max $S_{Q,50}$	
mean $\left[\text{kN/m}^2\right]$	COV [-]	98% quantile $\left[\text{kN/m}^2\right]$	mean $\left[\text{kN/m}^2\right]$	COV [-]
0.96	0.78	3.10	3.05	0.29
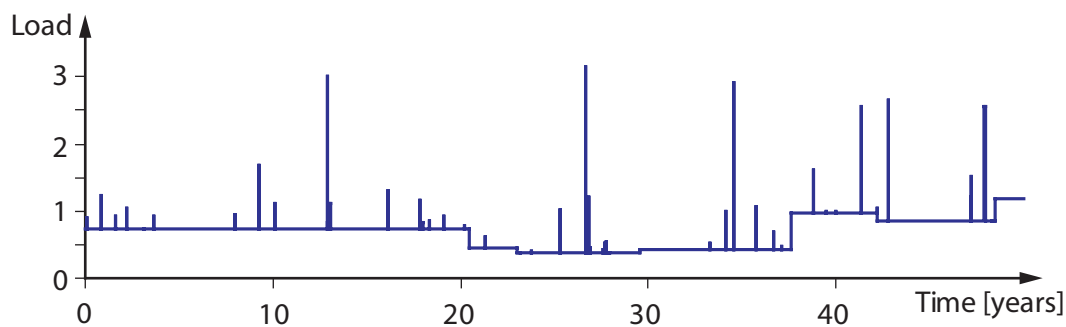
Figure 4-27:   A typical live load realization acting as midspan bending moment on a joist beam in an office space.

Result

The three DOL models discussed in section 4.3.3.2 are utilized for comparison. The parameters for timber with 20% moisture content as specified in Table 4-14 are used. The Nielsen model is applied with its simple format as given in Equation (4.64), i.e. only time under load is considered. The results from the calibration of k_{mod} factor for the case with live load in office space are shown in Table 4-18. The results show that the damage models give almost the same results (Köhler and Svensson (2002)).

Table 4-18:   Calibrated values of k_{mod} for the different damage models.

Foschi and Yao	Nielsen	Gerhards
0.77	0.76	0.75

4.3.4.4   Calibration Example – Snow Load

Snow Load Model

Snow on roofs of buildings is considered and a stochastic load model is formulated in accordance with the load model presented in Sørensen et al. (2002). Snow load on the ground

is modeled by triangularly shaped load pulses (snow packs). This is illustrated in Figure 4-28.
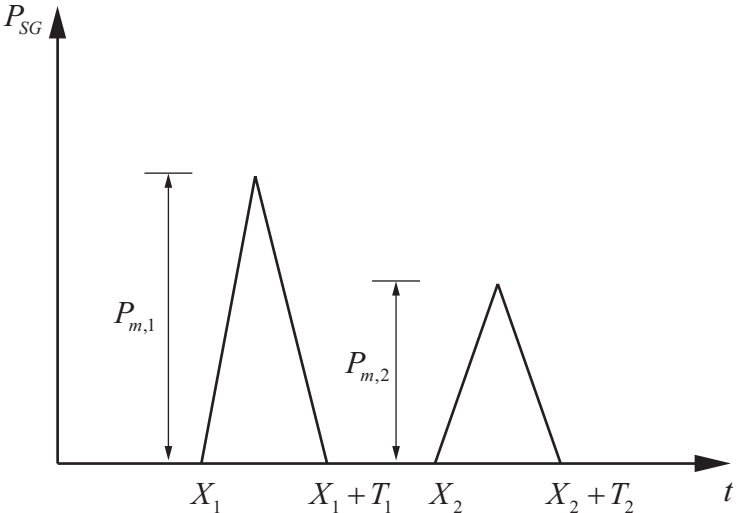
Figure 4-28:   Snowload at the ground modeled by triangular pulses.

Based on Danish snow data over 32 years from five locations the following load process parameters have been estimated (see in Sørensen et al. (2002)). The occurrence of a snow package at times $X_1, X_2, \ldots$ is modelled by a Poisson-process. The duration between snow packages is therefore exponential distributed with expected value $1/\lambda$, where λ is the expected number of annually snow packages. The magnitude of each snow package P_m is assumed to be Gumbel distributed. The duration of a snow package T_{SP} is assumed to be related to the snow package magnitude with $T_{SP} = X_T P_m$ where the factor X_T is exponential distributed. The load history on the ground $P(t)$ can be simulated and transformed to the roof load $Q(t)$ by introducing a Gumbel distributed shape factor C with $Q(t) = CP(t)$. The parameters for the stochastic models are summarized in Table 4-19.

Table 4-19:   Overview of the stochastic Models used in this example.

	Stochastic Variable		Distribution Type	Mean Value	Standard Deviation
Short term LS	Short-term strength	R_0	Log-normal	1	0.2
	Snow load (50 y max)	Q_S	Gumbel max	1	0.21
	Model uncertainty	X_M	Log-normal	1	0.05
Load model	Duration between snow pack [y]	$1/\lambda$	Exponential	1/1.175	-
	Max. per snow pack [kN/m^2]	P_m	Gumbel max	0.33	0.21
	Duration pack factor [d/kN/m^2]	X_T	Exponential	75	-
	Roof shape factor [-]	C	Gumbel max	1	0.35

The long term simulations are performed by using the simple Nielsen model with the parameters given in Table 4-14, timber with 11% moisture content.

Result

The modification factor k_{mod} is calibrated as previously described. A value of $k_{mod} = 0.8$ is found. This result is consistent with the results presented in Sørensen et al. (2002), where the same snow load model but different damage accumulation models are used in the calibration procedure. To illustrate the effect of damage α_κ to the strength of the timber material, the residual strength ratio $r_r(t)/r_0$ can be evaluated according to Equation (4.68). In Figure 4-29, one realisation of the load process and the corresponding residual strength ratio is given. Failure occurs when the residual strength ratio drops below the load effect as consequence of an extreme snow load, i.e. when $r_r(t)/r_0 < s(t)/r_0$ (Köhler (2002)). In the case illustrated in Figure 4-29 failure occurs after a time of approximately 32 years. The load history prior to failure seems not to be of significance to the damage and the residual strength respectively. A similar observation is made in Rosowsky and Bulleit (2002) where other damage accumulation models are investigated.
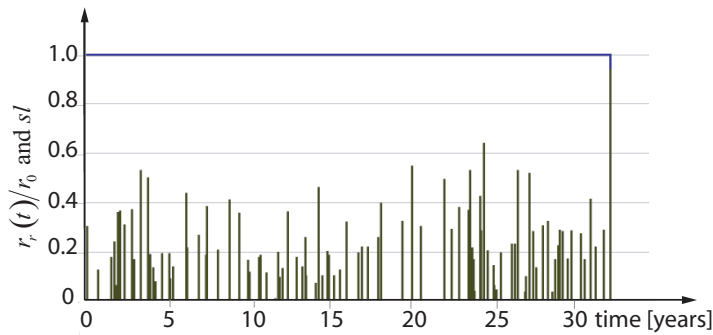
Figure 4-29   Maximum magnitude of each snow package and the residual strength of the timber specimen is plotted over lifetime.

In Figure 4-30, a snow load process is used where the standard deviation of the maximum load level of each snow package is lower compared to the example shown in Figure 4-29, $\sigma_{Pm} = 0.05$ compared to $\sigma_{Pm} = 0.21$. It is seen that the residual strength drops as a consequence of major snow loads several times until failure occurs. The damage accumulates with the number of major snow events.
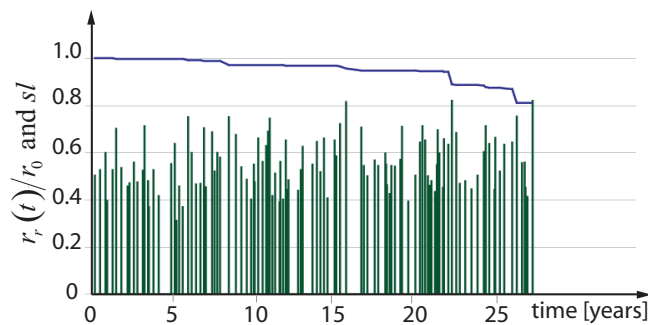
Figure 4-30   Maximum magnitude of each snow package with lower standard deviation and the residual strength of the timber specimen is plotted over lifetime.

Depending on the load level as well as the temporal characteristics of the underlying random load process failure may be considered as time independent. Rather than simulating complete load histories and incrementally accumulating damage, a time independent limit state function can be formulated. Only the load pulse that cause significant damage, may be considered for reliability analysis with the considered snow load characteristics. If the standard deviation of the maximum load level of a snow package is getting smaller, damage accumulates several times (Figure 4-30) and the time to failure has to be evaluated by simulation as described in this paper. The DVM-model does not include a threshold value η_D (compare the Foschi and Yao model, Equation (4.59)) below which no damage accumulates as some other damage accumulation models. However, through the highly non-linear properties of the model an effective threshold can be observed by analyzing the results of the simulations.

112

4.3.4.5   The Nielsen Model and Fatigue - Parametric Variable Load.

For timber structures as for structures made of any other material, in principle all types of loads must be anticipated. For the load types considered above, live load in buildings and snowload, it seems to be a reasonable assumption to regard damage solely a consequence of accumulated time under load. For some types of loads such as traffic load on bridges, wind loads on roofs and facades or the dynamic load on a rotor blade of a wind turbine it is intuitively understood that beside damage accumulation as a consequence of accumulated time under load, a significant damage contribution is due to the number of applied load cycles of given amplitude, i.e. due to fatigue effects. In Bonfield and Ansell (1991), the DOL-effect in wind turbine rotor blades is investigated considering timber as an elastic material, i.e. no damage caused by creep is considered.

In the calibration examples above (sections 4.3.4.3 and 4.3.4.4) and e.g. in Sørensen et. al. (2003), damage accumulation laws accounting for the visco-elastic damage accumulation are calibrated to long term test with structural timber specimen subjected to constant intensity loads. In the assessment of the k_{mod} factors for different load scenarios thus only the accumulated duration of load is taken into account, and fatigue effects disregarded.

In the following, two damage accumulation models are compared. The general Nielsen model for which the computational algorithm is illustrated in Figure 4-24 is considered. As previously mentioned this model is able to predict the lifetime of timber components subject to random time variant loads considering both creep and fatigue effects. Also the simple Nielsen model given in Equation (4.64) is considered. This model which also rests on the DVM-theory is compared with other damage accumulation models in section 4.3.4.3, where it is applied specifically for the purpose of calibration of k_{mod}.

Both models are used for the estimation of the time to failure of one timber specimen with the short term resistance r_0. A rectangular pulse process with constant amplitude and constant frequency as defined in Figure 4-23 is applied. The following load parameters are used: $p_{sl} = 0.5$, $\beta_{sl} = 0.5$, $sl_{\text{max}} = 0.6$, $f = 0.001$ Hz ($T = 100$s). In Figure 4-31 the residual strength ratio r_r/r_0 defined as $r_r/r_0 = \alpha_\kappa^{-0.5}$ and the maximum and minimum load intensities, sl_{max} and sl_{min} over the logarithm of time in hours are illustrated. A significant difference is observed in the predicted lifetimes, i.e. 14 and 60 years using the general and the simple model, respectively see also Figure 4-31.

It can be shown that a timber specimen is able to survive a reference lifetime period of 50 years applying a load as described above for $sl_{\text{max}} < 0.606$ for the simple model and $sl_{\text{max}} < 0.548$ for the general model.

In the following the general model is investigated in more detail. It is first examined whether the general model deviates significantly from the currently applied simpler damage accumulation model (without consideration of fatigue effect) for different types of random load processes.

A simple load process model is applied in the following, see Figure 4-32, where the rectangular load pulses are random in both their intensity and duration. The occurrence of load events at times $X_1, X_2, ...$ is modeled with the constant rate λ_S, i.e. the constant number of load events per year. The intensity of the load at a given load event P_m is assumed to be Gumbel distributed. The duration of a load event T_{LE} is assumed to be related to the load event intensity with $T_{LE} = X_T P_m$, where the factor X_T is assumed exponential distributed. The load model is illustrated in Figure 4-32.
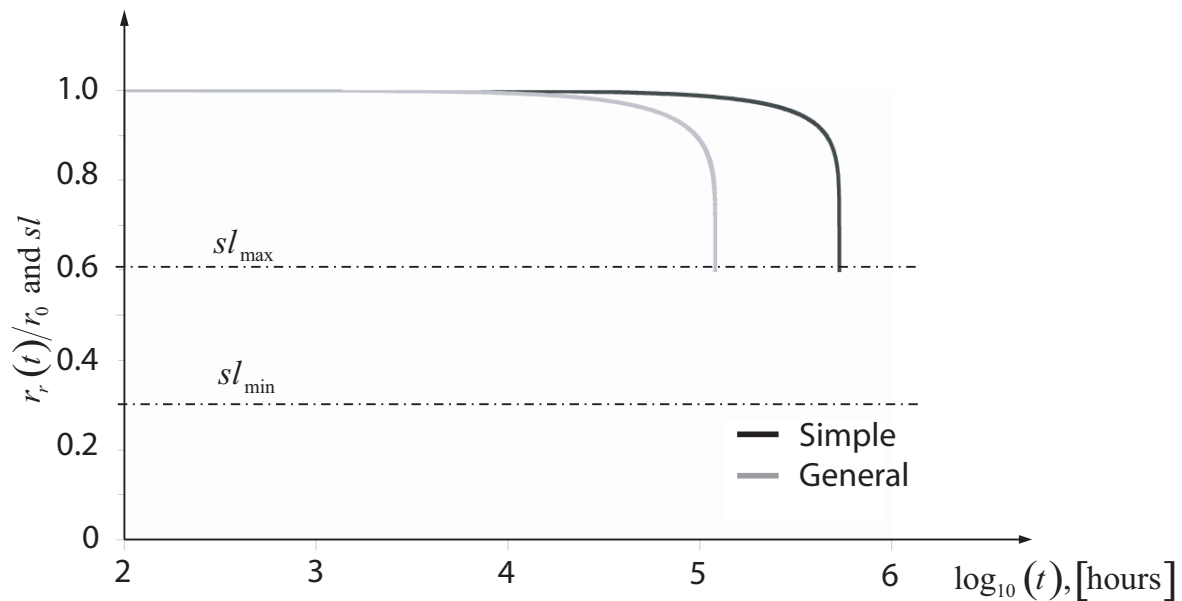
Figure 4-31   Predicted lifetime in accordance with using the simple model and the general model respectively.

To investigate the effect of the characteristics of the random load process on the model predictions, the variation of the intensity P_m and the number of load events per year λ_S are varied.
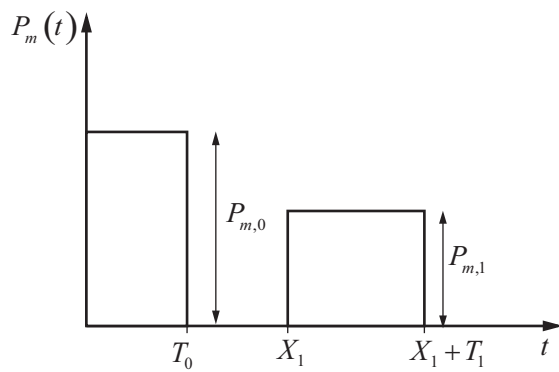
Figure 4-32   Load model applied in the example.

The parameters for the probabilistic models for the load, the long term strength and the short term strength are given in Table 4-20.

According to the presented procedure the modification factor k_{mod} is calibrated for the following cases. λ_S = 1, 4, 8, 16 (in 1/years) and $\sigma_{P_m} = 0.64$ according to Table 4-20; different numbers of load events per year are applied. The duration of the load events is decreasing by increasing number of load events per year so that the expected value of the time under load is the same for the considered load cases. In Figure 4-33 the results as obtained by the general model are illustrated and compared with the results obtained by using the simple model, i.e. the model in which fatigue effects are disregarded.

Table 4-20   Overview of the probabilistic model used in the example.

	Stochastic Variable		Distribution Type	Mean Value	Standard Deviation
Short term LS	Short-term strength	R_0	Log-normal	1	0.2
	Load, 50 years max	Q_S	Gumbel max	$f(\sigma_{P_m}, C)$	0.21
	Model uncertainty	X_M	Log-normal	1	0.05
Load model	Load events per year	λ_S	Exponential	C	-
	Intensity of the load event [kN/m^2]	P_m	Gumbel max	1	σ_{P_m}
	Load duration factor [d/kN/m^2]	X_T	Exponential	75/C	-
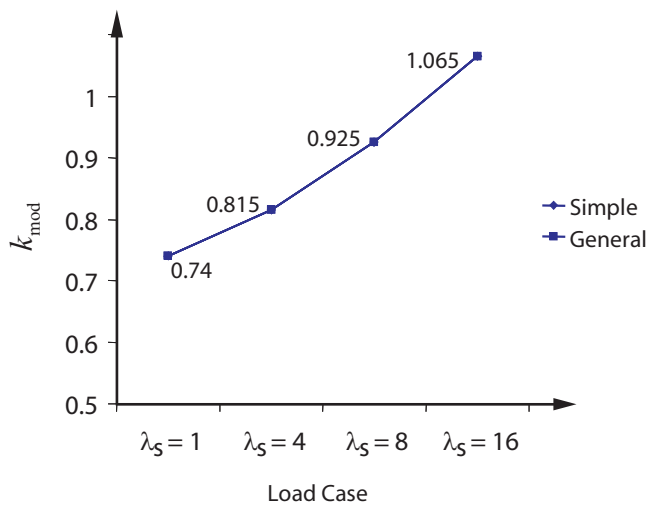
Figure 4-31   Calibrated k_{mod} factors for different load frequencies.

From Figure 4-31 it can be observed that the estimated values for the modification factor are virtually identical and independent on the choice of the damage accumulation model.

In Figure 4-32 the calibrated k_{mod} factors for different load cases are illustrated as a function of the coefficient of variation of the load intensity. The number of load events per year is constant with $\lambda_S = 16$, the expected value of the load duration factor is 4.7 d/kN/m^2 according to Table 4-20. The effect of varying the coefficient of variation in the range between 0.64 and 0.00001 is investigated, see Figure 4-32.
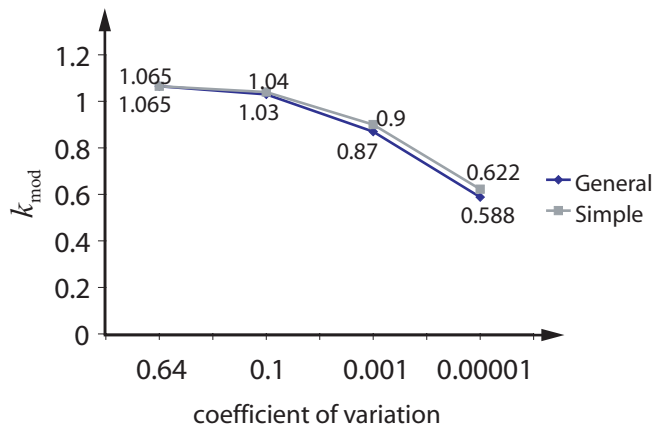
Figure 4-34   Calibrated k_{mod} factors as function of the coefficient of variation of the intensity of load events.

From Figure 4-34 it is seen that the smaller the coefficient of variation of the intensity of the load events, the larger the difference achieved by using the two different models.

4.3.5   SUMMARY AND CONCLUDING REMARKS, DOL EFFECTS

In section 4.3 an approach for the probabilistic modelling of the effect of load duration is presented. The method is exemplified for calibrating the design code short term strength modification factor k_{mod} for different characteristics of the applied loading process. The considered damage models are introduced. The Nielsen model takes basis in fracture mechanical considerations and facilitates the consideration both creep and fatigue effects. The two other models, the Gerhards model and the Foschi and Yao model take solely creep effects into account. The damage models are calibrated against duration of load tests using the maximum likelihood method. Furthermore, the damage models have been investigated and compared by applying several different load scenarios.

In section 4.3.4.3 the so called simple Nielsen model is compared with the other two models by calibrating k_{mod} for a live load scenario, using the three different DOL models. It is shown that the result is not sensitive to the particular DOL model which is used.

In section 4.3.4.4 the modification factor k_{mod} is also calibrated for a snow load scenario, this time only the simple Nielsen model is used. The result is in line with results for snow load calibration results found in the literature, where the Gerhards and the Foschi and Yao model is used. From section 4.3.4.3 and 4.3.4.4 it can be concluded, that the simple Nielsen model delivers similar results compared to other damage accumulation models.

In section 4.3.4.4 it is further observed that for a typical snowload realisation the damage accumulation process is highly non-linear, i.e. the undamaged state is directly leading into the full damage (failure) state (Figure 4-29). In Figure 4-30 it is illustrated that this is not the case when the variation of the amplitudes of each load cycle is decreased. Then, damage

accumulates as a consequence of several major load events.

In section 4.3.4.5 the general Nielsen model is compared with the simple Nielsen model. A significant difference in predicted lifetimes using the two different models can be observed in Figure 4-31. Under the given load conditions, a square wave process with constant load intensities, lifetime predictions obtained using the simple model are more than four times longer than those achieved using the general model. From this observation it can be concluded that, for the given harmonic square wave load process a significant fatigue effect might exist following the fracture mechanical modelling proposed by Nielsen (2000). This conclusion is also consistent with experimental evidence e.g. in Clorius (2001).

By applying random load processes with rectangular load pulses and random intensity and duration no significant fatigue effect is observed between the models in the frequency range considered. The estimated load duration modification factors k_{mod} are almost the same for both using the general and the simple models for the calibration.

By decreasing the coefficient of variation of the intensity of the load pulses P_m to nearly 0, i.e. P_m is nearly deterministic, a difference of the value of k_{mod} of 6% can be observed in the considered example.

The considered frequency range between 1 and 16 load cycles per year is, however, not representative for load scenarios likely to induce fatigue damages. In the present example this limited frequency interval is due only to the numerically cumbersome and time demanding calculations. It still remains to investigate higher frequency loads.

4.4   MOISTURE EFFECTS ON THE DURATION OF LOAD EFFECT

The DOL effect is dependent on the moisture content (mc) of the timber, i.e. the higher the moisture content, the shorter the time to failure. The DOL effect is also subject to variations in moisture content. Such variations increase creep significantly and shorten time to creep rupture (see e.g. Toratti (1992)). This effect is in general referred to as the mechanosorptive effect.

In line with the presented damage accumulation models for the duration of load effect, proposals for modelling the combined (damage) effect of moisture and duration of load exist. E.g. the models proposed in Fridley (1992) or in Toratti (1992) consider the moisture effect as an extra term in damage accumulation formulations similar to Equation (4.43). The parameters of these models are calibrated to rather limited data from experiments, i.e. can not be verified by a reasonable set of climate/load scenarios (Morlier (1994)). However, the combination of moisture and duration of load effects in a damage accumulation model still seems promising; current research projects focus into that direction (Sørensen and Svensson (2005), Nielsen (2005)).

In practical design, as in the Eurocode 5, the effect of moisture on the duration of load effect

is considered with the modification factor k_{mod} which is given for different climate exposures in design codes. Values for this factor are prescribed in a matrix for three different so-called service classes, i.e. different climate scenarios, and five different load classes, i.e. load scenarios. With a similar framework the stiffness degradation aspect is accounted for with the factor k_{def}, which is also prescribed in a matrix for different service and load classes. The different service and load classes according to the EC 5 are given in Table 4-21. The service classes sc are defined in regard to the average moisture content mc of the timber.

Table 4-21   Load and service classes according to the EC 5.

sc	mc [%]	Permanent ($t > 10$ years)	Long term ($0.5 < t < 10$ years)	Medium term ($0.25 < t < 6$ month)	Short term ($t < 1$ week)	Instantaneous
1	<12					
2	<20					
3	>20					

4.5   INTERRELATION OF MATERIAL PROPERTIES

As already discussed at the beginning of this chapter, other material properties are estimated based on the information about the reference material properties. In Equations (3.10)-(3.17) relationships based on experiments on European softwoods are given. The estimates derived with these equations are associated with uncertainties which are not quantified in the literature. Furthermore, only characteristic values or mean values are estimated with these formulas.

To get estimates for the probability distribution functions of other material properties the above equations are utilized as a basis. Based on several discussions within the COST action E 24 (2005) it is decided, as a simplification, to take the same interrelations as given for strength characteristic values also for the expected values for the strength related material properties. Furthermore, coefficients of variation of the other material properties and a correlation matrix is identified, both based on judgment and a result of several discussions within the COST action E24 (2005).

The bending moment capacity and the bending modulus of elasticity are assumed to be lognormal distributed. The density is assumed to be normal distributed.

Table 4-22   *Probabilistic models of other timber material properties. (quantities are tentative and basis for further discussion)*

Property	Distribution	Expected Values $E[X]$	Coefficient of variation $COV[X]$
Tension strength parallel to the grain:	lognormal	$E[R_{t,0}] = 0.6\, E[R_m]$	$COV[R_{t,0}] = 1.2\, COV[R_m]$
Tension strength perp. to the grain:	weibull	$E[R_{t,90}] = 0.015 E[P_{den}]$	$COV[R_{t,90}] = 2.5 COV[P_{den}]$
MOE - tension parallel to the grain:	lognormal	$E[MOE_{t,0}] = E[MOE_m]$	$COV[MOE_{t,0}] = COV[MOE_m]$
MOE - tension perp. to the grain:	lognormal	$E[MOE_{t,90}] = \dfrac{E[MOE_m]}{30}$	$COV[MOE_{t,90}] = COV[MOE_m]$
Compression strength parallel to the grain:	lognormal	$E[R_{c,0}] = 5\, E[R_m]^{0,45}$	$COV[R_c] = 0.8\, COV[R_m]$
Compression strength per. to the grain:	lognormal	$E[R_{c,90}] = 0.008\, E[P_{den}]$	$COV[R_{c,90}] = COV[P_{den}]$
Shear modulus:	lognormal	$E[MOE_v] = \dfrac{E[MOG_m]}{16}$	$COV[MOG_v] = COV[MOE_m]$
Shear strength:	lognormal	$E[R_v] = 0.2\, E[R_m]^{0.8}$	$COV[R_v] = COV[R_m]$

Table 4-23   *Correlation coefficient matrix. The values in this table are quantified by judgment; 0.8 ↔ high correlation, 0.6 ↔ medium correlation, 0.4 ↔ low correlation, 0.2 ↔ very low correlation.*

	MOE_m	P_{den}	$R_{t,0}$	$R_{t,90}$	$MOE_{t,0}$	$MOE_{t,90}$	$R_{c,0}$	$R_{c,90}$	MOG_v	R_v
r_m	0.8	0.6	0.8	0.4	0.6	0.6	0.8	0.6	0.4	0.4
MOE_m		0.6	0.6	0.4	0.8	0.4	0.6	0.4	0.6	0.4
P_{den}			0.4	0.4	0.6	0.6	0.8	0.8	0.6	0.6
$R_{t,0}$				0.2	0.8	0.2	0.5	0.4	0.4	0.6
$R_{t,90}$					0.4	0.4	0.2	0.4	0.4	0.6
$MOE_{t,0}$						0.4	0.4	0.4	0.6	0.4
$MOE_{t,90}$							0.6	0.2	0.6	0.6
$R_{c,0}$								0.6	0.4	0.4
$R_{c,90}$									0.4	0.4
MOG_v										0.6

It should be underlined that the information given in Table 4-22 and Table 4-23 is rather vague and associated with uncertainties. However, if no more information is available it can be taken as a reference. The information can be also utilized to quantify a prior distribution function as a basis for probability updating if more information becomes available (see Annex A).

5 PROBABILISTIC MODELLING OF THE PROPERTIES OF TIMBER CONNECTIONS

For timber structures, the structural performance depends to a considerable part on the connections between different timber structural members; connections can govern the overall strength, serviceability and fire resistance. Assessments of timber structures damaged after extreme events as storms and earthquakes often point to inadequate connections as the primary cause of damage (Foliente (1998)). Despite their importance timber connection design frameworks are not based on a consistent basis compared to the design regulations of timber structural components.

Explanations for this difference in progress of design provisions for members and connections can be found in the relative simplicity of characterising mechanical behaviour of members, as compared to connections. A diversity of connections types is used in practice and these types have infinite variety in arrangement. This usually precludes the option of testing large numbers of replicas for a reliable quantification and verification of statistical and mechanical models.

For commonly used connections, a distinction is made between carpentry joints and mechanical joints that can be made from several types of fasteners. An overview of timber connections can be found in the literature, e.g. in Thelandersson and Larsen (2003). The mechanical joints are divided into two groups depending on how they transfer the forces between the connected members. The main group corresponds to the joints with dowel type fasteners. Connections with dowels, nails, screws and staples belong to this group. The second type includes connections with fasteners such as split-rings, shear-plates and punched metal plates in which the load transmission is primarily achieved by a large bearing area at the surface of the members. In addition to connections with mechanical fasteners, also glued joints should be mentioned. This technique is mainly carried out using glued-in bolts for beam connections or large finger joints for frame corners, (Blass et al. (1995)).

In this chapter it is focused on connections with dowel type fasteners. On the example of timber to timber dowel type fasteners it is demonstrated how a probabilistic framework can be introduced. Therefore it is first focused on the physical modelling of this type of connections, while single fastener connections are at first considered. Beside a common physical model framework – the so called Johansen model – a model refinement considering timber splitting based on the work presented in Jorissen (1998) is introduced and discussed. The ingredients of the physical models, the material properties and their probabilistic modelling, are discussed. Different implementations of the considered models in present design formats are illustrated before it is examined how the effective number of fasteners for multiple fastener joints is commonly evaluated.

A large data base of load carrying capacity data of dowel type fastener connections described in Jorissen (1998) is utilized to illustrate the possible model verifications implied by

comparing model predictions with observations from the load bearing capacity tests. In the same line model uncertainties are assessed based on the similar database.

Different formats for possible probabilistic models are presented and the sensitivity of the model to the input parameters is assessed. The chapter is concluded with a discussion of the findings, the shortcomings in the presented approach and a perspective for further research is given.

5.1   JOINTS WITH DOWEL TYPE FASTENERS

Joints with dowel type fasteners are the most common joints in timber structures. Dowel type fasteners include bolts, dowels, nails and staples (see Figure 5-1). The main characteristic of this type of connections is that the fasteners are mainly laterally loaded.
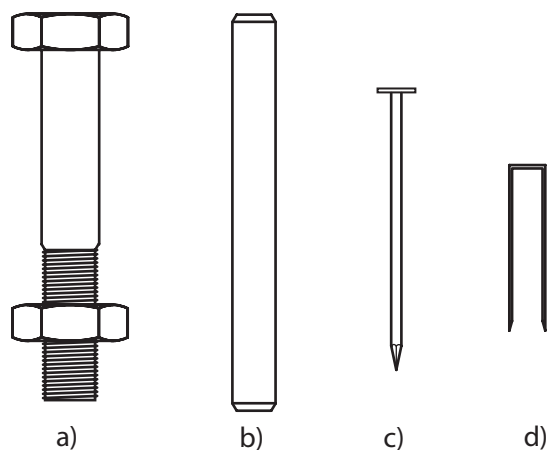
Figure 5-1   Different dowel type fasteners: a) Bolt, b) Dowel, c) Nail, d) Staple.

Laterally loaded joints with dowel type fasteners are illustrated in Figure 5-2. The load can be transferred through one or more shear planes per fastener.

By using dowel type fastener joints the load can be transferred in pure tension or compression, but also at an angle in e.g. truss joints. In Figure 5-3 two examples for timber to timber double shear fastener connections are given; a tension or compression joint (left) and a typical truss joint (right). Three timber components are connected, two so-called side members with the side member thickness d_s and one so-called middle member with thickness d_m. The fastener diameter is specified by $d_\varnothing$ and furthermore by the so-called end- and in-between distance for the side members, a_3 and a_1, are given in the left part of Figure 5-3.

Figure 5-2   Laterally loaded timber to timber joints with dowel type fasteners. Dowels in double shear (i.e. two shear planes per dowel (left)). Dowels in single shear (middle and right).

The load carrying capacity of dowel type fasteners is governed by four main characteristics:

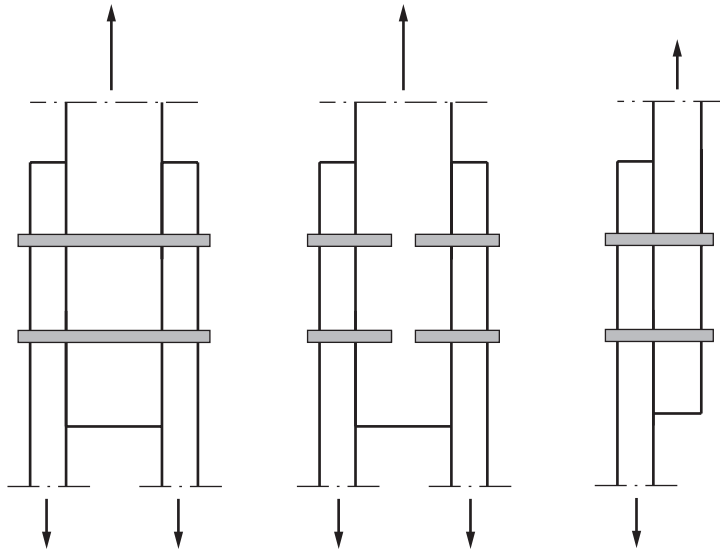- The embedding strength of the timber. The embedding strength is the property of a timber solid to resist the lateral penetration of a stiff fastener.

- The bending moment capacity of the dowel. The bending moment capacity is mainly influenced by the dowel diameter and the yield strength of the dowel material. A plastic deformation capacity is necessary to provide bending moment capacity even after considerable deformation of the dowel.

- The pulling out resistance of the dowel. Under special circumstances the so called pulling out resistance of dowel type fasteners can be mobilised even in lateral loading. A large bending deformation of the fastener is required. This effect is also referred to as the rope effect.

- The resistance against splitting. This resistance is mainly governed by a fracture mechanical phenomena.

Joints with dowel type fasteners usually contain more than one fastener. Modelling of the load bearing capacity of multiple fastener connections, however, is always based on the calculations made considering one fastener. This might be for traditional and practical reasons; since the physical behaviour of single fastener connections is rather complex, the behaviour is even more complicated for multiple fastener connections, not least due to the multitudinous configurations which could be considered.
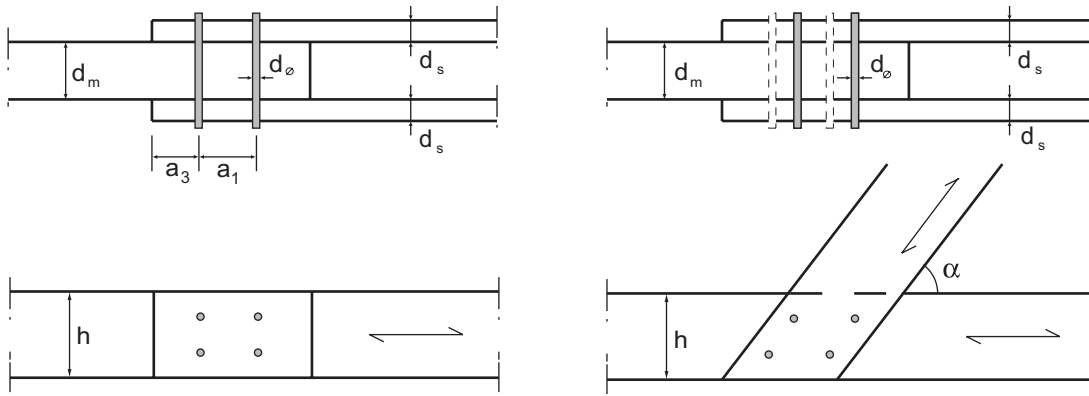
125

Figure 5-3   *Tension or compression joint (left) and a typical truss joint (right), where the load is transferred under the angle α .*

5.1.1   SINGLE FASTENER CONNECTIONS – JOHANSEN'S YIELD THEORY

The load bearing capacity of laterally loaded single dowel type fastener connections has been studied for several decades. In most timber design codes the so-called Johansen's Yield Model has been implemented for this type of connection. The embedding strength of timber and the bending capacity of the fastener are considered in this model. However, the model in its very first formulation (Johansen (1949)) is subject to rather strict assumptions. These are:

- The embedding behaviour of timber is idealised to be an ideal rigid-plastic type.

- All timber members of the connection have identical embedding strength properties.

- For single shear connections the involved members have the same thickness; for double shear connections the assembly is symmetric.

- Only the elastic bending capacity of the fastener is considered.

In Meyer (1957) these restrictions have been released; different material properties and member thickness are considered and the plastic bending capacity for the dowel type fastener can be taken into account. However, the modelling of double shear connections is restricted to symmetry in regard to its geometry and material properties. Despite of this historical background the formulations from Equation (5.1)-(5.4) are generally referred to as the Johansen Equations.

For double shear connections 4 different failure modes are differentiated; three different for the side members and one common for the middle member as illustrated in Figure 5-4. Note that for failure modes II and III two respectively four plastic hinges are developed.
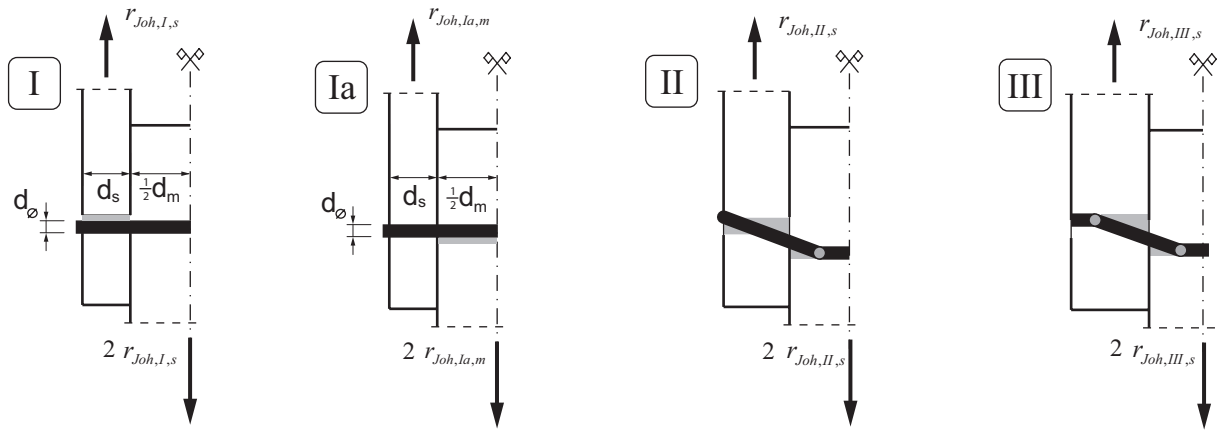
Figure 5-4   Johansen failure modes for double shear connections.

$$r_{Joh,I,s} = d_s \; d_\emptyset \; r_{h,s} \tag{5.1}$$

$$r_{Joh,Ia,m} = d_m \; d_\emptyset \; r_{h,m} \tag{5.2}$$

$$r_{Joh,II,s} = -\frac{d_s \; d_\emptyset \; r_{h,s} \; r_{h,m}}{2r_{h,s} + r_{h,m}} + \frac{1}{2}\sqrt{\left(\frac{2d_\emptyset \; d_s \; r_{h,s} \; r_{h,m}}{2r_{h,s} + r_{h,m}}\right)^2 + \frac{4\left(d_s^2 \; d_\emptyset \; r_{h,s} + 4m_y\right)d_\emptyset \; r_{h,s} \; r_{h,m}}{2r_{h,s} + r_{h,m}}} \tag{5.3}$$

$$r_{Joh,III,s} = \sqrt{\frac{4m_y \; d_\emptyset \; r_{h,s} \; r_{h,m}}{r_{h,s} + r_{h,m}}} \tag{5.4}$$

The parameters used in Equations (5.1) - (5.4) are:

$d_s \; / \; d_m$ the side/middle member thickness $[\text{mm}]$,

$d_\emptyset$ the diameter of the fastener $[\text{mm}]$,

$r_{h,s} \; / \; r_{h,m}$ the embedding strength of side/middle member $[\text{MPa}]$,

m_y the bending moment capacity of fastener $[\text{Nmm}]$.

$r_{Joh,I,s}, r_{Joh,II,s}, r_{Joh,III,s}$ is the load bearing capacity in $[\text{N}]$ of each side member according to failure modes I, II and III (see Figure 5-4) respectively. $r_{Joh,Ia,m}$ is the load bearing capacity in $[\text{N}]$ of the middle member according to failure mode Ia.

In the Johansen equations forces other than the force normal to the axis of the fastener are neglected. The load bearing capacity per shear plane is determined for any failure mode by static equilibrium or from the principle of virtual work. The governing failure mode is determined by the minimum capacity per shear plane, as:

$$r_{Joh} = \min\left(r_{Joh,I,s}, \frac{1}{2} r_{Joh,Ia,m}, r_{Joh,II,s}, r_{Joh,III,s} \right) \qquad (5.5)$$

As the fastener is assumed to exhibit ideal rigid-plastic behaviour, it can only translate and/or rotate as a rigid body or segments of it can behave as rigid bodies for failure modes, where one or more plastic hinges form in the fastener (compare Figure 5-4). The embedding of the fastener into the timber interface is also assumed to behave ideal rigid-plastic. The specification of the bending moment capacity of the fastener and the embedding strength of the fastener plays an important role in the Johansen equations.

5.1.2 SINGLE FASTENER CONNECTIONS – JORISSEN'S SPLITTING MODE

Beside the Johansen failure mechanisms, a failure mechanism associated with timber splitting is possible (Jorissen (1998)). Whether connections fail in timber splitting or according to one of the Johansen failure modes mainly depend on the positions of the fasteners; the distances from the fastener to the end of the timber member and the distance in between fasteners, both in direction parallel to the grain. In Figure 5-3 the end distance a_3 and the in between distance a_1 are specified. In general, design regulations provide guidelines for identifying connection geometries providing that the Johansen mechanisms are obtained and very brittle failure modes as timber splitting are avoided. These guidelines are in regard to minimum end distance and timber thickness both in relation with dowel diameters. However, tests by Jorissen (1998) show that connections with very rigid dowel type fasteners fail by timber splitting, even if the members are loaded parallel to the grain and designed according to the guidelines referred to above. In Jorissen (1998) a model based on fracture mechanical considerations is proposed to cover the splitting failure mode. According to Jorissen (1998) the splitting load bearing capacity of a member can be estimated as:

$$r_{splitt,i} = d_i\sqrt{\frac{g_{c,i}MOE_{0,i}d_\varnothing(2h - d_\varnothing)}{h}} \quad m_d = 1$$

$$(5.6)$$

$$r_{splitt,i} = 2d_i\sqrt{\frac{g_{c,i}MOE_{0,i}d_\varnothing(h - d_\varnothing)}{h}} \quad m_d = 2$$

with

$g_{c,i}$	the mixed mode fracture energy[1] $\left[N/mm\right]$,
$d_\varnothing$	the diameter of the dowel type fastener $\left[mm\right]$,
$MOE_{0,i}$	the modulus of elasticity parallel to the grain $\left[MPa\right]$,

---

[1] The mixed mode fracture energy is defined in section 5.1.3.3 and specifies a mixture between fracture opening failure mode and fracture sliding failure mode.

128

h the member width $[\text{mm}]$,

d_i the member thickness $[\text{mm}]$ (see Figure 5-3),

m_d the number of rows (perpendicular to the grain),

$r_{splitt,i}$ the load bearing capacity $[\text{N}]$.

Note that in Equation (5.6) it is differentiated between the case of one single row of fasteners[1] ($m_d = 1$) and two parallel rows ($m_d = 2$).

5.1.3 RELEVANT MATERIAL PROPERTIES

5.1.3.1 Embedding Strength

Several definitions of embedding strength exist for timber materials and when comparing test results it is of importance to be aware of these definitions. A quite common definition of the embedding strength is the definition according to the European test standard EN 383, which reads: the embedding strength is *"an average compressive stress at maximum load in a specimen of timber (…) under the action of a stiff linear fastener"*. The test configuration for parallel and perpendicular to grain tests is given in Figure 5-5. This standard defines the embedment strength as the highest embedment stress within 5 mm displacement for both parallel and perpendicular to grain tests. The load displacement diagrams for the embedding strength parallel and perpendicular to the grain are illustrated in Figure 5-6. For the parallel to grain test the maximum load is usually reached within 2 or 3 mm displacement and the load-displacement curves show a typical linear and full plastic branch. For tests perpendicular to the grain this is not the case. The load is increasing with increasing displacement and the measured embedding strength strongly depends on at which displacement it is defined. It should be underlined that in Johansen's yield model ideal rigid-plastic behaviour is assumed for the embedding strength. This might be reasonable for the case parallel to the grain, but it is a crude approximation for the case perpendicular to the grain (compare Figure 5-6).

In practice the embedding strength must be estimated based on indirect information, such as geometry or material properties which are related to the embedding strength. In most design codes the embedding strength is estimated based on information about the dowel diameter, the timber density and the force direction relative to the grain. These estimates are based on the analysis of experiment data.

---

[1] Rows of fasteners are defined in Figure 5-15.
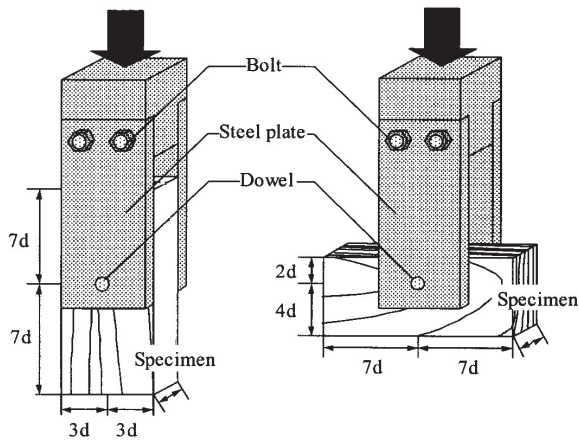
Figure 5-5   Embedment test according to EN 383. (Taken from Sawata and Yasumura (2002)).
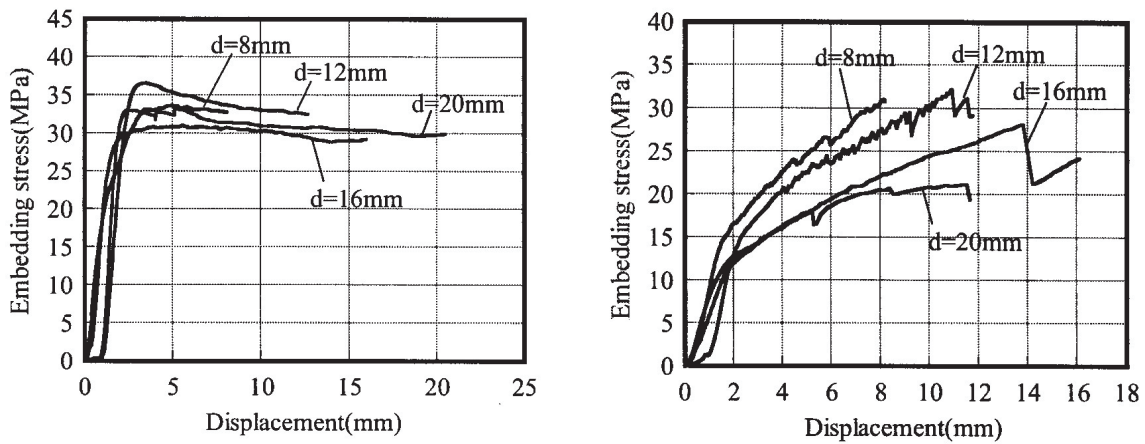
Figure 5-6   Load-displacement behaviour parallel (left) and perpendicular (right) to grain test. (Taken from Sawata and Yasumura (2002))

The embedment strength expressions in EC 5 (EN 1995-1-1:2004) are based on a comprehensive study by Whale and Smith (1986b) and Ehlbeck and Werner (1992). The influence of the timber density and the fastener diameter is derived by regression analyses. The following equations build the basis for the formulation found in the EC 5.

$$r_{h,0} = 0.082(1 - 0.01d_{\varnothing})\rho_{den} \text{ for dowels, coniferous and deciduous} \qquad (5.7)$$

$$r_{h,0} = 0.082\rho_{den}d_{\varnothing}^{-0.3} \text{ for nails (not pre-drilled), coniferous and deciduous} \qquad (5.8)$$

When the embedding strength perpendicular to the grain is estimated according to EC 5 the following formulations are utilised:

$$r_{h,90} = \frac{0.082\left(1-0.01d_{\varnothing}\right)\rho_{den}}{1.35+0.015d_{\varnothing}} \quad \text{for dowels, coniferous} \qquad (5.9)$$

$$r_{h,90} = \frac{0.082\left(1-0.01d_{\varnothing}\right)\rho_{den}}{0.9+0.015d_{\varnothing}} \quad \text{for dowels, deciduous} \qquad (5.10)$$

$$f_{h,90} = 0.082\rho_{den}d_{\varnothing}^{-0.3} \quad \text{for nails, coniferous and deciduous} \qquad (5.11)$$

with

$r_{h,0}$ the embedding strength parallel to the grain [MPa],

$r_{h,90}$ the embedding strength perpendicular to the grain [MPa],

ρ_{den} the timber density [kg/m^3],

$d_{\varnothing}$ the diameter of the fastener [mm].

Equations (5.7) - (5.11) specify an estimate of the embedding strength by given fastener diameter and density of the timber. In EC 5 the same expressions are used for the estimation of the 5%-fractile value. Therefore, it is assumed that a sufficiently good estimate for the 5%-fractile value of the embedding strength can be obtained by exchanging the expected value of the density by the 5%-fractile value. This is only true if it can be assumed that the uncertainty of the derived regression models is equal to zero.

In Leijten et al. (2004) embedding strength data is analysed. Data from research projects associated with the following references is used:

- Whale and Smith (1986b) and Ehlbeck and Werner (1992) (coinciding with data used for calibration of code formats, e.g. see the EC 5 formulations above),

- Vreeswijk (2003), Sawata and Yasamura (2002), Mischler (not published) (not yet considered in code drafting).

As in the EC 5 formulation it is found that the embedding strength mainly depends on the timber density and the diameter of the fastener. Eight cases are differentiated, namely coniferous and deciduous wood loaded parallel or perpendicular to the grain with pre-drilled (bolts and dowels) or non pre-drilled (staples and nails) fastener holes. For all cases it is found that the following model fits the data best:

$$r_h = a_h\rho_{den}^{b_h}d_{\varnothing}^{c_h}\varepsilon \qquad (5.12)$$

where,

r_h is the embedding strength $\left[\text{MPa}\right]$,

a_h, b_h, c_h are the model parameters $\left[-\right]$,

ρ_{den} is the timber density $\left[kg/m^3 \right]$,

$d_{\varnothing}$ is the diameter of the fastener $\left[mm \right]$,

ε is the error term $\left[MPa \right]$.

Rewriting Equation (5.12) as:

$$\ln\left(r_h \right) = a_h^* + b_h \ln\left(\rho_{den} \right) + c_h \ln\left(d_{\varnothing} \right) + \ln\left(\varepsilon \right) \quad \text{with} \ a_h^* = \ln\left(a_h \right) \tag{5.13}$$

and assuming that $\ln\left(\varepsilon \right)$ is normal distributed with zero mean and unknown standard deviation $\sigma_{\ln(\varepsilon)}$ the parameters a_h^*, b_h, c_h and the standard deviation $\sigma_{\ln(\varepsilon)}$ can be estimated with the maximum likelihood method, see e.g. Annex A. Therefore, the parameters and the standard deviation of the logarithm of the error term are normal distributed random variables. According to Leijten et al. (2004) the parameters of Equation (5.12) are:

Table 5-1   *Parameters for the estimation of the embedding strength based on Equation (5.12) according to Leijten et al. (2004).*

	Nails				Dowels			
	parallel		perpendicular		parallel		perpendicular	
	Coniferous	Deciduous	Coniferous	Deciduous	Coniferous	Deciduous	Coniferous	Deciduous
	n = 397	n = 120	n = 319	n = 80	n = 448	n = 285	n = 506	n = 37
$\mu_{A_h^*}$	-4.563	-5.533	-3.086	-7.905	-2.334	-2.441	-2.547	-2.245
$\sigma_{A_h^*}$	0.44	0.513	0.391	0.533	0.232	0.296	0.309	0.655
μ_{B_h}	1.345	1.507	1.148	1.887	1.066	1.091	1.099	1.128
σ_{B_h}	0.072	0.077	0.064	0.079	0.038	0.044	0.052	0.097
μ_{C_h}	-0.273	-0.181	-0.420	-0.418	-0.253	-0.253	-0.432	-0.455
σ_{C_h}	0.03	0.037	0.027	0.039	0.012	0.018	0.021	0.038
μ_{Σ_ε}	0.175	0.119	0.141	0.101	0.107	0.129	0.129	0.112
$\sigma_{\Sigma_\varepsilon}$	0.004	0.005	0.004	0.006	0.003	0.004	0.003	0.010
$\rho_{A_h^* B_h}$	-0.995	-0.994	-0.995	-0.994	-0.991	-0.986	-0.984	-0.987
$\rho_{B_h C_h}$	0.085	0.006	0.039	0.004	0.105	-0.115	-0.126	-0.129
$\rho_{A_h^* C_h}$	-0.182	-0.115	-0.138	-0.113	-0.235	-0.049	-0.055	-0.030

μ and σ are the mean values and the standard deviations of the parameters A_h^*, B_h, C_h and $\Sigma_{\ln(\varepsilon)}$. $\rho_{..}$ denotes the correlation between the parameters. With the presented information it is possible to express the probability distribution function of the embedding strength and to estimate values of the embedding strength based on this. The probability distribution function of the embedding strength $F_{R_h}\left(x \right)$ can be written as:

$$F_{R_h}\left(x \right) = P\left(\exp\left(A_h^* + B_h \ln\left(P_{den} \right) + C_h \ln\left(d_{\varnothing} \right) + \ln\left(\varepsilon \right) \right) \leq x \right) \tag{5.14}$$

where A_h^*, B_h, C_h and $\ln\left(\varepsilon \right)$ are introduced as normal distributed random variables.

However, it is important to note that the parameters of the model and consequently all estimates derived from this model are conditional on the set of data based on which the model is calibrated. It has to be assumed that the data set considered for deriving the model and its

parameters are representative.

Based on the above listed parameters the embedding strength parallel to the grain can be estimated with given density and dowel diameter and disregarding the uncertainty of the models as follows:

$$r_{h,0} = \frac{1}{96} \rho_{den}^{1.345} d_{\varnothing}^{-0.273} \quad \text{for nails, coniferous} \tag{5.15}$$

$$r_{h,0} = \frac{1}{253} \rho_{den}^{1.507} d_{\varnothing}^{-0.181} \quad \text{for nails, deciduous} \tag{5.16}$$

$$r_{h,0} = \frac{1}{10.3} \rho_{den}^{1.066} d_{\varnothing}^{-0.253} \quad \text{for dowels, coniferous} \tag{5.17}$$

$$r_{h,0} = \frac{1}{11.5} \rho_{den}^{1.091} d_{\varnothing}^{-0.253} \quad \text{for dowels, deciduous} \tag{5.18}$$
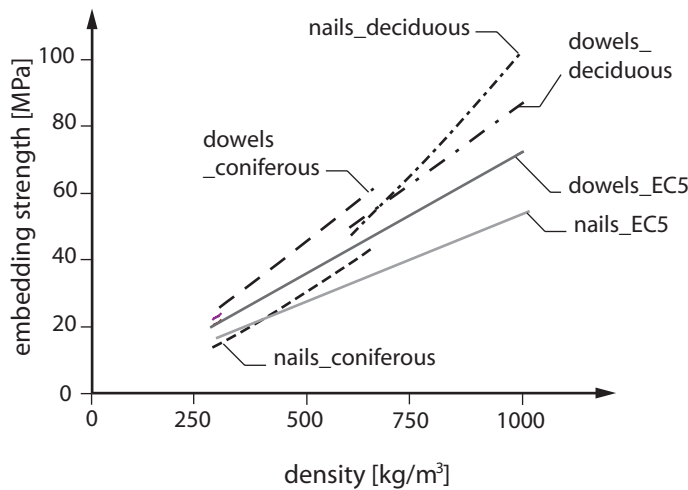
Figure 5-7   Comparison of the embedding strength parallel to the grain predictions according to Leijten et al. (2004) and the EC 5.

In Figure 5-7 Equations (5.7) and (5.8) (EC 5) and Equations (5.15) - (5.18) (Leijten et al.(2004)) are plotted as functions of the density ρ_{den} and given diameter (nails $d_{\varnothing} = 4mm$ and dowels $d_{\varnothing} = 12mm$) and compared. Except for nails coniferous, the EC 5 formulation gives lower estimates for the embedding strength.

5.1.3.2   Bending Moment Capacity

The bending moment capacity of a steel dowel type fastener is characterised through its yield moment. Johansen considered the elastic bending moment capacity $m_{y.el}$, which can be derived for circular cross sections as:

$$m_{y,el} = \frac{\pi}{32} f_y d_{\varnothing}^3 \qquad (5.19)$$

where f_y is the yield stress of the material of the fastener.

The plastic bending moment capacity for a circular cross section $m_{y,pl}$ is derived as:

$$m_{y,pl} = \frac{1}{6} f_y d_{\varnothing}^3 \qquad (5.20)$$

which requires large strains and therefore large bending rotations, of up to 45° in the fasteners, Blass et al. (2001). For mild steel the yield stress f_y in tension can in general be approximated by $f_y = 0.6 f_u$, where f_u is the ultimate tension stress of the steel material. Due to strain hardening at large bending rotations, the yield stress in bending is estimated by $f_y = 0.8 f_u$. In Figure 5-8 the stress – strain relation of mild steel is illustrated.
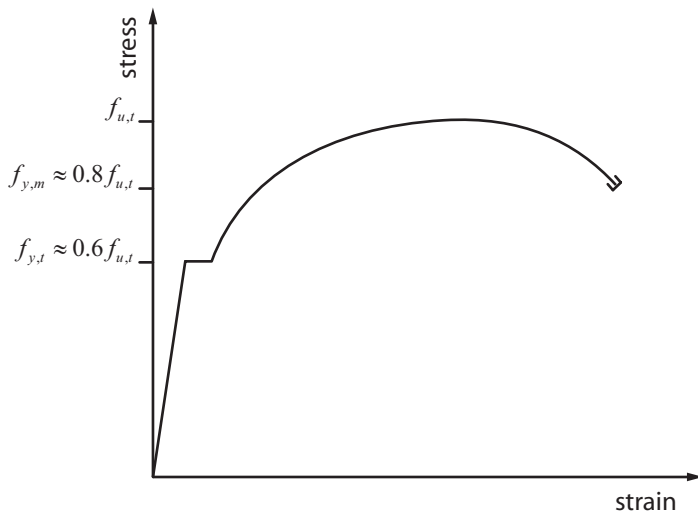
Figure 5-8   Stress – strain relation for mild steel. $f_{y,t}$ yield strength in tension, $f_{y,m}$ yield strength in bending, $f_{u,t}$ ultimate strength in tension.

In Europe the load carrying capacity and the deformation behaviour of connections with dowel type fasteners is assessed by tests according to EN 26891. Here the connection strength is defined as the maximum load before a deformation of 15 mm parallel to the load direction is observed. In Blass et al. (2001) it is shown that, considering the strength criteria of 15 mm relative displacement in the connection, an angle of 45° is rarely reached. Therefore the full plastic moment capacity cannot be mobilised. To quantify this effect an algorithm is derived to relate the plastification reached at 15 mm displacement for different dowel diameters and different joint geometries. As a result of this an alternative equation for the estimation of the bending yield moment of bolts and dowels in dowel type fastener connections is proposed in Blass et al. (2001), as:

$$m_y = 0.3 f_u d_\varnothing^{2.6}$$ (5.21)

The parameters 0.3 and 2.6 are identified by regression analysis. Note that Equation (5.21) is used in the present Eurocode 5 (EN 1995-1-1:2004).

In many tests recorded e.g. in Jorissen (1998) the load bearing capacity is reached at even lower displacements in the connection, when compared with the 15mm requirement in EN 26891. This is especially the case for multiple fastener joints. Therefore it may be assumed that even Equation (5.21) in some cases gives too optimistic estimates of the bending yield capacity.

5.1.3.3   Mixed Mode Fracture Energy

A fundamental material property in fracture mechanics is the (fracture) energy which is required to open a crack in a solid material. In fracture mechanics three different fracture modes are differentiated; the opening mode, the sliding mode and the tearing mode, compare Figure 5-9.
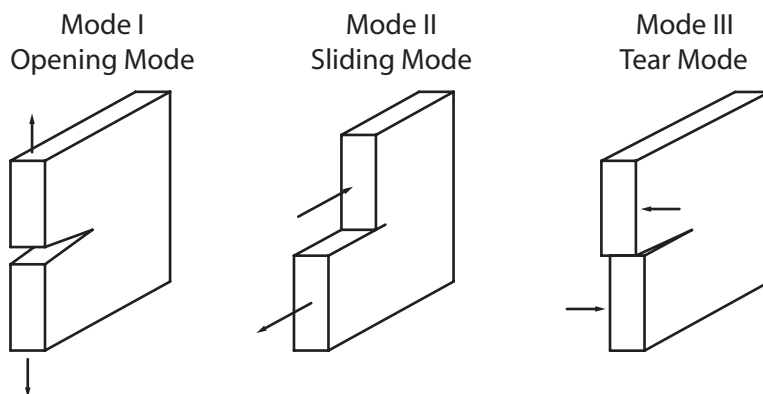
Figure 5-9   Three opening modes in fracture mechanics.

Generally, in dowel type fastener timber connections timber cracks are due to a combination of stresses perpendicular to the grain (opening Mode I) and shear (slide Mode II). The result is the so called mixed mode fracture. According to Petersson (1995) and Gustafsson (1992) the fracture energy in mixed mode I and II can be estimated as:

$$g_c = \frac{1}{\kappa_{g,1}} \left(1 + \frac{\kappa_{g,2}}{2\kappa_{g,1}} \left(1 - \sqrt{1 + \frac{4\kappa_{g,1}}{\kappa_{g,2}}} \right) \right)$$ (5.22)

where

$$\kappa_{g,1} = \frac{1 - \kappa_{g,3}}{g_{IIc}} \qquad\qquad \text{(a)}$$

$$\kappa_{g,2} = \frac{\kappa_{g,3}}{g_{Ic}} \qquad\qquad \text{(b)}$$

(5.23)

$$\kappa_{g,3} = \frac{\left(\dfrac{r_{t,90}}{r_v}\right)^2}{\left(\dfrac{r_{t,90}}{r_v}\right)^2 + \sqrt{\dfrac{MOE_{90}}{MOE_0}}} \qquad\qquad \text{(c)}$$

and

$$g_{Ic} = -162 + 1.07\rho_{den} \qquad \left[\frac{Nm}{m^2}\right] \qquad\qquad \text{(a)}$$

(5.24)

$$g_{IIc} = 3.5 g_{Ic} \qquad \left[\frac{Nm}{m^2}\right] \qquad\qquad \text{(b)}$$

where

g_{Ic} is the fracture energy required for opening mode I $[N/mm]$,

g_{IIc} is the fracture energy required for opening mode II $[N/mm]$,

ρ_{den} is the timber density $[kg/m^3]$,

$r_{t,90}/r_v$ is the ratio of tension strength perpendicular to the grain and shear strength,

MOE_{90} is the MOE perpendicular to the grain $[MPa]$,

MOE_0 is the MOE parallel to the grain $[MPa]$.

Simplification of the Mixed Mode Fracture Energy Model

In practice the input parameters of the above presented framework for deriving the mixed mode fracture energy may be not specified with high accuracy. E.g. in Jorissen (1998) the ratio of tension strength perpendicular to the grain and shear strength $r_{t,90}/r_v$ is assumed to be constant and approximated by 0.6. The ratio between the MOE perpendicular to the grain and the MOE parallel to the grain MOE_{90}/MOE_0 is assumed to be equal to 1/30. Based on these assumptions the above presented model can be simplified; thus the mixed mode fracture energy g_c can be modelled as a function of the density (Equation (5.25) and Figure 5-10):

$$g_c = 0.0013\rho_{den} - 0.1918 \qquad \left[\frac{Nmm}{mm^2} \right] \tag{5.25}$$
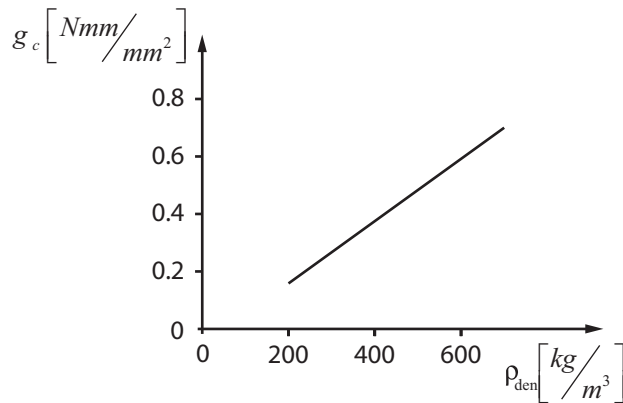
Figure 5-10   The mixed mode fracture energy as a function of the density.

5.1.4   THE BEHAVIOUR OF SINGLE FASTENER CONNECTIONS

The load-slip behaviour of single fastener connections is illustrated schematically in Figure 5-11. It is dependent on the slenderness of the fastener which can be expressed roughly as the ratio between the thickness of the middle member d_m and the diameter of the fastener $d_\varnothing$. In Figure 5-11 rigid corresponds to a ratio $d_m/d_\varnothing = 2$, rigid/slender to $d_m/d_\varnothing = 6$ and slender to $d_m/d_\varnothing = 12$.
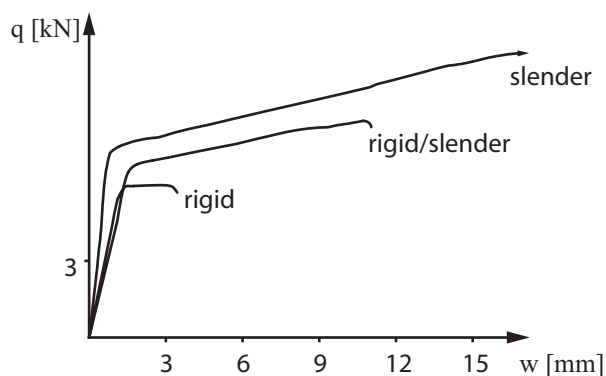
Figure 5-11   Influence of the slenderness of the fastener on the load-slip behavior of a timber to timber joint parallel to the grain, adapted from Jorissen (1998).

The slenderness ratio is also important for the assessment of the failure mode which can be expected in a joint with a specific configuration. In Jorissen (1998) slenderness ratios are introduced which divide expected rigid behaviour, rigid/slender behaviour and slender behaviour for double shear connections; corresponding to the Johansen failure modes I, II and

137

III specified in Equations (5.1)-(5.4). In Figure 5-12 the dependency between slenderness - ratio and failure mode is illustrated. The threshold values $\lambda_{gr;1}$ and $\lambda_{gr;2}$ can be quantified as:

$$\lambda_{gr;1} = \frac{d_s}{d_\varnothing} = 0.41\sqrt{\frac{f_y}{r_h}} \quad ; \quad d_m \geq 2d_s \tag{5.26}$$

$$\lambda_{gr} = \frac{d_s}{d_\varnothing} = 1.39\sqrt{\frac{f_y}{r_h}} \quad ; \quad r_m \geq 0.82r_s \tag{5.27}$$

Here, d_s is the side member thickness, $d_\varnothing$ is the dowel diameter, f_y the yield strength for bending, r_h the embedding strength and d_m the middle member thickness.
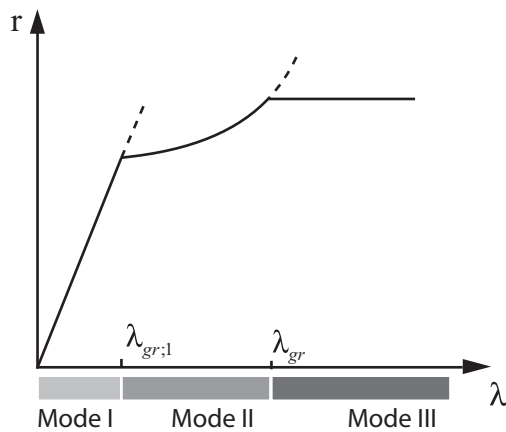
Figure 5-12   Graphical representation of the dependency between slenderness - ratio and (Johansen) failure mode. Characteristic capacity over slenderness - ratio (fixed diameter).

5.1.5   DESIGN FRAMEWORK FOR SINGLE DOWEL TYPE FASTENER CONNECTIONS

5.1.5.1   The Eurocode Design Format

According to EC 5 (EN 1995-1-1:2004) the design resistance r_d is calculated as (compare sections 2.4.2 and 4.3.4.2):

$$r_d = k_{\mathrm{mod}} z_d \frac{r_k}{\gamma_M} \tag{5.28}$$

where:

r_k is the characteristic value for the load bearing capacity,

z_d is the design variable,

138

γ_M is the partial factor for material property,

k_{mod} is a modification factor taking into account the effect of the duration of load and moisture.

The characteristic value r_k is equivalent to the 5%-fractile value of the underlying probability distribution function of the load bearing capacity.

The characteristic value of the resistance for dowel type fastener joints is derived from the Johansen equations (Equation (5.5)). In Equation (5.5) the index m specifies the middle member and s the side members which are assumed to have identical properties. The embedding strength and the fastener yield capacity are introduced as characteristic values (5%- fractile values). The characteristic value of the embedding strength is approximated by Equations (5.7) - (5.11) using the 5%- fractile value of the density; the characteristic value of the fastener bending moment capacity is approximated by Equation (5.21) using the 5%-fractile value of the tension yield strength of the fastener material.

The composite modification factor k_{mod} is taking into account the combined effect of load duration and moisture environment. k_{mod} values are tabulated in the EC 5 for different timber materials and it is distinguished between three 'service classes' (moisture environments) and five 'load duration classes' (compare section 4.4). The values given in the EC 5 are based on judgement and therefore mainly reflect tradition and experience. It is interesting to note that in the EC 5 design format for timber connections k_{mod} factors are directly applied on characteristic values of the resistance of connections (and not on a timber material property).

The partial safety factor for structural timber γ_M is 1.3 and in the EC 5 it is suggested to use the same value for the resistance of timber connections. In the present version of the EC 5 possible axial resistances of the fasteners are accounted for by multiplying factors on the equations for the failure modes II and III (Equations (5.3) and (5.4)). For these failure modes the fastener deformation is pronounced and the additional resistance can be explained by the so called rope effect, i.e. axial forces in the fastener due to transferred friction between the fastener shaft and the timber and on a compression force component due to possible washers. This effect, however, is hard to quantify and the factors are exclusively a result of judgement. In the present considerations these factors are thus not taken into account.

5.1.5.2 Simplified format according to DIN 1052:2004-08

Design formats based on the Johansen equations require the calculation of at least four equations for each failure mode. In design practice this is often considered as being too complicated and seen as a disadvantage of the Johansen equations.

In Blass et al. (1999) an alternative and simplified design framework is presented. It focuses on the case of slender fasteners and therefore ductile failure behaviour. It is suggested to aim for Johansen failure mode III and a minimum member thickness is introduced to induce slender failure mechanisms. For example for double shear timber to timber connections the

following minimum member thicknesses for side members $d_{s,req}$ and for middle members $d_{m,req}$ are proposed:

$$d_{s,req} = \left(2\sqrt{\frac{\varsigma_f}{1+\varsigma_f}} + 2 \right) \sqrt{\frac{m_y}{r_{h,s} d_\varnothing}}$$ (5.29)

$$d_{m,req} = \left(\frac{4}{\sqrt{1+\varsigma_f}} \right) \sqrt{\frac{m_y}{f_{h,m} d_\varnothing}}$$ (5.30)

ς_f is the ratio between the embedding strength of the middle member $r_{h,m}$ and the embedding strength if the side member $r_{h,s}$.

In the simplified design rules it is proposed to use the minimum member thickness and use the Johansen equation for failure mode III exclusively. If the minimum member thickness cannot be reached it is proposed to decrease the calculated joint capacity in a linear manner by multiplying the ratio between the member thickness and the minimal member thickness (see Equation (5.32)).

The resistance r_s of one fastener assuming that the minimum member thickness (Equation (5.29) and (5.30)) is used is given as:

$$r_s = r_{Joh,III,s} = \sqrt{\frac{4m_y \, d_\varnothing \, r_{h,s} \, r_{h,m}}{r_{h,s} + r_{h,m}}}$$ (5.31)

Here the index m specifies the middle member and s the side members which are assumed to have identical properties.

If the member thickness is smaller, the resistance r_s is decreased as:

$$r_s = \eta_{req} r_{Joh,III,s} \quad \text{with}$$

$$\eta_{req} = \min \left(\frac{d_s}{d_{s,req}}; \frac{d_m}{d_{m,req}} \right)$$ (5.32)

As in EC 5 the material properties for estimating the load bearing capacity r_s are introduced as 5%-fractile values. The 5%-fractile value of the embedding strength is estimated according to Equations (5.7) - (5.11) using the 5%-fractile value of the timber density; the characteristic value of the fastener bending moment capacity is approximated by Equation (5.21) by using the 5%- fractile value of the tension strength of the fastener material.

The effect of using the simplified design format can be illustrated by considering Figure 5-13.
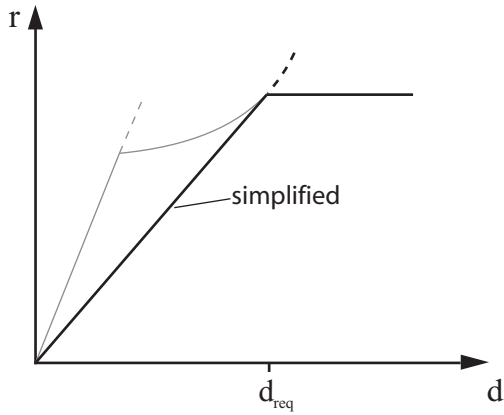
Figure 5-13   Effect of using the simplified design format on the predicted strength of the connection. Characteristic capacity over member thickness and fixed diameter.

In Figure 5-13 it can be observed that the strength predictions according to the simplified equations are always lower than predicted by using the complete Johansen equations.

5.1.5.3   Refined Design Format Considering Timber Splitting

As observed in a comprehensive test program documented in Jorissen (1998) the predictions of the load bearing capacity for cases when the Johansen failure mode I is governing are not properly reflecting the real load bearing capacity of connections with rigid fasteners. In this case Equation (5.6) (splitting) may be considered as more appropriate than Equations (5.1) and (5.2) (Johansen failure mode I).

According to the here presented refined design format the load bearing capacity is estimated based on the Johansen Equations (Equations (5.1)-(5.4)) and the splitting mode capacity according to Jorissen (Equation (5.6)). The relevant failure mode is equivalent to the failure mode corresponding to the minimum value of the load bearing capacity estimated according to Equations (5.1)-(5.4) and (5.6):

$$r_s = \min\left(r_{Joh,I,s}, \frac{1}{2}r_{Joh,Ia,m}, r_{Joh,II,s}, r_{Joh,III,s}, r_{splitt,s}, r_{splitt,m} \right)$$
(5.33)

The index m specifies the middle member and s the side members which are assumed to have identical properties.

The model predictions according to the refined design method are compared with the model predictions of the design framework according to EC 5 and the simplified design format according to DIN 1052:2004-08 presented in Section 5.1.5.2. A parameter study is carried out, considering different connection geometries and different material properties for timber and steel. (end distance: $a_3 = [5d_\varnothing; 8d_\varnothing]$; timber thickness: $d = [d_\varnothing; d_{req}]$; characteristic value of the timber density: $\rho_{den,k} = [300; 450]\ [\text{kg}/\text{m}^3]$; characteristic value of the bending moment capacity of the fastener material: $m_{y,k} = [300; 450]\ [\text{MPa}]$). Material properties are

introduced as 5%-fractile values of the underlying distribution functions. The result shows one characteristic pattern for all configurations considered (Figure 5-14): For the considered configurations the predictions according to Equation (5.6) never fall below the predictions following the simplified approach and never exceed the predictions according to Johansen I.
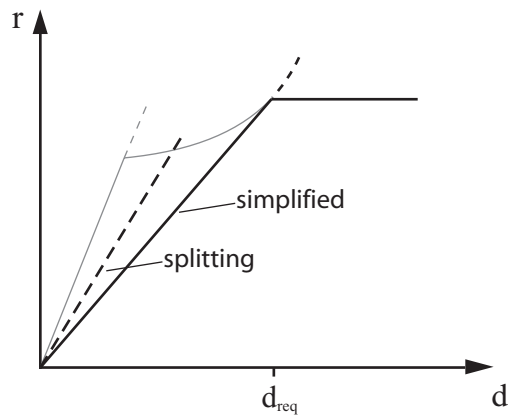
Figure 5-14   Predictions considering the splitting mode, compared to the simplified approach. Characteristic capacity over member thickness and fixed diameter.

5.2   EFFECTIVE NUMBER OF FASTENERS

In timber engineering practice, single dowel type fasteners are rarely used. So called multiple fastener connections are utilised; i.e. connections containing more than one fastener. In Figure 5-15 a multiple fastener connection is outlined. The connection is loaded in tension. Twelve fasteners are arranged in two rows.
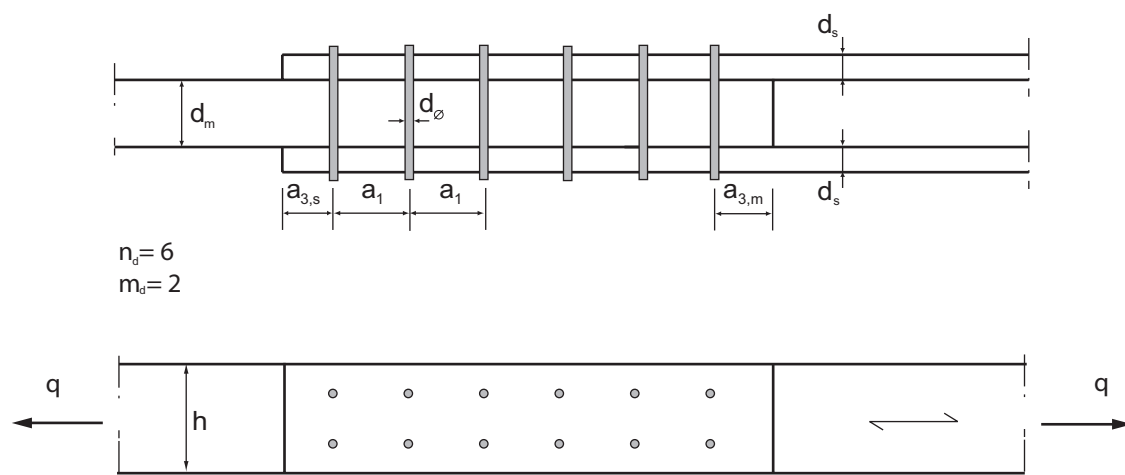
Figure 5-15   Multiple fastener connection loaded parallel to the grain in tension with $n_d = 6$ fasteners in $m_d = 2$ rows.

142

A multiple fastener connection in general fails at a load level lower than the load carrying capacity of a single fastener connection multiplied by the number of fasteners. In most national design codes this reduction in load bearing capacity is taken into account by introducing an effective number of fasteners $n_{d,ef}$ which is smaller than the real number of fasteners n_d. In general the load bearing capacity of multiple fastener connections $r_{multiple}$ is estimated as:

$$r_{multiple} = n_{d,ef} r_s \tag{5.34}$$

Different formulations for $n_{d,ef}$ can be found in the codes partly based on physical modelling and on experimental evidence. The present formulation in the EC 5 involves the in between distance a_1, the number of fasteners in a row n_d and the diameter of the fasteners $d_\varnothing$ and is based on Jorissen (1998):

$$n_{d,ef} = n_d^{0.9} \sqrt[4]{\frac{a_1}{13 d_\varnothing}} = 0.53 \, n_d^{0.9} \left(\frac{a_1}{d_\varnothing}\right)^{0.25} \tag{5.35}$$

In the Canadian code (CSA O86-1:2001) the slenderness $d/d_\varnothing$ of the fastener is also considered:

$$n_{d,ef} = 0.33 \, n_d^{0.7} \left(\frac{a_1}{d_\varnothing}\right)^{0.2} \left(\frac{d}{d_\varnothing}\right)^{0.5} \tag{5.36}$$

where d is the thickness of the component.

The common practice in the USA is described in the NDS (1997). The effective number of fasteners is based on an analytical study described in Lantos (1969). The multiple fastener connection is abstracted by one-dimensional elements. The elastic elongation stiffness EA of these elements and the foundation modulus[1] are considered for modelling the load bearing capacity of multiple fastener connections. The results of this study are tabulated in the US American code (NDS (1997)).

In Figure 5-16 the $n_{d,ef}$ - n_d relationships according to the different code formats are illustrated. It is clear that no agreement exists on the design values for $n_{d,ef}$. Although the design formulations in Canada or Europe are both experimentally based, for large n_d the difference reaches 90%.

---

[1] The foundation modulus specifies the gradient of the embedding stress - displacement diagram. (e.g. Figure 5-6)
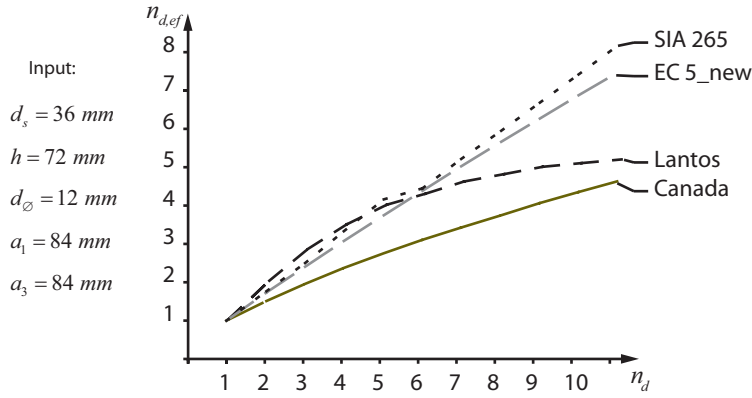
Figure 5-16 $n_{d,ef}$ *according to different design codes.*

The EC 5 design equation for $n_{d,ef}$ given in Equation (5.35) is based on Jorissen (1998). The parameters are estimated based on a comprehensive data base of 875 test observations supported by the results of a numerical model for the load bearing capacity of multiple fastener joints. All in all two different equations are proposed in Jorissen (1998). Besides the equation used in the EC 5 design format the other equation is equivalent to the one used in the Canadian code; the equations are rewritten as in Equation (5.37) and (5.38) respectively.

$$n_{d,ef} = a_n n_d^{b_n} \left(\frac{a_1}{d_\varnothing} \right)^{c_n} \tag{5.37}$$

$$n_{d,ef} = a_n n_d^{b_n} \left(\frac{a_1}{d_\varnothing} \right)^{c_n} \left(\frac{d}{d_\varnothing} \right)^{d_n} \tag{5.38}$$

a_n, b_n, c_n, d_n are model parameters,

a_1 the spacing parallel to the grain $[\text{mm}]$,

n_d the number of fasteners in a row in the grain direction,

d the member thickness $[\text{mm}]$.

The quantification of the parameters of Equation (5.37) and (5.38) depends on the basis of the load bearing capacity derivation of the single fastener joint. Two situations are differentiated:

a) R_s is based on Johansen Equations only (Equations (5.1)-(5.4)).

$$R_s = \min \begin{cases} \min \left[R_{Joh,II,s1}, R_{Joh,III,s1} \right] + \min \left[R_{Joh,II,s2}, R_{Joh,III,s2} \right] \\ \min \left[R_{Joh,Ia,m}, 2R_{Joh,I,s1}, 2R_{Joh,I,s2} \right] \end{cases} \tag{5.39}$$

See Johansen failure modes in Equations (5.1)-(5.4). Note that the Johansen failure mode I is assumed to be brittle, failure modes II and III are assumed to exhibit ductile behaviour.

144
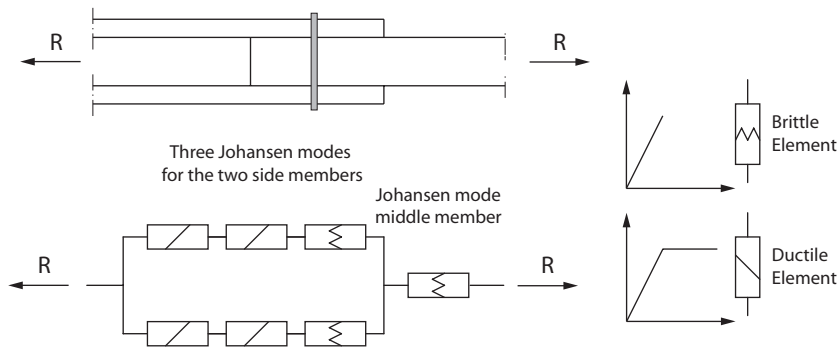
Figure 5-17   Schematic interaction of failure modes; a) R_s is based on Johansen Equations only (Equations (5.1)-(5.4)).

b) R_s is based on Johansen Equations and splitting (Equations (5.1)-(5.4) an Equation (5.6)).

$$R_s = \min \begin{cases} \min\left[R_{Joh,II,s1}, R_{Joh,III,s1} \right] + \min\left[R_{Joh,II,s2}, R_{Joh,III,s2} \right] \\ \min\left[R_{Joh,Ia,m}, 2R_{Joh,I,s1}, 2R_{Joh,I,s3} \right] \\ \min\left[R_{splitt,m}, 2R_{splitt,s1}, 2R_{splitt,s2} \right] \end{cases} \tag{5.40}$$

In Equation (5.39) and (5.40) the index m specifies the middle member, $s1$ and $s2$ the side members.
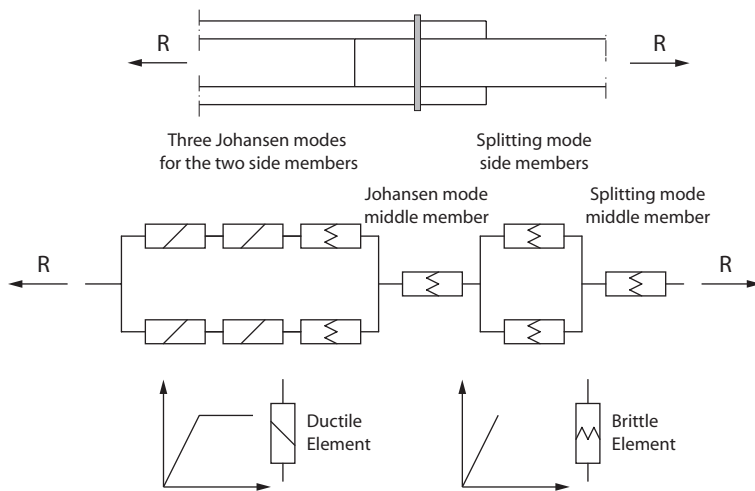
Figure 5-18   Schematic interaction of failure modes; b) R_s is based on Johansen Equations and splitting (Equations (5.1)-(5.4) and Equation (5.6)).

The following regression parameters are presented in Jorissen (1998):

Table 5-2   Regression parameters according to Jorissen (1998).

	1	2	3	4
	4-parameters Eq.(5.38) a)	4-parameters Eq. (5.38) b)	3-parameters Eq. (5.37) a)	3-parameters Eq. (5.37) b)
a_n	0.42	0.52	0.53	0.55
b_n	0.91	0.9	0.92	0.92
c_n	0.28	0.28	0.28	0.29
d_n	0.19	0.07	-	-

These parameters are derived by regression analysis, and therefore represent the parameters of the mean regression curve. In Jorissen (1998) it is found that these values are not appropriate for a design equation; they are rounded off and shifted in a way such that 5% of the observed and simulated data is larger than the predicted values.

Table 5-3   Design parameters according to Jorissen (1998).

	1	2	3	4
	4-parameters Eq.(5.38) a)	4-parameters Eq. (5.38) b)	3-parameters Eq. (5.37) a)	3-parameters Eq. (5.37) b)
a_n	0.37	0.43	0.53	0.56
b_n	0.9	0.9	0.9	0.9
c_n	0.3	0.3	0.25	0.25
d_n	0.2	0.1	-	-
			EC 5	

To demonstrate the consequence of the parameter differences in Table 5-2 and Table 5-3 $n_{d,ef}$ - n_d relationships for the case a) are illustrated in Figure 5-19. Four cases are compared; design parameters (Table 5-3) or regression parameters (Table 5-2) for the formulations with 3 or 4 parameters respectively. The curves are compared with the Canadian Design Equation (5.36). It can be observed that the differences within the different parameter sets suggested in Jorissen (1998) (Table 5-2 and Table 5-3) are rather small compared with the rather large difference compared to the formulation in the Canadian design code.
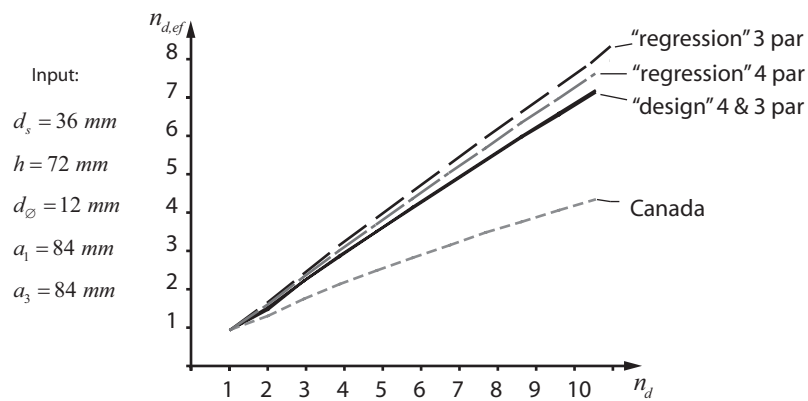
Figure 5-19 $n_{d,ef}$ *according to different suggestions in Jorissen (1998) compared to the formulation in the Canadian Design Code (CSA O86.1:2001).*

5.3 PROBABILISTIC MODEL FOR THE LOAD BEARING CAPACITY OF DOWEL TYPE FASTENER CONNECTIONS

In this section a model for the estimation of the load bearing capacity of dowel type fastener connections is derived. Therefore, at first two alternative models are presented and discussed. In this context when referring to a model two parts are considered separately; the physical and the probabilistic part. The physical part is based on proper mechanical hypothesises; i.e. here, the distinction of failure modes and the corresponding interaction between material and geometry parameters. The probabilistic part is concerned with the identification and the quantification of the parameters as random or deterministic variables and the quantification of model uncertainties.

As mentioned above two models are proposed;

a) A model where the physical part is closely related to the framework presented in the EC 5.

b) A model which is based on best possible knowledge, i.e. which accounts for the splitting mode, a refined embedding strength model and also a more complex equation for assessing $n_{d,ef}$.

The physical part of the models is summarised in Table 5-4:

Table 5-4   *Two alternative models for the load bearing capacity: a) traditional (Following EC 5), b) refinements according to failure mode and embedding strength evaluation.*

	a)	b)
Failure modes	$R_{Joh,\cdot,\cdot}$ according to Equations (5.1)-(5.4).	$R_{Joh,\cdot,\cdot}$ according to Equations (5.1)-(5.4); $R_{Splitt,\cdot}$ according to Equation (5.6).
Double shear capacity of single fasteners	$R_s = \min \begin{cases} \min\limits_{C=II,III}\left[R_{Joh,C,s1}\right] + \min\limits_{C=II,III}\left[R_{Joh,C,s2}\right] \\ \min\left[R_{Joh,Ia,m}, 2R_{Joh,I,s1}, 2R_{Joh,I,s2}\right] \end{cases}$	$R_s = \min \begin{cases} \min\limits_{C=II,III}\left[R_{Joh,C,s1}\right] + \min\limits_{C=II,III}\left[R_{Joh,C,s2}\right] \\ \min\left[R_{Joh,Ia,m}, 2R_{Joh,I,s1}, 2R_{Joh,I,s2}\right] \\ \min\left[R_{splitt,m}, 2R_{splitt,s1}, 2R_{splitt,s2}\right] \end{cases}$
Embedding strength	Based on density and diameter, according to Equations(5.7) - (5.11); e.g. for dowels parallel: $r_{h,0} = 0.082\left(1-0.01d_\varnothing\right)\rho_{den}$	Based on density and diameter, according to Equation (5.12), parameters according to Table 5-1: $r_h = a_h \rho_{den}^{b_h} d_\varnothing^{c_h} \varepsilon$
Yield Capacity	Based on the ultimate tension capacity of the fastener material and the diameter; according to Equation (5.21): $m_y = 0.3 f_u d_\varnothing^{2.6}$	Based on the ultimate tension capacity of the fastener material and the diameter; according to Equation (5.21): $m_y = 0.3 f_u d_\varnothing^{2.6}$
Mixed mode frac. energy	-	Based on the density; according to Equation (5.25): $g_c = 0.0013\rho_{den} - 0.1918 \quad \left[Nmm/mm^2\right]$
MOE	-	Based on density, according to Wood Handbook (1987): $moe_0 = 48\rho_{den}^{0.91}$
Main material properties	Ultimate tension capacity of the fastener material: f_u. Density of the timber material: ρ_{den}.	Ultimate tension capacity of the fastener material: f_u. Density of the timber material: ρ_{den}.
Geometry	Parameters modelled by deterministic values.	Parameters modelled by deterministic values.
Distance Requirements	Minimal end- and in-between distance according to EC 5. $a_1 \geq 4d_\varnothing$; $a_3 \geq 7d_\varnothing$.	Minimal end- and in-between distance according to EC 5. $a_1 \geq 4d_\varnothing$; $a_3 \geq 7d_\varnothing$.
Multiple fasteners	Based on single fastener connections as a reference (Equation (5.34); n_{ef} according to Equation (5.37), parameters according to Table 5-3 col. 3.	Based on single fastener connections as a reference (Equation (5.34); n_{ef} according to Equation (5.38), parameters according to Table 5-2 col. 2.

In the probabilistic part of the model input parameters have to be identified. The geometry parameters are assumed to be deterministic and the timber density ρ_{den} and the ultimate tension strength of the fastener material f_u are introduced as random variables. As well important is the identification and quantification of model uncertainties.

5.3.1 MODEL SENSITIVITIES

The models a) and b) (Table 5-4) are representing the load bearing capacity of single dowel type fasteners as a system of different failure modes. In order to assess the sensitivities of the different failure modes and of the input parameters a tentative reliability calculation using model a) is performed. According to this model, it is assumed that the Johansen failure modes *I* and *Ia* are brittle and the failure modes *II* and *III* are ductile. Furthermore, both side members are considered separately. The interaction of the different failure modes as illustrated in Figure 5-20 can be obtained (compare Figure 5-17).
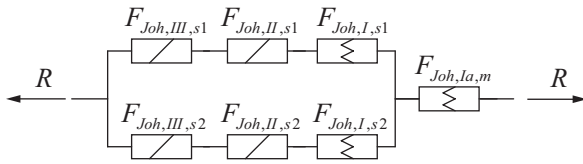
Figure 5-20   Interaction of failure modes.

The component failure events *F* associated with the different failure modes are indicated in Figure 5-20. The index *m* specifies the middle member, *s*1 and *s*2 the side members. System failure *SF* is related to the following combination of component failure events:

$$SF = F_{Joh,I,s1} \cup F_{Joh,I,s2} \cup F_{Joh,Ia,m} \cup \left(F_{Joh,II,s1} \cap F_{Joh,II,s2} \right) \cup \left(F_{Joh,III,s1} \cap F_{Joh,III,s2} \right)$$
$$\cup \left(F_{Joh,II,s1} \cap F_{Joh,III,s2} \right) \cup \left(F_{Joh,III,s1} \cap F_{Joh,II,s2} \right)$$

(5.41)

According to Equation (5.41) system failure occurs when one of the side members follows the failure mode *I*, the middle member follows the failure mode *Ia* or the side members are following both a failure mode *II* or *III*.

The governing combination of failure modes for the determination of the single fastener connection strength R_s can be quantified according to a set of limit state functions as e.g. presented here for one permanent and one variable load effect, S_G and S_Q:

$$g_1 = 2z_d R_{Joh,I,s1} X_M - S_G - S_Q = 0$$
$$g_2 = 2z_d R_{Joh,I,s2} X_M - S_G - S_Q = 0$$
$$g_3 = 2z_d R_{Joh,Ia,m} X_M - S_G - S_Q = 0$$
$$g_4 = z_d \left(R_{Joh,II,s1} + R_{Joh,II,s2} \right) X_M - S_G - S_Q = 0$$
$$g_5 = z_d \left(R_{Joh,III,s1} + R_{Joh,III,s2} \right) X_M - S_G - S_Q = 0$$
$$g_6 = z_d \left(R_{Joh,II,s1} + R_{Joh,III,s2} \right) X_M - S_G - S_Q = 0$$
$$g_7 = z_d \left(R_{Joh,III,s1} + R_{Joh,II,s2} \right) X_M - S_G - S_Q = 0$$

(5.42)

with

z_d is a design variable,

R is the resistance according to a Johansen failure mode,

S_G is the permanent load,

S_Q is the variable load,

X_M is the model uncertainty.

The failure probability p_f can be estimated as:

$$p_f = P\left(\bigcup_{i=1}^{7} g_i \leq 0\right) \tag{5.43}$$

The failure probability can be evaluated according to e.g. first or second order reliability method (FORM/SORM see e.g. Ditlevsen and Madsen (1996)). The equivalent reliability index β_E is defined as:

$$\beta_E = -\Phi\left(p_f\right) \tag{5.44}$$

The reliability analysis is performed by using the following input variables:

Table 5-5   Input variables for the tentative reliability calculation.

	timber density	yield capacity	permanent load	variable load	model uncertainty
	$P_{den}\left[kg/m^3\right]$	$F_u\left[MPa\right]$	$S_G\left[N\right]$	$S_Q\left[N\right]$	$X_M\left[-\right]$
distribution	Normal	Lognormal	Normal	Gumbel	Lognormal
mean value	450	427	1000	1200	1
st. dev.	45	17	100	480	0.1
COV	0.1	0.04	0.1	0.4	0.1
fractile	5%	5%	50%	98%	-
char. value	376	400	1000	2444	-
par. safety fac.	$\gamma_m = 1.3$		$\gamma_G = 1.35$	$\gamma_Q = 1.5$	-
geometry	member thickness		fastener diameter		fastener placing
	$d_m = 2d_s$		$d_\varnothing = 12mm$		$a_3 = 7d_\varnothing; a_4 = 3d_\varnothing$

The design variable z_d is derived according to the EC 5 design format, as:

$$z_d = \frac{\gamma_G S_{G,k} + \gamma_Q S_{Q,k}}{r_k} \gamma_M$$

(5.45)

The load characteristic values $S_{G,k}$ and $S_{Q,k}$ and the partial safety factors γ_M, γ_G and γ_Q are given in Table 5-5. The characteristic value for the resistance r_k is derived according to Equation (5.5) using the characteristic value for the embedding strength and the fastener bending moment capacity as given in Table 5-5.

To investigate different cases, i.e. different dominant failure scenarios a parameter study upon $d_m = [24mm, 160mm]$ is carried out.

5.3.1.1   Results

The equivalent reliability index β_E (Equation (5.44)) for different values for the middle member thickness d_m is calculated. In order to investigate the sensitivity of the results on the system model assumptions β_E-values for two alternative system model assumptions are also calculated; assuming that all Johansen failure modes are brittle and assuming that all Johansen failure modes are ductile (both in contrast to the assumptions in Table 5-4, Model a) brittleness for Johansen I and Ia and ductile behaviour for Johansen II and III).
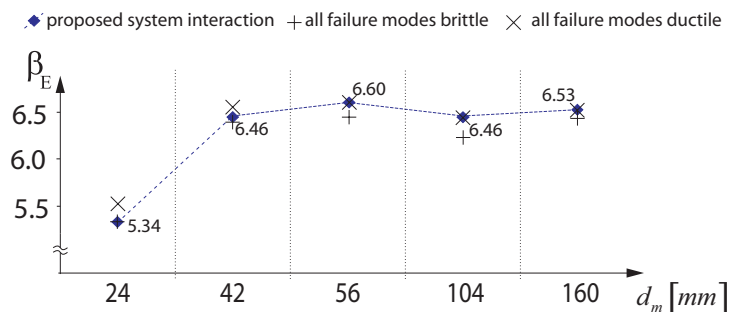
Figure 5-21   *The equivalent reliability index (Equation (5.44)) for different middle member thickness. The results of the proposed system are compared with the results of two alternative system model assumptions.*

The β_E-values range from 5.34 to 6.6 which is equivalent to a failure probability of $4.8 \cdot 10^{-8}$ and $2 \cdot 10^{-11}$ respectively. The results according to the alternative system model assumptions are in the same order of magnitude.

In Figure 5-22 the component (failure mode) sensitivities $\tau_{comp,j}$ are illustrated. $\tau_{comp,j}$ can be seen as a measure of the importance of a particular failure mode. E.g. for $d_m = 24mm$ the brittle failure modes I and Ia are relevant for the reliability calculation; for $d_m = 56mm$ exclusively failure mode II is relevant.

Ia	0.6	0.3	0.0	0.0	0.0
I	2x0.6	2x0.3	0.0	0.0	0.0
II	0.0	0.8	1.0	0.5	0.0
II/III	0.0	0.0	0.0	0.7	0.0
III	0.0	0.0	0.0	0.6	1.0
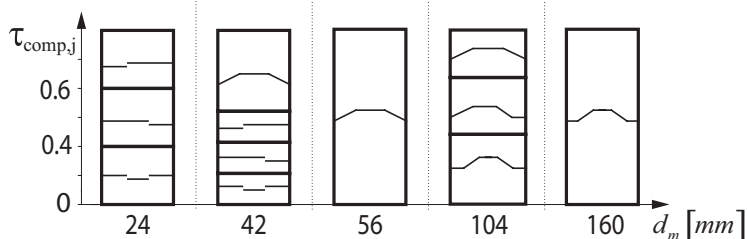
Figure 5-22   The componental (failure mode) sensitivities τ_i for different middle member thickness.

In Figure 5-23 the α - values, or sensitivity factors, of the basic variables are illustrated. The sensitivity factors are a measure for the relative importance of the uncertainty in the (stochastic) basic variables on the reliability index, (Madsen et al. (1986)). It can be observed that the uncertainty associated with the model uncertainty X_M and the variable load S_Q is dominating the result of the reliability calculation.
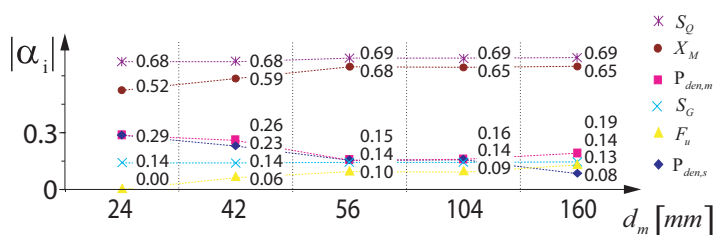
Figure 5-23   The sensitivity factors α_i for the basic variables for different middle member thickness.

5.3.1.2   Intermediate Conclusions and Discussion

Cases with different relevant failure mode combinations are considered. For all combinations it can be observed that the variables model uncertainty X_M and variable load S_Q are dominating the result of the reliability calculation. The evaluated β_E-values are significantly larger than usual target reliability indices ($\beta_{target} = 4.2$ according to the recommendations in JCSS (2001)). A possible reason for this could be the inappropriate quantification of the model uncertainty. Considering all the model assumptions integrated into the model a large variation of the model uncertainty can be expected. The possible sources of model uncertainty are briefly discussed next:

- Resistance is modelled as a consequence of the embedding strength of the timber and the plastic bending capacity of the fastener. Other possible effects on the resistance of dowel type connections are not considered.

- The embedding strength is defined as e.g. in EN 383. This standard defines the embedment strength as the highest embedment stress within 5 mm displacement for both

parallel and perpendicular to grain tests. Regression rules (associated with uncertainties) are evaluated based on these test data (Leijten et al. (2004), Whale and Smith (1986)). Further, the embedding stress strain relationship according to the Johansen equations is idealized with an ideal rigid-plastic model, which obviously does not reflect the real behaviour.

- The plastic bending capacity of the fastener is estimated by Equation (5.21), which is derived in Blass et al. (2001). The parameters 0.3 and 2.6 are found by applying an iterative procedure, estimating the activated plastic capacity for different geometrical configurations and for an assumed strength criterion of 15 mm relative displacement in the connection. In fact and as shown in Jorissen (1998) the ultimate relative displacement can be less than 15 mm.

- The system assumptions (Table 5-4) are idealisations and associated with uncertainties.

- The statistical modelling of the material properties, the timber density and the ultimate fastener capacity in tension is associated with model uncertainties.

Because of the high importance of the model uncertainty in reliability evaluation (Figure 5-23) and the several sources of uncertainty the model uncertainty is assessed in section 5.3.3 based on observations from experiments published in Jorissen (1998). But first the same data set is utilized to assess the proposed models empirically and to discuss some possible model verifications.

5.3.2   MODEL VERIFICATION

The presented models given in Table 5-4 are assessed and verified under consideration of a comprehensive data base, Jorissen (1998). Double shear timber to timber connections are loaded parallel to the grain in tension and compression. The fasteners are bolts without nuts. Teflon layers between the timber members are minimising the friction between the members. The motivation for these tests is to investigate the Johansen failure modes under additional consideration of a splitting mode. Undesired side effects as an axial tension force components in the fastener (rope effect) and friction between the timber members are minimised by having no nuts on the bolts and by introducing the Teflon layers respectively.

Table 5-6   Data base description:

$n = 564$	$n_d = [1;3;5;9]$	$m_d = [1;2]$	
$d_s = [12,60]\,mm$	$d_m = [24,80]\,mm$	$d_\varnothing = [10.65,19.75]\,mm$	$h = [6,9]\,d_\varnothing$
$a_1 = [3,12]\,d_\varnothing$	$a_2 = 3d_\varnothing$	$a_3 = [5,12]\,d_\varnothing$	

Material: North European timber, visual graded according to the Dutch class B (NEN 5466), which corresponds approximately to the European strength class C 24. The sample characteristics for density ρ_{den} are: mean value $m_{\rho_{den}} = 450.3$ and the standard deviation $s_{\rho_{den}} = 44.04$ both in $\left[kg/m^3\right]$; $n = 2700$.

Measurements: Within the experimental program, the following quantities are measured:

- the density of each side and middle member: $\rho_{den,s1}$, $\rho_{den,s2}$ and $\rho_{den,m}$,

- the load bearing capacity: r ,

- the end-displacement, i.e. the relative displacement at failure: w_Δ .

Based on the models presented in Table 5-4 assessments for the load bearing capacity of the test specimen are performed. Therefore, the measured timber densities are used together with the assumed ultimate tension strength of the fastener material and the specified geometry. As in Jorissen (1998), the ultimate tension strength f_u of the fastener material is approximated by:

$$f_u = 400 \text{ MPa} \tag{5.46}$$

The model assessments are compared with the observations from the experiments.

5.3.2.1 Single Fastener Connections

The first comparison is made for single dowel type fastener connections.

In the left part of Figure 5-24 model a) from Table 5-4 is utilised to assess the load bearing capacity r . The different failure modes according to Johansen are indicated in the Figure. Predictions of the load bearing capacity according to the Johansen equation for failure mode I (Equations (5.1) and (5.2)) are always larger than the load bearing capacity observed from the experiments and are therefore on the unsafe side. Mode II and III model calculations are smaller than the measured values. In the right part of Figure 5-24 model b) from Table 5-4 is utilised to calculate the load bearing capacity. Johansen failure mode I is entirely replaced by the splitting mode according to Jorissen (1998), i.e. for the configurations considered in this test programme Johansen failure mode I is never relevant. The predictions of the splitting

model are in good agreement with the measured values from the experiments. The Johansen modes II and III are also in better agreement with the measurements compared to model a). This might be due to the different model for the embedding strength.
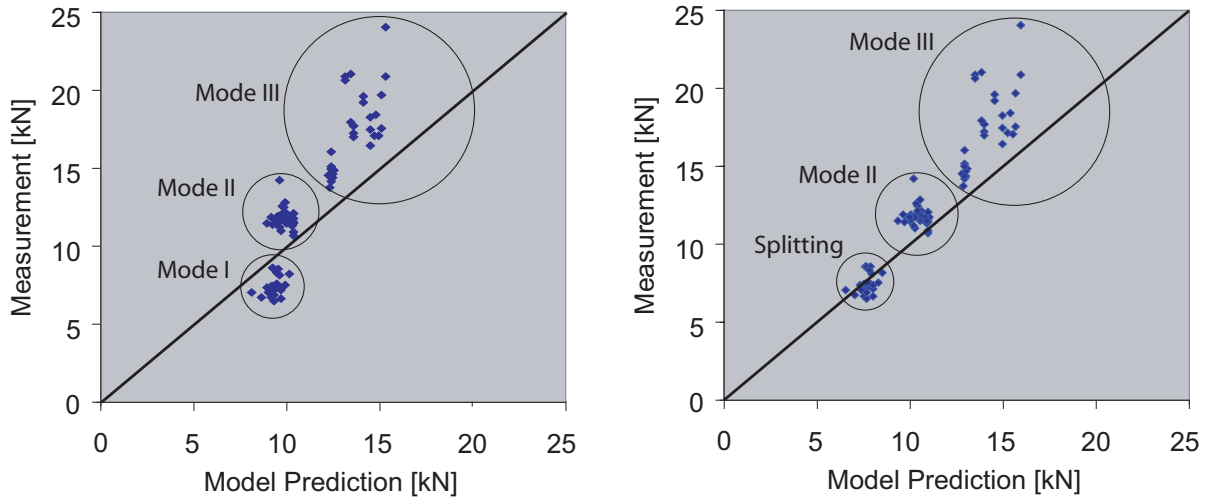
Figure 5-24   Comparison of model assessments and observations; predictions are made based on model a) (left) and model b) (right) from Table 5-4, (data from Jorissen (1998)).

For both models the results for semi rigid and slender fasteners (Johansen Modes II and III) are consistently lower than the experimentally assessed capacity of these connections. According to the Johansen model the load bearing capacity of a dowel type connection r is exclusively governed by the embedding strength of the timber r_h and the plastic bending moment capacity of the fastener $m_{y,pl}$. Other effects than friction between the timber side and middle members are not considered by the model. The reason for the special test configuration in Jorissen (1998) is to exclude these side effects as much as possible and to focus on the Johansen mechanisms. However, the consistent underestimation of the load bearing capacity by the model provokes a deeper thought in regard to what is modelled and what is really observed.

One reason for the deviation might be friction which occurs between bolt shaft and timber and this effect might increase the load bearing capacity. This effect is assumed to be proportional to the normal force between shaft and timber and different for the case of two plastic hinges (Mode II) and four hinges (Mode III) in the fastener (Figure 5-4). The model could be refined by introducing the two factors $k_{f,II}$ and $k_{f,III}$, as:

$$r_{Joh,II,s} = k_{f,II} \left[-\frac{d_s\, d_\varnothing\, r_{h,s}\, r_{h,m}}{2r_{h,s} + r_{h,m}} + \frac{1}{2} \sqrt{\left(\frac{2d_\varnothing\, d_s\, r_{h,s}\, r_{h,m}}{2r_{h,s} + r_{h,m}} \right)^2 + \frac{4\left(d_s^2\, d_\varnothing\, r_{h,s} + 4m_y \right) d_\varnothing\, r_{h,s}\, r_{h,m}}{2r_{h,s} + r_{h,m}}} \right] \quad (5.47)$$

$$r_{Joh,III,s} = k_{f,III} \sqrt{\frac{4m_y \, d_\varnothing \, r_{h,s} \, r_{h,m}}{r_{h,s} + r_{h,m}}} \qquad\qquad (5.48)$$

The factors are quantified by simple least squares technique minimising the difference between model calculation and observation, to $k_{f,II} = 1.19$ $k_{f,III} = 1.29$ for model b).
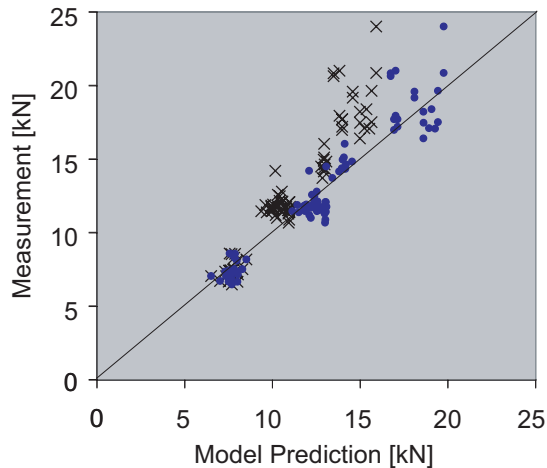
Figure 5-25   Comparison of model calculations (original, refined) with measurements, (data from Jorissen (1998)).

In Figure 5-25 the model calculations of the refined model b) are plotted and compared with the measurements. Due to the assumed friction effect the dots in the middle and upper part of the graph are shifted to the right.

The above results seem to be promising to capture common effects which might occur for any connection with dowel type fasteners. This would inherently include the assumption that the considered range of connections is representative for all dowel type connections, which obviously is not the case: Only few different diameters are considered, the bolts fit loose into the holes (in contrast to dowels, where the fit is tight); all tests are parallel to the grain, friction between the members is suppressed by the Teflon layers, etc.. The result has to be interpreted as an example and cannot be extrapolated to real situations. Therefore the idea of a design format with a factor taking into account a friction effect k_f as calibrated above is not followed further.

5.3.2.2   Multiple Fastener Connections

In Figure 5-26 model calculations following model a) and b) (Table 5-4) are compared with observations from tests. When comparing the two graphs a slight difference between the two models can be observed by visual inspection. Model b) seems to deliver more accurate predictions. However, the considerable differences in model formulations are not reflected in Figure 5-26.
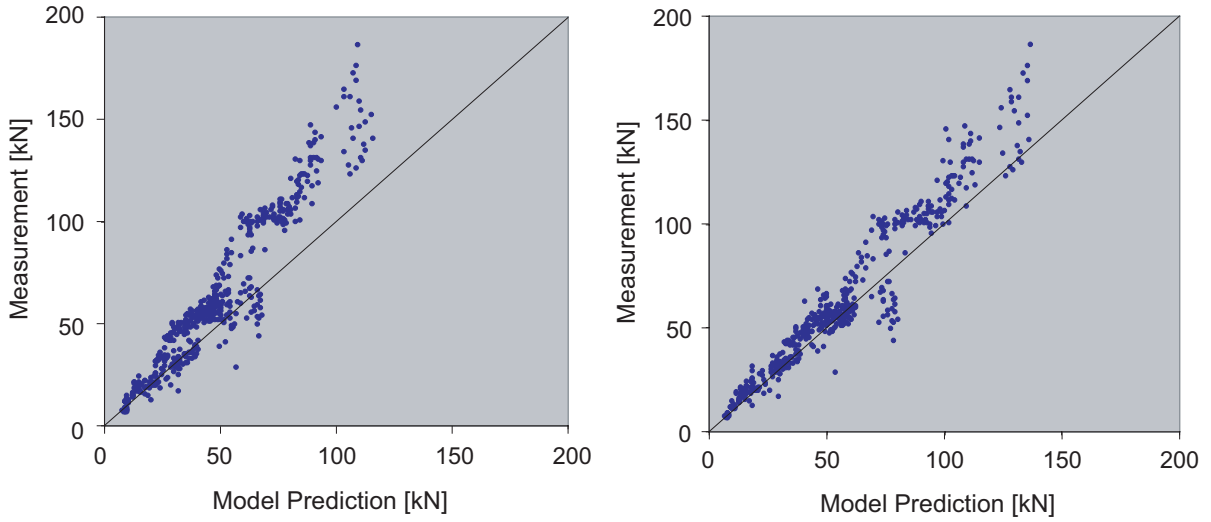
*Figure 5-26   Comparison of model calculations and measurements for multiple dowel type
fasteners (N = 474) for model a) (left) and b) (right), (data from Jorissen (1998)).*

5.3.2.3   Estimation of Model Parameters for the $n_{d,ef}$ - Equations

In Table 5-4, the $n_{d,ef}$ -equations are specified according to Equations (5.37) (Model a)) and
(5.38) (Model b)) with the corresponding parameters according to Jorissen (1998). These
parameters are derived based on the data base used herein with support of numerical
calculations. The same test observations as utilised by Jorissen and the calculated load bearing
capacity according to models a) and b) are utilized to reassess the parameters of the models.
Therefore the following regression equations based on Equations (5.37) and (5.38) can be
formulated:

$$r_{obs} = m_d n_{d,ef} r_s = m_d a_n n_d^{b_n} \left(\frac{a_1}{d_\varnothing} \right)^{c_n} r_s \ \varepsilon$$

$$\Leftrightarrow \ln \left(\frac{r_{obs}}{m_d r_s} \right) = \ln \left(n_{d,ef} \right) = \ln \left(a_n \right) + b_n \ln \left(n_d \right) + c_n \ln \left(\frac{a_1}{d_\varnothing} \right) + \ln \left(\varepsilon \right)$$

(5.49)

$$r_{obs} = m_d n_{d,ef} r_s = m_d a_n n_d^{b_n} \left(\frac{a_1}{d_\varnothing} \right)^{c_n} \left(\frac{d}{d_\varnothing} \right)^{d_n} r_s \ \varepsilon$$

$$\Leftrightarrow \ln \left(\frac{r_{obs}}{m_d r_s} \right) = \ln \left(n_{d,ef} \right) = \ln \left(a_n \right) + b_n \ln \left(n_d \right) + c_n \ln \left(\frac{a_1}{d_\varnothing} \right) + d_n \ln \left(\frac{d}{d_\varnothing} \right) + \ln \left(\varepsilon \right)$$

(5.50)

Assuming $\ln \left(\varepsilon \right)$ is following a normal distribution with zero mean and standard deviation σ_ε
the maximum likelihood method can be used to estimate the parameters of the model. Only
test data with $n_d > 1$ is used for this consideration. The number of observations is then
$n = 474$. For the estimation of the load bearing capacity of a single fastener r_s the models

157

presented in Table 5-4 are used with the input data specified in section 5.3.2.1.

The parameters of Equation (5.37) and (5.38) are estimated as follows (expected values):

Table 5-7   Parameters for estimating $n_{d,ef}$ according to Equations(5.37) and (5.38) (mean values).

	Model a)	Model b)
	3-parametric	4-parametric
	Equation (5.37)	Equation (5.38)
$E[A_n]$	0.604	0.419
$E[B_n]$	0.991	0.957
$E[C_n]$	0.211	0.183
$E[D_n]$	-	0.363
$E[\Sigma_\varepsilon]$	0.195	0.122

The evaluated parameters are utilised for further comparisons. The same models a) and b) as for Figure 5-26 is utilised with the difference that the parameters from above are used for the $n_{d,ef}$ - equation.
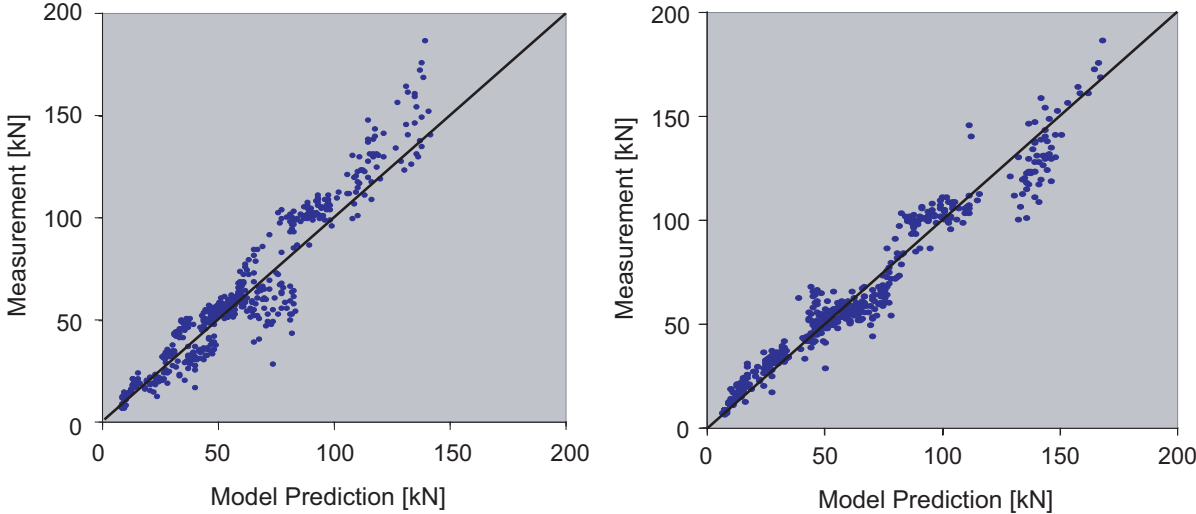
Figure 5-27   Comparison of model results. Reassessed parameters for Equations (5.37) and (5.38) and measurements for multiple dowel type fasteners (n = 474) , (data from Jorissen (1998)).

As illustrated in Figure 5-27 the model calculations are in good agreement with the test results. However, the models are mainly based on empirical considerations (the model parameters are calibrated to test observations) rather than on physical understanding (the strict

differentiation of the failure modes for single fasteners etc.). It is important to note that therefore the appearance of the models is mainly conditional to the tests considered for its verification. The physical differentiations made by modelling one single fastener and the involved calculation efforts are not consistent with the fact that the multiple fastener connection model is mainly governed by the $n_{d,ef}$ - equation. This fact is illustrated in the following.

As a simple example one could think of a very simple model. By setting up the mathematical framework of the model one could consider some physical hypothesis. The model of the capacity could be for instance be:

$$r_m = m_d a_n n_d^{b_n} \left(\frac{a_1}{d_\varnothing} \right)^{c_n} \left(\frac{d}{d_\varnothing} \right)^{d_n} \left(d_m d_\varnothing \ r_h \right)^{e_n} \varepsilon \tag{5.51}$$

where f_h is the embedding strength evaluated according to model b). The parameters of such a model could be estimated similarly to the approach used in Equation (5.50) to $\left(a_n; b_n; ...; e_n; \sigma_\varepsilon \right) = \left(0.43; 0.95; 0.19; -0.16; 1.087; 0.11 \right)$. The result is illustrated in Figure 5-28, left.

Alternatively, the embedding strength can be replaced by the timber density.

$$r_m = m_d a_n n_d^{b_n} \left(\frac{a_1}{d_\varnothing} \right)^{c_n} \left(\frac{d}{d_\varnothing} \right)^{d_n} \left(d_m d_\varnothing \ \rho_{den} \right)^{e_n} \varepsilon \tag{5.52}$$

The parameters of this model are estimated similar to the approach used in Equation (5.50) to $\left(a_n; b_n; ...; e_n; \sigma_\varepsilon \right) = \left(0.095; 0.95; 0.20; -0.07; 0.92; 0.11 \right)$. The result is illustrated in Figure 5-28, right.
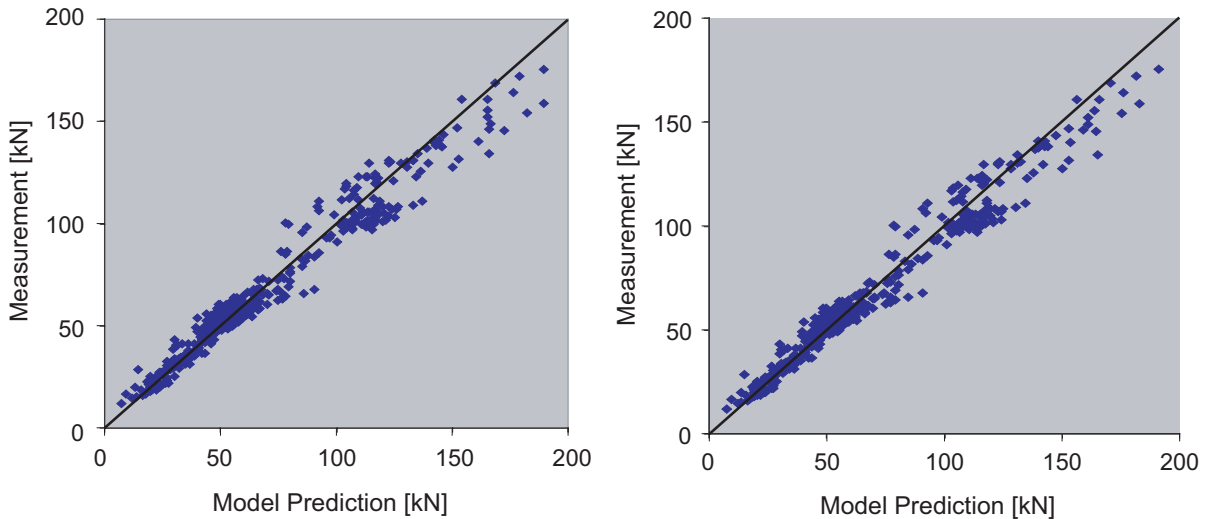
Figure 5-28   Comparison of model results according to Equation (5.51) and (5.52) with measurements for multiple dowel type fasteners $n_d < 1$ (n = 474), (data from Jorissen (1998)).

The models presented in Equation (5.51) and (5.52) do not include any steel material property, nor any differentiation or detailed description of failure modes. The result, however, is rather good. It is underlined that with Equation (5.51) and (5.52) no alternative models for multiple fastener connections are proposed. It is demonstrated, however, that models for multiple fastener connections are governed rather by the empirical $n_{d,ef}$ -equation than by physical consideration as the Johansen equations or the splitting mode.

5.3.3   EVALUATION OF THE MODEL UNCERTAINTY

Probabilistic models for uncertain load and resistance characteristics may in principle be formulated at any level of approximation within the range of a purely scientific mathematical description of the physical phenomena governing the problem at hand and a purely empirical description based on observations and tests. In engineering analysis the physical modelling is, however, normally performed at an intermediate level.

The proposed models for the load bearing capacity of double shear timber to timber connections with single and multiple dowel type fasteners is based on a strong hypothesis of the physical load bearing behaviour. However, some of the input variables of these physical models are uncertain and have to be modelled probabilistically. E.g. the formulation for the effective number of fasteners n_{ef} is found semi empirically, i.e. assuming that n_{ef} is a function of the number of fasteners n_d, the ratio between the fastener distance and the diameter $a_1/d_\varnothing$ and the ratio between the member thickness and the diameter $d/d_\varnothing$, a multiple linear formulation of the logarithms of the assumed model parameters is obtained (compare Equation (5.50)). Hereby both the identification of model parameters and the mathematical formulation of the model constitute the model assumptions. The appropriateness

160

of these model assumptions can be quantified by comparing model predictions and measurements from experiments. In the JCSS Probabilistic Model Code three possible representations of the model uncertainty are given:

$$Y = X_M f(X_1...X_n)$$
(5.53)

$$Y = X_M + f(X_1...X_n)$$
(5.54)

$$Y = f(X_{M,1}X_1, X_{M,2}X_2,..., X_{M,n}X_n)$$
(5.55)

with

Y the structural performance as a random variable,

$f(.)$ the model function,

X_M the model uncertainty as a random variable,

X_i the basic random variables.

For the model of the strength for single fastener connections the formulation in Equation (5.55) seems to be most appropriate since it differentiates between different model uncertainties for different variables within the model. For instance for the model presented in Table 5-4b) the mixed mode fracture energy is estimated based on the timber density, the embedding strength of the timber is estimated based on the timber density together with the diameter of the fastener, etc. These estimations are associated with uncertainties. However, the test configuration which is considered here does not facilitate observations of the mixed mode fracture energy or the embedding strength directly. The geometry of the connection and the timber density is measured first and thereafter the load bearing capacity of the connection is measured by destructive test. Based on these the model uncertainty can only be quantified as a factor relating the entire model with the density and the geometry as the input with the load bearing capacity as the output. Consequently the formulation of Equation (5.53) is utilised in this case and can be written as:

$$Y = X_{M,s} f_s(\mathbf{z}, \mathbf{X})$$
(5.56)

Here the model is represented as a function of a vector of random variables $\mathbf{X}$ and a vector of deterministic parameters $\mathbf{z}$.

In this case the model uncertainty can be quantified as log-normal distributed random variable X_M with the realisations:

$$x_m = \frac{y}{f(\mathbf{z}, \mathbf{x})} \tag{5.57}$$

If the mean value of X_M is not equal to 1 the model is biased.

For the three models discussed in section 5.3.2.1 the model uncertainty can be quantified.

Table 5-8   *Model uncertainties for the strength estimation of single dowel type fastener connections.*

	Model Uncertainty	Mean	St.dev
1	Model a)	1.117	0.240
2	Model b)	1.105	0.128
3	Model b) + Friction	0.995	0.087

Model a) tends to underestimate the load bearing capacity and is therefore biased. This holds also for Model b) but the standard deviation of the model uncertainty is much less than for Model a). Model b) + Friction is not biased and more accurate since the standard deviation of the model uncertainty is less. Referring to Figure 5-24 and Figure 5-25 it has to be noted that the model uncertainty is depending on the failure mode which is considered. For example, for Johansen failure mode I in Figure 5-24 the model is overestimating the obtained load bearing capacity, i.e. the model is biased and the mean value of the model uncertainty is less than one. This effect is not reflected by the overall model uncertainty which is assumed in the tentative reliability assessment in section 5.3.1. In particular, when considering the individual failure modes the model uncertainties are significantly different as seen in Table 5-9.

Table 5-9   *Model uncertainties for the strength estimation of single dowel type fastener connections. (failure modes are differentiated)*

		Mean	St.dev
Model a)	Joh I	0.802	0.061
	Joh II	1.202	0.080
	Joh III	1.278	0.131
Model b)	Splitt	0.974	0.077
	Joh II	1.112	0.066
	Joh III	1.205	0.122
Model b) + Friction	Splitt	0.974	0.077
	Joh II	0.959	0.065
	Joh III	1.045	0.095

Equation (5.56) can now be extended to the case of multiple fastener joints. Considering the

multiplicative formulation in Equation (5.34), the model uncertainty for multiple fastener joints can be expressed as:

$$Y = X_{M,s} f_s\left(\mathbf{z}, \mathbf{X}\right) X_{M,nef} f_{nef}\left(\mathbf{z}, \mathbf{X}\right)$$ (5.58)

It is not possible to assess the model uncertainty associated with the $n_{d,ef}$ model individually. It is, however, possible to quantify the model uncertainty as:

$$Y = X_{M,m}\left(f_m\left(\mathbf{z}, \mathbf{X}\right)\right)$$ (5.59)

For the models discussed in section 5.3.2.2 the model uncertainty can be quantified as given in Table 5-10.

Table 5-10   Model uncertainties for the strength estimation of multiple dowel type fastener connections.

Model Uncertainty	Mean	St.dev.
Model a)	1.256	0.253
Model b)	1.105	0.170
Model a), $n_{d,ef}$ according to Table 5-7.	1.019	0.201
Model b), $n_{d,ef}$ according to Table 5-7.	1.027	0.163
Pure empirical according to Equation (5.51)	1.06	0.107
Pure empirical according to Equation (5.52)	1.06	0.108

The values Table 5-10 are evaluated for all data not differentiating between different failure modes and different geometrical set ups.

5.3.4   LIMIT STATE FUNCTIONS FOR A SELECTED MODEL ALTERNATIVE

In the previous two sections the two alternative models are verified and model uncertainties for different representations of the model are derived. It is shown that it is possible to reduce model uncertainty by applying model verifications, i.e. re-calibrated model parameters and/or changed model representations. However, none of the proposed verifications is followed further here. The considered data set is small and not sufficiently representative. Furthermore, the same data set is used for both, the calibration of verified models and for the assessment of model uncertainty. Therefore, the relative low model uncertainty derived for the verified model should be judged with caution.

The model presented in Table 5-4 a) is taken as a basis for a model proposal; the model which is mainly following the design framework which can be found in the present version of the

EC 5. The timber density and the steel yield capacity in tension are introduced as random variables. The connection is modelled as a system of the different failure modes according to Johansen. The interaction of the different failure modes as illustrated in Figure 5-20 can be obtained.

5.3.4.1 Single Dowel Type Fastener Connections

As in Equation (5.42) the governing combination of failure modes for the determination of the single fastener connection strength R_s can be quantified according to a set of limit state functions as here for one permanent and one variable load effect, S_G and S_Q:

$$g_1 = 2z_d R_{Joh,I,s1} X_{M,I} - S_G - S_Q = 0$$
$$g_2 = 2z_d R_{Joh,I,s2} X_{M,I} - S_G - S_Q = 0$$
$$g_3 = 2z_d R_{Joh,Ia,m} X_{M,I} - S_G - S_Q = 0$$
$$g_4 = z_d \left(R_{Joh,II,s1} + R_{Joh,II,s2} \right) X_{M,II} - S_G - S_Q = 0 \qquad (5.60)$$
$$g_5 = z_d \left(R_{Joh,III,s1} + R_{Joh,III,s2} \right) X_{M,III} - S_G - S_Q = 0$$
$$g_6 = z_d \left(X_{M,II} R_{Joh,II,s1} + X_{M,III} R_{Joh,III,s2} \right) - S_G - S_Q = 0$$
$$g_7 = z_d \left(X_{M,III} R_{Joh,III,s1} + X_{M,II} R_{Joh,II,s2} \right) - S_G - S_Q = 0$$

with

z_d is a design variable,

R is the resistance according to a Johansen failure mode,

S_G is the permanent load,

S_Q is the variable load,

X_M is the model uncertainty.

In Equation (5.60) the index m specifies the middle member, $s1$ and $s2$ the side members. For the quantification of the model uncertainty X_M it is differentiated between the different failure modes. The model uncertainties for the failure modes are taken from Table 5-9, Model a).

The failure probability p_f can be estimated as in Equation (5.43) and can be evaluated according to e.g. first or second order reliability method (FORM/SORM see e.g. Ditlevsen and Madsen (1996)). The equivalent reliability index β_E is defined as in Equation (5.44).

5.3.4.2 Multiple Dowel Type Fastener Connections

In engineering design, the load bearing capacity of multiple fastener connections is assessed based on the estimated load bearing capacity of a single fastener multiplied by the effective number of fasteners $n_{d,ef}$, compare Equation (5.34). Accordingly, the proposed probabilistic

model for multiple fastener connections is based on the assessment of the single fastener load bearing capacity. The set of limit state functions, here for one permanent and one variable load effect, S_G and S_Q is given as:

$$g_1 = 2z_d n_{d,ef} R_{Joh,I,s1} X_M - S_G - S_Q = 0$$
$$g_2 = 2z_d n_{d,ef} R_{Joh,I,s2} X_M - S_G - S_Q = 0$$
$$g_3 = 2z_d n_{d,ef} R_{Joh,Ia,m} X_M - S_G - S_Q = 0$$
$$g_4 = z_d n_{d,ef} \left(R_{Joh,II,s1} + R_{Joh,II,s2} \right) X_M - S_G - S_Q = 0 \qquad (5.61)$$
$$g_5 = z_d n_{d,ef} \left(R_{Joh,III,s1} + R_{Joh,III,s2} \right) X_M - S_G - S_Q = 0$$
$$g_6 = z_d n_{d,ef} \left(R_{Joh,II,s1} + R_{Joh,III,s2} \right) X_M - S_G - S_Q = 0$$
$$g_7 = z_d n_{d,ef} \left(R_{Joh,III,s1} + R_{Joh,II,s2} \right) X_M - S_G - S_Q = 0$$

with

z_d is a design variable,

$n_{d,ef}$ the effective number of fasteners, according to Equation (5.35),

R is the resistance according to a Johansen failure mode,

S_G is the permanent load,

S_Q is the variable load,

X_M is the model uncertainty.

The model uncertainty is specified as in Table 5-10, EC a). The failure probability p_f can be estimated as given in Equation (5.43); the equivalent reliability index β_E is defined as given in Equation (5.44).

5.4   SUMMARY AND CONCLUDING REMARKS, TIMBER CONNECTIONS

Timber connections with dowel type fastener are addressed in this chapter. Calculation models for single dowel type fasteners are presented; beside the common Johansen equations a splitting mode according to Jorissen is introduced. The relevant material properties for dowel type fasteners are discussed and a new empirical equation for the estimation of the embedding strength is presented, which is based on a substantial embedding strength database consisting of data from North America, Europe and Japan.

Different design frameworks are discussed; the framework according to EC 5, a simplified one according to DIN 1052:2004-08 and a refined format also considering the splitting mode according to Jorissen (1998) are compared. Several equations for the estimation of the effective number of fasteners are introduced and compared.

Based on these findings two alternative probabilistic model frameworks for dowel type fastener connections are derived. One model, the traditional model, is based on the present design rules found in Eurocode 5, and therefore rests on a broad consensus in the research community. The other model, the refined model, features more recent research findings as failure mode of timber splitting and an alternative formulation for the embedding strength. Both models are assessed by considering test data from dowel type fastener connections. Some possible model verifications are identified and model parameters are reassessed. The model uncertainty is analysed for the two different models; it is observed that the model uncertainty is different for different failure modes and might be reduced by using verified parameters. The model predictions by using the refined model are closer to observed test data than the predictions made by using the traditional model.

However, the model improvements are not considered further when all the findings are summarised into a proposal for a probabilistic model for dowel type fasteners. The proposed model is based on the traditional model. The model uncertainty as evaluated under consideration of the test data is given.

The several promising achievements in regard to possible model refinements are not taken into account. The data set used in this study, although the number of observations is rather large, is not considered as representative for the entire domain of dowel type fasteners. In this context it should be mentioned that this statement also has to be considered when utilizing the model uncertainties quantified based on this test observations. However, the presented scheme for the verification of the model for the load capacity of connections with dowel type fasteners should be followed further under consideration of more experimental data.

6 PROBABILISTIC MODEL CODE - TIMBER

In chapter 4 and 5 existing knowledge about some aspects of the modelling of timber structures is reviewed, discussed and extended. However, the different aspects are treated rather independently. In this chapter it is the aim to envelope the above discussed aspects into a consistent modelling framework.

6.1 SCOPE AND LIMITATIONS OF THE PROPOSAL

The proposal contains models and limit state formulations which are found to be most relevant for the probabilistic analysis and code calibration of timber structures. The content of this proposal should serve as a general guideline and common reference, but also as a basis for further discussions in the research community; discussions on how to describe the rather complex strength and stiffness related behaviour of timber and timber related materials sufficiently precise and operational for engineering purposes.

The proposed probabilistic model code PMC for timber structures mainly concerns the modelling of material properties of solid structural timber and the modelling of dowel type fastener connections. The proposed models are predominantly based on test programs and investigations considering European and North American softwoods. For some other softwoods and especially for hardwood the underlying assumptions are less appropriate. It should also be noted that part of given numbers in this proposal should be considered as indicative values.

6.2 MODEL FRAMEWORK

In Figure 6-1 the general principle of the proposed modelling framework is illustrated. The framework takes basis in the reference material properties represented by random variables in the vector $\mathbf{X}$. As introduced in chapter 4 the reference material properties are the bending moment capacity R_m, the bending modulus of elasticity MOE_m and the timber density P_{den}. Other timber material properties are represented by random variables in the vector $\mathbf{Y}$. The material properties are seen in three different contexts. In the upper part of Figure 6-1 the material properties of test volumes measured under reference conditions[1] are specified with $\mathbf{X}^s$ and $\mathbf{Y}^s$. Test standards prescribe dimensions, duration and climate conditions for these tests. Nearly all available experimental evidence is related to tests performed according to these test standards, i.e. to the corresponding test volumes and conditions. In the middle part

---

[1] Reference test condition is defined in regard to the climate in which the volumes are conditioned prior to the test and in regard to the type of loading.

of Figure 6-1 the indicated material properties are related to reference volumes considered under reference conditions, $\mathbf{X}^0$ and $\mathbf{Y}^0$. A reference volume is defined as the volume for which the material properties are assumed to be constant. In the bottom part of Figure 6-1 the material properties under any conditions and any size of a component are represented with $\mathbf{X}^\alpha$ and $\mathbf{Y}^\alpha$.
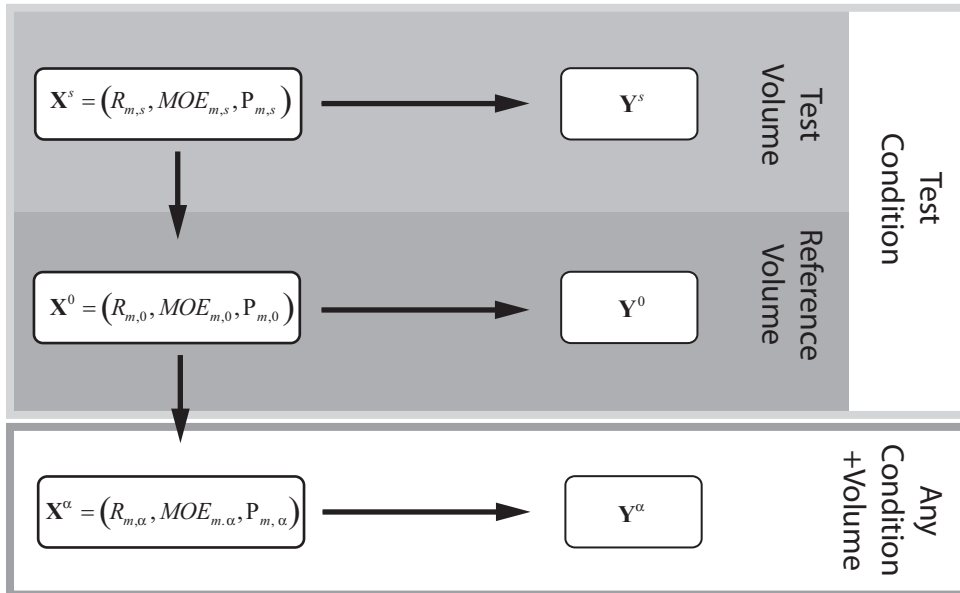
Figure 6-1   Model Framework. It is differentiated between different volumes and different conditions. The arrows indicate where models are proposed.

6.2.1   BASIC PROPERTIES

The reference properties of structural timber are:

the bending strength $r_{m,s}$ in $\left[MPa\right]$ and the

bending modulus of elasticity (MOE) $moe_{m,s}$ in $\left[MPa\right]$,

both measured on short-term standard test specimens evaluated according to ISO 8375[1] and the

timber density $\rho_{den,s}$ in $\left[kg/m^3\right]$,

measured according to ISO 3131[2].

The subscript s refers to material property according to a standardised test procedure.

For bending components it is assumed that the material properties of a cross section are

---

[1] symmetrical 4-point bending test, span $18h$ ($3 \cdot 6 \cdot h$) with $h \approx 150mm$, ramp load test duration $300 \pm 120s$, specimen conditioned at nominal climate, $20 \pm 2\,°C$, $65 \pm 5\%$ relative humidity.

[2] from a disc of full cross section, free of knots and resin pockets.

equivalent with the material properties of the reference volume; $r_{m,0}$, $moe_{m,0}$, $\rho_{den,0}$.

The reference material properties are sensitive to the deviations from the standard test conditions. The reference material properties of a cross section in situ (i.e. under any condition) can be estimated as:

Bending moment capacity in situ, $r_{m,0,\alpha}$:

$$r_{m,0,\alpha} = \alpha\big(Ex(s,\omega,\tau,t)\big)r_{m,0} \qquad (6.1)$$

Bending MOE in bending in situ, $moe_{m,0,\delta}$:

$$moe_{m,0,\delta} = \frac{MOE_{m,0}}{\big(1+\delta\big(Ex(s,\omega,\tau,t)\big)\big)} \qquad (6.2)$$

Density in situ, $\rho_{den,0}$:

$$\rho_{den,0} = \rho_{den,s} \qquad (6.3)$$

where $Ex(s,\omega,\tau,t)$ is the exposure of the structure to loads, humidity and temperature, over time t; $\alpha\big(Ex(.)\big)$ is a strength modification function, in general defined for a particular set of exposures; $\delta\big(Ex(.)\big)$ is a stiffness modification function, in general defined for a particular set of exposures.

Other material properties are estimated based on the reference material properties. Referring to section 4.5 expressions for the expected values $E[.]$ and the coefficient of variation $COV[.]$ are given in Table 6-1.

Table 6-1: Relation reference properties – other properties (based on section 4.5).

Property	Expected Values $E[X]$	Coef. of variation $COV[X]$
Tension strength par. to the grain, $r_{t,0}$:	$E[R_{t,0}] = 0.6\,E[R_m]$	$COV[R_{t,0}] = 1.2\,COV[R_m]$
Tension strength perp. to the grain, $r_{t,90}$:	$E[R_{t,90}] = 0.015E[P_{den}]$	$COV[R_{t,90}] = 2.5COV[P_{den}]$
MOE - tension par. to the grain, $moe_{t,0}$:	$E[MOE_{t,0}] = E[MOE_m]$	$COV[MOE_{t,0}] = COV[MOE_m]$
MOE - tension perp. to the grain, $moe_{t,90}$:	$E[MOE_{t,90}] = \dfrac{E[MOE_m]}{30}$	$COV[MOE_{t,90}] = COV[MOE_m]$
Compression strength par. to the grain, $r_{c,0}$:	$E[R_{c,0}] = 5\,E[R_m]^{0,45}$	$COV[R_c] = 0.8\,COV[R_m]$
Compression strength per. to the grain, $r_{c,90}$:	$E[R_{c,90}] = 0.008\,E[P_{den}]$	$COV[R_{c,90}] = COV[P_{den}]$
Shear modulus, mog_v:	$E[MOG_v] = {E[MOE_m]}\big/{16}$	$COV[MOG_v] = COV[MOE_m]$
Shear strength, r_v:	$E[R_v] = 0.2\,E[R_m]^{0.8}$	$COV[R_v] = COV[R_m]$

The relations are derived for standard test specimen properties tested under reference conditions. However, it is assumed that the relations can be used at any level, i.e. for reference volumes and for other climate and load conditions.

6.2.2 TYPICAL ULTIMATE LIMIT STATES

6.2.2.1 Components

The ultimate limit state equation for a cross section subjected to stress in one particular direction is given as:

$$g = z_d \, R \, X_M - \sum_i S_i \tag{6.4}$$

where z_d is a design variable, e.g. cross-sectional area, R is the resistance, e.g. tension strength, ΣS_i is the sum of all possible load effects, e.g. axial stresses, X_M is the model uncertainty.

The ultimate limit state equation for cross sections subjected to combined bending and tension stress parallel to grain is given as:

$$g = 1 - \left(\frac{1}{z_{d,A}} \frac{\sum_i S_{t,i}}{R_{t,0}} + \frac{1}{z_{d,M}} \frac{\sum_i S_{m,i}}{R_m} \right) X_M \tag{6.5}$$

where $z_{d,A}, z_{d,M}$ are design variables, e.g. the cross sectional area and the section modulus, $R_{t,0}, R_m$ are the tension strength and the bending moment capacity, $\Sigma S_{t,i}, \Sigma S_{m,i}$ are the sum of all possible load effects, e.g. axial stresses and bending stresses and X_M is the model uncertainty.

Ultimate limit state equations for cross sections subjected to other combined stresses can be formulated similarly.

6.2.2.2 Connections

The proposed limit state functions for dowel type fastener connections are given in section 5.3.4.

6.2.3 TYPICAL SERVICEABILITY LIMIT STATES

E.g. when a deflection exceeds an allowable deflection limit:

$$g(t) = \delta_L - W_\Delta \left(\Sigma S_i, MOE_m, t \right) X_M \tag{6.6}$$

where δ_L is an allowable deflection limit and $W_\Delta \left(\Sigma S_i, MOE_m, t \right)$ is the deflection at time t, depending on load effects ΣS_i and modulus of elasticity and X_M is the model uncertainty.

6.3 SIMPLE PROBABILISTIC MODEL

A rather simple but operational proposal for the quantification of the input parameters is presented in this section. The specifications may be seen as a common reference for, e.g. code calibration procedures.

6.3.1 BASIC PROPERTIES

The distribution type and the recommended coefficient of variation (cov) of the basic material properties for European softwood are given in Table 6-2. It is assumed that the properties of test specimen $r_{m,s}$, $moe_{m,s}$, $\rho_{den,s}$ are equivalent to the reference properties of cross sections in a structure $r_{m,0}$, $moe_{m,0}$, $\rho_{den,0}$.

Table 6-2: Probabilistic models for reference properties.

	Distribution	cov
Bending strength $R_m = R_{m,s}$	Lognormal	0.25
Bending MOE $MOE_m = MOE_{m,s}$	Lognormal	0.13
Density $P_{den} = P_{den,s}$	Normal	0.1

The proposed distribution functions for the other material properties are indicated in Table 6-3.

Table 6-3   Distribution functions for other material properties.

Property	Distribution Function
Tension strength par. to the grain, $R_{t,0}$:	Lognormal
Tension strength perp. to the grain, $R_{t,90}$:	2-p Weibull
MOE - tension par. to the grain, $MOE_{t,0}$:	Lognormal
MOE - tension perp. to the grain, $MOE_{t,90}$:	Lognormal
Compression strength par. to the grain, $R_{c,0}$:	Lognormal
Compression strength per. to the grain, $R_{c,90}$:	Normal
Shear modulus, MOG_v :	Lognormal
Shear strength, R_v :	Lognormal

6.3.2 CORRELATION MATRIX

The relations to other material properties are given in Table 6-1. Indicative values of the correlation coefficients are given in Table 6-4.

Table 6-4   Correlation coefficient matrix – indicative values.

	MOE_m	P_{den}	$R_{t,0}$	$R_{t,90}$	$MOE_{t,0}$	$MOE_{t,90}$	$R_{c,0}$	$R_{c,90}$	MOG_v	R_v
r_m	0.8	0.6	0.8	0.4	0.6	0.6	0.8	0.6	0.4	0.4
MOE_m		0.6	0.6	0.4	0.8	0.4	0.6	0.4	0.6	0.4
P_{den}			0.4	0.4	0.6	0.6	0.8	0.8	0.6	0.6
$R_{t,0}$				0.2	0.8	0.2	0.5	0.4	0.4	0.6
$R_{t,90}$					0.4	0.4	0.2	0.4	0.4	0.6
$MOE_{t,0}$						0.4	0.4	0.4	0.6	0.4
$MOE_{t,90}$							0.6	0.2	0.6	0.6
$R_{c,0}$								0.6	0.4	0.4
$R_{c,90}$									0.4	0.4
MOG_v										0.6

The values in Table 6-4 are quantified by judgment (COST E24 (2005)), such that 0.8 ↔ high correlation, 0.6 ↔ medium correlation, 0.4 ↔ low correlation, 0.2 ↔ very low correlation.

6.3.3 STRENGTH AND STIFFNESS MODIFICATION FUNCTIONS

Values for the strength modification function $\alpha(.)$ are quantified for discrete exposures $Ex(s,\omega,\tau,t)$ as specified in Table 6-5. The particular sets of exposures are defined as in EC 5 (ENV 1995-1-1:2004); different load duration classes and different service classes (sc) depending on the expected moisture content of the timber. The values for $\alpha(.)$ are taken from EC 5.

Table 6-5: Strength modification function table.

sc	Permanent ($t > 10$ years)	Long term ($0.5 < t < 10$ years)	Medium term ($0.25 < t < 6$ month)	Short term ($t < 1$ week)	Instantaneous
1/2	$\alpha = 0.6$	$\alpha = 0.70$	$\alpha = 0.80$	$\alpha = 0.9$	$\alpha = 1.1$
3	$\alpha = 0.5$	$\alpha = 0.55$	$\alpha = 0.65$	$\alpha = 0.7$	$\alpha = 0.9$

Values for the stiffness modification function $\delta(.)$ are quantified for discrete exposures $Ex(s,\omega,\tau,t)$ as specified in Table 6-7. The particular sets of exposures are defined as in the EC 5 (ENV 1995-1-1:2004); classified as in Table 6-5. The values for $\delta(.)$ are taken from the EC 5.

Table 6-6: Stiffness modification function table.

sc	Permanent ($t > 10$ years)	Long term ($0.5 < t < 10$ years)	Medium term ($0.25 < t < 6$ month)	Short term ($t < 1$ week)	Instantaneous
1	$\delta = 0.6$	$\delta = 0.5$	$\delta = 0.25$	$\delta = 0.0$	$\delta = 0.0$
2	$\delta = 0.8$	$\delta = 0.5$	$\delta = 0.25$	$\delta = 0.0$	$\delta = 0.0$
3	$\delta = 2.0$	$\delta = 1.5$	$\delta = 0.75$	$\delta = 0.3$	$\delta = 0.0$

6.3.4 MODEL UNCERTAINTIES FOR DIFFERENT ULTIMATE LIMIT STATES

The model uncertainties cover deviations and simplifications related to the probabilistic modelling and the limit state equations. The reference properties are determined by standardized tests. Therefore, model uncertainties related to estimation of other material parameters (e.g. tension and compression strengths) have to be accounted for. Geometrical deviations from specified dimensions, durations of load and moisture effects (damage accumulation) also contribute to model uncertainties if not explicitly accounted for in the stochastic modelling. Furthermore, the idealized and simplified limit state equations introduce model uncertainties. In Table 6-7 indicative values for model uncertainties related to components and connections are shown. The model uncertainty for components depends on the limit state (bending or e.g. combined stress effects) and how much the actual condition deviates from the standard test conditions. The model uncertainty for connections is based on statistical analysis of test data when compared to the calculation models in the limit state equations in section 5.3.3. It is noted that the expected value of X_M can be considered as a bias on the calculation models.

Table 6-7:   *Model uncertainties X_M for different limit states.*

		mean	st.dev.	Distribution
Component, e.g. Eq. (6.4)	Short term	1	0.05 – 0.10	Lognormal
Component, e.g. Eq. (6.13)	Long term	1	0.10	Lognormal
Dowel Type Connection, section 5.3.3.				
Single Fastener (Failure Mode I, II, III)	X_{MI}	0.8	0.12	Lognormal
	X_{MII}	1.2	0.15	Lognormal
	X_{MIII}	1.3	0.20	Lognormal
Multiple Fastener	X_M	1.25	0.3	Lognormal

6.4   POSSIBLE REFINEMENTS

6.4.1   MODELLING OF THE SPATIAL VARIATION OF TIMBER PROPERTIES

6.4.1.1   Bending moment capacity

Following the model proposed by Isaksson (1999) which is described in more detail in section 4.2.4.3, the bending moment capacity $r_{m,0}$ at a particular point j in component i of a structure/batch is given as:

$$r_{m,0} = r_{m,\mathrm{ij}} = \exp\left(\nu + \varpi_i + \chi_{ij}\right) \tag{6.7}$$

where ν is the unknown logarithm of the mean of all sections in all components, ϖ_i is the difference between the logarithm of the mean of the sections within a component i and ν. ϖ is normal distributed with mean value equal to zero and standard deviation σ_ϖ, χ_{ij} is the difference between the strength of weak section j in the beam i and the value $\nu + \varpi_i$. χ is normal distributed with mean value equal to zero and standard deviation σ_χ. ϖ and χ are statistically independent.

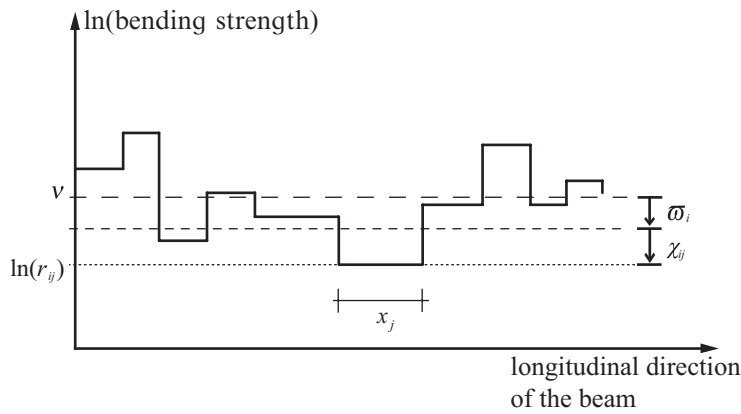Accordingly $R_{m,0}$ is a lognormal distributed random variable.

Figure 6-2   Section model for the longitudinal variation of bending strength.

It is assumed that the bending moment capacity of a cross section is related with the bending moment capacity of a test specimen $R_{m,s}$ as:

$$R_{m,0} = R_{m,s}^{\vartheta} \qquad (6.8)$$

where ϑ is a constant depending on the applied bending test standard and the characteristics of the timber.

The bending moment capacity $R_{m,0}$ is assumed to be constant within one segment (compare Isaksson (1999)). The discrete section transition is assumed to be Poisson distributed, thus the section length follows an exponential distribution.

The exponential distribution is given as:

$$F_X(x) = 1 - \exp(-\lambda x) \qquad (6.9)$$

For Nordic spruce the following information basis can be given (Isaksson (1999)):

The variation of the logarithm of the bending capacity $\ln(R_{m,0})$ is related by 40% to the variable ϖ and by 60% to the variable χ. The expected length of a section is $1/\lambda = 480mm$.

Table 6-8: ϑ-values for the estimation of the strength of weak sections.

See Equation *(6.8)*	EN	US	AUS
$\vartheta =$	1.05	1.03	1.02

The different values for ϑ given in Table 6-8 are due to the different definitions of bending strength of test specimen. The values are derived by simulation, see section 7.3.

6.4.1.2   Bending Modulus of Elasticity

The within component variation of the bending modulus of elasticity (MOE) is based on the within component variation model for bending moment capacity. The realizations of the MOE

are directly related to the realizations of the bending moment capacity following the model proposed for bending in the foregoing. The section MOE and the bending moment capacity are related as follows:

$$E\left[MOE_{m,0}\right] = 4000 + 150E\left[R_{m,0}\right]$$ (6.10)

where $E\left[.\right]$ is the expected value of the corresponding property. The regression coefficients are determined by judgement (based on the EN 338 strength class system, European softwoods).

$$COV\left[MOE_{m,0}\right] = 0.7COV\left[R_{m,0}\right]$$ (6.11)

where $COV\left[.\right]$ is the coefficient of variation of the corresponding property.

The discrete section transition is assumed to be Poisson distributed; for European softwoods the parameters of the section transition model can be taken from above.

It is noted that the empirical basis for the presented MOE model is rather scarce. However, if no better information is available and the within component variation of the MOE is of interest the proposed model is considered as a reasonable modelling basis for European softwoods.

6.4.2   DURATION OF LOAD EFFECT

The mechanism leading to strength reduction of a timber member under sustained load is referred to as creep rupture and is modelled by so-called cumulative damage models with the general form (compare section 4.3.2.2):

$$\frac{d\alpha_D}{dt} = h\left(s(t), r_0, \boldsymbol{\theta}\right) \text{ or } \frac{d\alpha_D}{dt} = h\left(s(t), r_0, \alpha_D, \boldsymbol{\theta}\right) \quad \text{for} \quad 0 \le \alpha_D \le 1$$ (6.12)

where t is time, α_D is the damage state variable which commonly ranges from 0 (no damage) to 1 (failure), the function $h(.)$ contains parameters $\boldsymbol{\theta}$ that must be determined from experiment observations, $s(t)$ is the applied stress and r_0 the failure stress under short term ramp loading.

The following long term limit state function is utilized:

$$g = 1 - X_M \alpha_D\left(S(t)\right)$$ (6.13)

where α_D is the damage state variable after the intended service life of a structure and X_M is the model uncertainty.

Three different models are proposed:

1.) The model referred to as the Gerhards model (Gerhards (1979)).

$$\frac{d\alpha_D}{dt} = \exp\left(-a_D + b_D \frac{s(t)}{r_0}\right) \quad \text{for} \quad 0 \leq \alpha_D \leq 1 \tag{6.14}$$

2.) The model referred to as the Foschi and Yao model (Foschi and Yao (1986)).

$$\frac{d\alpha_D}{dt} = a_D \left(\frac{s(t)}{r_0} - \eta_D\right)^{b_D} + c_D \left(\frac{s(t)}{r_0} - \eta_D\right)^{d_D} \alpha_D(t) \qquad \text{for} \quad \frac{s(t)}{r_0} \geq \eta_D$$

$$\frac{d\alpha_D}{dt} = 0 \qquad\qquad\qquad\qquad \text{for} \quad \frac{s(t)}{r_0} < \eta_D \tag{6.15}$$

3.) The model referred to as the Nielsen model (Nielsen 2000).

$$\frac{d\alpha_\kappa}{dt} = a_D \alpha_\kappa \left(\frac{s(t)}{r_0}\right)^2 \left(\left(\alpha_\kappa \left(\frac{s(t)}{r_0}\right)^2\right)^{-1} - 1\right)^{-\frac{1}{b_D}} \quad \text{for} \ 1 \leq \alpha_\kappa \leq \left(\frac{s(t)}{r_0}\right)^{-2} \tag{6.16}$$

The parameters in Equations (6.14)-(6.16) are:

α_D, α_κ is the damage state variable,

t is the time,

$s(t)$ is the load effect,

r_0 is the timber initial capacity,

$a_D, b_D, c_D, d_D, \eta_D$ are model parameters fitted to experimental results e.g. as in Sørensen et al. 2005 and section 4.3.3.

For model 3.) the limit state function given in Equation (6.13) is not valid. According to model 3.) a time variant limit state function can be given as:

$$g(t) = SL(t)^{-2} - X_M \alpha_\kappa \left(SL(t)\right) \tag{6.17}$$

where α_κ is the damage state variable after the intended service life of a structure, X_M is the model uncertainty and $SL(t) = S(t)/R_0$ is the load level.

6.4.3 UPDATING SCHEME FOR THE BASIC PROPERTIES

When information has been collected about the basic material properties the new knowledge implicit in that information might be applied to improve any previous (prior) estimate of the

material property. For the type of information e.g. it can be differentiated between direct and indirect information; i.e. direct measurements of the material property and the measurement of some indicator of the property respectively.

In the proposed framework new information in principle can be introduced at any stage of modelling. In the following the principle of considering new direct information e.g. in form of test results is presented. The utilisation of new indirect information, e.g. inform of grading indications, is illustrated with two different methods.

6.4.3.1 Updating - Direct Information

The bending strength R_m and the bending modulus of elasticity MOE_m are modelled by lognormal distributed random variables which can be represented through the normal distributed random variables $R_m^* = \ln(R_m)$ and $MOE_m^* = \ln(MOE_m)$. All basic properties may be represented with the uncertain mean value M and standard deviation Σ as illustrated in Equations (6.18) - (6.20).

$$R_m = \exp\left(R_m^*\right) \;\rightarrow\; R_m^* \sim N\left(\mathrm{M}_R, \Sigma_R\right) \tag{6.18}$$

$$MOE_m = \exp\left(MOE_m^*\right) \;\rightarrow\; MOE_m^* \sim N\left(\mathrm{M}_{MOE}, \Sigma_{MOE}\right) \tag{6.19}$$

$$\mathrm{P}_{den} \sim N\left(\mathrm{M}_\mathrm{P}, \Sigma_\mathrm{P}\right) \tag{6.20}$$

The parameters M and Σ of R_m^*, MOE_m^* and P_{den} are quantified with a Normal-Inverse-Gamma-2 distribution with the parameters m, s, n, v which is equivalent to the natural conjugate prior of a normal distribution with unknown mean and standard deviation. Given the parameters m, s, n, v the predictive distribution of R_m^*, MOE_m^* and P_{den} can be derived as:

$$F_{X|\hat{\mathbf{x}}}\left(x \mid m, n, s, v\right) = T_v\left(\frac{x-m}{s}\sqrt{\frac{n}{n+1}}\right) \tag{6.21}$$

where $T_v(.)$ is the student-t-distribution with v degrees of freedom.

The prior predictive distribution can be quantified with parameters $(m, s, n, v) = (m', s', n', v')$. See e.g. the JCSS Probabilistic Model Code, JCSS (2001) and Annex A.

New measurements on the material properties can be used for updating the parameters given above. For a sample of n observations $(\hat{x}_1, \hat{x}_2, ..., \hat{x}_n)$, the sample characteristics can be quantified as:

$$m = \frac{1}{n}\sum \hat{x}_i \tag{6.22}$$

$$s^2 = \frac{1}{n-1}\sum (m - \hat{x}_i)^2 \tag{6.23}$$

$$v = n-1 \tag{6.24}$$

(note that for observations on the bending moment capacity $r_{m,i}$ and the bending MOE $moe_{m,i}$, the natural logarithm of the observations, i.e. $\ln(r_{m,i})$ and $\ln(moe_{m,i})$ has to be used).

The parameters corresponding to the prior information m', s', n', v' and the sample characteristics m, s, n, v can be combined as (see e.g. Raiffa and Schlaifa (1960)) :

$$m'' = \frac{n'm' + nm}{n' + n} \tag{6.25}$$

$$n'' = n' + n \tag{6.26}$$

$$s''^2 = \frac{(v's'^2 + n'm'^2) + (vs^2 + nm^2) - n''m''^2}{(v' + \delta(n')) + (v + \delta(n)) - \delta(n'')} \tag{6.27}$$

$$v'' = (v' + \delta(n')) + (v + \delta(n)) - \delta(n'') \tag{6.28}$$

with:

$$\delta(x) \equiv \begin{cases} 0 & \text{for} \quad x \le 0 \\ 1 & \text{for} \quad x > 0 \end{cases} \tag{6.29}$$

and the posterior predictive distribution can be derived as

$$F_{X|\hat{x}}(x|m'', n'', s'', v'') = T_{v''}\left(\frac{x - m''}{s''}\sqrt{\frac{n''}{n'' + 1}}\right) \tag{6.30}$$

6.4.3.2   Updating - Indirect Information I

In this section a simple model for updating the statistical parameters of the Lognormal distribution for e.g. the bending strength of a given timber grade when new information becomes available in the form of machine grading results is described following Sørenson (2005) and Köhler et al. (2005).

The Lognormal distributed strength parameter R is assumed to have a coefficient of variation cov_R. Then $X = \ln R$ is Normal distributed with expected value M_X and standard deviation $\sigma_X^2 = \ln\left(\text{cov}_R^2 + 1\right)$. σ_X is assumed to be known and M_X is assumed to be Normal distributed with expected value μ_0 and standard deviation σ_0.

When machine grading is based on a measured indicator ι, typically related to the stiffness of a timber test specimen, for each grading technique the following relation with the bending strength is assumed:

$$\iota = b_0 r^{b_1} \cdot \varepsilon \tag{6.31}$$

where b_0 and b_1 are constants and ε is the error term which is assumed Lognormal distributed. $\ln(\varepsilon)$ is then Normal distributed and is assumed to have zero mean value and standard deviation $\sigma_{\ln(\varepsilon)}$. The parameters b_0, b_1 and $\sigma_{\ln(\varepsilon)}$ can be estimated using the Maximum Likelihood method as described in section 4.2.3.2.

Given n observations of the indicator $\iota_1, \iota_2, ..., \iota_n$ for n specimens from a given timber grade, the mean value of these can be estimated: $\bar{\iota} = 1/n \sum_{j=1}^{n} \iota_j$. The updated (predictive) distribution function for $X = \ln R$ is then Normal with expected value μ'' and standard deviation σ''':

$$\mu'' = \frac{\dfrac{n}{b_1}\left(\bar{\iota} - b_0\right)\sigma_0^2 + \mu_0 \sigma_X^2}{n\sigma_0^2 + \sigma_X^2} \quad \text{and} \quad \sigma''' = \sqrt{\sigma_X^2 + \frac{\sigma_0^2 \sigma_X^2}{n\sigma_0^2 + \sigma_X^2} + \left(\frac{(n/b_1)\sigma_0^2}{n\sigma_0^2 + \sigma_X^2}\right)^2 \sigma_\varepsilon^2} \tag{6.32}$$

The updated distribution for the strength R is then <u>Lognormal</u> with expected value $\mu_R'' = \exp\left(\mu'' + 0.5\sigma'''^2\right)$ and standard deviation $\sigma_R''' = \mu_R'' \sqrt{\exp\left(\sigma'''^2\right) - 1}$.

6.4.3.3   Updating - Indirect Information II (available test data – calibration of grading rules)

The probabilistic model for bending strength described in this section can be used for machine graded timber and is based on the model described in section 4.2.3.2. The probabilistic model can be described by the following steps:

For a given geographic region and a given type of species (e.g. Nordic Spruce) an initial (prior) distribution function $F_{R_m}(x)$ can be established for the bending strength R_m for non-graded timber. The recommended distribution function is Lognormal. The statistical parameters in the distribution function can be obtained using e.g. the Maximum Likelihood method. For the identification of lower grades it is recommended to fit the initial (prior) distribution function $F_{R_m}(x)$ to the data in the lower end (e.g. 30% of the data with lowest strengths); in order to obtain good models in the lower tail of the distribution function for the graded timber strength. This can be done using the Maximum Likelihood method, see section 4.2.3.2.

Machine grading is based on a measured indicator ι, typically related to the stiffness of a

timber test specimen. For each grading technique the following linear relation with the bending strength is assumed:

$$\iota = a_0 + a_1 r + \varepsilon \qquad\qquad (6.33)$$

where a_0 and a_1 are constants and ε is the lack-of-fit quantity which is assumed Normal distributed with zero mean value and standard deviation σ_ε. The parameters a_0, a_1 and σ_ε can be estimated using the Maximum Likelihood method which also gives the statistical uncertainty in form of standard deviations and correlation coefficients of the parameters a_0, a_1 and σ_ε.

After grading the updated (predictive) distribution function for the bending strength in grade no. j is obtained from:

$$F_{R_m,j}^U(x) = P\left(R_m \le x \middle| b_{L,j} \le I(x) \le b_{U,j}\right) \qquad\qquad (6.34)$$

where $b_{L,j}$ and $b_{U,j}$ are lower and upper limits of the grading indicator ι for grading no. j.

The updated distribution function $F_{R_m,j}^U(x)$ can then be used in reliability analyses. A detailed description of the method can be found in section 4.2.3.2.

6.5   CONCLUDING REMARKS

A proposal is presented for probabilistic modelling of timber material properties. The basic reference properties for timber strength parameters are described and some limit state equations for components and connections are formulated. The recommended probabilistic model for the basic properties is presented and indicative numerical values for the parameters are given. Refinements related to updating of the probabilistic model given new information, spatial variation of strength and duration of load effects are described.

The proposal can be seen as a guideline and common reference for probability based code calibration of timber design codes. However, the parameters of the proposed models need to be quantified on a broad and representative data base. Comprehensive experimental data concerning the basic timber phenomena already exist, especially resulting from research projects in North America, Europe and Australia. One major task for developing further the presented model code is to collect and assess existing experimental data. The timber research community is asked to contribute by making available experimental data for the quantification of model parameters for timber predominantly used for timber design.

The presented document does not cover all aspects of the design of timber structures. Beside solid timber other timber materials are utilized in timber engineering. Glued laminated timber is an example of an interesting timber material, frequently used in high performance load carrying structures. It is of utmost importance to develop consistent probabilistic models for

these timber materials, especially in the perspective of their potential competitiveness to other building materials such as steel and reinforced concrete.

The further development of the probabilistic model code for timber should constitute an important future task for the timber research community.

7 APPLICATIONS

7.1 ASSESSMENT OF DATA

In Appendix A a general outline for the characterisation of the statistical properties of samples is given. In this section the methods are applied on a data set consisting of $n = 175$ observations of bending moment capacity, $\mathbf{x} = (x_1, x_2, ..., x_n)^T$. The data is arbitrary but typical. It is assumed that the considered sample is obtained by random sampling.

7.1.1 NON-PARAMETRIC ASSESSMENT

To gain a first overview about the data set the order statistic of the sample is considered. Therefore it is assumed that the sample values are realisations of a random variable X. The data is ordered such that $x_1 \leq x_2 \leq x_3 ... \leq x_n$. Following Equations (7.1) and (7.2) the expected value and the variation of the cumulative distribution of each bending strength observation x_m, $F_X(x_m)$ are derived as:

$$E\left[F_X(x_m)\right] = \frac{m}{n+1} \tag{7.1}$$

$$VAR\left[F_X(x_m)\right] = \frac{m}{(n+2)(n+1)}\left(1 - \frac{m}{n+1}\right) \tag{7.2}$$

$E\left[F_X(x_m)\right]$ is plotted with its scatter band in Figure 7-1.

The scatter band is defined as $E\left[F_X(x_m)\right] \pm VAR\left[F_X(x_m)\right]^{0.5}$.

A plot of $E\left[F_X(x_m)\right]$ is often compared with a probability distribution function $F_X(x|\boldsymbol{\theta})$ for which the parameters $\boldsymbol{\theta}$ are calibrated to the same set of data. This implies that the probability specified in Equation (7.1) of an observation x_m is directly compared with the outcome of the probability distribution function $F_X(x_m)$. In the literature (e.g. in Foschi et al. (1989) or Ranta-Maunus et al. (2001)) the validity of probability distribution models to represent samples and underlying populations is often assessed based on visual judgements of these graphical representations. However, the scatter is not taken into account.
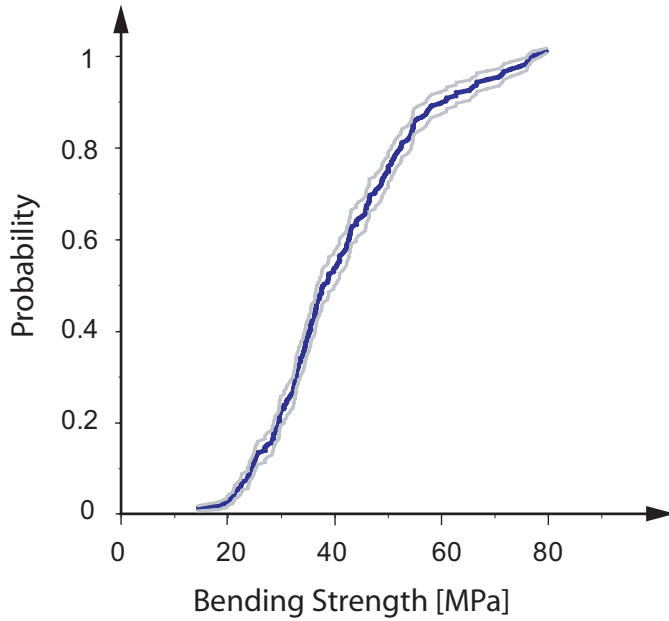
Figure 7-1   Plot of $E\left[F\left(x_m\right)\right]$ (thick line) and scatter band (enveloped by thin lines).

A common non-parametric evaluation of the 5%-fractile value is based on Equation (7.3) which specifies the probability that one further observation of X is not exceeding the value of x_m, as:

$$p\left(n,m;1,0\right)=\frac{m}{n+1} \tag{7.3}$$

For the considered sample the 5%-fractile value is estimated by linear interpolation and is equal to 21.82 MPa. The estimate is a so-called point estimate for the fractile value, only reflecting one characteristic of a specific sample.

According to Equations (7.4) and (7.5), the sample moments of the considered sample are evaluated as:

$$\overline{x}=\frac{1}{n}\sum_{i=1}^{n}\hat{x}_i \tag{7.4}$$

$$s^2=\frac{1}{n}\sum_{i=1}^{n}\left(\hat{x}_i-\overline{x}\right)^2 \tag{7.5}$$

Accordingly the sample moments of the considered sample are equal to $\overline{x}=40.9$ and $s=14.06$, both in MPa.

7.1.2   SELECTION OF A DISTRIBUTION FUNCTION AND PARAMETERS

A convenient approach to check the validity of a chosen distribution model is the use of probability paper. Probability paper for a given distribution model is constructed such that the cumulative probability density function for that distribution model will have the shape of a straight line when plotted on the paper. A probability paper is thus constructed by a non-linear transformation of the x and the y axis. The considered data set is plotted on Probability paper for a Normal, a Lognormal and a Weibull distribution. The transformations are indicated in the graph.
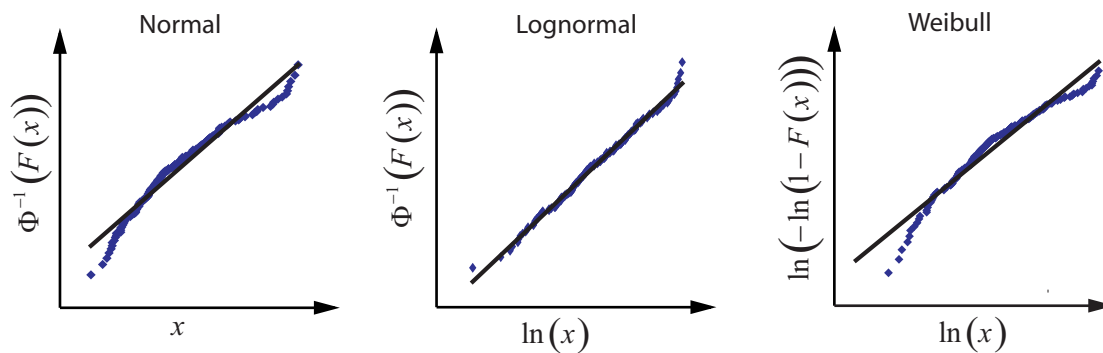

Figure 7-2   Probability paper for Normal, Lognormal and Weibull distributions.

Based on Figure 7-2 the lognormal distribution can be identified as most properly reflecting the statistical characteristics of the considered sample, especially in the lower tail regions of the distribution. It is well known that especially the behaviour of the probability distribution functions in the regions of the tails is of importance in reliability assessments. For load variables the upper tail is normally the most important whereas the lower tails are the important for resistance parameters (see e.g. Faber (2003)).

It thus remains to model timber material properties with special emphasis on a good representation in the lower tail region. One approach to estimate the probability distribution in the lower tail domain is by means of a censored Maximum Likelihood estimation where only observations in the lower tail domain i.e. below a given predefined threshold value are used explicitly. The other observations are only utilised implicitly to the extent that it is recognised that they exceed the threshold.

A general description of Maximum Likelihood method is given in Annex A on page 6. In this special case of a censored Maximum Likelihood estimation two different contributions to the likelihood are considered, i.e.:

$$L1 = \prod_{i=1}^{j} f\left(x_i \middle| \boldsymbol{\theta}\right) \tag{7.6}$$

and

$$L2 = P\left(X \geq x_G \middle| \boldsymbol{\theta}\right)^{n-j}$$

with: (7.7)

$$P\left(X \geq x_G \middle| \boldsymbol{\theta}\right) = 1 - F\left(x_i \middle| \boldsymbol{\theta}\right)$$

where $L1$ represents the likelihood of the j observations with values below or equal to the threshold value x_G. $L2$ represents the likelihood of the observations with values exceeding the threshold value x_G. $1 - F\left(x_G \middle| \boldsymbol{\theta}\right)$ is the probability that a value exceeds the threshold value x_G given the parameters of the probability distribution function $\boldsymbol{\theta}$. If n is the total number of observations $n - j$ is the number of observations exceeding the threshold value x_G.

The parameters are easily estimated by the solution of the optimisation problem:

$$\max_{\theta}\left(L1 \cdot L2\right)$$

(7.8)

The parameters $\boldsymbol{\theta}$ are estimated as normal distributed random variables with means and covariance quantifying the statistical uncertainty due to the relative small number of observations below the threshold.

The parameters $\boldsymbol{\theta}$ of the probability distribution functions estimated on the basis of Equation (7.8) have been found to exhibit moderate sensitivity to the choice of the threshold value x_G for moderately low values of x_G. The lower 30 % percentile value has been found to be a reasonable choice for x_G (Faber et al. (2004)).

For the considered bending strength observations, the maximum likelihood method is used to estimate the parameters of the 2-parameter Weibull, the Normal and the Lognormal distribution (compare Annex A). For means of comparison the parameters are calibrated to the entire data domain and by considering exclusively the data from the lower tail of the distribution. x_G is chosen to be equal to the lower 30% percentile value. In Table 7-1 the distribution parameters are summarized as correlated normal distributed random variables. In Figure 7-3 plots of both predictive distributions are compared with the quantile plot of the data.

Table 7-1   Distribution parameters calibrated to the considered bending strength data.

		Weibull		Normal		Lognormal	
	θ	w	k	μ	σ	ξ	δ
	μ_θ	45.76	3.09	40.91	14.02	38.61	0.342
All data	σ_θ	1.19	0.17	1.04	0.93	0.99	0.018
	ρ_θ	0.33		0.34		0	
	μ_θ	38.66	5.29	36.29	8.56	38.77	0.345
Lower tail	σ_θ	0.02	0.48	0.70	0.24	1.014	0.019
	ρ_θ	0.19		0.22		0.01	
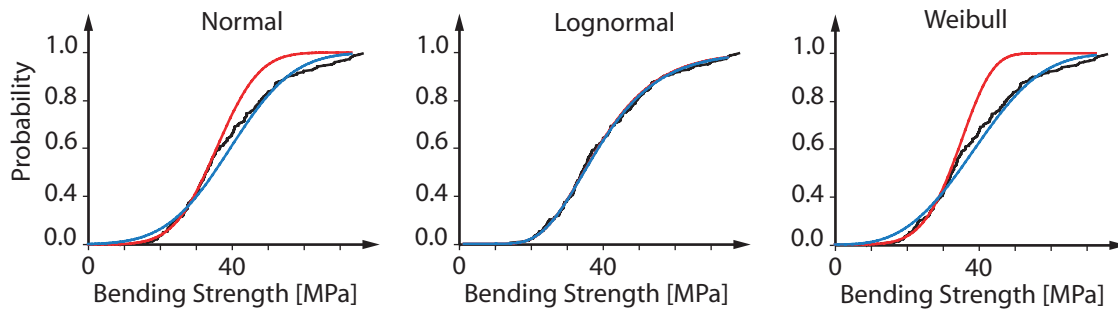
Figure 7-3   Plots of the predictive distribution functions in comparison with the $E\left[F\left(x_m\right)\right]$ plot; compare Figure 7-1.

Investigating the plots for the Weibull and the Normal distribution it can be found that the lower tail domain of the data (quantile plot) is significantly better represented by the distributions which are calibrated explicitly to the lower tail. For the Lognormal distribution it is evident that both distributions represent the entire data domain irrespectively which calibration method is used. It should be noted that this observation is not typical for bending strength data sets. For a comparison it is referred to Ranta-Maunus et al. (2001)) where a considerable amount of data bases is analyzed and documented.

7.1.3   ESTIMATION OF THE 5%- FRACTILE VALUE

As discussed in chapter 2, 5%-fractile values are used as characteristic strength values in deterministic design formats. It is of importance that the estimation of these values is fully consistent with the probabilistic modelling of strength related material properties. In the following the estimation of 5%-fractile values according to existing standards is discussed.

7.1.3.1 Standardized methods for the estimation of the 5%-fractile value

For timber materials several standardized methods for the estimation of the characteristic value x_k exist. Four different standards are considered here:

- EN 384: valid for solid timber,

- EN 14358: valid for wood based products,

- ISO 13910: valid for solid timber,

- ISO 12491: valid for all building products.

In the following these methods are briefly reviewed:

EN 384 – stratified sampling:

This method is based on stratified sampling, i.e. a sample is subdivided into at least 5 sub-samples j of size $n_j > 40$ and for each sub-sample the 5%-fractile value $x_{05,j}$ is assessed according to the order statistics method described in section 7.1.1. The value $\bar{x}_{05}$ is estimated as the weighted mean value of the 5%-fractile values of the sub-samples as:

$$\bar{x}_{05} = \frac{\sum_j n_j x_{05,j}}{\sum_j n_j} \qquad (7.9)$$

The characteristic value x_k is estimated as:

$$x_k = \min \begin{cases} \bar{x}_{05} \\ 1.2 \min_j x_{05,j} \end{cases} \qquad (7.10)$$

ISO 13910 – Weibull distribution

The sample 5%-fractile value x_{05} is estimated according to the order statistics method described in section 7.1.1. The data is calibrated to a 2-parameter Weibull distribution under explicit consideration of the lower tail data. The lower tail is defined with the threshold value x_G corresponding to the lower 15% of the data. The Weibull distribution is given in Annex A with the parameters w and k. v_{tail} is introduced as a approximation of the coefficient of variation of the Weibull distribution as:

$$v_{tail} = k^{-0.92} \qquad (7.11)$$

The characteristic value is given as:

$$x_k = \left[1 - 2.7\frac{v_{tail}}{\sqrt{n}}\right] x_{05} \tag{7.12}$$

where n is the sample size.

ISO 12491 – Normal distribution

The estimation of the characteristic value x_k is based on the sample mean $\bar{x}$ and standard deviation s as:

$$x_k = \bar{x} + k_s s \tag{7.13}$$

where k_s is a correction factor.

Equation (7.13) corresponds to a lower bound estimate at a given double sided confidence interval α_k. Accordingly k_s is given by:

$$k_s = -\frac{k_\alpha}{\sqrt{n}} \tag{7.14}$$

where n is the sample size and k_α is the α_k-percentile of the non-central t-distribution with n degrees of freedom and the non-centrality parameter λ_{nc} given as:

$$\lambda_{nc} = \Phi^{-1}(1-p)\sqrt{n} \tag{7.15}$$

where p is the fractile of interest (in this case equal to 0.05) and $\Phi(.)$ is the standard normal distribution function.

When the population standard deviation σ is assumed to be known Equation (7.13) is rewritten as:

$$x_k = \bar{x} + k_\sigma \sigma \tag{7.16}$$

where

$$k_\sigma = \Phi^{-1}(1-p) - \frac{\Phi^{-1}(\alpha_k)}{\sqrt{n}} \tag{7.17}$$

EN 14358 – Lognormal distribution

In the EN 14358 the approach of ISO 12491 is applied to a lognormal distribution.

7.1.3.2 Predictive 5%-fractile values

According to modern design codes as the Eurocodes (EN 1990:2002) characteristic values for strength related material properties have to be introduced as predictive values of the 5%-fractile. The general form of the predictive p%-fractile value can be given as:

$$x_{p,pred} = F_{X,pred}^{-1}(p) \quad \text{with} \quad f_{X,pred}(x) = \int f(x|\boldsymbol{\theta}) f_{\boldsymbol{\Theta}}''(\boldsymbol{\theta}|\hat{\mathbf{x}}) d\boldsymbol{\theta} \tag{7.18}$$

where $\hat{\mathbf{x}}$ are the sample observations, $\boldsymbol{\theta}$ are the parameters of the distribution function. The parameters $\boldsymbol{\theta}$ are realisations of the random vector $\boldsymbol{\Theta}$ with the posterior joint probability density function $f_{\boldsymbol{\Theta}}''(\boldsymbol{\theta}|\hat{\mathbf{x}})$ (compare in Annex with Equation (A.32)). Equation (7.18) can be generally solved by reliability methods as FORM/SORM or numerical integration, however, analytical solutions exists, e.g. for the case where X is normally distributed. In this case the predictive value of the p%-fractile $x_{p,pred}$ is given as:

$$x_{p,pred} = \exp\left(m + t_p(v) s \sqrt{1 + 1/n}\right) \tag{7.19}$$

where $\bar{x}$ is the sample mean, s the sample standard deviation, n is the sample size and v is defined by $v = n-1$. $t_p(v)$ is the p%-fractile value of the t-distribution with v degrees of freedom.

It should be noted that this method is fully consistent with the Bayesian updating scheme discussed later in this chapter.

7.1.3.3 Example

The described methods are used for some example calculations with the data set which is already used in section 7.1.1. The results are presented in Table 7-2.

It can be seen in Table 7-2 that the estimations for the 5%-fractile values are very sensitive to the applied estimation method. It can be noticed that the estimations which are based on the assumption that the data is normal distributed are rather low (row: 3, 5, 8 (all data)). It is also interesting to note, that the result of stratified sampling (row 1) differs significantly from the non-empirical approach according to Equation (A.8) (row 11). Consistent results are obtained when the parameters of a distribution function are calibrated to the lower tail domain of the data by using the maximum likelihood method. It can be seen that the resulting predictive fractile values are not very sensitive to the assumed distribution (compare row 8, 9, 10 (lower tail)). The method according to Equation (7.19) is fully consistent to the Bayesian updating scheme for normal distributed random variables. The method can also be used for lognormal distributed random variables by transforming the data accordingly. The estimates are sensitive to the assumed distribution (compare row 5 and 6).

Table 7-2   Different 5%-fractile values for the same sample.

row	Method			
1	EN 384, Equation (7.10)	stratified sampling		22.38
2	ISO 13910, Equation (7.12)	Weibull		20.86
3	ISO 12491, Equation (7.15)	Normal		16.60
4	EN 14358, Equation (7.15)	Lognormal		21.35
5	Predictive, Equation (7.19)	Normal		17.58
6	Predictive, Equation (7.19)	Lognormal		21.87
7	Predictive, Equation (7.18), Distribution and parameters as in Table 7-1:		all data	lower tail
8		Normal	17.75	22.02
9		Lognormal	21.95	21.90
10		Weibull	17.43	21.90
11	Non-parametric, Equation (A.8)			21.82

7.2 UPDATING OF RANDOM VARIABLES

7.2.1 NORMAL DISTRIBUTION WITH UNCERTAIN MEAN AND KNOWN STANDARD DEVIATION

The probability distribution of the bending strength of a sample of timber structural elements has to be estimated. As prior information it is known that the sample is assigned to be graded to a particular timber grade but it is neither known how the timber is graded nor where the ungraded material is coming from. The timber grade is specified by a 5%-fractile value of the bending strength. It is assumed that the bending strength is following a lognormal distribution and that the standard deviation of a typical batch is constant. Between batches of different suppliers it is implied that the location, i.e. the mean value, of the distribution is varying. Thus the mean value is uncertain.

The lognormal distribution is equivalent to the normal distribution, if the following transformation is applied:

$$F_X(x) = \Phi\left(\frac{\ln(x/\xi_X)}{\delta_X}\right) = \Phi\left(\frac{\ln(x) - \ln(\xi_X)}{\delta_X}\right) \Leftrightarrow F_Z(z) = \Phi\left(\frac{z - \mu_Z}{\sigma_Z}\right) \quad \text{for} \quad \begin{array}{l} z = \ln(x) \text{ and} \\ \mu_Z = \ln(\xi_X) \text{ and} \\ \sigma_Z = \delta_X \end{array} \quad (7.20)$$

Further, the coefficient of variation (cov) of the lognormal distribution is approximately equivalent to its parameter δ_X:

$$\text{cov} = \sqrt{\exp\left(\delta_X^2\right) - 1} \cong \delta_X \tag{7.21}$$

In the present example the prior information is quantified as follows: It is assumed that the 5%-fractile value of the predictive prior distribution matches the required 5%-fractile value of the bending strength of 24 MPa (corresponding to the European strength class C24, compare Table 3-3). Further, the coefficient of variation of the predictive distribution is assumed to be 0.3, where as 70% of the scatter is due to the constant standard deviation and 30% is due to the standard deviation of the uncertain mean.

The prior information is:

$$x \rightarrow \ln(x) = z : Z \sim N\left(M_Z, \sigma_Z\right); M_Z \sim N\left(\mu', \sigma'\right)$$

$$\sigma_Z = 0.25$$

$$\mu' = 3.67$$

$$\sigma' = 0.16$$

Based on the prior information the predictive distribution of Z is normal distributed with $\mu^P = \mu' = 3.67$ and $\sigma^P = \sqrt{\sigma'^2 + \sigma_Z^2} = 0.3$.

New information can be introduced, e.g. information from tests of the bending strength of a number of structural elements. Here the additional information is (arbitrary chosen values):

$$\hat{\mathbf{x}} = (20, 30, 50, 70, 80) \rightarrow \hat{\mathbf{z}} = \ln(\hat{\mathbf{x}}) = (3.0, 3.4, 3.9, 4.2, 4.4)$$

$$n = 5$$

$$\bar{z} = 3.87$$

Considering the prior information and the additional information from the tests the predictive distribution of Z is a normal distribution with the parameters: $\mu^U = \mu'' = 3.8$ and $\sigma^U = \sigma''' = 0.33$, (compare with Equation (A.33)).

Both distributions, i.e. before introducing new information and afterwards, are plotted in Figure 7-4. It is seen that by introducing new information the predictive probability distribution of the bending strength is shifted to the right, i.e. the expected strength values are higher than prior to the tests. It should be noticed that the new information is quantified by the mean value of the sample values and the number of observations within the sample, in this case $\bar{z} = 3.87$ and $n = 5$. Implicitly, it is assumed that the standard deviation of the drawn sample is already known with $s = 0.25$.

The predictive 5%-fractile value is calculated with (with σ assumed to be known):

$$x_{0.05, pred} = \exp\left(\mu + \Phi^{-1}(0.05)\sigma\right) \tag{7.22}$$

with $\Phi^{-1}(0.05) \approx -1.64$.

Prior to the tests with, $\mu^P = \mu' = 3.67$ and $\sigma^P = \sqrt{\sigma'^2 + \sigma_Z^2} = 0.3 \rightarrow x_{0.05, pred} = 24$ MPa .

Posterior to the tests with, $\mu^U = \mu'' = 3.8$ and $\sigma^U = \sigma''' = 0.33 \rightarrow x_{0.05, pred} = 24.7$ MPa .
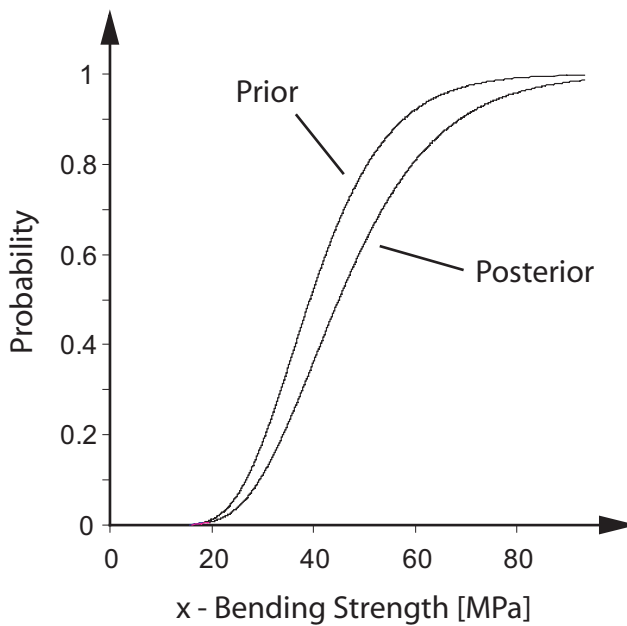

Figure 7-4   *Predictive probability distribution functions considering only prior information and considering both, prior and additional information (posterior).*

7.2.2 NORMAL DISTRIBUTION WITH UNCERTAIN MEAN AND STANDARD DEVIATION

Considering the same example as above, where the probability distribution of the bending strength of a sample of timber structural elements has to be estimated. Again, as prior information it is known that the sample is assigned to be graded to a particular timber grade but it is neither known how the timber is graded nor where the ungraded material is coming from. It is assumed that both, the mean value and the standard deviation are quite sensitive to the grading procedure and the origin of the timber. Consequently the prior information is leading to vague estimates of the parameters of the distribution; i.e. the mean and the standard deviation are both unknown.

The prior information is quantified inform of the parameters of the Normal-Inverse-Gamma-2 distribution (Equation (A.35)) m', s', n', v' . For this example the parameters are quantified by choice, but that the resulting prior predictive distribution function is very similar to the prior predictive distribution function from the example above:

$$x \rightarrow \ln(x) = z : Z \sim N(M_Z, \Sigma_Z)$$

$$m' = 3.7$$

$$n' = 5$$

$$s' = 0.25$$

$$v' = 6$$

The values of m' and s' are based on (abstract) samples of equivalent sizes of n' and v' respectively. Note that for the given parameter set the 'weight' of the prior information is relatively low.

New information can be introduced, e.g. inform of tests of the bending strength of a number of structural elements. The same sample as for the test sample above is used:

$$\hat{\mathbf{x}} = (20, 30, 50, 70, 80) \rightarrow \hat{\mathbf{z}} = \ln(\hat{\mathbf{x}}) = (3.0, 3.4, 3.9, 4.2, 4.4) \text{ with the sample characteristics:}$$

$$m = \bar{z} = 3.78$$

$$n = 5$$

$$s = 0.58$$

$$v = n - 1 = 4$$

Considering the prior information and the additional information from the tests the predictive distribution of Z is t-distributed (Equation (A.41)) with the parameters:

$$m'' = \bar{z}'' = 3.75$$

$$n'' = 10$$

$$s'' = 0.4$$

$$v'' = 11$$

Both distributions, i.e. before introducing new information and afterwards, are plotted In Figure 7-5.

The predictive 5%-fractile value is calculated with

$$x_{0.05, pred} = \exp\left(m + t_{0.05}(v) s \sqrt{1 + 1/n}\right) \tag{7.23}$$

where $t_{0.05}(v)$ is the 5%-fractile value of the student-t-distribution with v degrees of freedom.

Prior to the tests with, $(m', s', n', v') = (3.71, 5, 0.25, 6) \rightarrow x_{0.05, pred} = 24$ MPa .

Posterior to the tests with, $(m'', s'', n'', v'') = (3.75, 10, 0.4, 11) \rightarrow x_{0.05, pred} = 20$ MPa .
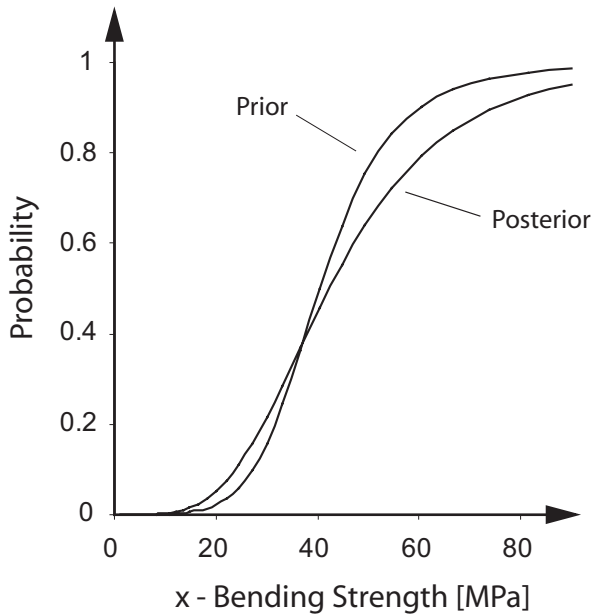
Figure 7-5   *Predictive probability distribution functions considering only prior information and considering both, prior and additional information (posterior).*
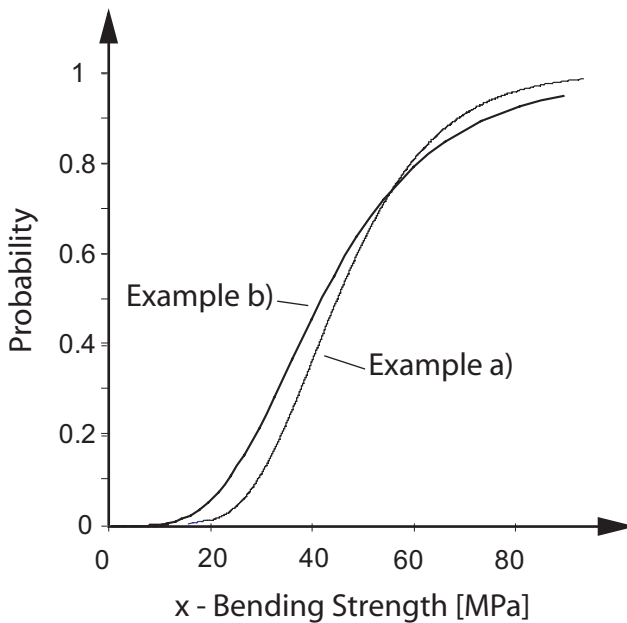

Figure 7-6   *Comparison of the posterior predictive distribution functions derived according to example a) and b).*

In Figure 7-5 it is seen that in this example the picture is quite different than in example a) above (Figure 7-4). Here the additional information is introduced in form of the mean value of the observed sample values, but also in form of the standard deviation of the sample ($s = 0.58$) which is significantly larger than presumed in example a). While the additional sample is exactly the same and the predictive prior distribution is similar, the predictive posterior is completely different (compare also with Figure 7-6).

When assuming known standard deviation, as for example a), the consistency of that assumption has to be proven carefully.

7.3 COMPARISON OF DIFFERENT BENDING TEST SPECIFICATIONS

To model the variation of strength and stiffness related material properties between components the variation on a meso level has to be taken into account, see chapter 4. Consider a timber producer, e.g. a saw mill, with a supply of timber raw material which can be assumed as stationary in its properties. It is further assumed that the production and selection schemes are constant. A typical output of the saw mill, e.g. normal construction timber of a specific size, can be assumed to be equivalent to a population and samples can be made to assess the characteristics of such a population. Full-size test can be performed to assess the variability of the load bearing capacity between the sampled components directly. Due to the sensitivity of the load bearing capacity of components not only to its size, but also to climate and loading conditions, test standards are used when investigating the between component variability.

Several probabilistic models where introduced to model the observed variation in strength and/or stiffness; e.g. the Normal distribution, the log-Normal distribution and the Weibull distribution. Large databases exist showing distribution parameters of specific populations of timber all tested according to certain test standards. These standards are in general associated with national guidelines or codes for testing structural timber. The most important ones are summarised in the following; to illustrate the differences the standards for the evaluation of bending strength are compared.

7.3.1 EUROPEAN STANDARDS EN 408 AND EN 384

The standard EN 408 specifies the laboratory methods for the determination of some physical and mechanical properties of structural timber. It is based on ISO 8375. A symmetrical four point bending configuration is used to evaluate the bending strength of components. The specimens have spans of 18 times the depth and the loads are introduced vertically at the third points; Figure 3-6. Maximum load shall be reached within 300 ± 120 secounds.

EN 384 defines the evaluation of characteristic values for the strength, stiffness and density of structural timber. Reference conditions for bending tests are specified as follows. A critical section of each specimen has to be identified and placed in between the loads in the centre third of the arrangement. The tension edge shall be selected at random and the reference moisture content shall be consistent with a surrounding climate corresponding to a temperature of 20°C and 65% relative humidity. The depth of the specimen shall be equal to 150mm.

7.3.2 AMERICAN SOCIETY FOR TESTING AND MATERIALS, ASTM D 4761-88 AND D 1990-91

The North American standard for testing the mechanical properties of timber and wood based material is ASTM D 4761-88. The span of bending specimens are also expressed as a multiple of the depth of the specimen. The span ranges from 17 times the depth to 21 times the depth. A four point bending configuration according to Figure 3-6 is prescribed. The time to failure shall be approximately 60 seconds; more than 10 and less than 600 seconds. According to ASTM D 1990-91, the North American standard for establishing allowable properties of visually graded timber, the critical zone shall be randomly located between the supports. The tension side shall be also selected at random. The moisture content of the timber shall be 13%.

7.3.3 AUSTRALIAN/NEW ZEALAND STANDARD, AS/NZ 4063:1992

This standard prescribes a random location of the test section. The test configuration is identical to ISO 8375, i.e. to EN 408.

Table 7-3   An overview comparison between different bending strength test procedures.

Origin/Code	Geometry	Climate/Moisture Content	Loading/Time to failure	Bias
Europe/EN 408 and EN 384	4 point bending (Figure 3-6) $L = 18\,H$ $H = 150$ mm	Conditioned at Temp.: 20°C Rel. Hum:: 65%	Ramp load, Time to failure: 300 s ± 120 s	(By judgment) weakest section in the middle. Tension side random.
North America/ ASTM D-4761-88 and 1990-91	4 point bending (Figure 3-6) $L = 17\,H - 21\,H$ $H = 150$ mm	Moisture Content: 13%	Ramp load, Time to failure: 60 s ~ (10s, 600s)	(By judgment) weakest section within supports. Tension side random.
Australia/New Zealand AS/NZ 4063:1992	4 point bending (Figure 3-6) $L = 18\,H$ $H = 150$ mm	Conditioned at Temp.: 20°C Rel. Hum:: 65%	Ramp load, Time to failure: 300 s ± 120 s	-

7.3.4 EVALUATING THE EFFECT OF DIFFERENT TEST STANDARDS

7.3.4.1 Duration of Load

When test data from different sources are assessed it is important to be aware of the different bending test specifications. As seen in chapter 2 timber material properties are sensitive to the

duration of the applied load. In the above introduced test standards average time to failure is specified. In the European and the Australian standard it is 300s, in the US standard it is 60s. It can be expected that the influence on the measurements is significant. The so-called Madison curve (Equation (4.41)) can be utilised to get an estimate of the effect of these load duration differences.

According to Wood (1949) the Madison curve is written as:

$$sl = 18.3 + 108.4 \ t_f^{-0.0464} \tag{7.24}$$

Where t_f is measured in seconds. According to the Madison curve the difference of bending strength measurements with a test of 60s duration are in average 6.5% larger than strength measurements with the test of 300s duration.

7.3.4.2 Weak Section Placing

The different test standards specify how to place the assumed weakest section in the bending test. The European standard requires placing the weakest section in the middle, high stressed region, according to the US standard the weakest section has to be placed within the supports and following the Australian standard the weakest section shall be placed randomly. The difference between the test standards in regard to placing the test specimen is illustrated in Figure 7-7. In the Figure the weakest section is indicated by a knot cluster. It can easily be imagined that the effect between the different specifications becomes larger when the length of the entire specimen increases. In practice it is in general not clear how long the specimen is.
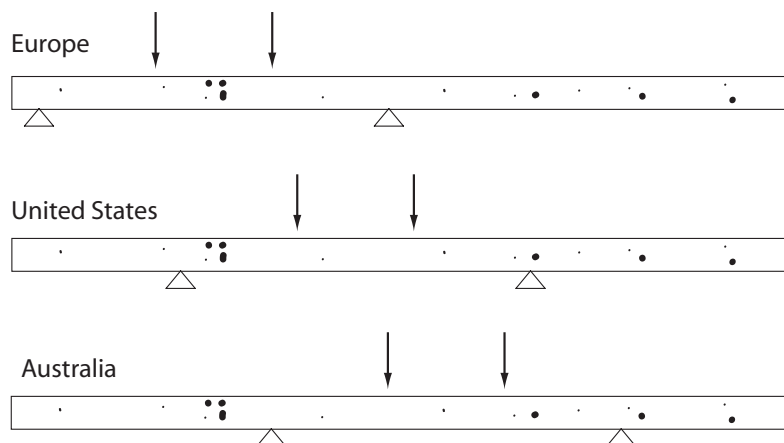

Figure 7-7   *Illustration of the effect of different weak section placing specifications; Europe (EN 384, weak section between load application), United States (ASTM D 1990-91, weak section between supports), Australia (AS 4063:1992, weak section at random).*

To illustrate the effect of the weak section placing specification the model derived in Isaksson

(1999) is utilized for simulations. The model is used as it is presented in the proposal for the probabilistic model code in chapter 6, page 174. The Monte Carlo Simulation technique (see e.g. Melchers (2001)) is used for the simulation of the random variables in the model. It is assumed that the beams have a length of 5 m. 1000 bending components are generated with a weak section distribution as indicated on page 174. The components are virtually tested according to the three different bending strength test specifications. The obtained data is utilized to calibrate the parameters of a lognormal distribution. The corresponding distribution functions are plotted together with the distribution function of the strength of the weak sections in Figure 7-8. The parameters of the distribution functions are given in Table 7-4.

Table 7-4   Distribution parameters corresponding to Figure 7-8.

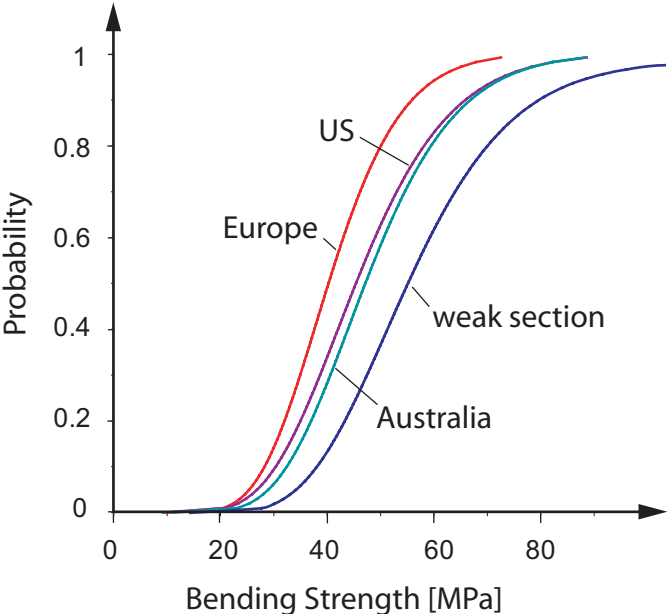|	ξ	δ
Weak sections	56.28	0.247
Europe	45.68	0.213
United States	50.36	0.247
Australia	51.95	0.232

Figure 7-8   Distribution Functions of simulated bending test specimen according to different national test standards.

The distribution functions shown in Figure 7-8 illustrate the difference between the bending moment capacity of test specimen and the bending moment capacity of all weak sections. As introduced in the proposal of the probabilistic model code in chapter 6 the capacity of a weak section corresponds to the capacity of a reference volume. An interesting question within the

probabilistic modelling of timber material properties is how to relate measurements on test specimen $r_{m,s}$ to the properties of reference volumes $r_{m,0}$. For the given example a simple relation is found with the form:

$$r_{m,0} = r_{m,s}^{\vartheta} \tag{7.25}$$

The parameter ϑ is calibrated for different test standards by using the least squares technique. The results are given in Table 7-5.

Table 7-5 ϑ-values for the estimation of the strength of weak sections.

See Equation *(6.8)*	EN	US	AUS
$\vartheta =$	1.05	1.03	1.02

According to Equation (7.25) the parameters of the lognormal distribution can be related as:

$$\xi_{r_{m,0}} = \left(\xi_{r_{m,s}} \right)^{\vartheta}$$
$$\delta_{r_{m,0}} = \left(\delta_{r_{m,s}} \right) \vartheta \tag{7.26}$$

It should be underlined that the given example is based on the within component bending moment capacity variation model and the corresponding model parameters as presented in Isaksson (1999) and chapter 6.

8 CONCLUSIONS AND OUTLOOK

8.1 CONCLUSIONS

8.1.1 RETROSPECT AND MOTIVATION

During the last decades structural reliability methods have been further developed, refined and adapted and are now at a stage where they are being applied in practical engineering problems as an decision support tool in connection with design and assessment of structures. Furthermore, basic knowledge concerning the actions on structures and the material characteristics has improved due to increased focus, better measuring techniques and international research co-operation. This knowledge has now reached a level where it enables experts to take into account uncertainties in material properties and actions when assessing the load carrying capacity, serviceability and service life of structures. This is not least due to the fundamental works on structural reliability methods performed within the Joint Committee on Structural Safety (JCSS) including, among others, the basic reports on actions on structures, basic reports on material resistances, the guideline for reliability based assessment of structures and the almost complete JCSS Probabilistic Model Code. These documents provide general guidelines for the use of structural reliability methods in practical applications and at the same time constitute the basis for ensuring that such analysis are performed on a theoretically consistent and comparative basis.

For materials such as concrete and steel, this has led to an increasingly more consistent evaluation of the safety or reliability, i.e. the probability that a structure will fulfil its function throughout its service life. Whereas some efforts in this direction have been undertaken also for timber; the developments, however, have been less impressive for several reasons:

- The variability of the material properties is much higher than for other building materials. This poses problems but also implies that the advantages of introducing reliability concepts may be greater.

- The material properties, and therefore also the probability of failure, depend on the entire load and moisture history of the structure.

In the last few years the interest in designing timber structures has steadily increased. The reason for this being an increased focus in society on sustainability and environmental aspects but also due to the positive effects of timber materials on the inner climate in residential buildings and excellent architectural possibilities. Furthermore, timber has been found technically and economically competitive compared with steel and concrete as a building material for a broad range of building structures such as e.g. large span roof structures and residential buildings.

It is thus now urgently important that a consistent basis for design of timber structures is established and documented in such a way that it may be accepted for implementation by the timber engineering and research community. Only then can a consistent basis for the design of timber structures be insured for the benefit of the society in general and for the parties with interest in the application of the timber as a building material in particular.

The development of a basis of design for timber structures is the main objective of this thesis.

8.1.2   APPROACH AND SUMMARY

The logical scheme of the development of a basis for the design of timber structures is constituted by successively following chapters 2 – 7.

In chapter 2 the main issues of structural reliability are reviewed and discussed. It is focused on the topics which are considered as most relevant for this thesis. The limit state principle is introduced; uncertainties and their influence on engineering decision making are discussed. Basic principles of the probabilistic modelling of loads and resistances are presented. The most essential methods of structural reliability and different probabilistic and deterministic design concepts are outlined and compared.

Chapter 3 addresses on timber as a structural material. The growth of a tree is described to illustrate how wood is produced. Many particularities of structural timber can be attributed to the growing conditions of a tree and the characteristics of the wood cell. The chapter is concluded with the definition of timber material properties at the so-called element level and the introduction of structural timber strength classes as a consequence of timber grading.

Chapters 4 and 5 represent the development part of the thesis. In chapter 4 a scheme for the probabilistic modelling of the material properties of solid timber is introduced, differentiating between three main aspects: scale dependency of timber material properties, time dependency and the interrelation between different material properties (see also Figure 4-2). The spatial variability is discussed in more detail, differentiating between different levels of variation. The corresponding perceptions constitute the basis for better understanding and assessment of the high variability of timber material properties. The properties of timber components depend on the load- and climate history to which they are exposed during their service lives. Different models of the strength degradation under sustained load are discussed, further developed and applied for reliability calculations. At the end of chapter 4, functional interrelations between different timber material properties are presented.

In chapter 5 the probabilistic modelling of timber connections is discussed, focusing on a particular type of connection: connections with parallel loaded double shear dowel type fasteners. Existing calculation frameworks are reviewed and discussed. A probabilistic calculation model is developed where the different failure modes of a connection are considered as a system reliability problem. A large database is used to calibrate the model uncertainty and to discuss possible refinements of the calculation model. The database,

however, was found to not be applicable for the development of an alternative calculation model for dowel type fastener connections.

In chapter 6 the conclusions are condensed into a proposed basis for the design of timber structures. After several discussions [1] it was decided to structure the proposal for the probabilistic model code for timber into several levels of sophistication. The basic level reflects the recent practice for reliability based code calibration. The bending strength and stiffness and the density of timber are referred to as reference material properties and are introduced as simple random variables. The basic limit state functions for components and connections are given. Furthermore, proposals are made regarding the different characteristics of timber on this simple level. Scale effects are disregarded and the time, load and moisture dependency is covered by deterministic factors for discrete time, load and moisture scenarios. Functional relationships for other material properties (based on the reference material properties) are given and probability distribution functions for the other material properties are proposed. Starting from this level, several possible refinements are proposed. New information might be introduced, and it is shown how different types of new information can be integrated by using a Bayesian updating scheme. Refinements in regard to the modelling of damage as a consequence of time load duration are proposed based on the models introduced in chapter 4. For the bending strength, a hierarchical spatial variability model is proposed and a method is presented for linking the properties of a cross section (which is considered as the reference starting point for the modelling of spatial variability) with the properties of a test specimen. However, some of the features explored in chapters 4 and 5 are not considered as being sufficiently verified for the implementation in an operational model code.

Within chapter 4 and 5 several examples for the discussed models are already given. In chapter 7 some further applications such as the assessment of experimental data, updating with new information etc. are exemplified.

8.1.3 ORIGINALITY OF WORK

The present work has one main objective; the development and the documentation of a proposed basis for probability based design of timber structures. The content of the proposal is mainly based on already existing knowledge. However, the attempt to combine this knowledge into a consistent and operational format is considered as new and original. The main features are:

- The presentation of a very basic model as a reference for simple reliability based code calibration which is fully consistent with possible refinements.

---

[1] e.g. with participants of the COST action E 24 (with many representatives of the timber research community) and members of the JCSS (as experts in the field of structural reliability)

- Interrelationships between different material properties based on expected values, coefficients of variation and correlations.

- The consistent treatment of material variability on different scales (micro, meso, macro).

- The illustration of how timber material properties can be updated in regard to different types of information.

During the development of the proposal several interesting issues are explored. The results have not all been applied in the proposed model code, but they also deliver valuable conclusions for the further development of the understanding of timber as a structural material. These results are:

- The development of a consistent probabilistic framework of graded timber material; the grading process is explicitly considered and a format of communicating the relevant information is proposed.

- Based on these results it is demonstrated how cost optimal grading strategies can be identified.

- A framework for the calibration of load duration modification factors is presented; a damage accumulation model based on fracture mechanical considerations is developed further for consideration of random load processes. It is found that the model is not sensitive to the number of load cycle repetitions when a random load process is considered.

- Based on experimental data existing models for the capacity of dowel type fasteners are reassessed and possible developments are discussed. The model uncertainty is quantified based on the data.

8.1.4   LIMITATIONS

The present work mainly concerns modelling the material properties of solid structural timber and the load bearing properties of connections. The proposed models are predominantly based on test programs and investigations considering North American and European softwoods. For some other softwoods, and especially for hardwood, the underlying assumptions are less appropriate. It should also be noted that part of the quantitative information in this thesis should be considered as indicative values. Timber connections are considered, however, all the concern is directed to one special type of connections; connections with parallel loaded double shear dowel type fasteners.

System effects are not addressed explicitly within this thesis. However, the proposal for the modelling of spatial variability can be used for performing research in this direction. Another aspect which is nearly neglected is the complex interrelation of timber material and moisture. In this case, the physical or biological deterioration of the timber should be considered in

addition to its strength and stiffness behaviour.

8.2   OUTLOOK

The main outcomes of this thesis are related to necessary pre-codification modelling aspects concerning the reliability of timber components in regard to strength and stiffness properties. An achievement of this thesis is that the work performed is fully compatible with the general probabilistic framework for establishing design basis developed by the Joint Committee on Structural Safety (JCSS).

During the course of writing this thesis, however, it has become apparent that several fundamental issues require more research and development. In particular, it is found that the present practice in regard to strategies to quality control of timber raw material as well as engineered timber introduces significant uncertainties regarding the performance of timber structural components, and the uncertainties cannot be quantified based on the present control practice. It is necessary to develop further a framework for the probabilistic modelling of timber grading as outlined in chapter 4 and to disseminate this within code and standard writing bodies and timber researchers.

An attempt to model the spatial variability of timber material properties is presented within the present thesis. More experimental work should be performed or reviewed to quantify the parameters of the presented models. The description of size effects has earned considerable recognition in the past research; no general consensus has been reached and future research should be directed in the development of a consistent framework for the description of size effects in structural timber elements.

Furthermore, it has been found that model uncertainties associated with high performance timber structural components such as glued laminated timber beams are unsatisfactorily high. It is of importance to direct future research in this direction, because engineered timber elements are promising products that may compete with steel in large span high performance load bearing structures.

More than for other building materials, the properties of timber structural components and systems have to be seen in direct combination with the loads and environment to which they are exposed to. Adverse effects in timber structures are not only related to critical load-strength combinations, but rather to moisture induced strength and stiffness degradation of structural elements. The mechanism behind this is the so called mechano-sorptive creep of timber on the one hand, but also degradation as a consequence of physical and/or biological decay (insects/fungi) on the other hand. Several research activities in the field of moisture effects in buildings have taken place, but the individual studies did not yet converge to a general consensus which could form a scientific basis for proper code formats and regulations facilitating the engineer to cope with the problem in daily design and maintenance. Therefore, more work is needed in this respect.

9 REFERENCES

AS 3519: Standards Australia: Timber – Stress graded – Procedures for monitoring structural properties. Sydney, Australia, 1997.

AS 4490: Standards Australia: Timber – Machine proof grading. Sydney, Australia, 1997.

ASHTO (1994): LRFD Bridge Design Specifications. American Association of State Highway and Transportation Officials, Washington, DC.

ASTM Book of Standards – Wood (Print and CD-ROM). Volume 04.10, July 2004.

ASTM D 245: Standard practice for establishing structural grades and related allowable properties for visually graded lumber. ASTM Book of Standards.

ASTM D 6570: Standard Practice for Assigning Allowable Properties for Mechanically-Graded Lumber. ASTM Book of Standards.

Bach L. (1973). Reiner Weisenbergs' theory applied to time dependent fracture of wood subjected to various modes of mechanical loading. Wood Science, 5(3), pp. 161-171.

Barenblatt G. I. (1962). The mathematical theory of equilibrium cracks in brittle fracture. Adv. Appl. Mech. 7, pp. 55-129.

Barrett J. D. (1974). Effect of size on tension perpendicular to grain strength of douglas fir. Wood and Fiber. 6(2), pp. 126-143.

Barrett J. D. and Fewell A. R. (1990). Size factors for the bending and tension strength of structural lumber. Proceedings of the 23th Meeting, International Council for Research and Innovation in Building and Construction, Working Commission W18 – Timber Structures, CIB-W18, Paper No. 23-10-3, Lisbon, Portugal, 1990.

Barrett J. D. and Foschi R. O. (1978). Duration of load and probability of failure in wood. Part I + II. Canadian Journal of Civil Engineering, 5(4):505-532.

Barrett J. D., Foschi R. O. and Fox S. P. (1975). Perpendicular to the grain strength of douglas fir. Canadian Journal of Civil Engineering. 2(1) pp. 50-57.

Basler E. (1961). Untersuchungen über den Sicherheitsbegriff von Bauwerken. Schweizer Archiv für angewandte Wissenschaft und Technik, Volume 4.

Benjamin J. R. and Cornell C. A. (1970). Probability, Statistics and Decision for Civil Engineers. McGraw-Hill Book Company, New York, USA.

Blass H.J. (editor) (1995) STEP 1: Timber Engineering, Basis of Design, Material Properties, Structural Components and Joints. Centrum Hout, The Netherlands.

Blass H.J., Bienhaus A. and Krämer V. (2001). Effective bending capacity of dowel-type fasteners. Proceedings PRO 22, International RILEM Symposium on Joints in Timber Structures. pp. 71-88.

Bohannan B. (1966). Effect of size on bending strength of wood members. USDA Forest Service, Research Paper FPL 56, Forest Products Laboratory, Madison, WI.

Bolotin V. V. (1969). Statistical Methods in Structural Mechanics. Holden-Day Series in Mathematical Physics.

Bonfield P. W., and Ansell M. P. (1991). The fatigue properties of wood in tension, compression and shear. Journal of Material Science. 26, pp. 4765-4773.

Boström L. (1994). Machine strength grading. Comparison of four different grading systems. Swedisch National Testing and Research Institute, SP REPORT 1994:49.

Bronstein I. N. and Semendjajew K. A. (1981). Taschenbuch der Mathematik. BSB B. G. Teubner Vertragsgesellschaft, Leipzig.

Caultfield D. F. (1985). A chemical kinetics approach to the duration of load problem in wood. Wood and Fibre Science, 17(4), pp. 504-521.

CEB (1976a): First Order Concepts for Design Codes. CEB Bulletin No. 112, Munich.

CIRIA (1977): Rationalization of Safety and Serviceability Factors in Structural Codes. CIRIA Report No. 63, London.

Clorius C. O. (2001). Fatigue in wood – an investigation in tension perpendicular to the grain. PhD Thesis, Department of Structural Mechanics and Materials, Technical University of Denmark.

Coder S. E. (1965). Localised deflection related to bending strength of lumber. Proceedings of the second symposium on non-destructive testing of wood. Washington State University, Pullman, WA.

Colling F. (1986). Influence of volume and stress distribution on the shear strength and tensile strength perpendicular to the grain. Proceedings of the 19th Meeting, International Council for Research and Innovation in Building and Construction, Working Commission W18 – Timber Structures, CIB-W18, Paper No. 19-12-3, Florence, Italy, 1986.

COMPUTERMATIC "Manual" (2000). MPC Measuring and Process Control Ltd., Chelmsford, Essex, England.

Cornell C. A. (1969). A Probability Based Structural Code. ACI-Journal, 66: pp. 974-985.

COST E 24 (2005) Reliability of Timber Structures. European Research Project, Meetings and Publications Documentation: http://www.km.fgg.uni-lj.si/coste24/coste24.htm.

Czomch I. (1991). Lengthwise variability of bending stiffness of timber beams. Proceedings of the International Timber Engineering Conference, London, UK , Vol.2, pp. 2158-2165.

Czomch I., Thelandersson S. and Larsen H. J. (1991). Effect of within member variability on the bending strength of structural timber. Proceedings of the 24th Meeting, International Council for Research and Innovation in Building and Construction, Working Commission W18 – Timber Structures, CIB-W18, Paper No. 24-6-3, Oxford, UK, 1991.

Der Kiureghian A., Lui P.-L. (1986). Structural reliability under incomplete probability information. Journal of Engineering Mechanics, 112(1), pp. 85-104.

Ditlevsen O. and Källsner B. (2004). Statistical series system size effects on bending strength of timber beams. Reliability and Optimization of Structural Systems – Maes & Huyse (eds). Taylor and Francis Group, London.

Ditlevsen O. and Madsen H.O. (1996). Structural Reliability Methods. Wiley, Chichester, UK.

Downing S. D. and Socie D. F. (1982). Simple Rainflow Counting Algorithms. International Journal of Fatigue. 4(1), pp. 31-40.

Dugdale D. S. (1960). Yielding of steel sheets containing slits. J. Mech. Phys. Solids 8, pp. 100-104.

Ellingwood B. and Rosowski D. V. (1991). Duration of load effects in LRFD for wood constructions. ASCE J. Struct. Eng. 117(2):584-599.

Ellingwood, B., MacGregor, J.G., Galambos, T.V. & Cornell, C.A. (1982): Probability Based Load Criteria: Load Factors and Load Combinations. ASCE, Journal of the Structural Division, Vol. 108, N0. ST5, 1982, pp. 978-997.

EN 1995-1-1, Eurocode 5: Design of timber structures; part 1-1: general rules and rules for buildings. Comité Européen de Normalisation, Brussels, Belgium, 2004.

EN 26891: Timber Structures – Joints made with mechanical fasteners – General principles for the determination of strength and deformation characteristics. Comité Européen de Normalisation, Brussels, Belgium, 1991.

EN 338: Structural Timber – Strength Classes. Comité Européen de Normalisation, Brussels, Belgium, 2003.

EN 383: Timber Structures; test methods; determination of embedding strength and foundation values for dowel type fasteners. Comité Européen de Normalisation, Brussels, Belgium, 1993.

EN 383: Timber Structures; test methods; determination of embedding strength and foundation values for dowel type fasteners. Comité Européen de Normalisation, Brussels, Belgium, 1993.

EN 408: European Standard: Timber structures - Structural Timber - Determination of some physical and mechanical properties. Comité Européen de Normalisation, Brussels, Belgium, 2004.

Ewan W. D., Kemp K. W. (1960). Sampling inspection of continuous processes with no autocorrelation between successive results. Biometrika 47, pp. 363-380.

Faber M. H. (2003). Risk and safety in Civil Engineering. Lecture Notes, Institute of Structural Engineering, Swiss Federal Institute of Technology, Zurich.

Faber M. H. and Sørensen J. D. (2003). Reliability based code calibration – the JCSS approach. Proceedings to the 9th International Conference on Applications of Statistics and Probability in Civil Engineering ICASP9, Volume 2, pp. 927-935, San Francisco, USA, July 6-9, 2003.

Faber M. H., Köhler J. and Sørensen, J. D. (2004). Probabilistic modelling of graded timber material properties. Journal of Structural Safety, 26(3), pp. 295-309.

Foliente, G.C. (1998). Design of timber structures subjected to extreme loads. *Prog. Struct. Eng. Mater.*, 1(3), pp. 236-244.

Foschi R. O. and Barrett J. D. (1975). Longitudinal shear strength of douglas fir. Canadian Journal of Civil Engineering, 3(2), pp. 198-208.

Foschi R. O. and Barrett J. D. (1980). Glued laminated beam strength: A model. ASCE Journal of Structural Division 106 (ST8).

Foschi R. O. and Yao Z. C. (1986). Another look at three duration of load models. Proceedings of the 19th Meeting, International Council for Research and Innovation in Building and Construction, Working Commission W18 – Timber Structures, CIB-W18, Florence, Italy, 1986.

Foschi R. O., Folz B. R. and Yao F. Z. (1989). Reliability-based Design of Wood Structures. Structural Research Series, Department of Civil Engineering, University of British Columbia, Vancouver, British Columbia, Canada. Report No. 34.

Fridley K. J. and Soltis L. A. (1992). Load-duration effects in structural lumber: strain energy approach. J. of Struct. Eng. ASCE, 118(9), pp. 2351-2369.

Galligan W., DeVisser D. (2004). Machine Grading Procedures under American Lumber Standard. Proceedings of the 8th World Conference of Timber Engineering, Lathi, Finnland.

Gerhards C. C. and Link C. L. (1987). A cumulative damage model to predict load duration characteristics in lumber. Wood and Fiber Science. 19(2), pp. 147-164.

Gerhards, C. C. (1979). Time-related effects of loads of wood strength. A linear cumulative damage theory. Wood Science. 19(2), pp. 139-144.

Glos P. (1981). Zur Modellierung des Festigkeitsverhaltens von Bauholz bei Druck-, Zug- und Biegebeanspruchung. Berichte zur Zuverlässigkeitstheorie der Bauwerke, SFB 96, Munich, Germany.

Glos P. (1995). Strength Grading. STEP 1: Timber Engineering, Basis of Design, Material Properties, Structural Components and Joints. Centrum Hout, The Netherlands.

Green D. W. and Kretschmann, D. E. (1997). Properties and grading of southern pine timber. Forest Products Journal, 47(9), pp. 78-85.

Gustafsson P. J. (1992). Some test methods for fracture mechanics properties of wood and wood adhesive joints. RILEM TC133-TF workshop, Bordeaux, France, 1992.

Hanhijärvi A., Galimard P. and Hoffmeyer P. (1998). Duration of load behaviour of different sized straight timber beams subjected to bending in variable climate. Holz als Roh- und Werkstoff, 56(5), pp. 285-293.

Hasofer A. M. and Lind N. C. (1974). An exact and invariant first order reliability format. ASCE, J. Eng. Mech. Div. 1974, pp. 111-121.

Hoffmeyer P. (1990). Failure of Wood as Influenced by Moisture and Duration of Load. Ph. D. Thesis, College of Environmental Science and Forestry Syracuse, State University of New York.

Hoffmeyer P. (1995). Wood as a Building Material. STEP 1: Timber Engineering, Basis of Design, Material Properties, Structural Components and Joints. Centrum Hout, The Netherlands.

Hohenbichler M., Rackwitz R. (1981). Non-Normal dependent vectors in structural safety. Journal of Engineering Mechanics, 107(6), pp. 1227-1238.

Isaksson T. (1999). Modelling the Variability of Bending Strength in Structural Timber. PhD-thesis, Lund Institute of Technology, Report TVBK-1015.

ISO 8375: Solid timber in structural sizes – determination of some physical and mechanical properties. International Organisation for Standardisation, 1985.

Johansen K.W. (1949). Theory of timber connections. International Association of Bridge and Structural Engineering, Publication No. 9, pp. 249-262, Bern, Switzerland.

Johansson C.-J., Brundin, J. and Gruber R. (1992). Stress grading of Swedish and German timber. A comparison of machine stress grading. SP REPORT 1992:23.

Johnson A. I. (1953). Strength, safety and economical dimensions of structures. Swedish State Committee for Building Research, Bulletin n. 22, p. 159.

Joint Committee of Structural Safety (JCSS, 2001). Probabilistic Model Code, Internet Publication: www.jcss.ethz.ch.

Jorissen A. (1998). Double shear timber connections with dowel type fasteners. PhD-Thesis, Delft University Press, Netherlands.

Jourez B, Riboux A and Leclercq A. (2001). Anatomical characteristics of tension wood and opposite wood in young inclined stems of poplar. IAWA (International Association of Wood Anatomists) Journal, 22, pp. 133–157.

Källsner B. and Ditlevsen O. (1994). Lengthwise bending strength variation of structural timber. IUFRO Sydney, Australia.

Källsner B. and Ditlevsen O. (1997). Experimental verification of a weak zone model for timber bending. IUFRO S5.02 Timber Engineering, pp. 389-404, Copenhagen, Denmark.

Kass A. J. (1975). Middle ordinate method measures stiffness variations within pieces of lumber. Forest Products Journal 25(3), pp. 33-41.

Kersken-Bradley M. (1981). Beanspruchbarkeit von Bauteilquerschnitten bei streuenden Kenngrössen des Kraftverformungsverhaltens innerhalb des Querschnitts. Dissertation, TU München.

Kersken-Bradley M. and Rackwitz R. (1991). Stochastic Modeling of Material Properties and Quality Control, JCSS Working Document, IABSE-publication, March 1991.

Kline D. E., Woeste F. E. and Bendtsen B. A. (1986). Stochastic model for the modulus of elasticity of lumber. Wood and Fiber Science, 18(2), pp. 228-238.

Köhler J. (2002). Probabilistic modelling of duration of load effects in timber structures using a fracture mechanics model. Proceedings 4th International Ph.D. Symposium in Civil Engineering, fib, Munich, September 2002.

Köhler J. and Faber M. H. (2003). A probabilistic creep and fatigue model for timber materials. Proceedings to the 9th International Conference on Applications of Statistics and Probability in Civil Engineering ICASP9, Volume 2, pp. 1141-1148, San Francisco, USA, July 6-9, 2003.

Köhler J., Faber M. H. (2003). A probabilistic approach to cost optimal timber grading. Proceedings of the 36th Meeting, International Council for Research and Innovation in Building and Construction, Working Commission W18 – Timber Structures, CIB-W18, Paper No. 36-5-2, Colorado, USA, 2003.

Köhler J., Faber M. H. (2004). Proposal for a probabilistic model code for design of timber structures. Proceedings of the 37th Meeting, International Council for Research and Innovation in Building and Construction, Working Commission W18 – Timber Structures, CIB-W18, Paper No. 37-104-1, Edinburgh, UK, 2004.

Köhler J., Svensson S. (2002). Probabilistic modelling of duration of load effects in timber structures. Proceedings of the 35th Meeting, International Council for Research and Innovation in Building and Construction, Working Commission W18 – Timber Structures, CIB-W18, Paper No. 35-17-1, Kyoto, Japan, 2002.

Kollmann F. F. P., Côté W.A. (1968). Principles of wood science. I – Solid wood, Springer- Verlag.

Lam F. and Varoglu E. (1991). Variation of tensile strength along the length of timber, Part 1 and 2. Wood Science and Technology 25, pp. 351-360 and pp. 449-458.

Larsen H. J. (1986). Eurocode 5 and CIB structural design code. Proceedings of the 19th Meeting, International Council for Research and Innovation in Building and Construction, Working Commission W18 – Timber Structures, CIB-W18, Paper No. 19-102-2, Florence, Italy, 1986.

Leicester R. H. and Breitinger H. O. (1994). Statistical control of timber strength. Proceedings of the 27th Meeting, International Council for Research and Innovation in Building and Construction, Working Commission W18 – Timber Structures, CIB-W18, Paper No. 27-17-1, Sydney, Australia, 1994.

Leijten A., Köhler J. and Jorissen A. (2004). Review of data for timber connections with dowel-type fasteners. Proceedings of the 37th Meeting, International Council for Research and Innovation in Building and Construction, Working Commission W18 – Timber Structures, CIB-W18, Paper No. 37-7-13, Edinburgh, UK, 2004.

Leijten A., Köhler J. and Jorissen A. (2004). Review of probability data for timber connections with dowel type fasteners. Proceedings of the 37th Meeting, International Council for Research and Innovation in Building and Construction, Working Commission W18 – Timber Structures, CIB-W18, Paper No. 37-7-6, Edinburgh, UK, 2004.

Lindley D. V. (1965). Introduction to Probability & Statistics. Cambridge University Press.

Madsen B. (1992). Structural Behaviour of Timber. Timber Engineering Ltd., Vancouver, Canada.

Madsen B. and Buchanan A. H. (1986). Size effects in timber explained by a modified weakest link theory. Canadian Journal of Civil Engineering 13(2), pp. 218-232.

Madsen H.O., Krenk S. and Lind N.C. (1986). Methods of Structural Safety. Prentice-Hall, Eaglewood Cliffs, NJ, USA.

Mattheck C. (1998). Design in nature: learning from trees. Springer, Berlin.

Melchers R. (1999). Structural Reliability: Analysis and Prediction. Ellis Horwood, Chichester, UK.

Meyer A. (1957). Die Tragfähigkeit von Nagelverbindungen bei Statischer Belastung. Holz als Roh- und Werkstoff. 15(2), pp. 96-109.

Mindess S., Nadeau J. S. and Barret J. D. (1975). Slow crack growth in douglas-fir. Wood Science 8(1) pp. 389-396.

Morgan J. N. and Sonquist A. (1963). Problems in the analysis of survey data and a proposal. J. Am. Statist. Assoc. 58, pp. 415-435.

Morlier P., Valentin G. and Toratti T. (1994). Review of the theories on long-term strength and time to failure. Proceedings COST 508 Workshop on Service Life Assessment of Wodden Structures, Espoo, Finland.

NBCC (1980): (National Building Code of Canada), National Research Council of Canada.

Nelder J. A., and Mead R. (1965). A simplex method for function minimization. Computer Journal 7: pp. 308-313.

NEN 5466: Kwaliteitseisen voor hout (KVH 1980). Houtsoort Europees vuren (in Dutch). Quality requirements for timber. Species European spruce. Netherlands Normalisatie Instituut, Delft, Netherlands, 1983.

Nielsen L.F. (1979). Crack failure of dead-, ramp- and combined loaded viscoelastic materials. Proceedings to the First International Conference on Wood Fracture, Banff, Alberta, Canada, 1979.

Nielsen L.F. (2000). Lifetime and Residual Strength of wood subjected to static and variable load – Part I +II. Holz als Roh- und Werkstoff. Vol. 58, pp. 81-90 and 141-152.

Nielsen L.F. (2005). On the Influence of Moisture and Load Variations on the Strength Behaviour of Wood. Proceedings of the international Conference on Probabilistic Models in Timber Engineering, Arcachon, France 2005.

Niemz P. (2004). Physik des Holzes. Lecture Notes (in German). ETH Zürich, Switzerland.

NLGA SPS2: National Lumber Grades Authority. Standard grading rules for Canadian lumber. Vancouver, Canada, 1998.

Norén B. (1986). Results of pair matching of wood for long-term loading. International workshop on duration of load in lumber and wood products. Forintek Canada Corperation, Special Publication, No SP27.

OHBDC (1983): (Ontario Highway Bridge Design Code), Ontario Ministry of Transportation and Communication, Ontario.

Pearson R. G. (1972). The effect of duration of load on bending strength of wood. Holzforschung, 26(4), pp. 153-158.

Petersson H. (1995). Fracture design analysis of wooden beams with holes and notches. Proceedings of the 28th Meeting, International Council for Research and Innovation in Building and Construction, Working Commission W18 – Timber Structures, CIB-W18, Paper 28-19-3, Copenhagen, Denmark, 1995.

Philpot T. A., Fridley K. J and Rosowsky D. V. (1994). Energy based failure criterion for wood. J. of Materials in Civil Engineering, 6(4), pp. 578-593.

Pöhlmann S. and Rackwitz R. (1981). Zur Verteilungsfunktion der Festigkeitseigenschaften bei kontinuierlich durchgeführter Sortierung. Materialprüfung 23, Hanser, Munich, Germany.

prEN 14081 part 1-4: Timber Structures – Strength Graded Timber with rectangular Cross Section. Comité Européen de Normalisation, Brussels, Belgium, 2003.

Rackwitz R. and Müller K. F. (1977). Zum Qualitätsangebot von Beton, II. Beton, 27(10), pp. 391-393.

Raiffa H. and Schlaifer R. (1960). Applied statistical decision theory. John Wiley & Sons Ltd. Chichester, UK.

Ranta-Maunus A., Fonselius M., Kurkela J. and Toratti T. (2001). Reliability Analysis of Timber Structures. VTT Research Notes, Espoo, Finland.

Ravindra, M.K. & Galambos, T.V. (1978): Load and Resistance Factor Design for Steel. ASCE, Journal of the Structural Division, Vol. 104, N0. ST9, 1978, pp. 1337-1353.

Riberholt H. and Madsen P. H. (1979). Strength of timber structures, measured variation of the cross sectional strength of structural lumber. Report R 114, Struct. Research Lab., Technical University of Denmark.

Rosenblueth, E. & Esteva, L. (1972): Reliability Basis for Some Mexican Codes. ACI Publication SP-31, 1972, pp. 1- 41.

Rosowsky D. V., Bulleit W. M. (2002). Load duration effects in wood members and connections: order statistics and critical loads. Structural Safety 2002, 24, pp. 347-362.

Rouger F. (1996). Application of a modified statistical segmentation method to timber machine strength grading. Wood and Fibre Science. 28(4).

Rouger F. (1997). A new statistical method for the establishment of machine settings. Proceedings of the 30th Meeting, International Council for Research and Innovation in Building and Construction, Working Commission W18 – Timber Structures, CIB-W18, Paper No. 30-17-1, Vancouver, Canada, 1997.

Rouger F. and Fewell A. R. (1994). Size effects in timber: Novelty never ends. Proceedings of the 27th Meeting, International Council for Research and Innovation in Building and Construction, Working Commission W18 – Timber Structures, CIB-W18, Paper No. 27-6-2, Sydney, Australia, 1994.

Sawata K., Yasumura, M. (2002). Determination of embedding strength of wood for dowel-type fasteners. Journal of Wood Science, 48, pp. 138-146.

Sharpely R. A. (1975). A theory of crack initiation and growth in viscoelastic media (3 parts). Int. J. of Fracture 11, pp. 141-159, 369-388, 549-562.

Showalter K. L., Woeste F. E. and Bendtsen B. A. (1987). Effect of length on tensile strength in structural timber. Forest Products Laboratory, Research paper FPL-RP-482. Madison, Wisconsin.

Sørensen, J.D. and Svenson S. (2005). Reliability Based Modeling of Moisture and Load Duration Effects. Proceedings of the international Conference on Probabilistic Models in Timber Engineering, Arcachon, France 2005.

Sørensen, J.D., Stang, B.D., Svensson, S. (2002). Effect of load duration on timber structures in Denmark. Proceedings 9th International Conference on Applications of Statistics and Probability in Civil Engineering(ICASP9), San Fransisco, USA, July 6-9, 2003, pp. 345-354.

Suddarth S. K. and Woeste F. E. (1977). Influence of variability in loads and modulus of elasticity in wood column strength. Wood Science 20(2), pp. 62-67.

Svensson S., Thelandersson S. and Larsen H. J. (1999). Reliability of timber structures under long term loads. Materials and Structures. 32, pp. 755-760.

Thelandersson S. and Larsen H. J. (2003). Timber Engineering. John Wiley & Sons Ltd. Chichester, UK.

Thörnquist T. (1990). Juventile wood in coniferous trees. The Swedish University of Agricultural Sciences. Department of Forest-Industry-Market Studies. Report 10.

Timell T. E. (1969). The chemical composition of tension wood. Svensk Papperstidning, 72: pp. 173–181.

Toft-Christensen P. and Baker M. J. (1982). Structural Reliability Theory and its Applications. Springer, 1982.

Van der Put T. A. C. M. (1989). Deformation and damage processes in wood. PhD thesis. Delft University press, Netherlands.

Walker J. C. F. (1993). Primary Wood Processing. Chapman & Hall.

Warren W. G. (1978). Recent developments in statistical quality control procedures for MSR. Proceedings of Fourth Nondestructive Testing of Wood Symposium. Vancouver, Canada.

Weibull W. (1939). A statistical theory of the strength of materials. Royal Swedish Institute for Engineering Research, Proceedings, 141, pp. 45.

Whale, L.R.J. and Smith, I. (1986). The derivation of design clauses for nailed joints in Eurocode 5, Proc. of the 19th CIB W18 meeting, Paper 19-7-6.

Wood Handbook: Wood as an Engineering Material. Agriculture Handbook 71. Forest Product Laboratory, U.S. Dep. Agric., Washington D.C., 1987.

Wood L.W. (1947). Behaviour of wood under continued loading. Eng. News-Record, 139(24), pp. 108-111.

Wood L.W. (1951). Relation of strength of wood to duration of load. Report no. 1916. Madison, USDA Forest service, Forest products laboratory. Report no. 1916.

ANNEX

A1

A CHARACTERISATION OF RANDOM PHENOMENA

In general two situations may be distinguished namely, the situation where a new probabilistic model is formulated from the very beginning; and the situation where an already existing probabilistic model is updated based on additional information. The formulation of probabilistic models is normally based on frequentistic information (i.e. data from tests) mostly combined with some physical considerations, experience and judgment (subjective information). Building a probabilistic model in general requires the following steps:

- assessment and statistical quantification (and qualification) of available data,

- selection of a distribution function,

- estimation of distribution parameters,

- model verification,

- model updating.

A1   NON-PARAMETRIC ASSESSMENT OF AVAILABLE DATA

To reach an overview and to get a crude idea about the statistical characteristics of a sample it is common to apply some descriptive procedures. In the following, the concept of Order Statistics and the Quantile Plot are introduced. It is also common to use the first two sample moments to characterise the sample.

Quantile Plot

A common method for quantifying the statistical properties of a test sample **x** is the non-parametric procedure. The test data is sorted (ranked) in ascending order according to its magnitude, as

$$x_1 \leq x_2 \leq x_3 \ldots \leq x_n \tag{A.1}$$

where n is the number of test specimen in the sample and the subscript is equal to the rank of the data value.

The quantile of the data value of rank m is

$$q_m = \frac{m - 0.5}{n} \tag{A.2}$$

An issue that may arise here is why the quantile is given by Equation (A.2) and not for example just by m/n. When evaluating a certain quantile the data set is split into two groups, an upper and a lower one. The 0.5 term in the numerator of Equation (A.2) means that the corresponding observation x_m is counted as being half in the one group and half in the other. The method is often used as a direct graphical representation of the data in a so-called

quantile plot.

Order Statistics

Let X be a continuous random variable with unknown distribution function $F(x)$ and the probability density function $f_X(x)$. n independent realisations of X are ordered such that $x_1 \leq x_2 \leq x_3 \ldots \leq x_n$. The observation of rank m, x_m is a realisation of the random variable X_m. X_m is determined from the observation that there are $m-1$ observations not larger and $n-m$ not less than X_m (considering an arbitrary number of samples of size n). The probability density function of X_m can be expressed as (Madsen et al (1986)):

$$f_{X_m}(x) = \frac{n!}{(m-1)!(n-m)!} F_X(x)^{m-1} \left[1 - F_X(x)\right]^{n-m} f_X(x)$$ (A.3)

Since the distribution model underlying X is not known, Equation (A.3) might have no further proposition. But if the function $F_X(x)$ itself is considered as a stochastic variable, instead of the variable X, the mean and the variance of $F_X(x_m)$ can be assessed by rewriting Equation (A.3) as:

$$f_{X_m}(x_m) dx_m = m \binom{n}{m} F_X(x_m)^{m-1} \left[1 - F_X(x_m)\right]^{n-m} dF_X(x_m)$$ (A.4)

The expected value of $F_X(x_m)$ is obtained by integration over the probability mass:

$$\begin{aligned}
E\left[F_X(x_m)\right] &= \int_{-\infty}^{\infty} F_X(x_m) f_{X_m}(x_m) dx_m \\
&= m \binom{n}{m} \int_0^1 F_X(x_m)^m \left[1 - F_X(x_m)\right]^{n-m} dF_X(x_m) \\
&= m \binom{n}{m} \frac{(n-m)!m!}{(n+1)!} \\
&= \frac{m}{n+1}
\end{aligned}$$ (A.5)

Accordingly the variance $VAR\left[F_X(x_m)\right]$ can be calculated as:

$$\begin{aligned}
VAR\left[F_X(x_m)\right] &= E\left[F_X(x_m)^2\right] - E\left[F_X(x_m)\right]^2 \\
&= \frac{1}{n+2} E\left[F_X(x_m)\right]\left(1 - E\left[F_X(x_m)\right]\right) \\
&= \frac{m}{(n+2)(n+1)}\left(1 - \frac{m}{n+1}\right)
\end{aligned}$$ (A.6)

A3

Equation (A.5) means that the expected value of the distribution function $F_X(x_m)$ evaluated at the observation of order m is equal to $m/(n+1)$; i.e. independent of the type of the distribution function.

Quantile Predictions

For quantile predictions the viewpoint is somehow different. Of interest is now the probability of exceeding the observation of order m from a sample of n independent observations M times in N future trails. Following Madsen et al. (1982) it can be shown that this probability is given as:

$$p(n,m;N,M) = \frac{\binom{N-M+m-1}{m-1}\binom{n-m+M}{M}}{\binom{n+N}{n}}$$ (A.7)

For example the probability that one further observation of the random variable X is not exceeding x_m is

$$p(n,m;1,0) = \frac{m}{n+1}$$ (A.8)

The probability that no of N further observations will exceed the maximum x_n is

$$p(n,n;N,0) = \frac{n}{N+n}$$ (A.9)

Equation (A.7) can be utilised to estimate fractile values of a random variable without any assumptions of the distribution model of the variable.

A2 SELECTION OF A DISTRIBUTION FUNCTION

A classical approach to select a proper distribution function for the representation of a random quantity is to postulate a hypothesis for the distribution family, then estimate the parameters for the selected distribution function on the basis of observations and finally perform statistical tests to verify the hypothesis. Statistical tests are, e.g., the χ^2 - goodness of fit test the Kolmogorov-Smirnov goodness of fit test or when comparing two hypothesises e.g. the likelihood ratio test. (see e.g. in Benjamin and Cornell (1971))

However, a quite big number of probability distribution functions exist, and it might not be reasonable to check all in regard to their validity. Furthermore, in most cases the amount of frequentistic information is limited and the statistical tests may thus lead to false conclusions. In many cases there are some physical considerations paired with experience which lead to the identification of a limited number of possible distributions. In practice the following

strategy is quite common:

First consider the physical arguments why a quantity may belong to one or the other distribution family.

Then check whether the statistical evidence (frequentistic information) is in gross contradiction with the assumed distribution.

E.g. if the bending strength of timber is considered, the following possible distribution models are selected for the following reason:

- Normal distribution: additive combination of random phenomena – traditionally used for ductile material failure. Probability for negative realisations.

- Lognormal distribution: multiplicative combination of random phenomena. Only positive realisations.

- 2-parametric Weibull distribution: extreme value distribution. Traditionally used for brittle material failure.

The distribution functions are introduced in Table A1.

A convenient method to check the validity of a chosen distribution model is the use of probability paper. Probability paper for a given distribution model is constructed such that the cumulative probability density function for that distribution model will have the shape of a straight line when plotted on the paper. A probability paper is thus constructed by a non-linear transformation of the x and the y axis. The transformations for the Normal, the Lognormal and the Weibull distribution are given in Table A2.

Table A2   Axis transformation for the construction of probability paper.

	x'-axis	y'-axis
Normal	x	$\Phi^{-1}(F(x))$
Lognormal	$\ln(x)$	$\Phi^{-1}(F(x))$
Weibull	$\ln(x)$	$\ln(-\ln(1-F(x)))$

Table A1   Normal, Lognormal and Weibull distribution functions.

	Density / Distribution Function	Range	Parm. Restrict.	Mean	Standard Deviation
Normal	$f_X(x) = \dfrac{1}{\sqrt{2\pi}\,\sigma}\exp\left[-\dfrac{1}{2}\left(\dfrac{x-m}{\sigma}\right)^2\right]$ $= \dfrac{1}{\sigma}\varphi\left(\dfrac{x-m}{\sigma}\right)$ $F_X(x) = \Phi\left(\dfrac{x-m}{\sigma}\right)$	$-\infty < x < \infty$	$\sigma > 0$	m	σ
Lognormal	$f_X(x) = \dfrac{1}{x\delta}\varphi\left(\dfrac{\ln\left(x/\xi\right)}{\delta}\right)$ $F_X(x) = \Phi\left(\dfrac{\ln\left(x/\xi\right)}{\delta}\right)$	$0 < x < \infty$	$\delta > 0$ $\xi > 0$ $\xi = median$	$\xi\exp\left(\dfrac{\delta^2}{2}\right)$	$\mu\sqrt{\exp\left(\delta^2\right)-1}$
Weibull	$f_X(x) = \dfrac{k}{w}\left(\dfrac{x}{w}\right)^{k+1}\exp\left[-\left(\dfrac{x}{w}\right)^k\right]$ $F_X(x) = 1-\exp\left[-\left(\dfrac{x}{w}\right)^k\right]$	$0 < x < \infty$	$w > 0$ $k > 0$	$w\Gamma\left(1+\dfrac{1}{k}\right)$	$w\sqrt{\Gamma\left(1+\dfrac{2}{k}\right)-\Gamma^2\left(1+\dfrac{1}{k}\right)}$

A3   ESTIMATION OF DISTRIBUTION PARAMETERS

The Method of Moments

Let the density function of a random variable X be given as f_X and x be every possible realisation of X, then the m th moment of X $m_X^{(m)}$ is given as:

$$m_X^{(m)} = E\left[X^m\right] = \int_{-\infty}^{\infty} x^m f_X(x)\, dx \quad \text{with } m = 2,3,4,5... \tag{A.10}$$

The m th central moment is given as:

$$m_{X,c}^{(m)} = E\left[\left(x - m_X^{(1)}\right)^m\right] = \int_{-\infty}^{\infty} \left(x - \mu_X\right)^m f_X(x)\, dx \quad \text{with } m = 2,3,4,5... \tag{A.11}$$

The characteristic of a random variable X can be expressed with the moments. E.g. the mean

value μ_X and the variance σ_X^2 of X can be derived, based on the first and second centralized moment respectively:

$$\mu_X = m_X^{(1)} = \int_{-\infty}^{\infty} x f_X(x) \, dx \tag{A.12}$$

$$\sigma_X^2 = \int_{-\infty}^{\infty} (x - \mu_X)^2 f_X(x) \, dx \tag{A.13}$$

Moments have proven to be useful numerical descriptors of the characteristics of random variables, i.e. a random variable can be completely described through its moments. They are also used to characterise the statistical properties of samples. The sample mean value and the sample variance can be derived based on the first and second centralized moment respectively. Considering a sample with n realisations of the variable X the sample mean (first sample moment) and the sample variance (second sample moment) are given in Equation (A.14) and (A.15) correspondingly.

$$\overline{x} = \frac{1}{n} \sum_{i=1}^{n} \hat{x}_i \tag{A.14}$$

$$s^2 = \frac{1}{n} \sum_{i=1}^{n} (\hat{x}_i - \overline{x})^2 \tag{A.15}$$

Note that these are sample descriptors and independent of any assumption of a possible distribution function of X.

Similar as the sample mean and the sample variance, sample moments of higher order, e.g. the sample coefficient of skewness and the sample coefficient of kurtosis can be derived from Equation (A.10). However, different samples drawn from the same random variable X might have different sample moments. The real moments of X are not known and they might be considered as random variables itself. The sample moments are just realisations of these random variables.

To capture the uncertainty associated with the sample moments the following way of thinking might be helpful: Prior to a test nothing is known about its outcomes, it is just known that there will be realisations of the random variable X, i.e. $X_1, X_2, X_3, ..., X_n$, which is a general description of the sample consisting of n observations. The sample mean and the sample variance can be written as

$$\overline{X} = \frac{1}{n} \sum_{i=1}^{n} X_i \tag{A.16}$$

A7

$$S^2 = \frac{1}{n} \sum_{i=1}^{n} \left(X_i - \overline{X} \right)^2 \tag{A.17}$$

With some further calculus (see, e.g. Benjamin and Cornell (1970)) the expected value and the variance of the sample mean and the sample variance can be expressed as

$$E\left[\overline{X} \right] = m_X \qquad Var\left[\overline{X} \right] = \frac{1}{n} \sigma_X^{\ 2} \tag{A.18}$$

$$E\left[S^2 \right] = \frac{n-1}{n} \sigma_X^{\ 2} \qquad Var\left[S^2 \right] = \frac{2(n-1)}{n^2} \sigma_X^{\ 2} \tag{A.19}$$

The expected value of the sample mean is equivalent to the mean of the underlying random variable X. The variation of the sample mean is given for the case where the individual observations can be considered to be mutually independent. This is the case, e.g. if the sample is obtained through random sampling. Also for random samples, the expected value of sample variance is given which is not equivalent to the variance of the underlying random variable. In other words, on the average over many different samples, S^2 will not be equal to σ_X^2 for which it has been introduced to serve as an estimator. Therefore S^2 is called a biased estimator of σ_X^2. As the variance of the sample mean the variance of the sample variance is also a function of the number of observations and the variance of the underlying random variable X.

As shown the sample moments can be used to obtain estimates of the real moments of the random variable and the uncertainty associated with this estimation can be quantified. Obviously in practice mostly only one sample is considered, i.e. only one realisation of sample moments is obtained. The uncertainty of this one realisation can be addressed, by exchanging m_X with $\overline{x}$ and σ_X with s.

Assuming the random variable X is following a probability distribution function F_X the parameters of the distribution can be estimated. However, the uncertainty associated with the distribution type assumption cannot be assessed by the method of moments.

The Method of Maximum Likelihood

The principle of the Method of Maximum Likelihood is to find a set of parameters of an assumed probability distribution function which most likely reflects the statistical behaviour of the underlying set of data (sample). The format of the method can be derived by means of the following considerations. Supposing that the parameters $\mathbf{\theta} = \left(\theta_1, ..., \theta_n \right)^T$ of the distribution of X are known, the joint probability distribution of a (random) sample $X_1, X_2, X_3, ..., X_n$ can be written as:

$$f_{\mathbf{X}}(\mathbf{x}|\mathbf{\theta}) = f_{X_1,X_2,X_3,...,X_n}(x_1,x_2,x_3,...,x_n|\mathbf{\theta}) = f_{X_1}(x_1)f_{X_2}(x_2)\cdots f_{X_n}(x_n) = \prod_{i=1}^{n} f_X(x_i|\mathbf{\theta}) \quad \text{(A.20)}$$

In other words Equation (A.20) can be seen as a relative measure for the belief that the sample $X_1, X_2, X_3, ..., X_n$ belongs to the distribution function with given parameters $\mathbf{\theta} = (\theta_1,...,\theta_n)^T$. Obviously in general the situation is contrary. A sample $\hat{\mathbf{x}} = \hat{x}_1, \hat{x}_2, \hat{x}_3, ..., \hat{x}_n$ is observed and the set of distribution parameters is not known. In that context Equation (A.20) can be similarly seen as a relative measure for the likelihood that the distribution determined by $\mathbf{\theta}$ is reflecting the statistical behaviour of the sample $\hat{\mathbf{x}}$. Over the entire domain of all possible parameters $\mathbf{\theta}$ the likelihood $L(.)$ that the parameters belong to the sample is:

$$L(\mathbf{\theta}|\hat{x}_1, \hat{x}_2, ..., \hat{x}_n) = \prod_{i=1}^{n} f_X(\hat{x}_i|\mathbf{\theta}) \quad \text{(A.21)}$$

The maximum likelihood estimators can now be defined as the set of parameters $\hat{\mathbf{\theta}}$ which are most likely representing the set of sample values, i.e. the set of parameters which maximise the likelihood function $L(.)$ over the entire domain of $\mathbf{\theta}$.

$$\hat{\mathbf{\theta}} = \max_{\mathbf{\theta}} L(\mathbf{\theta}|\hat{x}_1, \hat{x}_2, ..., \hat{x}_n) \quad \text{(A.22)}$$

To illustrate the nature of the likelihood function a set of sample values $\hat{\mathbf{x}}$ is considered and the exponential distribution is chosen as a proper distribution function for the sample. The probability density function for the exponential distribution is:

$$f(x|\lambda) = \lambda \exp(-\lambda x) \quad \text{(A.23)}$$

Then by given realisations of X, i.e. $\hat{\mathbf{x}} = \hat{x}_1, \hat{x}_2, ..., \hat{x}_n$ the joint probability density is

$$f_{\mathbf{X}}(\hat{\mathbf{x}}|\lambda) = \prod_{i=1}^{n} f_X(\hat{x}_i|\lambda) = \lambda \exp(-\lambda \hat{x}_1) \lambda \exp(-\lambda \hat{x}_2) \cdots \lambda \exp(-\lambda \hat{x}_n)$$

$$= \lambda^n \exp\left(-\lambda \sum_{i=1}^{n} \hat{x}_i\right) = L(\lambda|\hat{\mathbf{x}})$$

(A.24)

which is equivalent to the likelihood function given λ.

For illustration the likelihood function for a given sample is sketched in Figure A1.
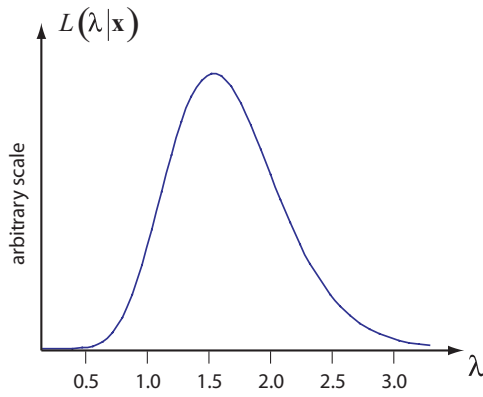
Figure A1   Likelihood function on λ

According to Figure A1 the likelihood function is attaining its maximum at $\lambda = 1.58$, the parameter which is most likely representing the considered sample. As an intuitive interpretation, the likelihood function might also be helpful to asses the likelihood of every possible parameter. In Figure A1 for example 1.5 might be a more likely estimate for λ than 2.5.

In general, it might be advantageous to consider the logarithm of the likelihood function. The log likelihood is written as:

$$\ln\left[L\left(\boldsymbol{\theta}|\hat{\mathbf{x}}\right)\right] = l\left(\boldsymbol{\theta}|\hat{\mathbf{x}}\right) = \ln\left[\prod_{i=1}^{n} f_X\left(\hat{x}_i|\boldsymbol{\theta}\right)\right] = \sum_{i=1}^{n} \ln\left[f_X\left(\hat{x}_i|\boldsymbol{\theta}\right)\right] \tag{A.25}$$

Then the maximum may be obtained by solving a set of m equations

$$\sum_{i=1}^{n} \frac{\partial}{\partial \theta_j} \ln\left[f_X\left(\hat{x}_i|\boldsymbol{\theta}\right)\right] = 0 \qquad j = 1, 2, ..., m \tag{A.26}$$

However, the solution of the system might not always be possible in a closed form. For complex problems, computer-automated search functions like e.g. the simplex method (Nelder and Meat (1965)) can be employed to find the values $\hat{\boldsymbol{\theta}}$ which maximise the likelihood function.

Properties of the Maximum Likelihood estimators

As for the method of moments the estimators are, before the experiment, random variables and can be studied as such. Their properties are well known and intensively studied in the literature (Lindley (1965)). For large samples ($n > 15$) the estimators $\hat{\boldsymbol{\theta}}$ are approximately normal distributed (due the summation form in Equation (A.25)). Their means are asymptotically equal to the true parameter values $\boldsymbol{\theta}$; which means, the estimators are asymptotically unbiased. The covariance matrix $\mathbf{C}$ for the parameters $\boldsymbol{\theta} = \left(\theta_1, \theta_2, ..., \theta_n\right)^T$ may be obtained through the inverse of the Fischer information matrix $\mathbf{H}$:

$$\mathbf{C}_{\boldsymbol{\Theta}\boldsymbol{\Theta}} = \mathbf{H}^{-1} \tag{A.27}$$

with components given by:

$$H_{ij} = -\left.\frac{\partial^2 l}{\partial\theta_i\partial\theta_j}\right|_{\boldsymbol{\theta}=\hat{\boldsymbol{\theta}}} \tag{A.28}$$

E.g. the variance of θ_i is asymptotically equal to:

$$Var\left[\hat{\boldsymbol{\theta}}\right] = -\frac{1}{nE\left[\dfrac{\partial^2 l}{\partial\theta_i^2}\right]} \tag{A.29}$$

Contrary to the method of moments the estimations of the distribution variables are studied in regard to their uncertainty and not the sample moments. The main properties of the maximum likelihood estimates are:

- For large data samples the distribution parameters $\boldsymbol{\theta}$ are Normal distributed.

- Maximum likelihood estimates are consistent: For large n the estimates converge to the true value of the parameters of the distribution.

- Maximum likelihood estimates are unbiased: For all sample sizes the parameter of interest is calculated correctly.

- Maximum likelihood estimates are efficient: The estimate has the smallest variance.

- Maximum likelihood estimate is sufficient: All the information of the observations is utilized.

- The solution of MLM is unique.

- The probability distribution for the problem at hand has to be known.

A4   UPDATING

When information has been collected about a quantity of interest the new knowledge implicit in that information might be applied to improve any previous (prior) estimate of the value of the property. For the type of information it can be differentiated between so-called equality type and inequality type information. Equality type information is corresponding to measured variables and inequality type information denotes the information carried with a measurement that some variable is greater than or less than some predefined limit. It can also be differentiated between direct and indirect information; i.e. direct measurements of the quantity of interest and the measurement of some indicator of the quantity respectively. Examples for the different types of information are given in Figure A2.

A11

	direct	indirect
equality	standard tests	grading indication
inequality	proof-loading	status inspections

Figure A2   Examples for combinations of different types of information.

The framework of doing updating is Baysian statistics, which uses the Bayes theorem, see e.g. Ang and Tang (1975).

Updating Random Variables using Direct Information

A random quantity is represented by the random variable X with the probability distribution function $F_X(x)$. The parameters $\mathbf{\theta} = (\theta_1, \theta_2, ..., \theta_n)^T$ of the distribution function are not known with accuracy; i.e. they are product of engineering knowledge, physical understanding or earlier observations of the quantity. The parameters $\mathbf{\theta}$ are in general expressed as random variables itself specified by the so-called prior density function $f_{\mathbf{\Theta}}'(\mathbf{\theta})$. The uncertain parameters can be updated based on new observations of realizations of the random quantity X, $\hat{\mathbf{x}} = (\hat{x}_1, \hat{x}_2, ..., \hat{x}_n)^T$.

The general scheme for updating of the parameters $\mathbf{\theta} = (\theta_1, \theta_2, ..., \theta_n)^T$ is:

$$f_{\mathbf{\Theta}}''(\mathbf{\theta}|\hat{\mathbf{x}}) = \frac{f_{\mathbf{\Theta}}'(\mathbf{\theta}) L(\mathbf{\theta}|\hat{\mathbf{x}})}{\int f_{\mathbf{\Theta}}'(\mathbf{\theta}) L(\mathbf{\theta}|\hat{\mathbf{x}}) d\mathbf{\theta}} \tag{A.30}$$

where $f_{\mathbf{\Theta}}''(\mathbf{\theta}|\hat{\mathbf{x}})$ is the posterior distribution function of the parameters $\mathbf{\theta}$. The likelihood function $L(\mathbf{\theta}|\hat{\mathbf{x}})$ represents the knowledge gained by the observation of $\hat{\mathbf{x}}$. It can be interpreted as the likelihood of observing $\hat{\mathbf{x}}$ under the assumption that $\mathbf{\theta}$ takes its current set of values – it may be written as $p(\hat{\mathbf{x}}|\mathbf{\theta})$.

The Likelihood function is proportional to the joint conditional probability of making the observations $\hat{\mathbf{x}}$:

$$L(\mathbf{\theta}|\hat{\mathbf{x}}) \propto \prod_{i=1}^{n} f_{\mathbf{X}|\mathbf{\Theta}}(\hat{x}_i|\mathbf{\theta}) \tag{A.31}$$

where n is the number of observations.

Based on the updated distribution of the parameters $f_\Theta''(\theta|\hat{\mathbf{x}})$, it is possible to calculate the predictive distribution of the random property X, as:

$$f_\Theta^U(x) = \int f_X(x|\theta) f_\Theta''(\theta|\hat{\mathbf{x}}) d\theta \tag{A.32}$$

Closed form solutions for the predictive and the posterior distribution can be found for special types of probability distribution functions (known as natural conjugate distributions) in e.g. Raiffa and Schlaifer (1961). These solutions are the analytical basis for the updating of random variables and cover a number of distribution types which are in common use in structural engineering. In cases where no analytical solution is available FORM/SORM techniques (Madsen et al. 1986) can be used to integrate over the possible outcomes of the uncertain distribution parameters.

Inference: Normal Distribution with uncertain mean and known standard deviation

A normal distributed variable X, with the parameters $\theta = (M_X, \sigma_X)^T$ is considered. The standard deviation σ_X is assumed to be known and the mean value M_X is considered as random variable. It can be shown, that the natural conjugate distribution for M_X is the normal distribution, i.e. $M_X \sim N(\mu', \sigma')$ is the prior distribution. n new observations $\hat{\mathbf{x}}$ of X are made and the sample characteristics $\bar{x}$ and s are quantified.

The posterior distribution function of the mean can be given as (Ditlevsen and Madsen (1996)):

$$f''(\mu_X) = \frac{1}{\sqrt{2\pi}\sigma''} \exp\left(-\frac{1}{2}\left(\frac{\mu_X - \mu''}{\sigma''}\right)^2\right) \tag{A.33}$$

where:

$$\mu'' = \frac{\dfrac{\mu'}{n} + \dfrac{\bar{x}}{n'}}{\dfrac{1}{n} + \dfrac{1}{n'}} \quad \text{and} \quad \sigma'' = \sqrt{\frac{\dfrac{\sigma_X}{n}\dfrac{\sigma'}{n'}}{\dfrac{\sigma'^2}{n} + \dfrac{\sigma'^2}{n'}}} \quad \text{and} \quad n' = \frac{\sigma_X^2}{\sigma'^2}$$

The predictive distribution can then be given as:

$$f(x|\hat{\mathbf{x}}) = \frac{1}{\sqrt{2\pi}\sigma'''} \exp\left(-\frac{1}{2}\left(\frac{x - \mu''}{\sigma'''}\right)^2\right) \tag{A.34}$$

with:

$$\sigma''' = \sqrt{\sigma''^2 + \sigma_X^2}$$

As seen in Equation (A.33) and (A.34) the posterior distribution and the predictive distribution are both normal which is a convenient property especially for repeated updating.

A13

Inference: Normal Distribution with uncertain mean and standard deviation

Considered is a normal distributed variable X, with the parameters $\boldsymbol{\theta} = \left(M_X, \Sigma_X\right)^T$. The mean and the standard deviation are regarded as random variables. An analytical solution for the updating scheme can be found by using the natural conjugate prior for the distribution of $\boldsymbol{\theta}$, which in this case is the Normal-Inverse-Gamma-2 distribution. The Normal-Inverse-Gamma-2 distribution is defined through (compare e.g. Rackwitz (1983)):

$$f_{M,\Sigma}\left(\mu, h | m', s', n', v'\right) = f_M\left(\mu | m', hn'\right) f_\Sigma\left(h | s', v'\right)$$

$$= \frac{\sqrt{hn'}}{\sqrt{2\pi}} \exp\left(-\frac{1}{2}\left(\frac{\mu - m'}{1/\sqrt{hn'}}\right)^2\right) \frac{1}{2\Gamma(v'/2)}\left(\frac{1}{2}v's'^2 h\right)^{\frac{1}{2}v'-1} \exp\left(-\frac{1}{2}v's'^2 h\right) v's'^2 \qquad (A.35)$$

$$-\infty < \mu < \infty; \quad h \geq 0; \quad s', v', n' > 0$$

where $m' = \bar{x}'$ is the mean of a sample of equivalent size n' and s' is the standard deviation of a sample of equivalent size $v' + 1$. The uncertain variability is expressed by the precision $h = 1/\sigma^2$. Equation (A.35) is the natural conjugate prior distribution function of the parameters $\boldsymbol{\theta} = \left(M_X, \Sigma_X\right)$.

By observing n sample values $\hat{\mathbf{x}}$ from X the following statistics may be drawn:

$$m = \bar{x} = \frac{1}{n}\sum \hat{x}_i$$

$$s^2 = \frac{1}{n-1}\sum\left(m - x_i\right)^2$$

$$v = n - 1$$

For the posterior distribution function the parameters m', s', n', v' in Equation (A.35) are exchanged the parameters m'', s'', n'', v'' given by:

$$m'' = \frac{n'm' + nm}{n' + n} \qquad (A.36)$$

$$n'' = n' + n \qquad (A.37)$$

$$s''^2 = \frac{\left(v's'^2 + n'm'^2\right) + \left(vs^2 + nm^2\right) - n''m''^2}{\left(v' + \delta(n')\right) + \left(v + \delta(n)\right) - \delta(n'')} \qquad (A.38)$$

$$v'' = \left(v' + \delta(n')\right) + \left(v + \delta(n)\right) - \delta(n'') \qquad (A.39)$$

with:

$$\delta(x) \equiv \begin{cases} 0 & \text{for} \quad x \leq 0 \\ 1 & \text{for} \quad x > 0 \end{cases} \tag{A.40}$$

The predictive distribution is of student type and is given with:

$$F_{X|\hat{x}}(x|m'',n'',s'',v'') = T_{v''}\left(\frac{x-m''}{s''}\sqrt{\frac{n''}{n''+1}}\right) \tag{A.41}$$

where $T_v(.)$ is the student-t-distribution with v degrees of freedom.

Quantification of prior information

As described and illustrated before, Baysian statistics provides a proper framework for updating random variables and failure probabilities taking into account additional information. The basic assumption in Baysian statistics is that prior information is always available and can be quantified. If no information is available, the state of knowledge (or in this case the state of ignorance) can still be quantified by so-called non informative priors (Lindley (1965)). However, for engineering problems some prior information generally exist and the Bayesian interpretation of probability[1] enables to introduce even vague subjective judgement as quantified prior information. According to the confidence about the subjective judgement the prior information can be weighted. For example consider the bending strength of a timber supply of a sawmill which is planned to be continuously tested. It is assumed that the supply is stationary. It is planned to draw a sample of 20 test specimens from the output every first Monday of every month. From a neighbouring sawmill it is known that the mean and the coefficient of variation of the bending strength are around 56 MPa and 25% respectively. If it is believed that the supply for the considered sawmill is very similar, this information can be utilized for the quantification of the prior distribution. Depending on how strong the belief of similarity of the outputs of the two sawmills is, the prior information can be weighted; i.e. the parameters n' and v' can be estimated correspondingly.

Another possibility is the quantification of prior information based on data. Consider the example above, where the prior information of the bending strength of a sawmill timber supply has to be quantified. Distribution parameters from several neighbouring sawmills are available and a significant scatter within these parameters can be observed. It is assumed that the parameters are following the natural conjugate prior distribution and that the parameters of the supply of interest are members of this distribution. In case of the assumption of normal distributed bending strength with unknown mean and standard deviation the conjungate prior

---

[1] Interpretations of probability.

Bayesian: probability of A, $P(A)$, is the degree of belief that the event A occurs.

Frequentistic: Probability is understood as a relative frequency; i.e. $P(A) = n_A/n_{total} \quad n_{total} \rightarrow \infty$

is Normal-Inverse-Gamma-2 distributed with the parameters (m', s', n', v'). The parameters (m', s', n', v') can directly estimated based on the parameter pairs from the other supplies $\bar{x}_i$ and s_i with $m_i = \bar{x}_i$ and $h_i = 1/s_i^2$ (Rackwitz (1983)):

$$\bar{x}' = \frac{\hat{h}}{\bar{h}} \tag{A.42}$$

$$n' = \left(\breve{h} - \frac{\hat{h}^2}{\bar{h}} \right)^{-1} \tag{A.43}$$

$$s' = \bar{h}^{-1/2} \tag{A.44}$$

$$\tilde{h} = \psi\left(\frac{v'}{2}\right) - \ln\left(\frac{v'}{2\bar{h}}\right) \tag{A.45}$$

with:

$$\bar{h} = \frac{1}{k} \sum_1^k h_i; \qquad \tilde{h} = \frac{1}{k} \sum_1^k \ln(h_i); \quad \hat{h} = \frac{1}{k} \sum_1^k h_i m_i; \quad \breve{h} = \frac{1}{k} \sum_1^k h_i m_i^2;$$

and

$$\psi\left(\frac{v'}{2}\right) = \ln\left(\frac{v'}{2}\right) - \frac{1}{v'} - \frac{1}{3v'^2} + \frac{2}{15v'^4} - \frac{16}{63v'^6} + \dots$$

The determination of v' requires the numerical solution of Equation (A.45). However, for sufficiently large v' (order of magnitude $v' > 6$) v' can be approximated with

$$v' \approx \left(\ln(\bar{h}) - \tilde{h} \right)^{-1} \tag{A.46}$$